UNIVERSIDADE FEDERAL DE SÃO CARLOS
CENTRO DE CIÊNCIAS BIOLÓGICAS E DA SAÚDE
PROGRAMA DE PÓS-GRADUAÇÃO EM ECOLOGIA E RECURSOS NATURAIS

AVALIAÇÃO DA INFLUÊNCIA DE BORDA EM VEGETAÇÃO HETEROGÊNEA COM ANÁLISE DE PADRÃO ESPACIAL

Pavel Dodonov

SÃO CARLOS
2015

FEDERAL UNIVERSITY OF SÃO CARLOS
CENTER OF BIOLOGICAL AND HEALTH SCIENCES
POST-GRADUATION PROGRAM IN ECOLOGY AND NATURAL RESOURCES

ASSESSMENT OF EDGE INFLUENCE IN HETEROGENEOUS VEGETATION USING SPATIAL PATTERN ANALYSIS

Pavel Dodonov

SÃO CARLOS
2015

UNIVERSIDADE FEDERAL DE SÃO CARLOS
CENTRO DE CIÊNCIAS BIOLÓGICAS E DA SAÚDE
PROGRAMA DE PÓS-GRADUAÇÃO EM ECOLOGIA E RECURSOS NATURAIS

AVALIAÇÃO DA INFLUÊNCIA DE BORDA EM VEGETAÇÃO HETEROGÊNEA COM ANÁLISE DE PADRÃO ESPACIAL

Pavel Dodonov

Tese apresentada ao Programa de Pós-Graduação em Ecologia e Recursos Naturais, para obtenção do título de doutor em Ecologia e Recursos Naturais

Orientação: Profa. Dra. Dalva Maria da Silva Matos
Co-orientação: Profa. Dra. Karen A. Harper

SÃO CARLOS
2015

Ficha catalográfica elaborada pelo DePT da
Biblioteca Comunitária/UFSCar

D646ai

Dodonov, Pavel.
Avaliação da influência de borda em vegetação heterogênea com análise de padrão espacial / Pavel Dodonov. -- São Carlos : UFSCar, 2015.
240 f.

Tese (Doutorado) -- Universidade Federal de São Carlos, 2015.

1. Conservação. 2. Cerrados. 3. Influência de borda. 4. Cadeias de Markov. 5. Transformada de Wavelet. I. Título.

CDD: 574.5247 (20ª)

UNIVERSIDADE FEDERAL DE SÃO CARLOS

Centro de Ciências Biológicas e da Saúde
Programa de Pós-Graduação em Ecologia e Recursos Naturais

Folha de Aprovação

Assinaturas dos membros da comissão examinadora que avaliou e aprovou a Defesa de Tese de Doutorado do candidato Pavel Dodonov, realizada em 20/02/2015:

Dalva M. Silva Matos
Profa. Dra. Dalva Maria da Silva Matos
UFSCar

Luciano E. Lopes
Prof. Dr. Luciano Elsinor Lopes
UFSCar

Prof. Dr. Marcus Vinicius Cianciaruso
UFG

Prof. Dr. Milton Cezar Ribeiro
UNESP

Tadeu Siqueira
Prof. Dr. Tadeu de Siqueira Barros
UNESP

The Road goes ever on and on
Down from the door where it began
Now far ahead the Road has gone
And I must follow, if I can,
Pursuing it with eager feet
Until it meets a larger way
Where many paths and errands meet.
And whither then? I cannot say.
(J. R. R. Tolkien)

Agradecimentos gerais

À minha coorientadora Karen Harper, pelo direcionamento e pela ajuda nestes últimos anos;

À minha orientadora Dalva Matos, pelos muitos anos de orientação;

Ao Conselho Nacional de Desenvolvimento Científico e Tecnológico (CNPq) pelo financiamento desta pesquisa (processo 141623/2011-0);

Ao Programa Científico de Treinamento do Norte (Northern Scientific Training Program – NSTP), ao Conselho de Pesquisa em Ciências Naturais e Engenharia do Canadá (Natural Sciences and Engineering Research Council of Canada – NSERC) e ao Fundo de Pesquisas do Norte (Northen Research Fund) pelo apoio financeiro à pesquisa de campo de dois meses em Churchill, MB, Canada;

Ao Programa Líderes Emergentes nas Américas (Emerging Leaders in the Americas Program – ELAP) por financiar a minha pesquisa de seis meses no Canadá;

Ao Instituto Florestal de São Paulo e à Estação Ecológica de Itirapina, pela permissão de trabalho e pelo apoio logístico;

Ao Centro de Estudos do Norte de Churchill (Churchill Northern Studies Centre) e o seu pessoal, especialmente LeeAnn Fishback, pelo apoio logístico na pesquisa de campo em Churchill;

A Cinthya Santos, pela ajuda infinita em campo, ajuda e apoio infinito com o desenvolvimento do trabalho, e apoio mental também infinito;

A minha co-orientada Andreza Lanza, pela ajuda na morfotipagem e identificação de plantas infinitas, e pela experiência de orientação;

Às muitas pessoas que me ajudaram em campo no Brasil: Natália Rosatti, Marcelo Leite, Ariel Viscardi, Renata Muylaert, Maria Luiza Zambom, Luiz Arruda, Rafael Xavier, Viviane Pereira, Ingrid Paneczko, Bárbara Rupert, Paulo Rubim, Cinthya Santos, Andreza Lanza, Zaryf Dahroug, Raquel Miatto, Gabriela Lobato, Carolline Fieker, Isabela Lucena, Marina Telles, Carolina Stella Gonçalves, Bianca Rantin, Marcos Henrique Silva, Matheus Reis, Davi Munhoz, Elaine Dantas, Talita Alvarenga, Fernanda Tibério, Luana Hortenci, Vanessa Lazaro, Julie Scaloppi, Amanda Mello, Renata Vilar, Jaqueline Siquitelli, Rayane Maciel, Camila Leite;

A Amanda Lavalle e Danielle StLouis, pelo trabalho de campo conjunto em Churchill;

A Danilo Muniz, Rafael Xavier, Prof. Yoshio Tamashiro, Prof. Marco Batalha, Francisco Santos e Marcelo Leite, pela ajuda com identificação de plantas;

A Genevieve Berard por ajuda na coleta dos dados de altimetria em Churchill;

Ao Departamento de Ecologia da Unesp (Rio Claro), pelo empréstimo de altímetro usado na coleta de dados de altimetria no Brasil;

Às pessoas lindas do Lab. de Ecologia e Conservação (UFSCar), especialmente Fernanda Tibério, Rafael Xavier e Talita Sampaio, pelo trabalho conjunto, pela ajuda, pelas discussões, pela companhia;

Às pessoas lindas do Lab. de Ecologia Espacial e Conservação (Unesp), pelas discussões, pela companhia, por me mostrar os diversos caminhos da ecologia espacial;

Às pessoas lindas do Grupo de Estudos e Pesquisa em Educação Ambiental e da Trilha da Natureza (UFSCar), por me mostrar outros caminhos dentro da Academia;

A Carlos Zucco por sugestões no capítulo sobre métodos;

Aos professores Milton Ribeiro, Hugo Sarmento e Marco Batalha pela avaliação do meu exame de qualificação;

Aos professores Marcus Cianciaruso, Milton Ribeiro, Luciano Lopes e Tadeu Siqueira, pela avaliação da tese e pelas valiosas sugestões;

Aos meus amigos de Halifax, especialmente Caroline Franklin, Jordi Segers, Angela Ni, 안창규, John McQuaid, Cameron Elley, e Yu Baoui;

Às pessoas do Centro de Pesquisas do Norte de Churchill, especialmente Ryan Rimas, Matthew Morrison, Hannah Boehm, Thanushi Eagalle, Morgan Roblin e Genevieve Berard;

À minha família;

A outras pessoas que me ajudaram a manter um pouco de sanidade nestes quatro anos de doutorado – Yashiro Yamamoto Sensei, Harumi Nakahara Sensei, Juliana Padilha, Carolina Stella, Roberta Freitas, Carolina Zanelli, Felipe Oliveira, Marcos Henrique, Raquel Miatto, Amelina Aquino, Ariadne Sabbag, Luana Hortenci, Jaqueline Siquitelli, Anderson Nakano, Felipe Rinaldi.

General acknowledgments

To my cosupervisor Karen Harper, for guidance and help during the last years. Long live the Edge Queen! :);

To my supervisor Dalva Matos, for the long years of supervision;

To the National Council for Scientic Research and Development (Conselho Nacional de Desenvolvimento Científico e Tecnológico - CNPq) for funding this research (grant 141623/2011-0);

To the Northern Scientific Training Program (NSTP), the Natural Sciences and Engineering Research Council of Canada (NSERC) and the Northern Research Fund (NRF), for financial support to the two-month research in Churchill, MB, Canada;

To the Emerging Leaders in the Americas Program (ELAP) for funding my six-month research in Canada;

To the Forestry Institute of São Paulo and the Itirapina Ecological Station for fieldwork permissions and logistic support;

To the Churchill Northern Studies Centre and its staff, especially LeeAnn Fishback, for logistic support during the fieldwork in Canada;

To Cinthya Santos, for help in the field, aid with the development of this study, and general support;

To my co-supervised student Andreza Lanza, for help with plant morphotyping and for the supervisor experience;

To the many people who helped me in the field in Brazil: Natália Rosatti, Marcelo Leite, Ariel Viscardi, Renata Muylaert, Maria Luiza Zambom, Luiz Arruda, Rafael Xavier, Viviane Pereira, Ingrid Paneczko, Bárbara Rupert, Paulo Rubim, Cinthya Santos, Andreza Lanza, Zaryf Dahroug, Raquel Miatto, Gabriela Lobato, Carolline Fieker, Isabela Lucena, Marina Telles, Carolina Stella Gonçalves, Bianca Rantin, Marcos Henrique Silva, Matheus Reis, Davi Munhoz, Elaine Dantas, Talita Alvarenga, Fernanda Tibério, Luana Hortenci, Vanessa Lazaro, Julie Scaloppi, Amanda Mello, Renata Vilar, Jaqueline Siquitelli, Rayane Maciel, Camila Leite;

To Amanda Lavalle and Danielle StLouis, for the joint fieldwork in Churchill;

To Danilo Muniz, Rafael Xavier, Prof. Yoshio Tamashiro, Prof. Marco Batalha, Francisco Santos and Marcelo Leite, for help with plant identification;

To Genevieve Berard for aid in collecting altimetry data in Churchill;

To the Department of Ecology of the São Paulo State University (Rio Claro) for lending the altimeter used to collect altimetry data in Brazil;

To the people of the Ecology and Conservation Lab (UFSCar), especially Fernanda Tibério, Rafael Xavier and Talita Sampaio, for the joint work, help, discussions and company;

To the people of the Spatial Ecology and Conservation lab (Unesp), for the discussions, company, and for showing me the paths of spatial ecology;

To the people of the Study and Research Group in Environmental Education and of the Trail of Nature (UFSCar), for showing me other paths in Academia;

To Carlos Zucco for suggestions on the general methods chapter;

To the professors Milton Ribeiro, Hugo Sarmento and Marco Batalha for evaluating my qualification exam;

To the professors Marcus Cianciaruso, Milton Ribeiro, Luciano Lopes and Tadeu Siqueira for the final evaluation of the thesis and their insightful suggestions;

To my friends in Halifax, especially Caroline Franklin, Jordi Segers, Angela Ni, 안창규, John McQuaid, Cameron Elley, and Yu Baoui;

To the people at the Churchill Northern Studies Centre, especially Ryan Rimas, Matthew Morrison, Hannah Boehm, Thanushi Eagalle, Morgan Roblin, and Genevieve Berard;

To my family;

To other people who helped me maintain some sanity during these four years of PhD – Yashiro Yamamoto Sensei, Harumi Nakahara Sensei, Juliana Padilha, Carolina Stella, Roberta Freitas, Carolina Zanelli, Felipe Oliveira, Marcos Henrique, Raquel Miatto, Amelina Aquino, Ariadne Sabbag, Luana Hortenci, Jaqueline Siquitelli, Anderson Nakano, Felipe Rinaldi.

Resumo

A influência de borda, o conjunto de modificações no ambiente natural próximo a bordas abruptas antrópicas ou naturais, é uma séria ameaça à biodiversidade em ambientes fragmentados. Exemplos comuns de influência de borda incluem um aumento na abundância de espécies exóticas e mudanças na estrutura e/ou composição da vegetação. Bordas de distúrbios lineares, como rodovias, linhas de transmissão elétrica e aceiros, merecem atenção especial devido à sua ubiquidade na paisagem. Embora tais distúrbios sejam muito mais estreitos do que outros usos de solo antrópicos, eles podem afetar as comunidades vegetal e animal adjacentes. A combinação da influência de borda com a variação natural da vegetação pode resultar em padrões complexos que não são facilmente detectáveis. No entanto, a variação natural via de regra não é levada em conta em estudos de influência de borda. Nós usamos uma abordagem de padrão espacial para estudar a influência de borda de distúrbios lineares estreitos, levando também em conta a variação da vegetação (natural e/ou por histórico de distúrbios), no cerrado brasileiro e no ecótono floresta-tundra canadense. Nossos principais objetivos eram: 1) estudar a heterogeneidade na cobertura de graminóides nativos e exóticos, diversidade estrutural e composição de espécies e 2) verificar se o padrão espacial das diferentes variáveis-resposta é afetado por bordas antrópicas. Objetivos secundários incluem 3) explorar as diferentes formas em que a transformação de *wavelets* (“pequenas ondas”) e simulações Monte Carlo podem ser usadas para estudar a influência de borda, 4) comparar diferentes índices de diversidade estrutural e 5) verificar se os padrões espaciais de diferentes espécies vegetais estão relacionados aos seus traços de história de vida. Nós amostramos três transectos de 300 a 1350 m de comprimento, três no Brasil e dois no Canadá. Os transectos continham uma a cinco bordas antrópicas e uma a dez bordas naturais, e foram divididos em parcelas contíguas de 1x1 m. Dentro de cada parcela nós estimamos a cobertura de graminóides nativos e invasores (dois transectos no Brasil), amostramos diferentes elementos estruturais para medir a diversidade estrutural (dois transectos no Brasil e os dois transectos canadenses) i identificamos as espécies de plantas, assim como suas síndromes de dispersão e formas de vida (um transecto no Brasil). Nós analisamos o dado por meio de transformação de *wavelets* contínua e discreta e análise de multiresolução, e determinamos a influência de borda por meio de aleatorizações completas, simulações por cadeia de Markov e modelos autoregressivos. Embora alguns padrões relacionados a bordas foram observados para a maior parte das variáveis, eles não foram observados em todas as bordas e padrões similares também foram observados longe de bordas. Os diferentes índices de diversidade estrutural mostraram padrões similares e os traços funcionais das espécies, especificamente forma de vida e síndrome de dispersão, não foram relacionados à distribuição espacial das diferentes espécies. A principal conclusão deste estudo é que, embora bordas de distúrbios lineares estreitos, especificamente aceiros, podem alterar a estrutura da vegetação e a composição de espécies, as condições na borda não são necessariamente diferente do que pode ser observado devido à variação natural nas comunidades vegetal em vegetação não-florestal..

Palavras-chave: cadeia de Markov, cerrado, diversidade estrutural, efeitos de borda, gramíneas invasoras, modelos autoregressivos, padrão espacial, síndromes de dispersão, transformação de *wavelet*, tundra.

Abstract

Edge influence, the set of modifications in the natural environment next to abrupt anthropogenic or natural edges, is a serious threat to biodiversity in fragmented environments. Common examples of edge influence include an increased abundance of exotic species and modifications in vegetation structure and/or composition. Edges of linear disturbances, such as roads, powerlines, and firebreaks, are especially important due to their ubiquity in the landscape. Although such disturbances are much narrower than other anthropogenic land uses, they have been shown to affect adjacent plant and animal communities. The combination of edge influence with the natural variation in vegetation may lead to complex and not easily discernible patterns. However, this natural variation is not usually taken into account in studies of edge influence. We employed a spatial pattern approach to study edge influence from narrow linear disturbances while accounting for variation in vegetation (both natural and from disturbance history), in Brazilian cerrado and in Canadian forest-tundra ecotone. Our main objectives were 1) to assess the overall heterogeneity in the cover of native and invasive graminoids, structural diversity and species composition, and 2) to verify whether the spatial pattern of different response variables is affected by anthropogenic edges. Secondary objectives include: 3) to explore different ways in which wavelet transforms and Monte Carlo simulations may be used to assess edge influence, 4) to compare different structural diversity indices, and 5) to assess whether the spatial patterns of different plant species are related to their functional traits. We sampled five 300-1350 m-long transects, three in Brazil and two in Canada. The transects contained one to five anthropogenic edges and one to ten natural edges and were divided into contiguous 1x1 m quadrats. In each quadrat, we estimated the cover of native and invasive graminoids (two transects in Brazil), sampled different structural elements to measure the structural diversity (two transects in Brazil and the two Canadian transects), and identified plant species and their dispersal syndromes and lifeforms (one transect in Brazil). We analyzed the data by means of continuous and discrete wavelet transforms and multiresolution analysis, and assessed significance by means of full randomizations, Markov chain simulations, and autoregressive models. Although some edge-related patterns were apparent for most variables, they were not observed at all edges, and similar patterns were also observed far from edges. The different structural diversity indices showed similar patterns, and species traits, namely lifeform and dispersal syndrome, were not related to the spatial distribution of different species. The main conclusion of our study is that although narrow linear disturbance edges may alter vegetation structure and species composition, the conditions at edges are not necessarily different from what may be observed due to the natural variation in plant communities in non-forest vegetation.

Keywords: autoregressive models, cerrado, dispersal syndromes, edge effects, invasive grasses, Markov chain, spatial pattern, structural diversity, tundra, wavelet transform.

Contents

Chapter 1. Introduction

1.1 Literature review

In human-altered landscapes there is a profusion of edges between natural communities and anthropogenic land uses (Saunders et al. 1991, Fahrig 2003). These edges may result in significant differences in ecosystem structure, composition and/or function near edges in relation to reference interior forest, a process known as known as edge influence (Harper et al. 2005a). Common examples of edge influence on plant communities include changes in vegetation structure, such as lower canopy cover (Harper et al. 2004) or increased abundance of lianas at the edge, Magrach et al. 2014); abundance of different species, as some species may favor edges whereas other avoid them (Santos et al. 2014, Hauck et al. 2014); a lower number of plant species at the forest edge (Hofmeister et al. 2013) Lippok et al. 2013), and changes in interspecific interactions, for example with a dietary narrowing (Falcão et al. 2011) and increased nectar robbing leading to lower reproductive success (Magrach et al. 2012). Another common example is an increase in the abundance of exotic species next to edges, which has been observed in grassland, savanna and forest environments (Pivello et al. 1999a, b, Honnay et al. 2002, Cilliers et al. 2008). However, generalizations of edge-related patterns are not easily made, as different studies often find different or even opposite patterns. For example, although vegetation height has been observed to be lower at edges than in reference conditions in tropical rainforest (Didham and Lawton 1999, Vaughn et al. 2014), it has also been found to be taller or have a non-monotonic pattern at edges in the Brazilian cerrado, possibly due to reduced competition (Dodonov et al. 2013).

Among the land uses that have been shown to affect the adjacent plant communities, linear disturbances such as roads, power lines, railroads, firebreaks, and tourist trails are especially important. Linear disturbances such as roads and powerlines are omnipresent infrastructure features and result in severe impacts in tropical forests (Laurance et al. 2009), whereas firebreaks are important for the management of protected areas, and recreational trails are common in areas with ecotourism activities (Ballantyne et al. 2014). Although these disturbances are much narrower than plantations and clearcuts, their edges have been shown to affect microclimate and vegetation structure (Delgado et al. 2007, Pohlman et al. 2007, Smit and Asner 2012), plant growth (Bowering et al. 2006), species composition (Avon et al.

2010) and plant-insect interactions (Huang et al. 2009, Pires et al. 2014). A large number of studies on the effects of linear disturbances on both plants and animals has been performed at road edges (e.g. Delgado et al. 2013, Rotholz and Mandelik 2013). Edge influence at road edges probably results from a combination of the creation and maintenance of the linear disturbance, vehicle traffic, and pollution (Eigenbrod et al. 2009, Bettez et al. 2013). However, edge influence has also been observed at maintained linear disturbances with low or no vehicle traffic, such as powerlines and firebreaks (Smit and Asner 2012, Pires et al. 2014). A more detailed study on the effects of this latter type of disturbance may aid in understanding how the simple creation and maintenance of these features influences the adjacent vegetation.

Edge-related patterns caused by different land uses may be superimposed on the natural variation in vegetation (Guerra et al. 2013), resulting in complex and not easily discernible patterns. Plant communities have a characteristic spatial structure composed of alternating areas with high and low values (patches and gaps) of species abundance, vegetation height and other characteristics (Dale 1999). Spatial pattern and other characteristics of the vegetation may be influenced by factors such as intra- and inter-specific competition (Wiegand et al. 2005; Strand et al. 2007), soil properties (Ruggiero et al. 2002), past disturbance (Strand et al. 2007) and stage of succession (Harper et al. 2005b). Thus, on a scale of hundreds of meters to kilometers, the formation of different vegetation types may be related to the variation in soil characteristics; for example, richer soil patches may be occupied by forest vegetation, and poorer soil by savanna (Ruggiero et al. 2002). Alternating patches with dominance of trees or grasses may also result from spatially variable rainfall and inter-tree competition in savannas (Wiegand et al. 2005). Topography and hydrography also influence the structure of vegetation and the distribution of different species (Brosofske et al. 1999, Silva et al. 2010, Lippok et al. 2014). At a scale of meters, gap dynamics in forests result from an alternation of areas with high and low canopy cover (Bradshaw and Spies 1992), and similar patterns may be observed in tropical grasslands (Cilliers et al. 2008). The cover of different plant species may also be affected by variation in microtopography and soil characteristics at smaller scales (Marchand and Houle 2006). Finally, disturbances such as insect outbreaks and wildfire may result in different patch types at a landscape scale (James et al. 2010; Fischer et al. 2012), as well as increases in heterogeneity at a local scale (Werner 2010; Dodonov et al. 2014a).

The superposition of edge influence on the natural variation in a plant community may complicate the detection of edge-related patterns. Studies on edge influence usually compare samples at different distances from the edge with those located in interior references conditions (Didham & Lawton 1999, Harper and Macdonald 2011). Although this approach has provided many results on the intensity and extent of edge influence in various ecosystems (Didham and Lawton 1999, Dodonov et al. 2013, Harper et al. 2014), it may be of limited use in patchy and/or highly fragmented environments, where effects of two or more edges may combine (Porensky and Young 2013). Therefore, a different method may be needed to study edge influence in environments with many edges and/or high natural heterogeneity, such as riparian buffers, ecotones between open and closed vegetation, and savannas.

As an alternative, studies of spatial pattern that span both edge and interior (when available) may provide insight into both the natural variability in spatial pattern across the landscape and on the change in this pattern near edges. Sampling with a large set of small contiguous quadrats makes it possible to have both small- and large-scale pattern assessments (Dale 1999), thus allowing the determination of edge-related patterns at different scales. Although studies on spatial pattern often focus only on the scales of variation without considering where different patterns may be observed, recent developments, such as wavelet transforms, enable the assessment of both the scales of variation and the location of the different patterns (Dale and Mah 1998, Keitt and Urban 2005). Combined with the use of different null models, these analyses permit an assessment of the significance of patterns observed at different scales in relation to different null hypotheses, permitting inferences regarding the underlying ecological processes, including edge influence (Rouyer et al. 2008, James et al. 2010).

1.2 Objectives

We employed a spatial pattern approach, combined with wavelet transforms and different null models, to assess the natural heterogeneity and edge-related patterns in heterogeneous environments, namely the Brazilian cerrado and the Canadian forest-tundra ecotone (Supplementary Material 1.1-1.5). Our main objectives were: 1) to verify whether the spatial patterns of different response variables – invasive grasses, vegetation structural diversity and plant species composition – are affected by linear disturbance edges, with a special emphasis on firebreaks, and 2) to explore different ways in which wavelet analysis and null models may be used to study edge influence in patchy vegetation. Secondary objectives included 3) to assess patterns in different response variables at ecotones between forest and savanna and at natural lakeshore edges, 4) to introduce a dissimilarity-based measure of structural diversity, and 5) to verify whether functional traits, namely lifeform and seed dispersal syndromes, are related to the spatial distribution of different species.

1.3 General methods

1.3.1 Sampling and analysis for an assessment of spatial pattern

We performed our sampling along transects 300 to 1334 m in length, divided into contiguous 1x1 m quadrats; the response variables used are explained in Chapters 2, 3 and 4. The transects encompassed different plant communities, e.g. forest and savanna, as well as anthropogenic linear disturbance, mostly firebreaks. This sampling is analogous to regularly sampled time series, with the difference that, whereas time series are directional, our data were not. Notwithstanding this difference, the explanation below may be applied to time series analysis, as the signal, here represented by a spatial transect, may also be represented by a time series. The use of either contiguous or regularly spaced quadrats permits the detection of patterns that exist at different scales, thus enabling a thorough assessment of the spatial variation in the response variables (Dale 1999). However, regularly spaced quadrats or other sampling schemes may give misleading results because the spacing of the quadrats may interfere with the detection of the underlying spatial pattern and because small-scale patterns may only be detected with contiguous quadrats (Dale 1999). We thus chose to use contiguous quadrats, which, among other advantages, permit the detection of patterns at all scales greater than the quadrat size. However, for the same sampling effort, regularly spaced quadrats permit to have longer transects. Thus, the choice to use contiguous or spaced quadrats must consider the tradeoff between sampling effort, transect length, and resolution. As edge influence often extends for distances of less than ten meters (Harper et al. 2005), the capacity to detect small-scale patterns was a requirement for our sampling design, and we chose to maximize resolution instead of transect length or number of transects.

Spatial pattern analysis assesses the pattern of alternating areas with high (patch) and low (gap) values of a response variable, for example the cover of a species (Dale 1999). We used wavelet analysis (Burrus et al. 1998, Dale and Mah 1998, Percival and Walden 2000), a form of spatial pattern and time series analysis that permits an assessment of both the scales and the locations of the observed patterns, whereas analyses such as the three-term local quadrat variance (3TLQV) and Fourier analysis only permit the detection of the scales of variation (Dale and Mah 1998, Keitt and Urban 2005, Dong et al. 2008). Wavelet analysis is therefore appropriate to analyze signals with multiple scales of variation, such as the one in Figure 1.1 a and b. Specifically we used scaleogram plots (a way of showing the patterns that occur at different scales, Figure 1.1 c) in Chapter 3, wavelet scale variance (Figure 1.1 d) in Chapters 3 and 4, univariate and bivariate wavelet position variance (Figure 1.1 e; Hudgins and Huang, 1996, Dale and Mah 1998, Rosenberg and Anderson, 2011) in Chapter 2, multiresolution analysis (an analysis that shows the patterns that exist at different discrete scales without the lower-scale patterns or noise, Figure 1.2 Percival and Walden 2000) in Chapter 4, and a wavelet-based measure of similarity in spatial pattern (Rouyer et al. 2008) in Chapter 4. We provide a brief general explanation of wavelets and the related analyses below.

1.3.2 General overview of wavelet analysis

Wavelet analysis has been used for pattern detection and analysis in spatial and temporal data in plant ecology, animal behavior, marine biology and other fields (Bradshaw and Spies 1992, Rouyer et al. 2008, James et al. 2010, Leise et al. 2013). This analysis may be used for data such as a time series or a spatial transect, with a response variable measured preferentially at regular (or contiguous) intervals. Response variables may be, for example, the cover of a plant species or a measure of species diversity in a quadrat for spatial data, or the activity level of an animal for temporal data. The data is usually unidimensional, but bidimensional wavelets for spatial data also exist (James et al. 2011).

A central concept in wavelet analysis is the wavelet template, a function with the shape of a small, localized wave (therefore the term “wavelet”) (figure 1.3). One characteristic of all wavelet templates is that they integrate to zero, meaning that the result of the multiplication will be equal to zero when there is no variation in the data. Thus, wavelet transforms measure the variation that exists in the response variable; however, the detected patterns depend on the wavelet template. Common templates include the Haar wavelet (a step function equal to zero throughout most of the transect that changes to 1 and then to -1 before becoming again equal to zero; Figure 1.3 a), which shows abrupt changes in the response variable, and the Mexican hat wavelet (a second-order derivative of the Gaussian distribution; Figure 1.3 b), which is symmetric and shows areas with large values (peaks) surrounded by areas with small values, and may thus be used to show the location of patches at different scales (Dale and Mah 1998).

One form of wavelet analysis is the continuous wavelet transform (CWT), a highly redundant transformation of the data that shows the adjustment of the data to a wavelet template at contiguous scales of 1, 2... *j* m, where *j* is the maximum scale of variation in the response variable examined. This is done by multiplying the signal by the wavelet template centered at the first quadrat, then at the second quadrat, and so on until the last quadrat. This shows how similar is the signal to the shape of the wavelet template at each position along the transect. The wavelet template is then expanded and this analysis is repeated for a larger scale. When all scales have been analyzed, the result shows how well the data adjust to the wavelet template at each position along the transect for different scales, thus permitting the assessment of different scales of pattern in the response variables. The redundancy comes from the fact that the transform for a given scale is not uncorrelated (i.e. not orthogonal) to the previous and next scales (Percival and Walden 2000).

The result of wavelet analysis – the wavelet transform – is a set of coefficients representing the correspondence between the data and the wavelet template at different positions along the data series (Burrus et al. 1998, Percival and Walden 2000). The wavelet transform can be arranged as a *j* x *k* matrix, with *j* as the number of different scales and *k* as the number of quadrats or positions along the data series (Burrus et al. 1998). The finest scale is the one that represents differences between adjacent quadrats. The maximum scale examined depends on the length of the data series, as at high scales the wavelet template will always extend beyond the borders of the data series, thus precluding a valid interpretation of the results; the maximum scale that may be used for the Mexican hat wavelet is 25% of the data series length (Rosenberg and Anderson 2011b). (Parts of the wavelet transform for which the wavelet template extended beyond the limits of the signal, and therefore are not easily interpretable, are often removed from the result. The result is a semicircular or triangular shape of the scaleogram, as in Figure 1.1 c).

In the wavelet transform, each finer scale provides details that are absent at a coarser scale. Thus, if the Mexican hat wavelet is used, a coarse scale may show areas with overall large or small cover of a given species, whereas a fine scale may show irregularities in the cover of this species within these areas. Alternatively, with the Haar wavelet, a large scale would show where an extensive stretch with a large cover encounters an extensive stretch with a small cover. This set of coefficients may be shown graphically as a scaleogram (figure 1.1c), which shows the scales on the Y axis, the positions along the data series on the X axis, and the value of the wavelet transform at each scale and each position as a color or grayscale map (Dale and Mah 1999, Rouyer et al. 2008).

1.3.3 Position and scale variance and covariance

The CWT may undergo further transformations, for example by calculating the variance across scales or across positions along the data series (Dale and Mah 1998). As all wavelet templates integrate to zero, the values of the CWT are a measure of the variation at a given scale in a given position. These values may be summarized as either scale or position variance (Figure 1.1 d, e). Wavelet scale variance (Figure 1.1 d) is calculated as the average of the squared CWT coefficients for each scale across all positions; the coefficients are squared because the wavelet transform coefficients may assume both positive and negative values, whereas variance is necessarily positive. The result is interpreted in the same way as a 3TLQV and a Fourier analysis, with peaks in variance indicating the predominant scales of spatial pattern or to cycles of periodicity in the case of temporal data (Dale 1999). Alternatively, instead of looking for peaks, the scale variance at all scales may be compared to 95% confidence intervals resulting from null models (see below), with the scales above the confidence intervals being considered as significant.

In turn, wavelet position variance (Figure 1.1 e) is a measure of the amount of variation at each position across all scales are considered. It is calculated by summing the squared CWT across the scales for each position and dividing them by the number of scales (Dale and Mah 1998). This analysis may be used to detect parts of the data series with abrupt changes or a large amount of variation in the spatial pattern, especially when considered alongside the original data (Figure 1.1 e).

An extension of wavelet variance that may be used to assess the relationship between two response variables is wavelet covariance (Hudgins and Huang 1996). Wavelet scale covariance is calculated by multiplying the wavelet coefficients of two response variables and calculating the average of this product across all positions for each scale (Rosenberg and Anderson 2011a), and it shows the scales at which the two response variables are positively or negatively correlated. As such, it is similar to the three-term local quadrat covariance (3TLQC; Dale 1999). Similarly, wavelet position covariance is calculated by multiplying the wavelet coefficients of two response variables and calculating their product's average across all scales for each location along the data series (Rosenberg and Anderson 2011a). Parts of the data series where both variables vary in the same direction (either both increasing or both decreasing) will therefore have positive wavelet position covariance, and parts of the data series in which one variable increases while the other decreases will have negative position covariance. Wavelet position covariance will be close to zero in more homogenous areas in which there is little variation in at least one of the response variables.

1.3.4 Discrete wavelet transform and multiresolution analysis

Another form of wavelet analysis is the discrete wavelet transform (DWT), which may also be used to perform a multi-resolution analysis and assess the spatial patterns of the response variables at different scales (Keitt and Urban 2005). Unlike the continuous wavelet transform, which is performed on continuous scales, i.e. 1, 2. … 329, 330 m (if a maximum scale of 330 m is used), the discrete wavelet transform is performed only dyadic scales, equal to powers of 2, e.g. 2, 4, 8… 256 m (Percival and Walden 2000). As few scales are analyzed, the DWT is much more computationally efficient than the CWT. In addition, the coefficients calculated from each scale are uncorrelated, thus removing the redundancy that exists in the CWT (Percival and Walden 2000). On the other hand, the fewer scales analyzed mean that the DWT is somewhat less informative than the CWT.

The DWT proceeds by dividing the original signal into a detail component, representing the variation between adjacent values, and a smooth component, representing the average value of the signal. The detail component is obtained by multiplying the signal by a wavelet function, which is the same as the wavelet template or wavelet function used in the CWT. In turn, the smooth component is calculated by multiplying the signal by a scaling function, which does not integrate to zero and is not used in the CWT (figure 1.3 c, d; Burrus et al. 1998, Percival and Walden 2000). The smooth component is then analyzed in the same way, resulting in a detail and a smooth component for the second scale of analysis. This procedure is repeated until the final scale the variation at which is analyzed, and the last coefficient, known as scaling coefficient, represents the mean values at the next larger scale (Percival and Walden 2000, Keitt and Urban 2005; figure 1.2).

Multiresolution analysis permits to perform the backward process, i.e. reconstruct the smooth signal at each scale, thus exploring the patterns at larger scales without the smaller-scale variation (Percival and Walden 2000, Keitt and Urban 2005). The smooth signal is, therefore, the reconstructed signal at each scale, without the lower-scale patterns or noise. Several wavelet templates are available for this analysis; we used Daubechie's least-asymmetrical S16 wavelet template because it is similar in shape to the Mexican hat wavelet, but is more appropriate for a discrete wavelet transform (Percival and Walden 2000).

1.3.5 Wavelet-based similarity analysis

Rouyer et al. (2008) introduced a similarity analysis based on wavelets. This analysis proceeds by first calculating wavelet transforms for each of a set of response variables and covariance matrices between pairs of wavelet transforms. These covariance matrices are then subjected to a multivariate analysis (singular value decomposition), which extracts singular vectors associated to common patterns of decreasing importance between the two wavelet transforms. By projecting each wavelet spectrum onto its corresponding singular vector, a measure showing how the frequency patterns changes in space (or in time), the leading pattern, is obtained. A measure of dissimilarity is then obtained by comparing the singular vectors and the leading patterns; identical, or parallel, vectors and patterns give a dissimilarity of zero. The dissimilarity measure recommended by Rouyer et a. (2008) is calculated by calculating the angle between each pair of corresponding segments of the two singular vectors and leading patterns. One characteristic of this analysis is that similarity is influenced by areas with greater variability, whereas areas where the response variable, e.g. the cover of a species, is homogeneous (which often represents species absence), will have little influence on the result (Rouyer et al. 2008). The dissimilarity coefficients may then be treated with analyses based on distance matrices, such as ordinations (metric and non-metric multidimensional scaling), cluster analysis, and analyses to determine the effect of external factors (e.g. lifeform) on the pattern of the wavelet transform (such as the multivariate permutational analysis of variance – PERMANOVA; Anderson 2001).

1.3.6 Null models and assessments of significance

The significance of the wavelet transform and related analyses (wavelet variance, multi-resolution analysis etc.) may be assessed by randomization or Monte Carlo tests. The simplest randomization test involves complete spatial randomness, in which the quadrats are randomly redistributed along the data series (Manly 2007). This, however, is not an ecologically meaningful model as it does not consider the autocorrelation structure of the response variables (Rouyer et al. 2008, James et al. 2010). We therefore assessed the significance of the wavelet analysis by comparing them with patterns expected under different null models that consider different aspects of the data (Table 1.1), and based our interpretation on the null models which seamed most ecologically meaningful.

We based our models on complete spatial randomness (CSR), a first-order Markov chain process (MC1), or a second-order autoregressive process (AR2). The models used may either treat the data series as homogeneous, i.e. with no differences in the spatial pattern between parts of the transect, or as composed of different sections (different plant communities in our case) with different spatial patterns. The null models were: 1) homogeneous complete spatial randomness, which assumes a stationary spatial pattern and does not consider different plant communities along the data series (CSRh); 2) complete spatial randomness that accounts for differences between different plant communities (e.g. grassland, forest, firebreaks) (CSRs); 3) a first-order Markov chain process that is also stationary along the entire data series (MC1h); 4) a first-order Markov chain process that includes linear disturbances (i.e. firebreaks and a railroad) (MC1d); 5) a first-order Markov chain process that accounts for differences between plant community types (MC1s); and 6) a second-order autoregressive process that also accounts for differences between plant community types (AR2s). We differentiate between plant communities, corresponding to continuous parts of the data series occupied by the same vegetation, and plant community types, corresponding to all areas occupied by the same type of vegetation even if they are not continuous. For example, the ecotone areas on both sides of a forest patch correspond to two plant communities but one single plant community type.

Models were generated in the following manner (pseudocodes in Supplementary Material 1.1, except for model 6):

1) CSRh: Data were reshuffled without replacement.

2) CSRs: Data were reshuffled as in CSRh but only within each plant community.

3) MC1h: We generated a transition matrix for the cover of a quadrat based on the cover of the immediately adjacent quadrats. We then assigned the value of a random quadrat to a random position along the data series and randomly assigned cover to the adjacent quadrats according to probabilities in the transition matrix corresponding to the first quadrat. This step was then repeated for each new quadrat until reaching the end of the data series in both directions using the transition matrix that corresponds to the previously assigned quadrat.

4) MC1d: This null model is similar to MC1, but the position of the firebreaks and the response variable’s pattern associated with them is included in the model. The data were

simulated as in MC1, but firebreaks were omitted from the transition matrix. Distances along the data series corresponding to the firebreaks were then replaced by random reshuffling of values only from within the corresponding firebreak.

5) MC1s: Transition matrices were generated as in MC1 but separately for each section. After simulating data for one section, a random start was chosen for the next section and the process was repeated until reaching the end of the data series.

6) AR2s: Similar to MC1s, but using autoregressive functions (predicting the value of a quadrat from the two previous quadrats) calculated separately for each section. One difficulty in using this model is that autoregressive models are directional (James et al. 2010), whereas our data were not. We therefore calculated AR2 models both ways (towards the end and towards the beginning of the data series), and used the average of the two models to create a combined AR2 model. As it was not possible to calculate AR2 functions for the narrow disturbances, data from the disturbances were randomized as in CSRs.

For each variable, we simulated 4999 datasets (Chapter 2) or 999 datasets (Chapters 3 and 4) under a subset of the null models and performed wavelet analysis on each of these datasets. We then determined wavelet position variance and covariance for the simulated datasets in the same way as for the original data. In the case of bivariate wavelets, we calculated wavelet covariance from the simulated datasets of the two variables. We used the randomized datasets to establish one-tailed 95% confidence intervals for wavelet variance and two-tailed 95% confidence intervals for wavelet covariance, scaleograms and MRA analyses; assessment of significance was computationally unfeasible for the wavelet-based similarity analysis. For the bivariate position covariance we used two-tailed confidence intervals corresponding to the 0.025 and 0.975 quantiles. Thus, for each response variable (or combination of response variables in the case of bivariate wavelets) along each data series we had five confidence intervals corresponding to the five models, each calculated from 5000 or 1000 datasets.

The results of the six null models on a simulated dataset are shown in Figures 1.4, 1.5 and 1.6. Based on these results and on theoretical considerations, we assumed that peaks in wavelet position variance that were not significant in relation to any null model can be accounted for by a random distribution of the response variable, whereas peaks significant when compared to a CSR model but not to the corresponding MC1 or AR2 model may be accounted for by small-scale autocorrelation. In the same way, patterns that were not significant in relation to the CSRs, MC1s or AR2s models were assumed to be caused by differences between adjacent sections and are not related to edges. Thus, we assumed that significant patterns located close to edges represent edge influence. Figures 1.4 and 1.5 also show that the confidence intervals may be somewhat conservative, i.e. fail to detect known edge-related patterns, which gives us more confidence that the patterns detected indeed represent ecological processes. Throughout the study, we based our conclusions on only one model in each chapter (MC1s in Chapter 2, CSRs and Chapter 3 and AR2s in Chapter 3). The results of all models except for AR2s on real datasets are shown in Supplementary Material 2.3 and 2.4. The performance of the different null models on a real dataset is also discussed in Chapter 2.

1.3.6 Software used

All analyses were performed in R 2.15.3 software (R Core Team 2013), except for the wavelet analyses in Chapter 2, which were performed on each randomized dataset in Passage 2.0 (Rosenberg & Anderson 2011b) by creating a batch file to save the output as text files. The codes used for the null models and wavelet analyses are available in Supplementary Material 2.2, 3.1 and 4.1. All wavelet analyses in R were performed with the *wmtsa* library (Constantine and Percival 2012), with the functions *wavCWT*, *wavDWT*, *wavMRD* and *reconstruct*. Code for the wavelet similarity analysis was kindly provided by T. Rouyer (Rouyer et al. 2008).

Tables

Table 1.1. Comparison among the five different null models used in this study, two of which were based on complete spatial randomness (CSR) and three on a first-order Markov chain process (MC1). In the model names, h stands for homogeneous (no differences among plant communities), s stands for sections (considers the different plant communities or sections of the data series), and d stand for disturbance (assumes the data series is homogeneous except for firebreaks and other anthropogenic disturbances).

Assumptions	CSRh	CSRs	MC1h	MC1d	MC1s	AR2s
No autocorrelation	Yes	Yes	No	No	No	No
No effect of disturbances	Yes	No	Yes	No	No	No
No differences between plant communities	Yes	No	Yes	Yes	No	No

Figures

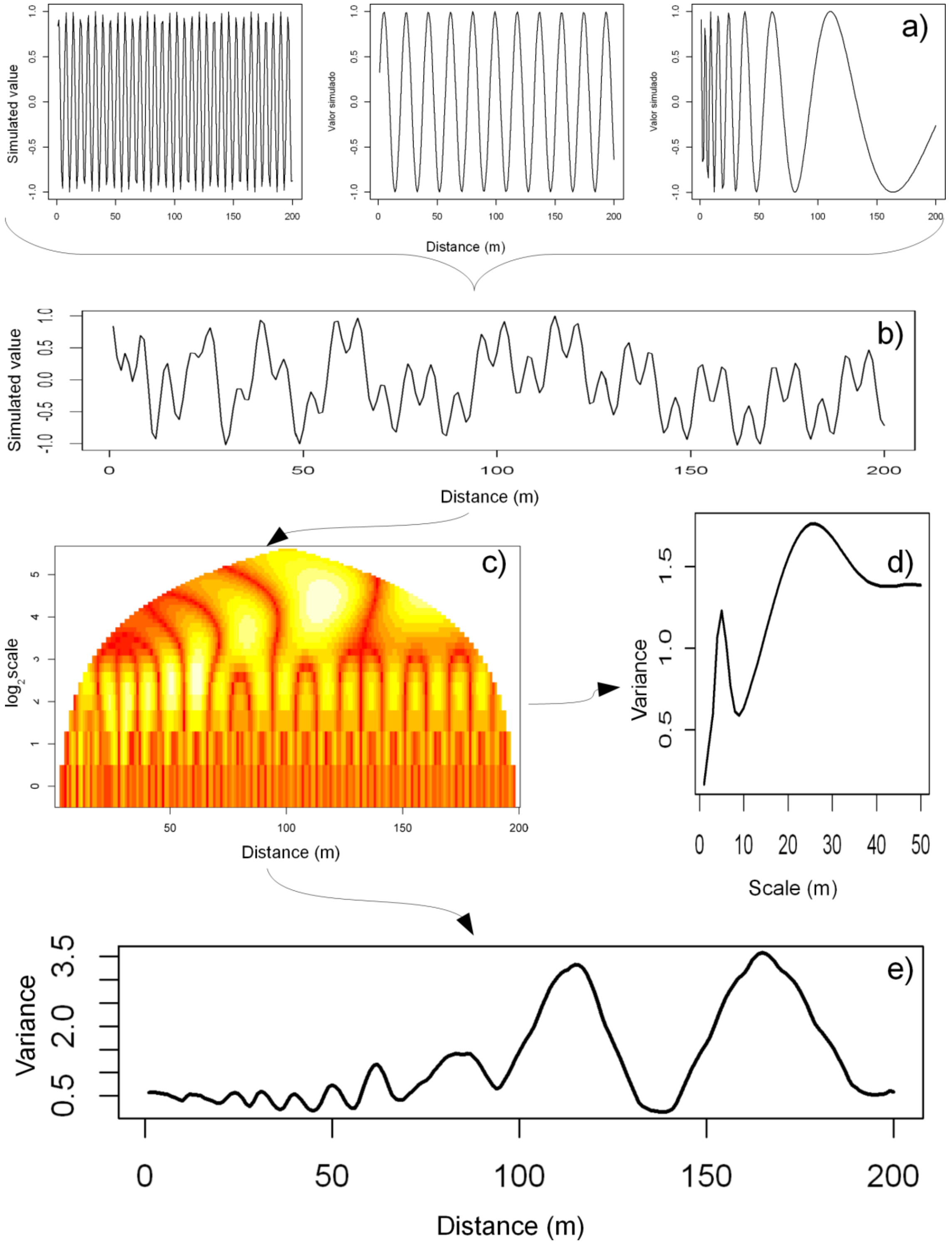

Figure 1.1 Example of two stationary and one none-stationary signals (a) composing an artificial signal (b) and results of the wavelet analysis performed on it: scaleoram (c), wavelet scale variance (d) and wavelet position variance (e). The signal was generated in R as the sum of the signals *sin(x)*, *sin(x/3)* and sin*(x/m)* where *m* is a arithmetic progression from 0.5

to 4.0.

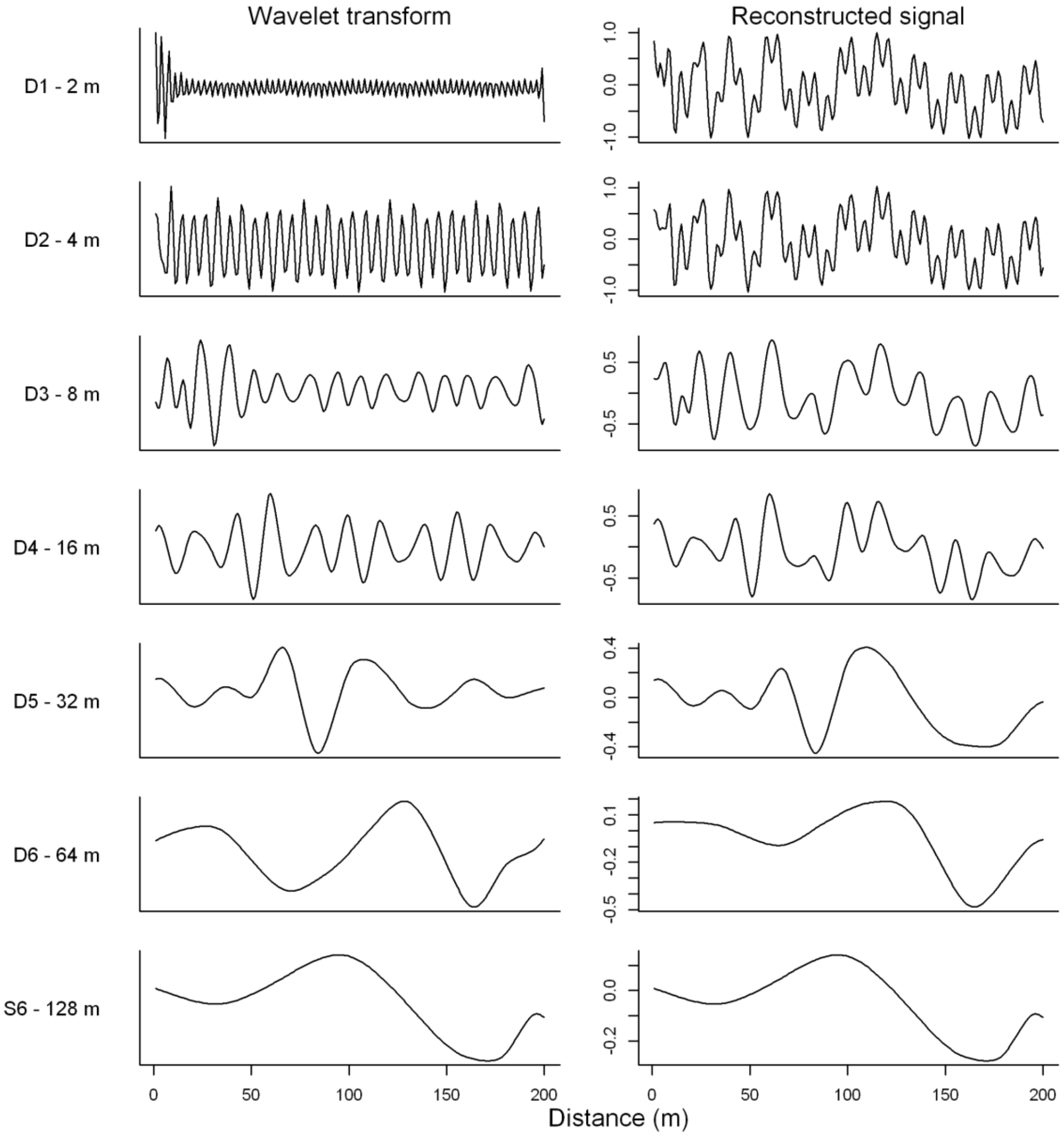

Figure 1.2 Example of a multi-resolution analysis on the same signal as in figure 1.1. The left side shows the discrete wavelet transform coefficients at each scale and the right side shows the reconstructed signal for a given scale, i.e. without the lower-scale patterns. The coefficients D1-D6 are called detail coefficients, whereas the coefficient S6 is the smooth coefficient.

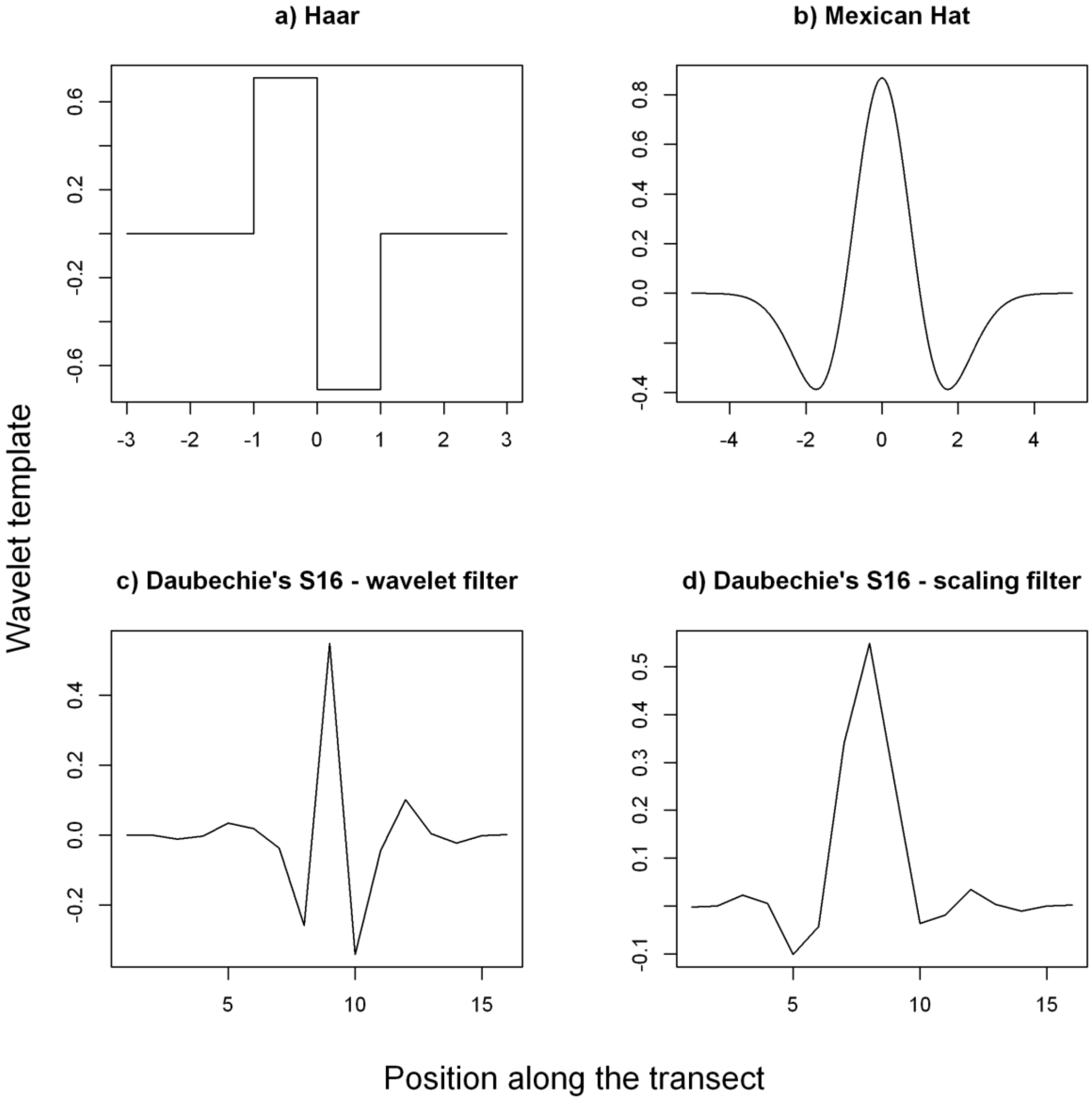

Figure 1.3 Wavelet templates (also known as wavelet functions or filters) for the a) Haar and b) Mexican Hat, and the c) wavelet and d) scaling filters for Daubechie's least asymmetrical S16 wavelet, created with the wmtsa package (Constantine and Percival 2012) in R. All wavelet. The wavelet transform shows the correspondence between the signal and the chosen template at each scale analyzed.

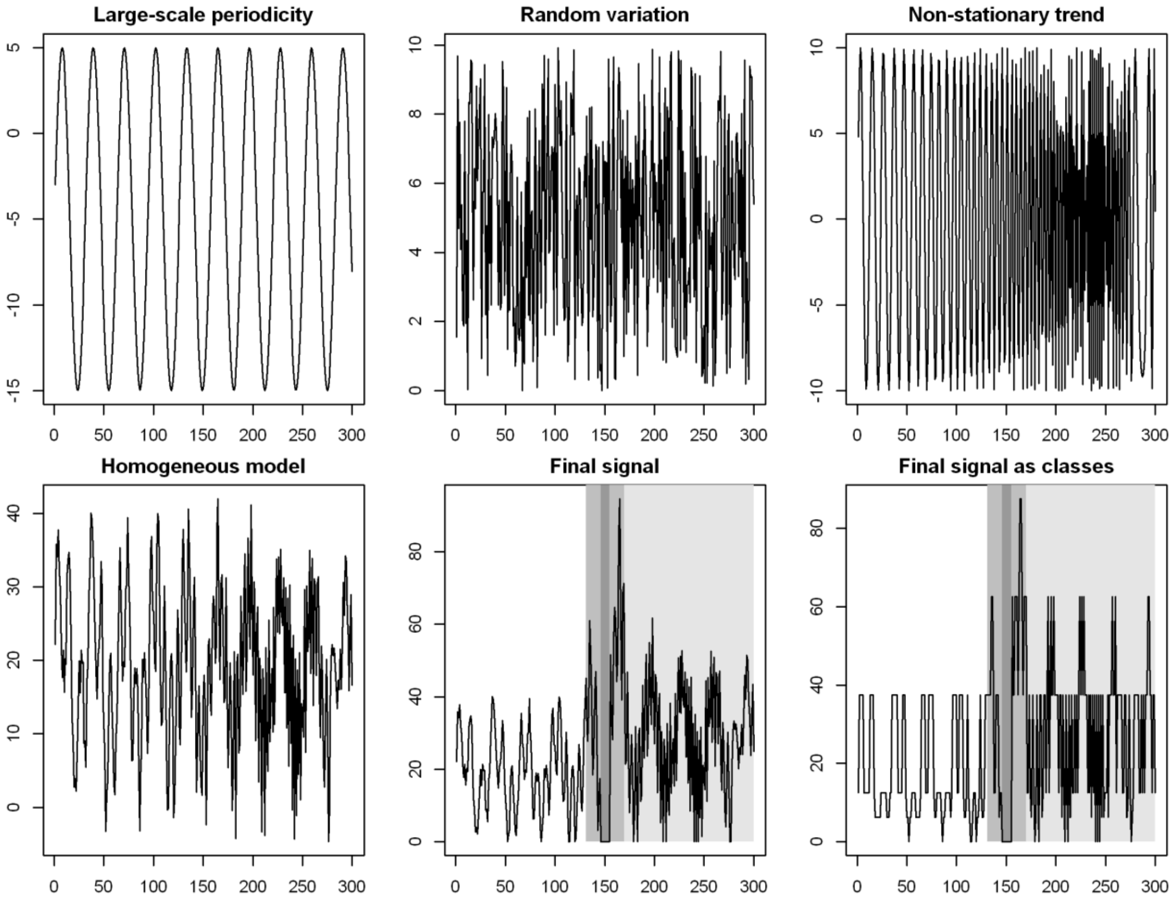

Figure 1.4 Example of an artificial signal composed by periodic variation, random variation and a non-stationary trend with the addition of a disturbance, edge influence and differences between two parts of the signal and the same signal transformed into discrete classes. The homogeneous model includes all sources of variation except for edge influence and difference between sections. White and light gray background represent parts of the signal with different mean values, medium gray represents an area subjected to edge influence, and dark gray represents a disturbance (“firebreak”) with zero values. Periodic variation was simulated as *sin(x/5)*10-5*; random variation was simulated as a uniform random variable ranging from 0 to 10; and the non-stationary trend was simulated as *sin(x/m)*, where *m* is an arithmetic progression from 2 to 0.5. The different areas were simulated by multiplying all the values in one of them by 1.5, and edge influence was simulated by multiplying the values by 1.5 once more.

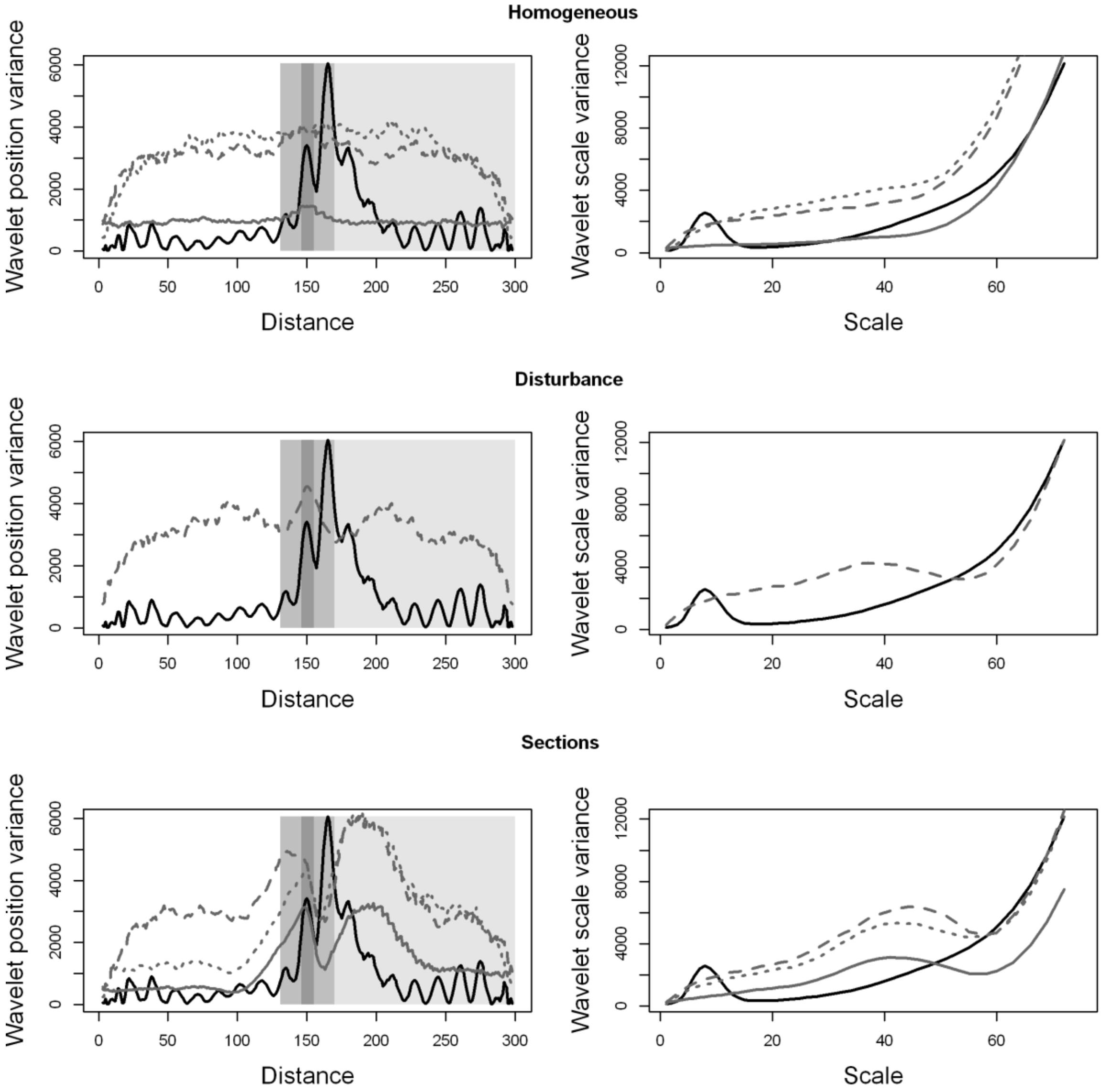

Figure 1.5. Results of the Mexican Hat wavelet analysis on the final signal of figure 1.3, with position (left) and scale (right) variance and confidence intervals for complete spatial randomness (CSR), first-order Markov chain (MC1) and second-order autoregressive (AR2) null models, for scales from 1 to 75 m. See figure 1.3 for a description of the signal and the colors. The black line represents the original wavelet position and scale variance. The gray lines represent the confidence intervals for the different null models: CSR (solid line), MC1 (dashed line) and AR2 (dotted line). The top plot shows homogeneous confidence intervals (CSRh, MC1h and AR2h models), the middle ones account for the presence of the firebreak (MC1d), and the bottom ones account for differences among the sections of the data series (CSRs, MC1s and AR2s models). Notice how peaks in position variance occur some distance from the borders between the sections (different-colored areas).

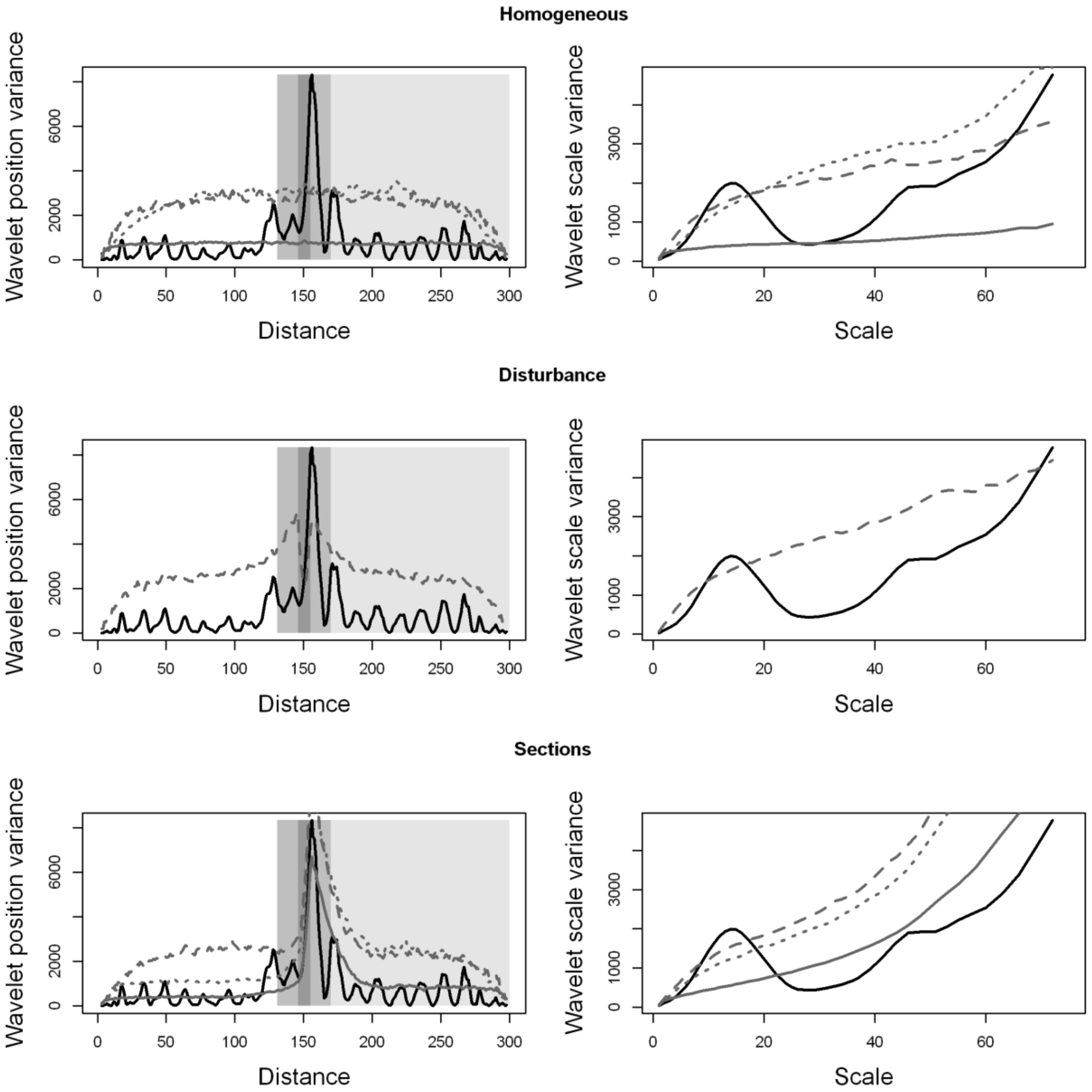

Figure 1.6. Results of wavelet analysis with the Haar wavelet on the final signal of figure 1.3, with position (left) and scale (right) variance and confidence intervals for complete spatial randomness (CSR), first-order Markov chain (MC1) and second-order autoregressive (AR2) null models, for scales from 1 to 75 m. See figures 1.3 and 1.4 for explanation of the colors and the confidence intervals. Notice how peaks in position variance are located at the transitions between sections (different-colored regions). Notice also that the confidence intervals for the Haar wavelet appear to be more conservative than for the Mexican hat wavelet.

Supplementary material description

SM 1.1-1.3: Photos of the study sites in the Federal University of São Carlos (SM 1.1 and 1.2) and the Itirapina Ecological Station (SM 1.3), all in Brazilian cerrado, São Paulo state, South-eastern Brazil.

SM 1.4-1.5: Photos of the study sites in a lichen heath tundra (SM 1.4) and an ecotone area (SM 1.5), both in the Canadian forest-tundra ecotone near the Churchill Northern Studies Centre, Manitoba, western Canada.

Chapter 2. Edge influence on the spatial pattern of native and invasive graminoids in Brazilian cerrado[1]

Resumo

A vegetação natural é espacialmente heterogênea em diversas escalas, devido tanto a processos naturais quanto a atividades antrópicas. Mudanças relacionadas a bordas na comunidade vegetal contribuem para esta heterogeneidade, enquanto que um alto grau de heterogeneidade intrínseca dificulta a detecção desta influência de borda. Um exemplo comum de influência de borda é uma maior abundância de espécies invasoras em bordas do que no interior da floresta, o que pode afetar a regeneração de espécies nativas e outros processos ecológicos. Os nossos objetivos eram: 1) verificar como diferentes tipos de bordas afetam os padrões espaciais de diferentes graminóides e 2) estudar a variação espacial na relação entre gramíneas nativas e invasoras. Nós amostramos gramíneas nativas, ciperáceas nativas e duas gramíneas invasoras (*Urochloa decumbens* e *Melinis minutiflora*) ao longo de dois transectos muito compridos (de 733 e 1334 m) em uma paisagem heterogênea no cerrado brasileiro, com cada transecto atravessando quatro a cinco distúrbios lineares estreitos, em sua maioria aceiros. Nós usamos variância e covariância de posição de *wavelets* para determinar a localização das áreas com maior variabilidade espacial e comparamos os resultados com intervalos de confiança criados a partir de modelos nulos por cadeia de Markov que levam em conta a autocorrelação de pequena escala nas variáveis-resposta e a existência de diferentes comunidades vegetais ao longo dos transectos. Os padrões espaciais das ciperáceas nativas e de *M. minutiflora* eram os mais heterogêneos, enquanto que gramíneas nativas e *U. decumbens* ocorreram de forma mais homogênea ao longo dos transectos. Os padrões próximo a bordas de aceiros não eram consistentemente diferentes dos modelos nulos, mas as áreas já dominadas por gramíneas invasoras aparentemente afetaram a vegetação adjacente. Embora as duas gramíneas invasoras via de regra estiveram negativamente correlacionadas com os graminóides nativos, correlações positivas também foram observadas, indicando que espécies nativas e exóticas podem coexistir em certas condições. Os resultados indicam que bordas de aceiro não necessariamente resultam em padrões fora da variação natural na cobertura de diferentes graminóides no cerrado brasileiro.

---

[1] Previous versions of this chapter were presented at the 8th Annual Canadian Society for Ecology and Evolution conference in Kelowna, BC, Canada, in May 2013, and at the I International Symposium of Ecology and Conservation in Belo Horizonte, MG, Brazil, in August 2014.

Chapter 2. Edge influence on the spatial pattern of native and invasive graminoids in Brazilian cerrado

Abstract

Natural vegetation is spatially heterogeneous at a variety of scales, due to natural processes and anthropogenic activities. Edge-related changes in the plant community contribute to this heterogeneity, whereas high inherent heterogeneity complicates the detection of this edge influence. One common example of edge influence is greater abundance of invasive species at edges compared to interior forest, which may affect native species regeneration and other ecological processes. Our objectives were: 1) to assess how different types of edges affect spatial patterns of different graminoids, and 2) to assess the spatial variation in the relationship between native and invasive species. We sampled native grasses, native sedges and two invasive grasses (*Urochloa decumbens* and *Melinis minutiflora*) along two very long transects (733 and 1334 m) across a heterogeneous Brazilian cerrado landscape, each transect crossing four to five narrow linear disturbances, mostly firebreaks. We used wavelet position variance and covariance to assess the location of areas with greater spatial variability and compared the results with confidence intervals created from a Markov chain null model which accounts for small-scale autocorrelation in the response variables and for the existence of different plant communities along the transects. The spatial patterns of native sedges and *M. minutiflora* were the most patchy, whereas native grasses and *U. decumbens* were distributed more homogeneously. Patterns next to firebreak edges were not consistently different from the null models, but areas already dominated by invasive grasses appeared to affect the adjacent vegetation. Although the two dominant invasive species were usually negatively correlated with native graminoids, positive correlations were also observed, possibly indicating that native and invasive species may coexist in certain conditions. The results indicate firebreak edges do not necessarily result in patterns outside the natural variation in the cover of different graminoids in the Brazilian cerrado.

2.1. Introduction

Invasive species, especially invasive grasses, may have severe negative effects on the environment by displacing native species (Almeida-Neto et al. 2010), hampering germination and growth of native seedlings (Hoffman and Haridasan 2008), modifying fire dynamics (Hoffman et al. 2012) and altering vegetation structure as a whole (Molinari and D’Antonio, 2014). Expansion patterns of invasive species may vary among species and environments. At a given site, invasive species may advance as a continuous front with short dispersal distances and high abundances in new areas of establishment, or in a more patchy or heterogeneous manner, with the establishment of new individuals at farther distances from previously occupied areas (Hengeveld 1989). The combination of different dispersal strategies with ecological processes such as competition and with natural variation in soil properties and vegetation structure may result in complex spatial patterns in the distributions of invasive species. Thus, different invasive species may have different spatial patterns, as has been observed, for example, for two invasive grasses in the Brazilian cerrado (Pivello et al. 1999a, b).

These patterns may be modified by anthropogenic edges; increased abundance of exotic species close to edges has been often observed in forest (Gieselman et al. 2013, LaPaix et al. 2012), savanna (Pivello et al. 1999a,b, Dodonov et al. 2013) and grassland (Morgan 1998, Cilliers et al. 2008) environments. In grassland and savanna areas, however, invasive grasses are also often found far from edges (Pivello et al. 1999a,b, Cilliers et al. 2008), possibly due to heterogeneous soil characteristics or to the presence of leafcutter ant mounds (Coutinho 1982). Processes such as gap-phase dynamics may also result in patterns similar to those observed at edges, with localized increases in the cover of invasive grasses that are not related to anthropogenic disturbances or edges with other land uses or vegetation types (Cilliers et al. 2008, Gray et al. 2012). This complicates the assessment of edge influence on these species, as edge influence is more difficult to detect in heterogeneous environments (Harper et al. 2005a). Therefore, it is important to account for patterns of natural environmental heterogeneity when studying effects of anthropogenic edges on vegetation.

We used a spatial pattern approach to assess the effects of firebreak edges on the distribution of native and invasive graminoids in the Brazilian cerrado, a highly heterogeneous vegetation type with grassland, savanna and forest phytophysiognomies, making it a good study model. Although firebreaks are important for avoiding catastrophic fires in protected savanna areas, these linear disturbances may lead to changes in vegetation structure (Smit and Asner 2012), and possibly favor the dispersal and establishment of invasive species. Our main objectives in this study were: 1) to assess whether the spatial patterns of invasive and native graminoids are affected by firebreak edges, and 2) to assess whether firebreak edges increase the negative effects of invasive graminoids on native ones. We also present different null models that may be used to assess wavelet significance, and discuss their appropriateness for this type of study.

2.2. Methods

2.2.1 Study sites and species

We conducted this study in two areas dominated by cerrado vegetation in São Paulo state, southeastern Brazil: a cerrado area in the Federal University of São Carlos (21°58'34"S, 47°52'31"W; Supplementary Material 1.1) and the Itirapina Ecological Station (22°14'46"S, 47°52'39"W; Supplementary Material 1.3) (Figure 2.1)[2]. Cerrado vegetation encompasses a wide range of vegetation types with a large variation in vegetation structure ranging from open fields to forests with a continuous canopy layer (Coutinho 1978, Ribeiro and Walter 2008). These areas are often interspersed with riparian or gallery forests along rivers. The cerrado phytophysiognomies in these sites include savanna of typical cerrado and more open savannas known as *campo cerrado* and *campo sujo*, as well as *campo limpo* grassland (Ribeiro and Walter, 2008). Graminoids, which were the focus of our study, may account for over 90% of the biomass in the *campo limpo* and *campo sujo* phytophyisiognomies but for about 30% of the biomass in *campo cerrado* and typical *cerrado* (Kauffman et al. 1994).

The area in São Carlos is mostly composed of typical cerrado with some degraded *campo sujo* areas dominated by the African grass *Urochloa decumbens.* Some parts of this area were used as eucalypt plantations until the 1990s, after which the cerrado regenerated naturally. The cerrado of Itirapina is occupied by more open vegetation, mostly *campo sujo*, but also has grassland areas invaded by *U. decumbens*. Both areas contain corridors of riparian vegetation, but only the one in Itirapina was sampled. The predominant soils are dystrophic oxisols in São Carlos (Dantas and Batalha 2011) and oxisols and entisols in Itirapina (Reis and Zanchetta 2006). The climate is humid subtropical in both areas, with a yearly precipitation of around 1400 mm and an average yearly temperature of around 22ºC (Oliveira and Batalha 2005, Reis and Zanchetta 2006).

We explored the overall cover of native grasses (Poaceae) and sedges (Cyperaceae) and of invasive grasses. Two invasive grasses were dominant in our study areas, the signal grass, *Urochloa decumbens*, and the molasses grass, *Melinis minutiflora*. Both are considered serious threats to the *cerrado* vegetation, but have different spatial patterns. *U. decumbens*

---

[2] The transect in Itirapina was also sampled for structural diversity (Chapter 3), and the transect in São Carlos was also sampled for species composition (Chapter 4).

usually form a continuous cover, whereas *M. minutiflora* tends to have a patchy distribution (Pivello et al. 1999b). Both are C4 grasses native to Africa (Klink and Joly, 1989). *M. minutiflora* has been shown to negatively affect native species by hindering seedling growth and altering the fire regime (Hoffman and Haridasan 2008, Hoffman et al. 2012).

We did not differentiate between native grasses and exotic non-invasive grasses (e.g. *Melinis repens*) because these latter exotic grasses occur with low frequencies and are not considered a conservation threat in the *cerrado* (R. O. Xavier, pers. comm.). We did not differentiate between species of native grasses due to difficulties in identifying some of the species without reproductive organs and because our main focus was on the distribution of invasive grasses and their overall effects on all native grasses. However, according to other studies performed in our study sites, native grasses include *Andropogon bicornis, A. leucostachyus, Schizachyrium condensatum*, and other species of the genera *Andropogon*, *Aristida*, *Axonopus*, *Chloris, Digitaria*, *Panicum*, *Paspalum* and *Tristachya*. Sedges include species of the genera *Bulbostylis, Fimbristylis*, *Rhynchospora* and *Cyperus* (Urbanetz et al. 2013; R. O Xavier, unpublished data; P. Dodonov, unpublished data). Both the grasses and sedges include C3 and C4 species (Klink and Joly 1989, Sage et al. 2011).

2.2.2 Sampling design

We sampled graminoids along a 1334 m-long transect in São Carlos and a 733 m-long transect in Itirapina. The transects spanned respectively four and five narrow 5-20 m wide firebreaks and sections of vegetation with different characteristics and phytophysiognomies including *campo sujo* grassland, typical *cerrado*, riparian forest and degraded areas (Table 1). We differentiated between recently created or frequently used firebreaks (e.g. vehicle use), which had almost bare soil, and regenerating firebreaks, which were found only in Itirapina and were characterized by low frequency of disturbance and a scarce plant cover.

We divided each transect into 1x1 m contiguous quadrats; we used contiguous quadrats because regularly spaced quadrats or other sampling schemes may not show small-scale patterns or give misleading results because the spacing of the quadrats may interfere with the detection of the underlying spatial pattern (Dale 1999). Within each quadrat, we visually estimated the cover of the two species of invasive grasses, and the total cover of native grasses and sedges, using six cover classes: 0, 0 - 0.125, 0.125 - 0.25, 0.25 - 0.50, 0.50 - 0.75, and 0.75 - 1.00. The mid-points of each class (0, 0.0625, 0.1875, 0.375, 0.625, and 0.875) were used in the analyses.

2.2.3 Data analysis

We used continuous wavelet transforms, with the Haar wavelet and a maximum scale of 170 m, corresponding to 12 to 23% of the transect length. We used this scale because edge influence seldom extends to greater distances (Harper et al. 2005a).To assess the spatial variation of native and invasive graminoids along each transect, we calculated wavelet position variance by summing the squared wavelet coefficients across the scales for each position, and dividing them by the number of scales (Dale and Mah 1998, Percival and Walden 2000). For each position along the transect, wavelet position variance indicates the total amount of variation at different scales, and may be used to detect changes in the spatial pattern along the transect, especially when considered alongside the original data. We also used bivariate wavelet position covariance (Hudgins and Huang 1996) to assess the relationship between the native and invasive graminoids. Wavelet position covariance will be close to zero in more homogenous areas in which there is little variation in one or both response variables and in areas in which the two variables vary independently. These analyses are explained in section in Chapter 1.3.

We used 95% confidence intervals for five null models, each with 4999 simulations, to assess significance of the wavelet position variance and covariance: 1) homogeneous complete spatial randomness, which assumes a stationary spatial pattern along the transect and does not consider the different plant communities along the transects (CSRh); 2) complete spatial randomness that accounts for differences between different plant communities (e.g. grassland, forest, firebreaks) (CSRs); 3) a first-order Markov chain process that is also stationary along the entire transect (MC1h); 4) a first-order Markov chain process that includes disturbance created by linear disturbances (i.e. firebreaks and a railroad) (MC1d); and 5) a first-order Markov chain process that accounts for differences between the plant community types (MC1s). We differentiate between plant communities, corresponding to continuous parts of the transect occupied by the same vegetation, and plant community types, corresponding to all areas occupied by the same type of vegetation even if they are not continuous. We used one-tailed confidence intervals for wavelet position variance and two-tailed confidence intervals for wavelet position covariance. Details on the models are presented in Chapter 1 and pseudocodes in Supplementary Material 2.1.

We used R 2.1.5.3 (R Core Team 2013) to create the randomized datasets for each variable (R codes in Supplementary Material SM 2.2). We then analyzed these datasets in Passage 2.0 (Rosenberg & Anderson 2011b) by creating a batch file to perform the wavelet analysis on each randomized dataset and save the output as text files. Afterwards, we imported the text files into R 2.15.3 to calculate the bivariate wavelets and 95% confidence intervals.

2.3. Results

Abundance of different graminoids varied between the two sites and among different sections of the transect (Table 2). In São Carlos, native sedges were absent from the invaded grassland and firebreaks, and the invasive grass *M. minutiflora* was also absent from the firebreaks. In Itirapina, native sedges were absent from the railroad, *U. decumbens* was absent from the ecotones and was found in a single quadrat in the forest, and *M. minutiflora* was absent from forest, ecotone, firebreaks (both maintained and regenerating), and the railroad. Apart from this, all graminoids were found throughout both transects. Of the different categories of graminoids, native grasses were usually the most frequent and had the greatest cover, except in invaded grasslands.

2.3.1 Confidence intervals for the five null models

There were large differences among the five confidence intervals obtained for each variable (Supplementary Material 2.3, Figure A1). The MC1 confidence intervals were consistently higher than the CSR ones of the same type (MC1h compared to CSRh, MC1s to CSRs), and there were fewer significant changes in cover when the MC1 intervals were used. Therefore, part of the spatial variability in the data may be attributed to small-scale autocorrelation (i.e. changes in cover indicated by peaks in wavelet position variance that were significant compared to the CSR intervals but not the MC1 intervals). In addition, confidence intervals for the models which consider differences in cover between sections or vegetation types (CSRs and MC1s) were quite different from the others, showing the importance of among-section variability for the spatial patterns. The MC1d confidence intervals were similar to the MC1h ones, except in firebreaks and their immediate vicinity.

The MC1d intervals were usually narrower within the firebreaks, reflecting the low variation in cover in these areas, but were often wider next to them, probably due to differences between the firebreaks and the rest of the transect.

Interestingly, the CSRh and MC1h confidence intervals were usually (but not always – Supplementary Material 2.3, Figure A1 b, i) higher than the CSRs and MC1s confidence intervals, respectively, except close to transitions between sections, and some peaks in wavelet variance were only significant when differences between sections were considered (Supplementary material 2.3, Figure A1 a, b, g, h). For example, for native sedges in Itirapina, only some of the changes were significant when compared to the MC1h and MC1d models (Supplementary material 2.3, Figure A1 a). When differences among plant communities were taken into account, more changes in cover were significant except close to ecotones (Figure 3a).

This was especially noticeable for the bivariate wavelets (Supplementary Material 2.3, Figure A2), in which the MC1h and MC1d confidence intervals were almost always either above or slightly below the MC1s ones, as were the CSRh intervals in relation to the CSRs ones. The only exceptions were at the borders between some sections, where the MC1s and CSRs confidence intervals were sometimes much wider than the others.

2.3.2 Spatial patterns of different graminoids

Since we consider Markov chain confidence intervals that take into account differences between sections as the most meaningful, we focus our results on trends in wavelet variance as compared with the MC1s confidence intervals.

The distribution of sedges was especially patchy, with a lot of empty quadrats and large variation in cover (Figure 2a, b). There were many changes in cover along both the Itirapina and the São Carlos transects, both near and far from firebreak edges and from edges between different vegetation types (Figure 3a, b). The greatest variation in sedge cover was observed in regenerating cerrado in São Carlos, whereas sedge distribution in Itirapina appeared to be equally variable throughout the transect. It is worth noting the great variation in sedge cover at the ecotone in Itirapina, with some highly significant patterns. In one of the ecotones, the peak in wavelet position variance for sedges was the same height as the peak observed in the null model, but these two peaks were located at different parts of the ecotone. This shift probably indicates that the greatest change in sedge cover is not located directly at the border between the forest and the ecotone, but is instead closer to the center of the ecotone.

Native grasses were more homogeneously distributed throughout the transects, although their cover varied widely among sections (Figure 2c, d). For example, they were nearly absent from the invaded grassland, which was dominated by *U. decumbens*, and from the riparian forest in Itirapina. Even though there were some significant changes in the *campo sujo*, typical cerrado and ecotone areas, changes in grass cover were much less conspicuous than those for sedges (Figure 3c, d). Few of the changes observed in Itirapina were significant, indicating that small-scale autocorrelation may account for a large part of the variation in the distribution of native grasses. In São Carlos, however, the null model accounted for a much smaller proportion of the peaks except at the *Urochloa*-dominated grassland, where almost all the variation in native grasses was within the confidence interval. Most significant patterns were between edges and the centers of the sections in Itirapina and close to the centers of the sections in São Carlos, and there were no significant patterns close to the firebreak edges. Similar to sedges, there was also a large variation in cover between the forest and ecotone areas in Itirapina, but this variation was significant in only one of the two ecotones. The shift in the peak observed for sedges at an ecotone in Itirapina was also observed at the same ecotone for native grasses.

Invasive grasses also varied widely among sections, especially in Itirapina (Figure 2e, f). In Itirapina, they were dominant in the highly invaded area and were also found, albeit with a much lower frequency, in one *campo sujo* area, but were absent from ecotone and forest areas and from the other *campo sujo*. Conversely, they were found with reasonably high cover throughout the transect in São Carlos, although they were more abundant in a highly invaded area and close to a firebreak edge. Much of the variation in invasive grasses may be accounted for by the null model (Figure 3e, f), especially in Itirapina. The greatest variation, as indicated by peaks in position variance, was observed in areas with the highest cover. There were significant or marginally significant peaks in invasive grass cover in relation to all null models close to one firebreak in Itirapina and two firebreaks in São Carlos. In São Carlos, however, there were also some significant changes in the center of the regenerating cerrado area.

When the two invasive species were considered separately, there were marked differences in their patterns. *U. decumbens* was the dominant invasive grass in Itirapina, but not in São Carlos (Figure 2g,-j; Table 2). Thus, the spatial pattern of *U. decumbens* was essentially the same as for the total invasive grasses in Itirapina (Figure 3e, g). In São Carlos, *U. decumbens* was concentrated mostly at the ends of the transect close to highly invaded areas where its spatial pattern was highly variable (Figure 2h), with several significant changes (Figure 3h). It was much less common along the rest of the transect, where most of its variation in cover could be explained by spatial autocorrelation. *M. minutiflora* occurred in only some parts of the *campo sujo* areas in Itirapina but was found throughout the entire transect in São Carlos (Figure 2i, j; Table 2). In both areas its pattern was quite patchy, with highly significant peaks in relation to all null models (Figure 3i, j). Abrupt changes in the cover of *M. minutiflora* were observed in different parts of the transect, usually at intermediate distances from firebreak edges regardless of vegetation type. In São Carlos its pattern was quite similar to that of the combined invasive grasses.

2.3.3 Bivariate relationships between graminoids

Both positive and negative significant relationships were observed in relation to the confidence intervals, but negative ones were slightly more common (Figure 4). One exception is the relationship between native sedges and *M. minutiflora* in Itirapina, which had conspicuous positive correlations in the invaded grassland and the campo sujo (Figure 4c). Positive peaks in wavelet covariance, indicating positive correlation, were often, but not always, observed close to the negative ones. The greatest heterogeneity in bivariate correlations was observed in invaded grassland and campo sujo in Itirapina and in regenerating cerrado in São Carlos (e.g. Figure 4a, g, j). As in the univariate analyses, relationships involving native sedges were more heterogeneous with greater peaks in wavelet covariance than those with native grasses.

Few edge-related patterns were observed for wavelet covariance. In Itirapina, there was a highly significant negative relationship between native sedges and both total invasive grasses and *U. decumbens* next to the firebreak between the invaded area and the campo sujo (Figure 4a, b), with a marginally significant positive correlation next to it. A negative relationship was observed at the same firebreak between native grasses and both total invasive grasses and *U. decumbens* (Figure 4d, e). This negative correlation, however, was above the upper confidence interval for both models. Therefore, when the differences in the cover of different graminoids between the plant communities were taken into account, the null models predicted a less negative correlation between native and invasive species than the one observed. This is likely due to a greater cover of *U. decumbens* than would be expected under the null model immediately after the firebreak combined with a reasonably large cover of native grasses. In São Carlos, significant or marginally significant correlations, mostly negative, were observed between native grasses and sedges and all groups of invasive grasses close to the invaded area at the end of the transect (Figure 4g-l).

2.4. Discussion

Both study sites had a substantial cover of invasive graminoids at edges and throughout the transect. Thus, as has been previously observed elsewhere (Pivello et al. 1999a, b), invasive species are not restricted to edges at our study sites, and their distribution may be governed by other processes, such as gap-phase dynamics (Cilliers et al. 2008) and variation in vegetation structure and/or soil properties. Still, many of the observed patterns did not deviate significantly from the null models, indicating that small-distance dispersal and random variation may account for a large part of the variation in the distribution of both native and invasive species. In addition, when edge-related patterns were observed, similar patterns were usually also observed far from edges. Thus, patterns observed at edges, such as an increased abundance in invasive grasses, were not exclusive of the edge environment.

2.4.1 Null models and confidence intervals

The randomization and Monte Carlo simulation tests we used to assess the significance of the observed patterns have two main advantages: they do not assume that the data follow a normal or other pre-defined distribution, and they allow different null hypotheses to be tested (Manly 2007). However, the validity of these tests depends on the null model being tested, as an ecologically unreasonable null model will lead to unreliable confidence intervals (Manly 2007). As we used five different null models to simulate the data, we were able to assess the differences between the different confidence intervals and to select the most ecologically meaningful ones. The use of different null models also enabled us to infer the processes that may have caused the observed patterns, in an approach similar to the one advocated by McIntire and Fajardo (2009).

Comparing fully random (CSR) and Markov chain (MC1) null models enabled us to assess the importance of small-scale autocorrelation in determining ecological patterns. Whereas CSR models represent a fully random distribution, which is unlikely in an ecological system, the Markov chain models may be related to ecological processes such as dispersal and intraspecific competition (James et al. 2010). In our study, we assumed that the

MC1 models represent short-distance dispersal (neighborhood diffusion, Hengeveld 1989) through both vegetative and sexual reproduction. Deviations from the MC1 models may represent the establishment of invasive species at new sites through long distance dispersal, as observed especially for *M. minutiflora* at both sites and, less conspicuously, for *U. decumbens* in São Carlos.

Both short- and long-distance dispersal and consequent establishment also depend on site characteristics such as soil, microclimate, vegetation structure and anthropogenic disturbance (Honnay et al. 2002). We found noticeable differences in the cover and frequency of some graminoid groups between different sections of the transects. The confidence intervals that considered these differences between sections, namely CSRs and MC1s, were markedly different from the homogeneous ones, especially for the bivariate relationships between different graminoids, for which the homogeneous confidence intervals were either wider or slightly narrower. This is probably due to the existence of sections where one or both of the response variables were nearly absent, resulting in very low wavelet covariance values for the MC1s and CSRs confidence intervals. Conversely, the MC1d model, which only incorporates anthropogenic disturbances, was quite similar to the MC1h one and does not reflect the larger-scale variation in cover among the plant communities. Thus, as full randomization is not ecologically likely, we based most of our conclusions on the Markov chain confidence intervals that consider differences between the plant communities.

To our knowledge, this is the first study that incorporates prior knowledge on the difference in vegetation structure and land use in the calculation of wavelet confidence intervals. However, studies that use wavelet position variance usually seek to identify boundaries and compare their location with boundaries between different land uses or boundaries identified with other techniques (Brosofske et al. 1999, James et al. 2010). Our objectives, however, were to assess the influence of these previously known edges on the spatial pattern of different grasses.

2.4.2 Spatial pattern of native and invasive graminoids

Despite substantial variation, there were some consistent patterns of native and invasive grasses. For example, native sedges were very patchy at both sites, whereas the cover of native grasses was more homogeneous, with less conspicuous changes in cover along the transects. Different patterns were also observed for the two invasive grasses, with *M. minutiflora* having a much patchier distribution than *U. decumbens*. This result agrees with previous observations that whereas *U. decumbens* tends to form a continuous cover over an area, *M. minutiflora* usually occurs in scattered patches (Pivello et al. 1999b). The combined invasive grasses followed the pattern of the dominant species – usually *U. decumbens* in Itirapina and *M. minutiflora* in São Carlos.

Part of the variation in cover of the different graminoids may be accounted for by the different plant communities and linear disturbances along the transects. For example, contrary to the invasive species, native sedges and grasses showed significant or marginally significant patterns at the ecotone areas in Itirapina, possibly reflecting spatial variation in soil and light. The near absence of the invasive grasses from the forest may be due to their reduced growth in shaded environments (Klink and Joly 1989), which probably also applies to most of the native grasses and sedges found in our study sites, as both grasses and sedges contained at least some C4 species. The absence of invasive grasses from the ecotone areas in Itirapina, which were not shaded, was probably due to the waterlogged soil, to which these species are not well adapted (Dias-Filho and Carvalho 2000); however, *M. minutiflora* has been observed to grow in a wet field in Itirapina (R. O. Xavier, unpublished data).

Effects of firebreaks on adjacent vegetation appear to be minimal, as there were no consistent patterns of conspicuous changes in cover close to firebreaks. This may seem surprising, as other studies have detected changes in vegetation next to forest roads, trails and firebreaks, in temperate forests and tropical savanna (Avon et al. 2010, LaPaix et al. 2012, Smit and Asner 2012). Roads and other linear corridors are known to facilitate the dispersal of invasive species (Gelbard and Belnap 2003, Penone et al. 2012). Expansion of invasive grasses, especially *U. decumbens*, seems to take place mostly close to areas already dominated by it rather than at firebreak edges; changes in invasive grass cover were more conspicuous next to the invaded areas. This expansion may have been favored by changes in vegetation structure, which may take place close to edges in the cerrado and other savanna areas (Lima-Ribeiro 2008, Smit and Asner 2012, Dodonov et al. 2013), and was probably due to greater propagule pressure. Vegetative expansion is not a likely reason as it would be precluded by the firebreaks, acting as a physical barrier, between the invaded area and the adjacent vegetation.

The relationship between invasive and native graminoids also varied along the transects, as shown by the existence of both positive and negative wavelet covariance. Negative covariance may indicate displacement of native species by the invasive ones, which would agree with other studies on the effects of invasive grasses on different groups of plants in the cerrado (Hoffman and Haridasan 2008, Almeida-Neto et al. 2010). The negative effects on native grasses were especially conspicuous and could be seen throughout both transects, without a clear relationship with edges or other landscape features. Less conspicuous effects on sedges were probably due to their naturally patchy distribution, hampering the detection of significant correlations with the spatial pattern of invasive grasses.

Positive covariance indicates the opposite pattern, i.e. areas in which an increase in the cover of invasive grasses coincides with an increase in the native ones. Although negative covariance probably represents negative effects of the invasive species on the native ones, the opposite is not necessarily true. With the exception of some species adapted to waterlogged soil or to the deep shade of the riparian forest, native grasses and sedges found in our study sites are typical of open savanna and grassland environments (Klink and Joly, 1989) and therefore have similar ecological requirements to the invasive grasses, which are native to African savannas. Thus, positive covariance is probably a result of the physical environment and/or vegetation structure, with some sections offering good conditions for both invasive and native species, as we observed in parts of the regenerating *cerrado* in São Carlos and of the *campo sujo* in Itirapina.

The existence of both positive and negative covariance may indicate the existence of different stable states (*sensu* Petraitis 2013), with invasive graminoids dominating the community in some but not all cases, has been previously suggested for the invasive bracken fern (Miatto et al. 2011). The coexistence between invasive and native species would be more likely in areas that have been less impacted by human activities or that are undergoing regeneration. This balance could also be altered by disturbance, such as an increase in the frequency and/or intensity of fires, leading to a different stable stage (Petraitis 2013), with an increased dominance of the invasive grasses and displacement of the native ones. As firebreaks decrease the probability of large-scale disturbances, they may also hamper the spread of invasive grasses. Thus, at our study sites, the possible edge influence from firebreaks appears to be outweighed by the disturbance control enabled by them.

2.5. Conclusions

Edge-related changes in cover were apparent only for the invasive signal grass, *U. decumbens*, and only next to areas already dominated by it. The lack of conspicuous edge influence on native sedges and the invasive molasses grass, *M. minutiflora*, is likely associated with their patchiness. The lack of edge influence on native grasses, which are more homogeneous, probably indicates that they have not yet been displaced by the invasive species or, alternatively, have been homogeneously displaced in areas where the invasive species dominate. This is corroborated by the existence of both positive and negative relationships between native and invasive species throughout our transects, which show that although displacement may occur, it has not yet occurred along the entire length of the transects. However, the more common and conspicuous nature of negative relationships indicates that the invasive species have already altered the spatial pattern of the native ones. This influence is not restricted to edges, but may be seen throughout the study sites, as do peaks in cover of the two invasive grasses. Thus, firebreak edges do not appear to significantly increase the cover of invasive species in the Brazilian cerrado when considering the natural variation in vegetation.

Acknowledgments

We thank the many people who helped us in the field, especially Cinthya C. Santos, Viviane C. Pereira and Carolline Z. Fieker. We also thank Marco A. Batalha, Milton C. Ribeiro and Hugo M. Sarmento for suggestions to a previous version of this manuscript. PD was financed by the Brazilian National Council for Scientific and Technological Development (CNPq grant 141623/2011-0) and the Emerging Leaders in the Americas Program (ELAP), of the Canadian Department of Foreign Affairs and International Trade.

Supplementary material description

SM 2.1: Pseudocodes for the generation of the five null models used.

SM 2.2: R code used for the generation of the five null models.

SM 2.3: Confidence intervals for the five null models in the univariate and bivariate analyses.

Tables

Table 1. Different plant communities along the two study transects in São Carlos and Itirapina.

São Carlos			Itirapina		
Section	Plant community[1]	Starting distance (m)	Section	Plant community[1]	Starting distance (m)
1	Invaded grassland	1	1	Railroad	1
2	Firebreak	33	2	Invaded grassland	13
3	Invaded grassland	36	3	Firebreak	120
4	Firebreak	105	4	Regenerating firebreak	122
5	Typical cerrado	109	5	Campo sujo	133
6	Firebreak	332	6	Regenerating firebreak	420
7	Regenerating cerrado	337	7	Ecotone	432

8	Firebreak	546	8	Forest	463
9	Regenerating cerrado	550	9	Ecotone	598
10	Firebreak	1329	10	Campo sujo	629
			11	Firebreak	669

[1] Invaded grassland: grassland with sparse trees and shrubs, and largely dominated by the invasive grass *Urochloa decumbens*; firebreak: a dirt road with almost no vegetation; typical cerrado: savanna vegetation with an open canopy, and both woody and herbaceous strata; regenerating cerrado: an area of cerrado previously occupied by a Eucalypt plantation with some remaining eucalypt trees; railroad: a railroad on the border of the Itirapina study site; regenerating firebreak: a firebreak with herbaceous plant cover due to lack of maintenance; campo sujo: grassland area with native grasses, and sparse shrubs and trees; ecotone: transition area between campo sujo and forest with a partially waterlogged soil; forest: a riparian forest around a narrow (1-2 m wide) stream.

Table 3. Mean cover and frequency (Freq.) of native sedges, native grasses, invasive grasses, and two invasive grass species in the different vegetation and land use types along our two transects. Mean cover considered only quadrats with a cover greater than zero, and frequency was calculated by dividing the number of quadrats with cover greater than zero by the total number of quadrats in the corresponding vegetation type. Vegetation or land use types are organized in order of increasing disturbance or decreasing tree cover (see Table 1 for additional information on land use types).

Plant community type	Native sedges		Native grasses		Invasive grasses		*U. decumbens*		*M. minutiflora*	
	Cover	Freq.	Cover	Freq.	Cover	Freq.	Cover	Freq.	Cover	Freq.
São Carlos										
Typical cerrado	0.10	0.04	0.17	0.64	0.32	0.69	0.24	0.23	0.31	0.57
Regenerating cerrado	0.11	0.21	0.23	0.78	0.29	0.49	0.23	0.13	0.28	0.42
Invaded grassland	N/A[1]	0.00	0.42	0.54	0.61	0.95	0.52	0.77	0.41	0.59
Firebreak	N/A	0.00	0.06	0.09	0.06	0.14	0.06	0.14	N/A	0.00

Itirapina										
Forest	0.09	0.16	0.09	0.07	0.06	0.01	0.06	0.01	N/A	0.00
Ecotone	0.33	0.35	0.51	0.87	N/A	0.00	N/A	0.00	N/A	0.00
Campo sujo	0.16	0.16	0.41	0.85	0.25	0.13	0.28	0.08	0.18	0.04
Invaded grassland	0.23	0.09	0.09	0.25	0.60	0.99	0.61	0.97	0.06	0.05
Regenerating firebreak	0.07	0.52	0.11	0.52	0.13	0.39	0.13	0.39	N/A	0.00
Firebreak	0.06	0.13	0.59	0.88	0.06	0.13	0.06	0.13	N/A	0.00
Railroad	N/A	0.00	0.63	0.08	0.41	0.42	0.41	0.42	N/A	0.00

[1] N/A: average cover could not be calculated because there were no quadrats with this plant group in this plant community type.

Figures

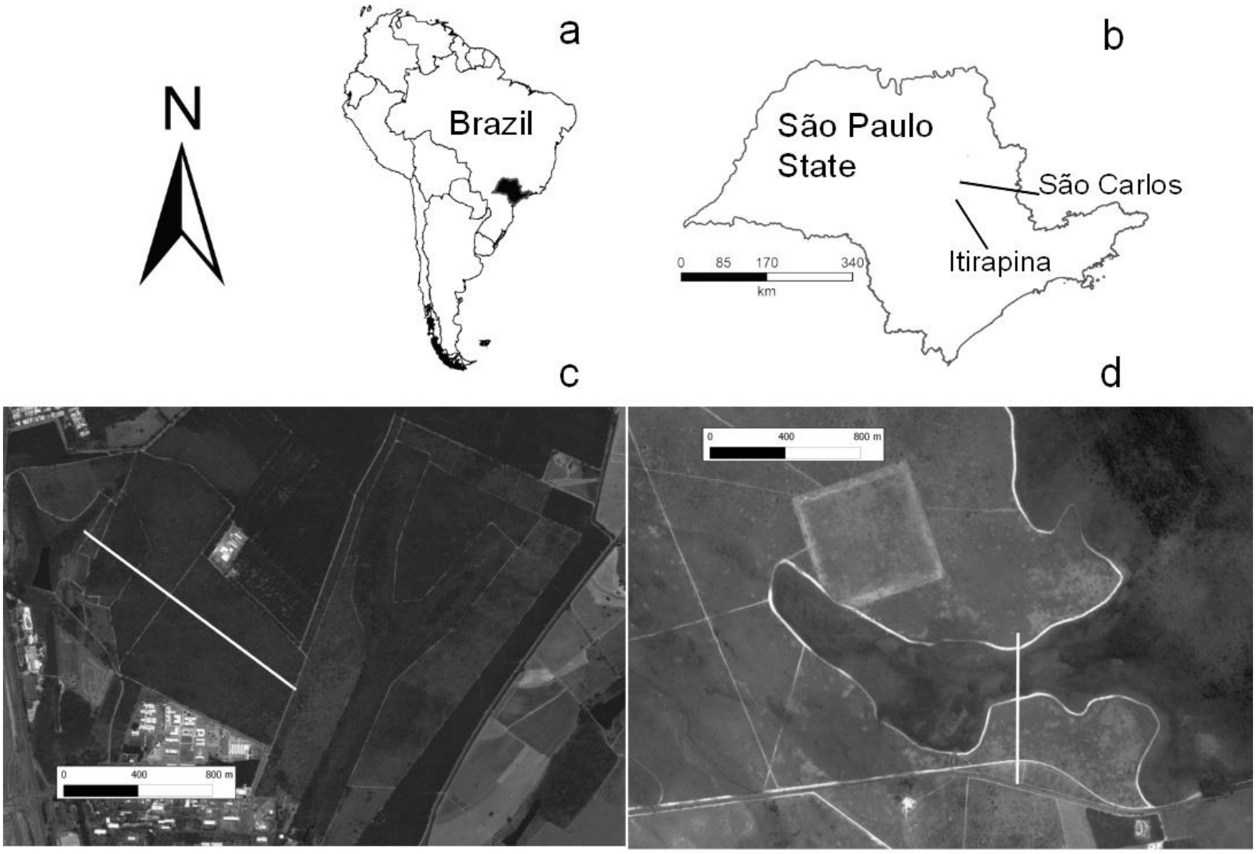

Figure 1. Location of São Paulo state in southeastern Brazil (a), the study areas in São Paulo state (b), and the transects in São Carlos (c) and Itirapina (d). The satellite images were obtained with the OpenLayers plugin in the Quantum GIS software.

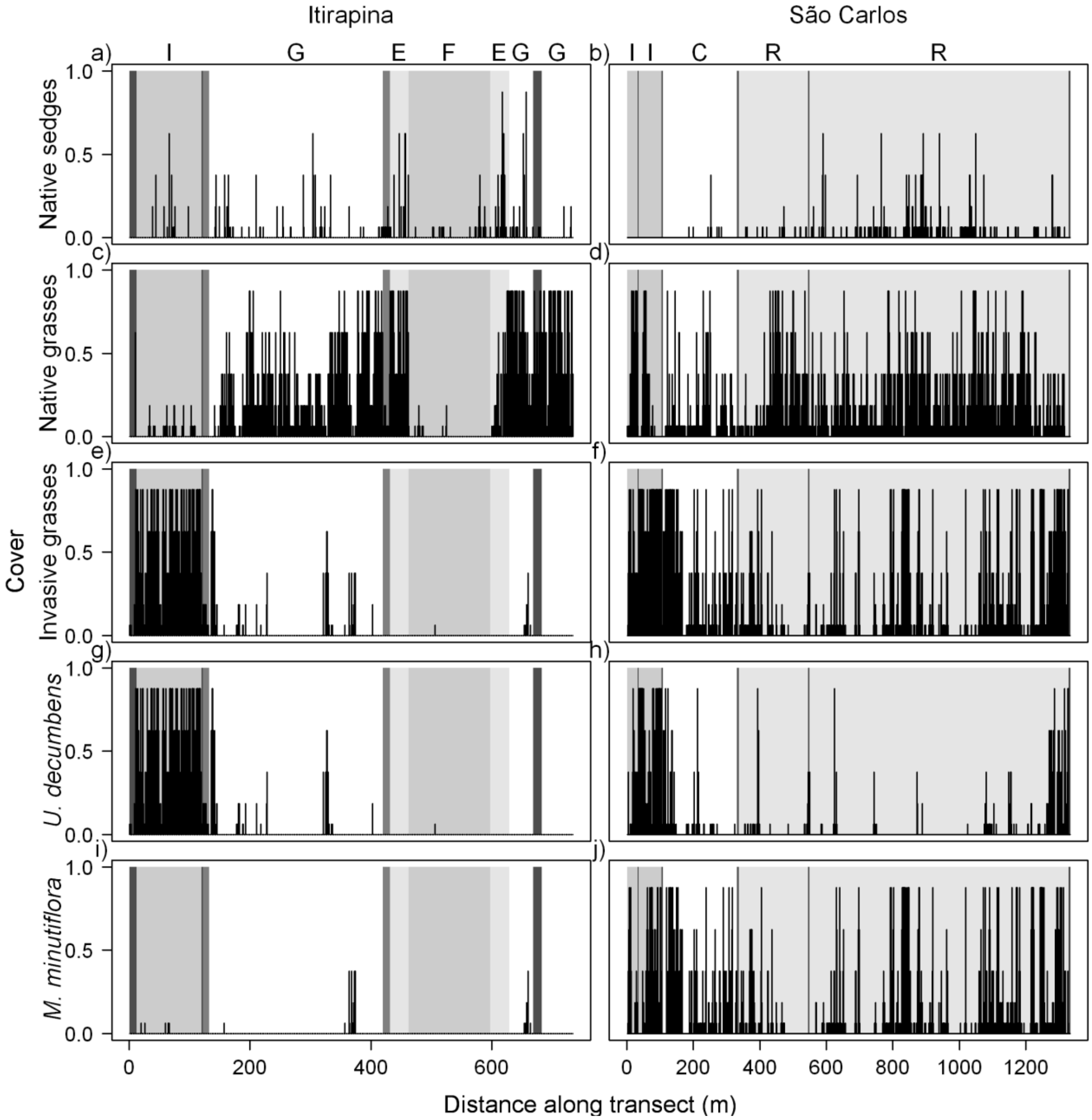

Figure 2. Cover of native sedges, native grasses, invasive grasses combined and the two invasive grass species, *Urochloa decumbens* and *Melinis minutiflora*, along the study transects in Itirapina and São Carlos. Linear disturbances are represented by darker shades of gray (dark gray for railroad and maintained firebreaks, medium-dark gray for regenerating firebreaks). Different phytophysiognomies are represented by different shading and labels above the plots: invaded grassland (I, medium gray), *campo sujo* grassland (G, white), ecotone (E, light gray), forest (F, medium gray), typical *cerrado* (C, white) and regenerating cerrado (R, light gray). See Table 1 for more details on the linear disturbances and phytophysiognomies.

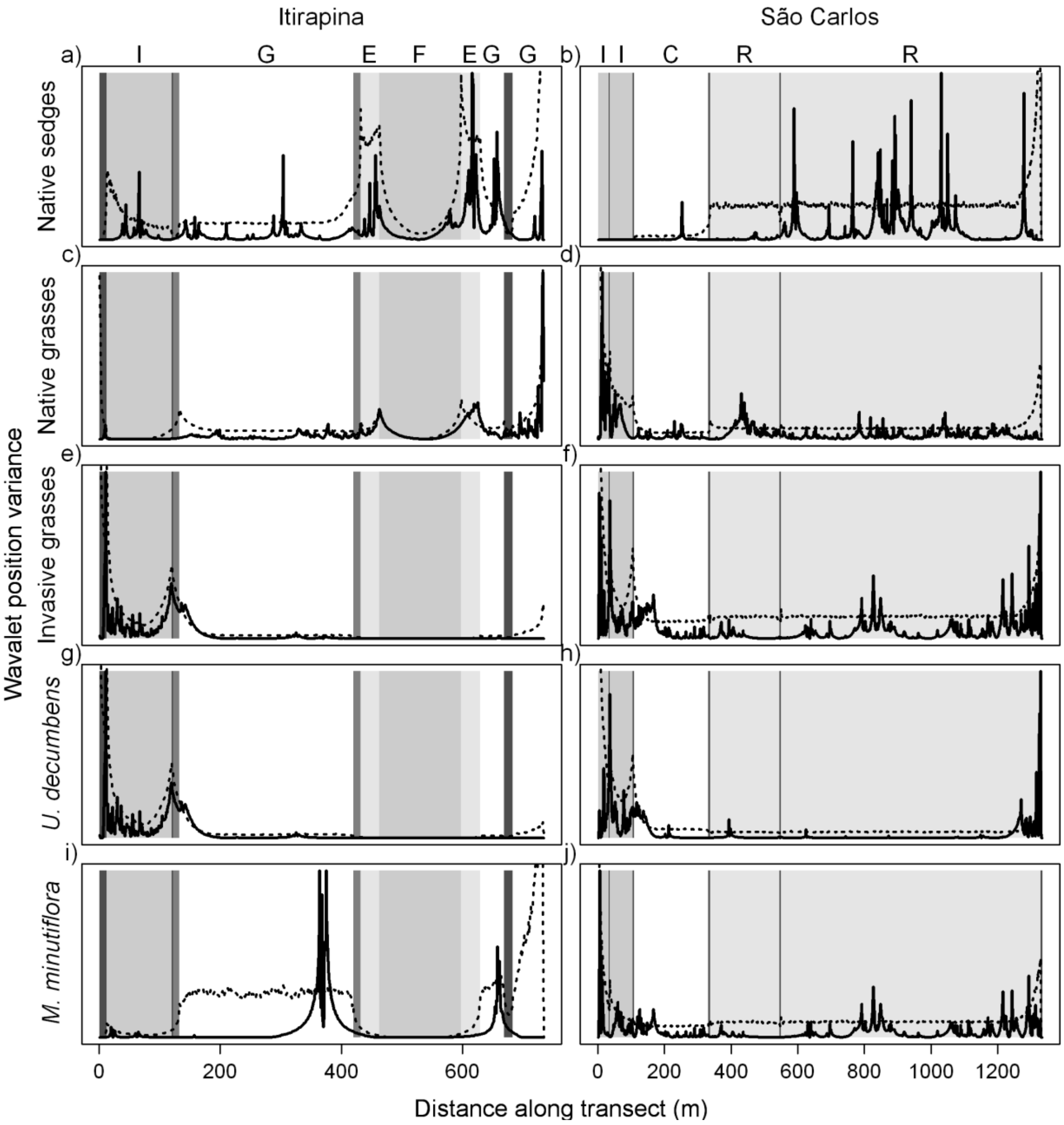

Figure 3. Wavelet position variance (solid black line) and confidence intervals calculated using different null models for native sedges, native grasses, combined invasive grasses, and the invasive grass species *Urochloa decumbens* and *Melinis minutiflora* for the two study transects. The wavelet template used was the Haar wavelet, calculated for scales 1 to 176 m in Itirapina and 1 to 173 m in São Carlos. The dashed line represents a first-order Markov Chain null model with different parameters for each plant community type in the transect (MC1s). See Table 1 and Figure 2 for more details.

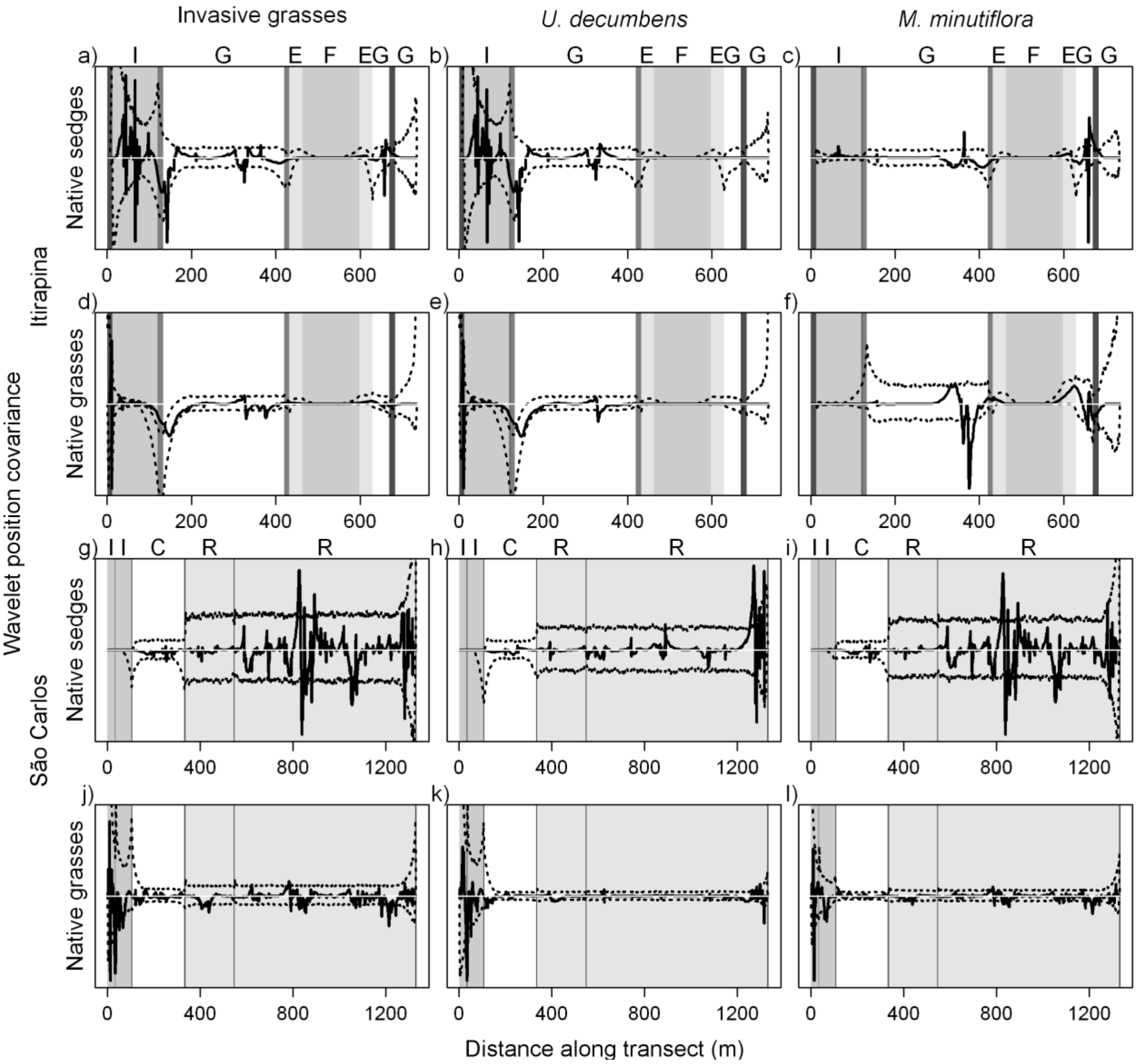

Figure 4. Bivariate position covariance (solid black line) between the native graminoids (sedges and grasses) and the invasive ones (combined invasive grasses, *Urochloa decumbens* and *Melinis minutiflora*), for the two study transects. The wavelet template used was the Haar wavelet, calculated for scales from 1 to 176 min Itirapina and 1 to 173 m in São Carlos. The dashed line represents a first-order Markov Chain null model with different parameters for each plant community type in the transect (MC1s). The white line represents covariance equal to zero. See Table 1 and Figure 2 for more details.

Chapter 3. Effects of natural and anthropogenic edges on plant structural diversity in cerrado and the forest-tundra ecotone[3]

Resumo

Sabe-se que a influência de borda afeta diferentes aspectos da estrutura da vegetação, incluindo sua altura, a densidade de árvores adultas e jovens e a cobertura de dossel. No entanto, a influência de borda sobre a diversidade estrutural, uma medida da variação entre os elementos estruturais presentes na vegetação, ainda foi pouco explorada. A influência de borda pode se combinar com a variação natural na estrutura da vegetação, complicando a detecção de padrões relacionadas a bordas, especialmente em ambientes heterogêneos com um estrato arbóreo descontínuo. Nós usamos uma abordagem de padrão espacial para 1) estudar a variação natural nos diferentes aspectos da diversidade estrutural e 2) verificar se a diversidade estrutural é afetada por bordas naturais e antrópicas. Nós colocamos um total de quatro transectos, dois no cerrado no Sudeste do Brasil e dois na transição entre tundra e floresta boreal no Oeste do Canadá. Os transectos tinham de 300 a 750 m de comprimento e eram subdivididos em parcelas contíguas de 1x1 m, e nós anotamos os elementos estruturais (elementos da vegetação com diferentes formas de vida e tamanhos, incluindo indivíduos tanto vivos quanto mortos, e diferentes substratos, como solo exposto, água e cascalho) presentes em cada parcela. Nós usamos duas medidas de diversidade estrutural, 1) o número de elementos estruturais presentes e 2) uma medida calculada a partir das dissimilaridades em forma de vida, classes de tamanho e outras características dos elementos estruturais, e usamos transformações de *wavelet* contínuas e testes de aleatorização para analisar a variação estrutural na diversidade estrutural em diferentes escalas. As escalas de padrão espacial eram maiores em vegetação mais aberta, e padrões relacionados a bordas foram observadas próximo tanto a bordas naturais quanto a bordas antrópicas. No entanto, padrões similares foram observados tanto perto quanto longe de bordas, indicando que a influência de borda não resulta necessariamente me padrões fora da variação natural da diversidade estrutural da vegetação. Mesmo assim, nós mostramos que, assim como outros aspectos da estrutura da vegetação, a diversidade estrutural é afetada por influência de borda até mesmo em ambientes com um alto grau de heterogeneidade natural.

---

[3] A first version of this study was presented at a seminar on functional diversity at the State University of São Paulo, in March 2014.

Abstract

Edge influence has been shown to affect different aspects of vegetation structure, including vegetation height, tree and sapling density, and canopy cover. However, edge influence on structural diversity, a measure of the variation among the structural elements present in the vegetation, has been little explored. Edge influence may superimpose on the natural variation in vegetation structure, complicating the detection of edge-related patterns, especially in patchy environments with a discontinuous tree layer. We employed a spatial pattern approach to assess 1) natural variation in different aspects of structural diversity and 2) effects of natural and anthropogenic edges on structural diversity. We established four transects, two in the Brazilian cerrado in south-eastern Brazil and two in the tundra-boreal forest transition in western Canada. The transects were 300 to 750 m long and subdivided into 1x1-m contiguous quadrats, and we noted the structural elements (vegetation elements with different life forms and sizes, including both live and dead elements, and elements of the substrate, such as bare soil, water, and gravel) present in each quadrat. We used two measures of structural diversity: 1) the number of structural elements present and 2) a measure calculated from the dissimilarities in category, size class and other characteristics of the structural elements. We used continuous wavelet transforms and randomization tests to assess the spatial variation in structural diversity at different scales. The scales of pattern were greater in more open vegetation, and edge-related patterns were observed next to natural and anthropogenic edges. However, similar patterns were observed both close to and for from edges, indicating that edge influence does not necessarily result in patterns outside the natural variation in plant structural diversity. Still, we showed that, similar to other aspects of vegetation structure, structural diversity is affected by edge influence even in patchy environments with a high degree of natural heterogeneity.

3.1. Introduction

Spatial patterns of vegetation structure may be caused by natural variation in environmental factors, patchy disturbances (Fischer et al. 2012, Dodonov et al. 2014a), animal activity (Asner et al. 2009) or influence from surrounding plant communities and anthropogenic land uses. One example of this is the patchy structure of savanna vegetation, which is characterized by alternating patches dominated by woody or herbaceous vegetation (Wiegand et al. 2005, 2006). Even greater variation may be observed at ecotones, for example between forest and non-forest vegetation, as these ecotones may have elements of both vegetation types. Gradients in vegetation structure may also be observed in areas undergoing regeneration (Dodonov et al. 2014b). Finally, anthropogenic edges may also result in different patterns in vegetation structure when compared to reference conditions (Didham and Lawton 1999, Dodonov et al. 2013).

Edge influence on vegetation structure may extend from a few meters to tens of meters at both natural and anthropogenic edges (Didham and Lawton 1999, Harper and Macdonald 2001, Delgado et al. 2007). Different aspects of vegetation structure have been shown to be affected by edge influence, including vegetation height (Delgado et al. 2007, Dodonov et al. 2013), canopy cover (Didham and Lawton 1999), tree and sapling density (Harper and Macdonald 2001), and woody cover (Smit and Asner 2012). Another important measure, which is also related to the ones mentioned above, is structural diversity, or the variability in the number and types of structural elements (components of the vegetation with different life forms, sizes etc) present in the vegetation (Harper et al. 2005b). Structural diversity is often used in studies of plant populations and on vegetation in general (Jimu et al. 2012, Ozdemir and Donoghue 2013), and may be seen as a measure of the complexity of the vegetation (McElhinny et al. 2005). Measures of structural diversity may include information on the size, growth forms, and development stages of individual plants. These measures may also include both live and dead plants, as they are important structural features in different vegetation types (Harper et al. 2005b, McElhinny et al. 2005). Thus, structural diversity may provide important information on the vegetation as a whole.

An assessment of spatial heterogeneity and edge-related patterns of structural diversity is also important because structural diversity may be related to different ecological processes. Structural diversity of deadwood may be related to fuel availability and therefore to fire dynamics, which are heavily influenced by the amount and type of fuel available, as has been shown in the cerrado (Hoffmann et al. 2012). Structural diversity also influences fauna by providing different possibilities for nesting and foraging (Tews et al. 2004, Coppedge et al. 2008). For example, one study showed a positive relationship between the structural diversity of a temperate forest and the occurrence of several bat species, which are highly dependent on the forest structure (Jung et al. 2012). Animal species may also affect structural diversity, e.g. by foraging or trampling the vegetation, as has been observed in an African savanna (Asner et al. 2009). Therefore, structural diversity may be used as a link between plant and animal communities in an area or between vegetation and ecological processes such as disturbances.

Given the large number of processes to which structural diversity may be related, it makes sense to use different measures of structural diversity depending on the research question. We calculated several different, but related, measures of structural diversity and assessed their spatial variation in heterogeneous environments. The study sites, located in the Brazilian cerrado and the Canadian sub-arctic, are characterized by an alternation of patches of open and closed vegetation, and contain several natural and anthropogenic edges. Our specific objectives were: 1) to describe the spatial variation of structural diversity in each environment, 2) to determine the scales with the greatest variation for different measures of structural diversity, and 3) to verify the existence of edge-related patterns in structural diversity next to natural and anthropogenic edges and to compare these patterns with the natural heterogeneity.

3.2. Methods

3.2.1 Study sites

We performed this study in the Brazilian cerrado in São Paulo, south-eastern Brazil, and the subarctic forest-tundra ecotone in Manitoba, western Canada (Figure 1). We placed two transects in each area. The two cerrado transects[4] were located in Itirapina Ecological Station (22°14'46"S, 47°52'39"W; Supplementary Material 1.3) and in the cerrado reserve of the Federal University of São Carlos (21°58'34"S, 47°52'31"W; Supplementary Material 1.2) and the two sub-arctic transects were located near the Churchill Northern Studies Centre (58º43’59’’N, 93º48’52’’W; Supplementary Material 1.4 and 1.5) (Figure 1).

The transects were 300 to 750 m long and comprised a number of different plant communities as well as natural (lakeshore, savanna-forest boundaries) and anthropogenic (railroad, road, firebreak) edges (Table 1). The transect in Itirapina, hereafter “savanna transect”, spanned open savanna vegetation with a continuous grass layer and scattered trees (known as “campo sujo”, Coutinho 1978) and a riparian gallery forest. The transect in São Carlos, hereafter “woodland transect”, spanned more closed vegetation with shrubby to woodland savanna (“typical cerrado” to “dense cerrado”, Ribeiro & Walter 2008) as well as a riparian gallery forest. One of the subarctic transects, hereafter “tundra transect”, passed mostly through lichen heath tundra vegetation with a forest-tundra transition, two lakes, and a gravel road. The other subarctic transect, hereafter “ecotone transect”, passed through areas

---

[4] The transect in Itirapina Ecological Station was also sampled for invasive grasses (Chapter 2).

characterized as forest-tundra ecotone, an alternation of tundra-like vegetation with prostrate shrubs and lichens and a more or less dense shrub and tree layer (Table 1).

3.2.2 Sampling

Each transect was composed of 1x1 m contiguous quadrats. This sampling enabled us to detect both fine and coarse scale patterns that could go undetected if we used spaced quadrats (Dale 1999). In each quadrat, we sampled different structural elements and classified them according to characteristics such as diameter, height, and decay class (Table 2). Structural elements included bare soil, water, fine woody debris, litter, grasses, other graminoids, prostrate shrubs, herbaceous plants, live and dead shrubs, woody resprouts, and live and dead trees. We classified all structural elements in height classes, and woody elements (fallen branches, shrubs, woody resprouts, and trees) in diameter classes. As we only used presence/absence data, the cover or density of the structural elements was not considered.

We used different height classes for the different transects according to the specific characteristics of each area. For the savanna transect, the height classes were: <0.7 m, 0.7-1.3 m, 1.3-2.0 m, 2-3 m, 3-5 m, 5-8 m and 8-15 m. The first three classes represent heights more intensely damaged by fire (Miranda et al. 2002), whereas the other height classes represent the maximum vegetation height in different cerrado phytophysiognomies (Ribeiro & Walter 2008). For the woodland transect we used the same height classes, with the subdivision of the first class into three (< 0.1 m, 0.1-0.4 m, 0.4-0.7 m) and the addition of a class >15 m. For the tundra and ecotone transects, we used the height classes <0.1 m, 0.1-0.4 m, 0.4-1.0 m, 1.0-1.6 m, 1.6-3.0 m, 3-5 m and >5 m, representing the variation in height found along these transects. The diameter classes used in all transects were <0.6 cm, 0.6-2.5 cm, 2.5-5.0 cm, 5-15 cm, 15-30 cm and >30 cm. The first two classes represent 1- and 10-hour fuel classes (Schimmel and Granström 1997), and the other classes were chosen because they represent the diameter distributions observed in the study systems (P. Dodonov, personal observation).

We also measured the variation in altitude along the transects to create topographic profiles. However, due to equipment availability, we used different methods in the cerrado and the subarctic. In the cerrado, we walked along the transects with an altimeter and marked the points along the transect at which there was an altitude change and the corresponding altitude. The altimeter was calibrated immediately before sampling at a location with known altitude (Brazilian Institute of Geography and Statistics' geodesic station 93671) close to the woodland transect. In the subarctic, we placed Trimble Juno ST GPS devices along the transects, every 20 m or where there were perceivable changes in topography, and recorded at least 1000 waypoints with the TerraSync^{TM} software, calculating altitude as the average of these waypoints.

3.2.3 Measurement of structural diversity

We used two measures of structural diversity. The first, which we call structural richness (StrS), is simply the number of different structural elements in a quadrat. The second measure, a dissimilarity-based measure of structural diversity (StrD), also takes into account the characteristics of the different structural elements. This measure is based on a dissimilarity matrix between the structural diversity elements and is calculated in a similar way to measures of functional and phylogenetic diversity (Petchey and Gaston 2006). Its main advantage is that it gives greater weight to structural elements that are less similar to other elements in the same quadrat. Thus, if two quadrats have the same number of structural elements, the one in which the elements are less similar to one another will have a greater structural diversity. Before calculating this index, we described each structural element according to its characteristics: plant vs. substrate, life form (broad and specific), standing vs. fallen, live vs. dead, woody vs. non-woody stem, and diameter and height classes (Table 2). StrD was then calculated for each quadrat by 1) attributing a weight to each descriptor of the different structural elements (Table 3), 2) calculating the dissimilarity matrix between the structural elements, 3) clustering the elements according to the dissimilarity matrix, and 4) summing the lengths of the cluster branches to calculate structural diversity. We used Gower dissimilarity because it may be used simultaneously for categorical and quantitative variables (Legendre and Legendre 1998). We selected weights based on the descriptors we considered most important for the ecological processes related to each structural diversity measure.

We calculated both indices for five measures of structural diversity: overall, live, woody, dead, and substrate. On one hand, this increases the probability of a type I error; however, it also provides a more thorough description of the spatial variation in structural diversity in the communities studied. Whereas overall diversity included all structural elements, live diversity included only live plants, woody diversity included only woody plants (both live and dead), dead diversity included all dead plants as well as fine woody debris and litter, and substrate diversity included bare soil, litter and ground plants such as prostrate shrubs and grasses. We chose these categories because they may represent different processes: woody plants for structural succession, dead plants for fuel and therefore fire intensity, and substrate for seedling establishment. We also used different weights for the descriptors in each measure, and some descriptors were not used in all measures (Table 3). Two elements with the same classification according to the descriptors used for a given measure (e.g. two trees in the same size classes, regardless of their species) were considered as one single element.

3.2.4 Data analysis

We used scaleograms for continuous wavelet transform (CWT) to assess the spatial pattern of structural diversity at different scales. This analysis is explained in section 1.3. We calculated the continuous wavelet transform (CWT) for all structural diversity measures along all transects, with the Mexican Hat wavelet and a maximum scale of 75 m, corresponding to 25% of the shortest transect. Prior to analysis we added zeroes to the extremities of the transect to enable calculation of the wavelet at the transect's edges, and afterwards we removed the cells of the position-scale matrix that were influenced by the transect's boundaries. We assessed significance from 999 restricted randomizations, in which data were randomly sorted only within a given plant community or section of the transect (Table 1). We performed these restricted randomizations instead of full randomizations because our interest was in the patterns within each plant communities, not in the differences between them. We performed the CWT on each of the 999 randomized datasets, and used the results to create 95% confidence intervals. As we used restricted randomizations, these confidence intervals show patterns that could be expected if the structural diversity varied randomly within each plant community or section of the transects. We considered the coefficients of the CWT for the original data as significant if they were outside these confidence intervals, and we assumed that significant patterns located close to edges represent edge influence.

We also calculated scale variance as the average of the squared CWT coefficients for each scale across all positions. To determine the significant scales of spatial pattern in each transect, we compared scale variance to one-tailed 95% confidence intervals calculated from the randomized datasets and considered all scales that were above the confidence interval as significant. This is different from the common approach in which peaks in the variance x scale plot are used to determine the most important scales (Dale and Mah 1998). We used all significant scales instead of looking for peaks because the shape of the curve may be influenced by the existence of different plant communities, which have been accounted for by the confidence intervals.

All analyses were performed in the R 2.15.3 software (R Core Team 2013). Structural diversity was calculated with the aid of the packages *cluster* (Maechler et al. 2012) and *vegan* (Oksanen et al. 2013), and the wavelet transforms were calculated with the package *wmtsa* (Constantine and Percival 2012). The codes used to calculate the structural diversity indices, to perform the wavelet transforms and to calculate their significance are available in Supplementary Material 3.1.

3.3. Results

Vegetation height, estimated as the maximum height class of the structural elements within the quadrats, varied greatly among and within the transects (Figure 2), and appeared to be related to topography. Along the savanna transect, the greatest heights were found in lower areas occupied by the riparian forest and transition areas (Figure 2A). A similar pattern was observed in the woodland transect, although the differences in vegetation height were smaller (Figure 2B). Vegetation height along the tundra transect was more homogeneous, with minor peaks at lakeshore and road edges (Figure 2C). The ecotone transect was characterized by scattered patches with taller vegetation, mostly corresponding to tree clumps in some of the lower areas and to forest vegetation on higher ground (Figure 2D).

3.3.1 Structural diversity measures

The patterns described below refer to both indices of structural diversity, StrS and StrD, unless specified otherwise.

There were some consistent patterns in the structural diversity measures when considering the plant communities composing each transect (Table 4; Figure 3). Thus, disturbances (railroad, roads and firebreaks) had much smaller structural diversity than the undisturbed areas, although there was not much variation among the disturbance types. However, structural diversity of these areas was not completely absent, probably due to the existence of a few plants and litter.

Along the savanna transect, structural diversity tended to be greater in taller vegetation, increasing from the invaded grassland to the *campo sujo* to the transition area and riparian forest. This was most evident for live and woody diversity. One exception was dead diversity, which was greater in *campo sujo* and the transition area. Conversely, there was much less variation along the woodland transect, but structural diversity was slightly greater in the typical *cerrado* and the riparian forest than in the regenerating *cerrado* and the transition area. Although StrS in the transition area was slightly greater than in the regenerating cerrado, the reverse was observed for StrD, indicating that the elements in the transition area were more similar to each another.

The tundra transect was relatively homogeneous, but structural diversity were slightly greater in the wetland. Woody diversity, however, was greater in the transition area, which contained more trees and shrubs. Along the ecotone transect, structural diversity was greatest in the transition area except for woody diversity, which was greatest in the forest. Live and dead diversities were similar between the forest and wetland in this transect, whereas substrate diversity was greater in the wetland.

3.3.2 Scales of spatial pattern

In general, scales of spatial pattern were greater along the savanna and tundra transects, which were characterized by more open vegetation, than along the woodland and ecotone transects. For the savanna transect, almost all measures of structural diversity showed significant patterns at scales of around 7 to 75 m (Table 5). The most noticeable exception was substrate StrD, which had significant patterns at scales 3 to 48 m and 72 to 75 m, but not at scales from 50 to 70 m. Along the tundra transect, all measures had significant patterns at scales of around 5 to 75 m, except for live diversity, with significant patterns at scales of around 15 to 75 m (Table 5).

Conversely, along the woodland and ecotone transects, characterized by a more closed vegetation with a larger number of trees, smaller scales of spatial pattern, up to approximately 20 m, were dominant. Along the woodland transect, overall and dead diversity showed significant patterns at scales of around 3 to 15 m, whereas the other measures were significant at scales of around 5 to 30 m. Overall StrD also had a significant pattern at 44 to 51 m, and substrate StrD at 58 to 75 m (Table 5). Patterns along the ecotone transects were similar, with significant scales mostly of around 3 to 20 m. Exceptions included woody StrS, significant at scales of 2 to 75 m, live diversity, with significant patterns at scales of around 3 to 20 m but also of around 50 to 75 m (Table 5).

3.3.3 Edge-related patterns

Although there was some noticeable edge influence at road and firebreak edges, it was not conspicuous, and similar patterns were often also seen throughout the transects far from edges (Figures 4 and 5, with higher-resolution colored Figures in Supplementary Material 3.2). Thus, edge-related patterns were not outside the natural, non edge-related variation in vegetation structure. Some measures of structural diversity (overall, live, woody and dead

StrS, and woody StrD) had low values next to the railroad in the savanna transect at scales of 2 to 8 m (Figure 4), but similarly low values were also observed in the center of the invaded grassland along the same transect. There were also areas with either lower or greater structural diversity at most firebreak edges at scales of 4 to 16 m in the *campo sujo*. Along the woodland transect, a small peak in dead structural diversity was observed next to one firebreak, at a scale of approximately 4 m. Peaks in structural diversity were observed next to the firebreaks separating the regenerating cerrado from the typical cerrado and the typical cerrado from the transition area, at scales of approximately 4 to 30 m. Along the tundra transect, peaks in structural diversity were observed on both sides of the gravel road at scales of approximately 4 to 30 m (Figure 5). No patterns were apparent next to the gravel road along the ecotone transect.

Some patterns were also apparent next to the natural edges. In the tundra, two distinct scales of pattern were evident next to large water bodies. At a large scale, of approximately 16 to 75 m, structural diversity appeared to be greatest approximately 20 to 50 m from the lake (Figure 5). The significant positive values at large scales within the lakes probably reflect this pattern, as the values in the center of the lake at these scales are influenced by the vegetation at the lake edges. However, at smaller scales, of approximately 4 to 16 m, structural diversity at lake edges was lower. Patterns observed along the ecotone transect were more complex. Large-scale patterns of greater structural diversity were observed at some distance from the lake, similar to the tundra transect. However, these peaks were not accompanied by small-scale patterns of smaller structural diversity, except for live diversity on one side of the lake (Figure 3). Interestingly, these large-scale patterns were not observed elsewhere along either of these transects, indicating that unique patterns of vegetation structure may be found close to large water bodies (Figures 3 and 5). Along the ecotone transect, there were peaks in structural diversity next to pond edges at scales varying from 4 to 32 m, but similar patterns were also observed elsewhere along this transect.

Patterns at edges between different plant communities were not easily discernible, as these boundaries often coincided with firebreak, road, or pond edges. In addition, the patterns at boundary areas were also observed elsewhere along the transects. Along the savanna transect, peaks in structural diversity were observed at the boundaries between the forest and transition areas at scales of approximately 30 to 40 m, and between the transition area and *campo sujo* at scales of 4 to 16 m (Figure 4). There were also patterns at scales of approximately 20 to 70 m at the boundary between invaded grassland and *campo sujo*, with a lower structural diversity in invaded grassland and greater diversity in *campo sujo*. Along the woodland transect, a peak in structural diversity was observed in typical *cerrado* next to the transition area at scales of 8 to 16 m. A peak in structural diversity was also observed in the riparian forest close to the boundary with typical *cerrado*, but only for live and dead StrD and substrate StrS (Figures 4, G-J). We did not detect any patterns related to boundaries between plant communities along the tundra transect. The peaks in structural diversity next to pond edges along the ecotone transect, as described above, may also reflect the effect of boundaries between plant communities, as one pond was located between a wetland and a transition area and the other between a forest and a transition area.

3.4. Discussion

There were spatial patterns in structural diversity at a variety of scales at all of our study sites for all of our structural diversity measures. As the analysis takes into account the differences between plant communities composing each transect, the significant patterns show that the plant communities composing each transect are not homogeneous, but are themselves composed of alternating patches with high and low structural diversity. Interestingly, with some exceptions, similar scales of spatial pattern were found for most of the structural diversity measures within each transect. This may be partially explained by the relationships between the structural diversity measures – for example, in forest areas, with large numbers of woody plants, live and woody diversity will probably vary in a similar manner. Some relationships, albeit weak, have been previously observed between, for example, canopy and understory structure in forest areas (Kembel and Dale 2006, Halpern and Lutz 2013), and our results indicate that variation in one aspect of the vegetation structure may be used to a certain degree to predict variation in another aspect.

In addition, the savanna and tundra transects showed similar scales of spatial pattern, as did the woodland and ecotone transects. Conversely, the scales of spatial pattern were quite different between savanna and woodland and between tundra and ecotone. Thus, the overall structure of the vegetation, whether more open or more closed, appears to be a more important factor than region or biome for determining the scales of variation. In environments with little tree cover (tundra and *campo sujo* savanna), small-scale spatial patterns may reflect factors such as microsite requirements and competition between adjacent plants (Strand et al. 2007), whereas patterns at larger scales, up to 75 m, may reflect relationships with soil fertility and/or topography (Gamon et al. 2012).

Conversely, the dominant scales of pattern in the more closed vegetation along the woodland and ecotone transects were smaller, usually up to 30 m, and appear to be related to the woody vegetation. Between-tree competition may result in conspicuous patterns as larger trees hamper the growth of other trees around them due to competition for light, water or other resources, as tree cover has been previously shown to affect the spatial pattern of vegetation (Batllori et al. 2009). Tree patterns may also modify the spatial pattern of undergrowth vegetation (Wiegand et al. 2006). Although larger scales of pattern were more common in the more open vegetation, they were also observed for some measures of structural diversity in the ecotone and woodland transects. It is likely that they result from the same factors as in the more open vegetation, such as variation in soil fertility and topography, but are less conspicuous because of the high influence of tree cover.

Some edge-related patterns, albeit not very clear, were observed for structural diversity measures at all transects. Previous studies have shown that anthropogenic edges may affect different aspects of vegetation structure, including vegetation height (Didham and Lawton 1999, Dodonov et al. 2013), canopy structure (Vaughn et al. 2014) and the density of trees and saplings (Harper and Macdonald 2001), and our data corroborate these studies by showing that structural diversity may be affected as well. Edge influence from anthropogenic edges occurred at smaller scales than the patterns at boundaries between plant communities, which occurred at smaller scales than patterns related to large water bodies. Thus, soil and topography gradients at the transitions between plant communities result in larger-scale patterns than edge-related gradients resulting from narrow firebreaks and low-traffic roads.

Anthropogenic edges such as roads and firebreaks may modify adjacent vegetation by several mechanisms related to energy and organism flow (Ries et al. 2004); for example by enabling greater irradiation, water runoff, and seed rain (Pohlman et al. 2007, Smit and Asner 2012, Gorchov et al. 2013), which may also result in changes in species composition at the edge. However, as our transects spanned relatively open vegetation without a closed canopy, edge-related changes in microclimate may be within the natural range of variation (but see Dodonov et al. 2013). Thus, edges in our study do not appear to create unique habitats in terms of structural diversity, but instead increase the probability of occurrence of a habitat type that may also be naturally found in a given vegetation type. Patterns at natural transitions may result from gradients in soil characteristics and topography, and possibly the occurrence of different plant species. Large-scale patterns related to lakes may reflect variation in soil fertility and depths, with a deeper permafrost layer.

Although some patterns were more evident for either StrS or StrD, overall the results obtained for the two indices were similar. This was not unexpected, as dissimilarity-based diversity measures are known to be highly correlated to the number of species or pseudospecies (Petchey and Gaston 2006). Some scales of pattern, however, were only apparent for StrD. Thus, larger scales of pattern were observed in the woodland transect for overall and substrate diversity with the StrD index. This may indicate that, although the number of structural elements may vary randomly at these scales, the similarity between them is spatially structured. Our StrD index may also have been biased by the lack of information on all descriptors for all structural elements. This was in large part due to our aim to include all structural elements in our sampling. If the study is aimed on a single type of structural diversity, e.g. woody diversity, the same variables may be measured for all structural elements, permitting a more precise calculation of this index.

`

3.5. Conclusion

Similar scales of pattern observed between transects in different biomes indicate that vegetation structure, whether open or closed, is a potential predictor of the scales of spatial pattern of structural diversity. Different aspects of structural diversity appear to show similar patterns, indicating that the structural diversity of part of the vegetation may be used to predict general patterns. Finally, our study showed that the assessment of both edge-related patterns and of natural heterogeneity in vegetation structure may provide insights into the effects of anthropogenic disturbances. Patterns observed at edges were usually not outside the range of natural variation in structural diversity, indicating that edges may modify vegetation structure without creating unique environments.

Acknowledgments

We are grateful to the many people who helped us in the field, especially Cinthya C. Santos, Bianca Rantin, Amanda A. Lavalle, Danielle St. Louis and Rayane Maciel; to the Forestry Institute of São Paulo State and to the Churchill Northern Studies Centre for permissions for fieldwork and logistic support; to Genevieve Berard for aid in collecting altimetry data from the subarctic transects; to the Ecology department of the São Paulo State University for providing the altimeter used in the cerrado transects; and to the Brazilian Council for Scientific and Technological Development (CNPq, grant 141623/2011-0), the Emerging Leaders in the Americas Program (ELAP), the Northern Scientific Training

Program (NSTP), the Natural Sciences and Engineering Research Council of Canada (NSERC), and the Northern Research Fund (NRF) for financial support.

Supplementary material description

SM 3.1 – Codes used to create the null models, to calculate structural diversity, to perform the wavelet analyses, to calculate the confidence intervals and to exclude the non-significant wavelet results.

SM 3.2 – Colored high-resolution Figures of the wavelet results.

Tables

Table 1. Different plant communities along each of the four transects.

Plant community	Description	Locations (m)
Savanna		
Railroad	A railroad bordering the protected area	1-12
Invaded grassland	An area dominated by the invasive grass *Urochloa decumbens* with scattered trees	13-119
Firebreak	Maintained firebreak with no regrowth	120-121, 669-682
Regenerating firebreak	Non-maintained firebreak with low grass and/or herbaceous plants	122-132, 420-431
Campo sujo	A savanna with a continuous grass layer and scattered trees	133-419, 629-668, 683-734
Transition	Transition between savanna and riparian forest	432-462, 598-628
Riparian forest	Tall gallery forest around a narrow 1-2 m stream	463-597
Woodland		
Firebreak	Maintained firebreak with no regrowth	1-8, 56-61, 71-75, 296-301
Regenerating cerrado	A woodland savanna regenerating after a eucalypt plantation with residual eucalypt trees	9-55
Cerrado	Woodland savanna, with a herbaceous layer and discontinuous canopy	62-70, 239-295
Transition	Transition between savanna and riparian forest	76-114
Riparian forest	Tall forest around a narrow 1-2 m stream	115-238
Tundra		
Tundra	Lichen heath tundra dominated by lichens and prostrate shrubs	1-228, 550-681
Lake	Large water bodies with no vegetation	229-336, 420-549
Wetland	Vegetation on waterlogged soil, mostly grasses	337-419
Gravel road	A road with little traffic	682-705
Ecotone	A transition area between treeless tundra and forest	706-747
Ecotone		
Wetland	Vegetation on waterlogged soil, mostly grasses	1-47
Ecotone	Transition area between treeless tundra and forest	57-195, 205-207, 224-225, 346-367
Forest	An open-canopy boreal forest	377-462
Road	A road with little traffic	196-204
Pond	Small water bodies with some vegetation	48-56, 208-223, 368-376
Lake	Large water body with no vegetation	226-345

Table 2. Structural elements for cerrado (savanna and woodland) and subarctic transects (tundra and ecotone) and their descriptors. Di: diameter; Ht: total height; Hi: intermediate height; De: decomposition.

Category (broad)	Category (specific)	Plant/soil	Standing	Woody	Live	Additional classification
Savanna and woodland transects						
Water	Running water	soil	N/A[1]	N/A	N/A	-
	Still water	soil	N/A	N/A	N/A	-
Soil	Rock	soil	N/A	N/A	N/A	Ht
	Soil	soil	N/A	N/A	N/A	-
Animal burrows	-	soil	N/A			
Termite mounds	-	soil	yes	N/A	N/A	Ht
Litter	Tree bark	plant	no	yes	no	-
	Fern leaves	plant	no	no	no	-
	Pine leaves	plant	no	no	no	-
	Tree leaves	plant	no	no	no	-
	Twigs	plant	no	yes	no	Di
Ground vegetation	Lichens	plant	no	no	yes	-
	Moss	plant	no	no	yes	-
Graminoids	Native grasses	plant	yes	no	yes	Ht
	Native sedges	plant	yes	no	yes	Ht
	Invasive grass - *Melinis minutiflora*	plant	yes	no	yes	Ht
	Invasive grass - *Urochloa decumbens*	plant	yes	no	yes	Ht
	Dead graminoids	plant	yes	no	no	Ht
Herbaceous plants	Bromeliads	plant	yes	no	yes	Ht
	Ferns	plant	yes	no	yes	Ht
	Lycopods	plant	yes	no	yes	Ht
	Palms	plant	yes	no	yes	Ht
Resprouts	Non-woody resprouts	plant	yes	no	yes	Ht
	Woody resprouts	plant	yes	yes	yes	Di, Ht
Tree-like plants	Eucalypts	plant	yes	yes	yes/no	Di, Ht, Hi, De[2]
	Tree ferns	plant	yes/no[3]	yes	yes/no	Di, Ht, Hi, De[2]
	Palm trees	plant	yes/no	yes	yes/no	Di, Ht, Hi, De[2]
	Roots	plant	no	yes	yes	Di
	Other trees	plant	yes/no	yes	yes/no	Di, Ht, Hi, De[2]
Vines	Non-woody vines	plant	yes	no	yes	Ht
	Woody vines	plant	yes	yes	yes	Di, Ht
Tundra and ecotone transects						
Rock	Gravel	soil	N/A	N/A	N/A	-
	Rock	soil	N/A	N/A	N/A	Ht
Soil	Soil	soil	N/A	N/A	N/A	-
Litter	Broadleaf litter	plant	no	no	no	-
	Conifer needles	plant	no	no	no	-
	Other litter	plant	no	no	no	-

Category (broad)	Category (specific)	Plant/soil	Standing	Woody	Live	Additional classification
	Graminoid litter	plant	no	no	no	Ht
	Herbaceous litter	plant	no	no	no	-
	Twigs	plant	no	no	no	Di
Lichens	Crustose lichens	plant	no	no	yes	-
	Dead lichens	plant	no	no	no	-
	Foliose lichens	plant	no	no	yes	-
	Cladonia spp.	plant	no	no	yes	-
	Other fruticose lichens	plant	no	no	yes	-
Moss	*Sphagnum* spp.	plant	no	no	yes	-
	Other moss	plant	no	no	yes	-
Herbaceous plants	Horsetails	plant	yes	no	yes	Ht
	Forbs	plant	yes	no	yes	Ht
	Graminoids	plant	yes	no	yes	Ht
	Other herbaceous plants	plant	yes	no	yes	Ht
Shrubs	Prostrate shrubs	plant	no	no	yes	Ht
	Tall shrubs	plant	yes	yes	yes/no	Di, Ht, De[2]
Trees	Roots	plant	no	yes	yes	Di
	Layering trees	plant	yes	yes	yes	Di, Ht, Hi
	Trees with treeskirt[3]	[2]plant	yes	yes	yes	Di, Ht, Hi
	Other trees	plant	yes/no	yes	yes/no	Di, Ht, Hi, De[2]

---

[1] N/A: this descriptor was not applied for this variable.

[2] Hi was considered only for live elements and Dec only for dead elements.

[3] yes/no: Both options were possible for these structural elements.

[4] treeskirt: low branches forming a protection against snow around the tree's trunk.

Table 3. Structural elements and the weights of their different descriptors used in the five structural diversity measures.

		Weights									
Measure	Elements used	Category (broad)	Category (specific)	Plant/soil	Standing	Woody	Live	Diameter	Total height[1]	Intermediate height[1]	Decay
Overall	All	1	0.5	1	1	1	1	0.7	0.7	0.3	0.7
Live	All live vegetation	1	0.7	N/A[2]	1	1		0.7	1		
Woody	All woody elements, excluding twigs	1	0.5	N/A[2]	1	N/A	1	0.7	1	0.5	0.7
Dead	All dead elements	1	0.5	N/A[2]	1	1	N/A[2]	0.5	1	0[3]	1
Substrate	Soil, graminoids, moss, lichens, and herbaceous plants	1	1	1	0.5	1	1	0.2	0.7	0[3]	0[3]

[1] Total height: height of the tallest branch or leaf of the structural element; intermediate height: height of the first branching for trees, the first leaves for palms and treeferns, and of the treeskirt for trees with treeskirts.

[2] N/A: the descriptor did not vary in the corresponding measure

[3] Weight of 0: we did not include this descriptor in the measure.

Table 4. Mean ± standard deviation of the structural diversity indices in the different plant communities along each transect.

	StrS					StrD				
Plant communities	Overall	Live	Woody	Dead	Substrate	Overall	Live	Woody	Dead	Substrate
Savanna										
Invaded grassland	5.0 ± 1.9	2.7 ± 1.2	1.0 ± 1.0	2.0 ± 1.1	3.6 ± 1.1	1.8 ± 0.8	1.0 ± 0.6	0.2 ± 0.4	0.7 ± 0.7	1.5 ± 0.6
Campo sujo	8.2 ± 2.1	3.4 ± 1.3	1.8 ± 1.6	4.0 ± 1.6	5.1 ± 1.1	3.0 ± 0.6	1.3 ± 0.5	0.3 ± 0.4	1.5 ± 0.4	2.5 ± 0.6
Transition	11.8 ± 3.8	6.1 ± 2.4	4.1 ± 2.7	5.2 ± 2.0	5.8 ± 1.6	3.2 ± 0.8	1.9 ± 0.6	0.7 ± 0.5	1.7 ± 0.5	2.3 ± 0.7
Forest	11.8 ± 2.8	6.2 ± 2.0	4.0 ± 2.2	4.5 ± 1.4	5.4 ± 1.6	3.5 ± 0.7	2.2 ± 0.6	1.0 ± 0.6	1.1 ± 0.6	2.1 ± 0.9
Regenerating firebreak	4.7 ± 0.8	1.5 ± 0.8	0.0 ± 0.0	2.2 ± 0.9	4.6 ± 0.7	2.3 ± 0.3	0.2 ± 0.3	0.0 ± 0.0	0.8 ± 0.5	2.5 ± 0.3
Firebreak	4.7 ± 1.5	1.7 ± 0.9	0.3 ± 0.6	2.0 ± 0.8	4.1 ± 1.0	2.4 ± 0.4	0.4 ± 0.5	0.0 ± 0.0	0.8 ± 0.5	2.4 ± 0.3
Railroad	4.3 ± 2.2	1.2 ± 1.5	0.3 ± 0.9	2.3 ± 1.6	3.7 ± 1.8	1.8 ± 0.9	0.3 ± 0.6	0.1 ± 0.2	0.8 ± 0.6	1.8 ± 1.0
Woodland										
Regenerating cerrado	11.7 ± 3.3	6.1 ± 2.7	3.3 ± 2.2	4.6 ± 1.1	6.8 ± 1.8	3.6 ± 0.6	1.9 ± 0.6	0.7 ± 0.5	1.5 ± 0.5	2.8 ± 0.6
Typical cerrado	13.0 ± 2.9	7.6 ± 2.4	4.8 ± 2.8	5.0 ± 1.2	6.6 ± 1.3	3.2 ± 0.5	2.1 ± 0.5	0.9 ± 0.6	1.7 ± 0.3	2.4 ± 0.5
Transition	11.8 ± 2.3	6.7 ± 1.8	4.4 ± 1.8	4.6 ± 1.2	5.6 ± 1.7	3.0 ± 0.6	1.9 ± 0.5	0.9 ± 0.5	1.3 ± 0.5	2.0 ± 0.9
Forest	12.8 ± 2.1	7.3 ± 2.2	4.7 ± 2.1	5.0 ± 1.3	6.7 ± 1.5	3.3 ± 0.6	2.2 ± 0.7	1.2 ± 0.6	1.5 ± 0.5	2.4 ± 0.6
Firebreak	5.0 ± 3.9	1.5 ± 2.6	0.4 ± 0.9	2.4 ± 1.7	4.1 ± 2.5	1.9 ± 1.1	0.4 ± 0.7	0.1 ± 0.2	0.7 ± 0.7	1.9 ± 1.0
Tundra										
Tundra	11.7 ± 2.3	7.1 ± 1.7	1.3 ± 1.2	3.9 ± 1.3	11.1 ± 2.2	4.2 ± 0.8	2.6 ± 0.6	0.2 ± 0.3	2.3 ± 0.7	4.6 ± 0.8
Wetland	12.8 ± 2.3	8.3 ± 1.8	1.3 ± 1.1	3.8 ± 1.0	12.4 ± 2.1	4.5 ± 0.6	2.9 ± 0.6	0.2 ± 0.3	2.5 ± 0.5	5.1 ± 0.7
Ecotone	11.4 ± 3.1	6.7 ± 2.0	1.7 ± 1.4	3.7 ± 1.2	10.1 ± 2.6	4.4 ± 1.1	2.6 ± 0.9	0.4 ± 0.5	2.3 ± 0.7	4.5 ± 1.1
Road	4.7 ± 3.6	1.8 ± 2.0	0.3 ± 0.6	1.6 ± 1.4	4.6 ± 3.6	2.1 ± 1.6	0.7 ± 0.9	0.0 ± 0.2	0.7 ± 0.8	2.3 ± 1.8
Ecotone										
Wetland	11.5 ± 2.3	7.0 ± 1.3	2.0 ± 1.2	3.9 ± 1.5	9.5 ± 1.7	3.4 ± 0.8	2.5 ± 0.6	0.3 ± 0.3	2.0 ± 0.6	3.4 ± 0.8
Ecotone	12.3 ± 2.4	7.7 ± 1.7	2.2 ± 1.6	4.1 ± 1.4	10.1 ± 2.1	3.7 ± 0.7	2.7 ± 0.6	0.4 ± 0.4	2.1 ± 0.6	3.7 ± 0.8
Forest	11.6 ± 3.1	7.0 ± 2.1	2.8 ± 1.7	4.1 ± 1.6	8.8 ± 2.0	3.3 ± 0.7	2.5 ± 0.9	0.6 ± 0.5	1.9 ± 0.7	2.9 ± 0.6
Pond	9.3 ± 4.6	5.1 ± 3.8	2.1 ± 1.9	3.4 ± 1.6	7.2 ± 3.2	3.0 ± 0.7	1.6 ± 1.4	0.3 ± 0.4	1.6 ± 0.7	2.8 ± 0.8
Road	6.8 ± 5.4	2.6 ± 3.4	1.0 ± 1.7	1.7 ± 2.3	5.8 ± 3.7	2.5 ± 1.6	1.0 ± 1.3	0.2 ± 0.4	0.6 ± 1.0	2.7 ± 1.5

Table 5. Significant scales of spatial pattern (in m) for the different structural diversity measures along the four transects.

		Savanna	Woodland	Tundra	Ecotone
Overall	StrS	11-75	6-16	5-75	2-16
	StrD	5-9, 14-75	3-13, 44-51	5-75	5-15
Live	StrS	13-69	6-29	14-75	3-20, 51-75
	StrD	12-75	6-34	17-75	3-19, 48-75
Woody	StrS	11-75	3-23	3-75	2-75
	StrD	6-7, 13-75	3-33	3-75	2-23
Dead	StrS	9-75	3-14	4-75	2-15
	StrD	7-75	4-15	5-75	3-17
Substrate	StrS	3-75	3-31	6-75	3-20
	StrD	3-48, 72-75	2-18, 58-75	5-75	3-19

Figures

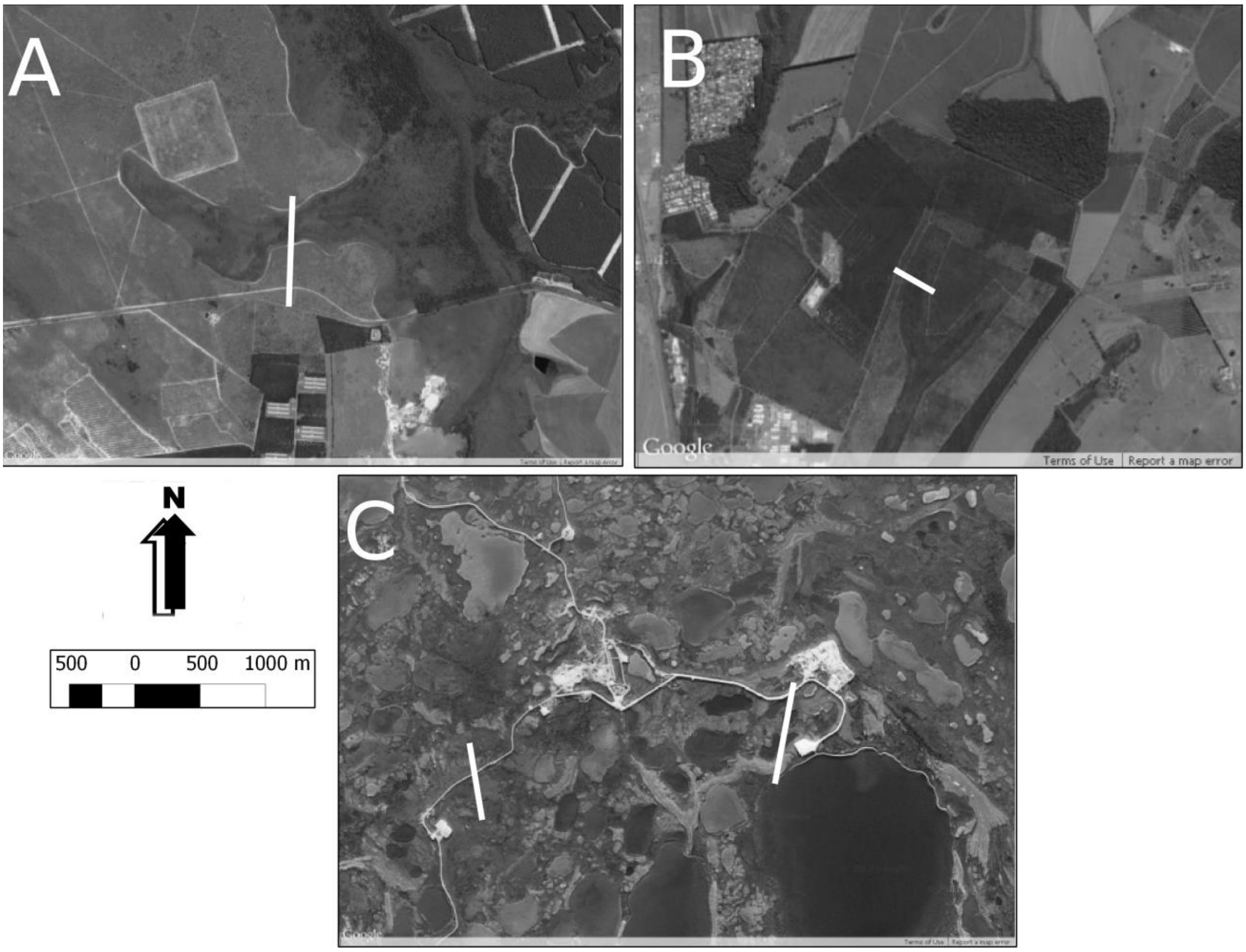

Figure 1. Satellite images of the study transects (white lines): a) the savanna transect at the Itirapina Ecological Station, b) the woodland transect in the cerrado reserve at the Federal University of São Carlos (both in São Paulo state, south-eastern Brazil), and c) the tundra (west) and ecotone (east) transects near the Churchill Northern Studies Centre (in Manitoba, western Canada).

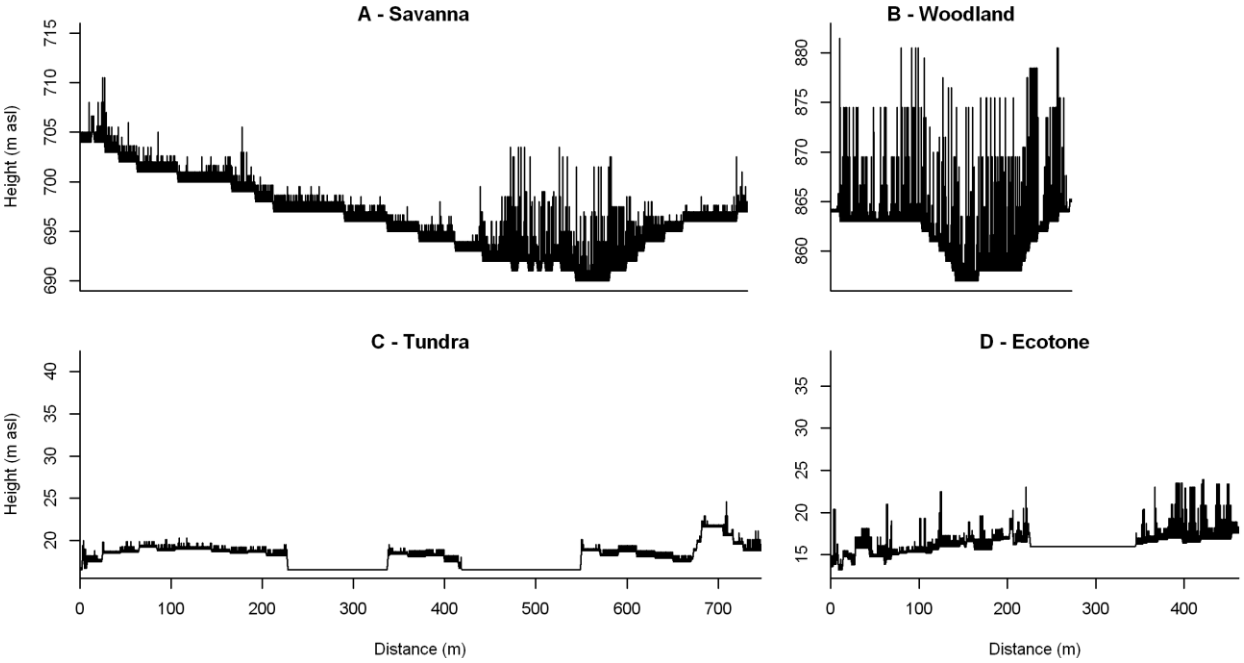

Figure 2. Topographic profile and vegetation structure of the four transects. The lower continuous line represents the ground layer and the vertical bars represent the maximum height of vegetation in each quadrat. The height range is equal in all plots to facilitate comparisons.

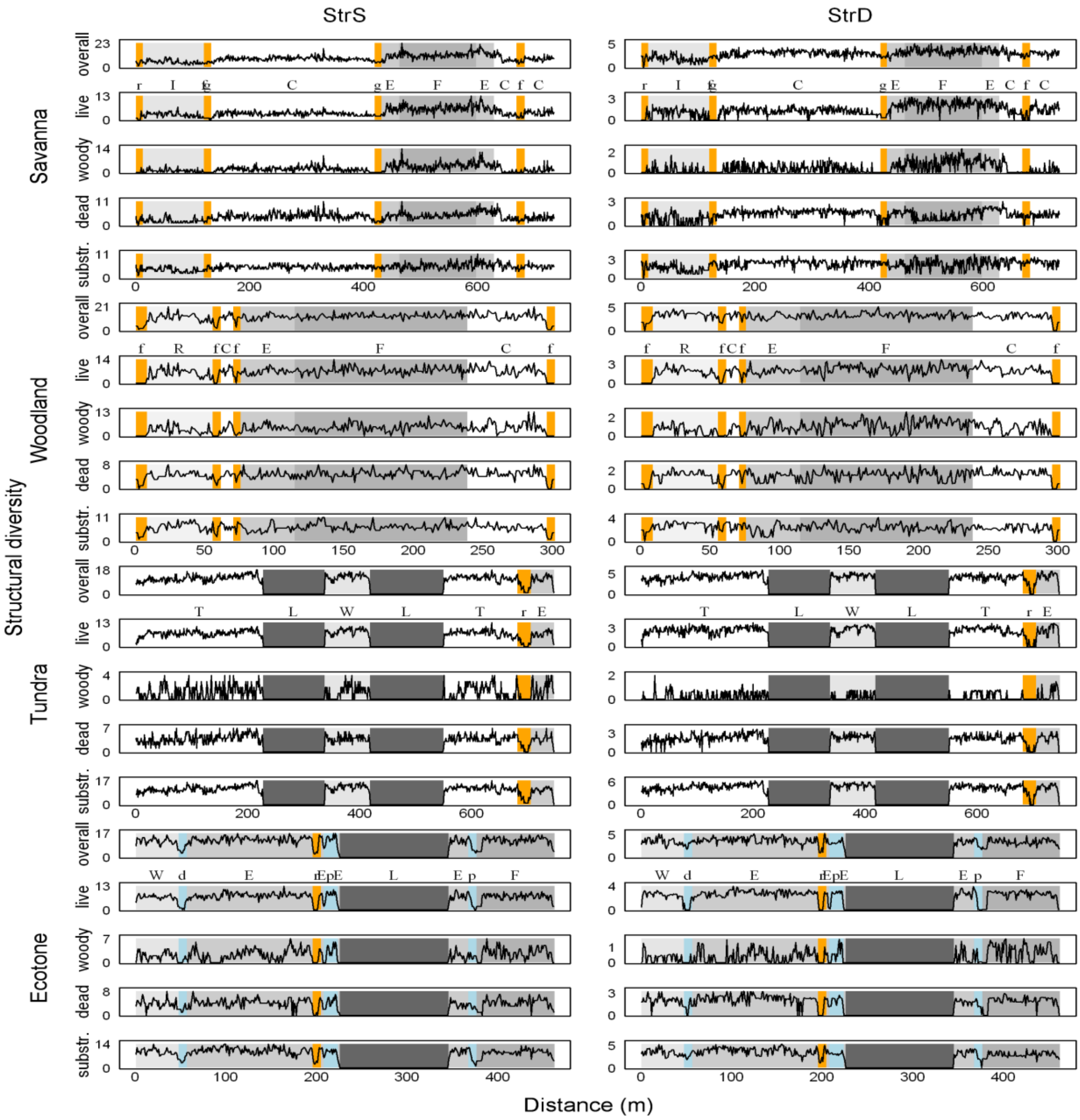

Figure 3. Variation in the number of structural elements (StrS) and the dissimilarity-based structural diversity index (StrD) for the different structural diversity measures along the savanna, woodland, tundra, and ecotone transects. The different colors and letters above the overall plots represent the plant communities composing each transect, with lowercase letters corresponding to disturbances or narrow areas: railroad and gravel road (r), invaded grassland (I), firebreak (f), regenerating firebreak with grass (g), savanna vegetation - *campo sujo* in Itirapina and typical *cerrado* in São Carlos (C), savanna-forest or tundra-forest transitions (E), riparian or boreal forest (F), regenerating cerrado with eucalypt trees (R), tundra (T), lakes (L), wet grassland (W), and pond (P). Refer to Table 1 for details.

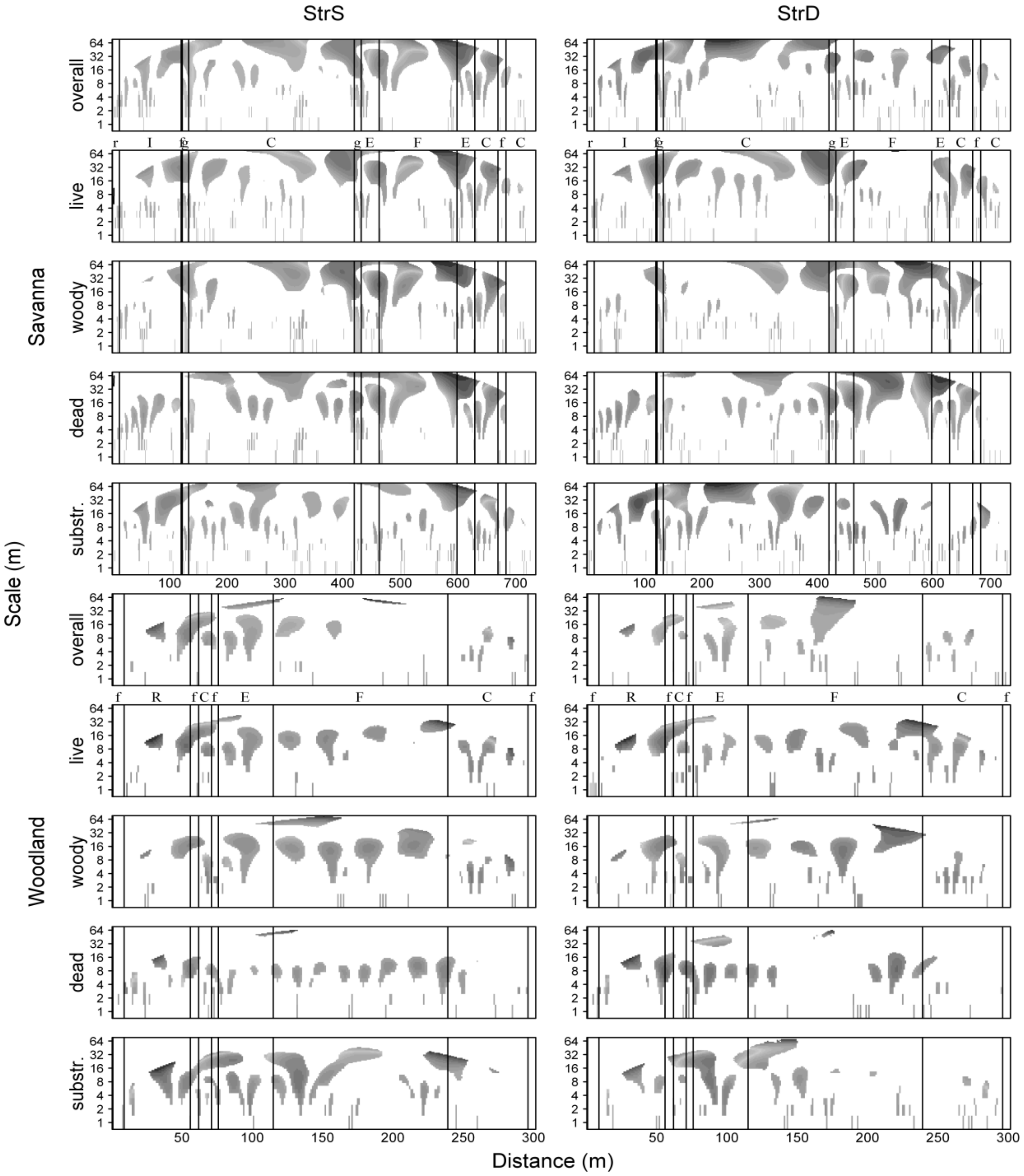

Figure 4. Results of the wavelet analysis of the number of structural elements (StrS) and the dissimilarity-based structural diversity index (StrD) for the different structural diversity measures along the savanna and woodland transects. Shades of gray indicate positions and scales for which the wavelet transform was significant (outside the 95% confidence interval). Light gray indicates negative wavelet transform values (gaps in structural diversity) whereas darker colors indicate positive values (patches). See Table 1 and Figure 1 fore details.

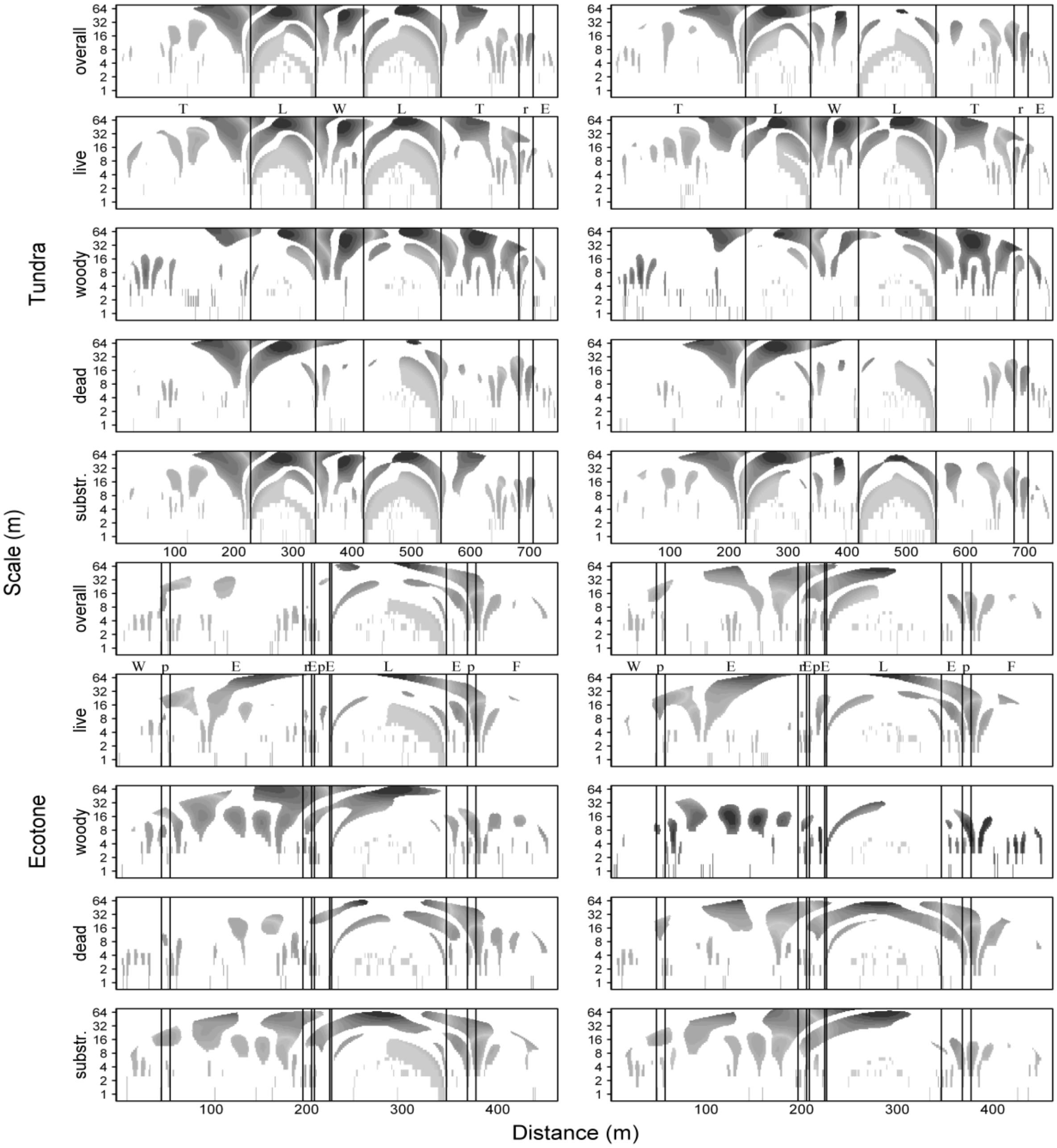

Figure 4. Results of the wavelet analysis of the number of structural elements (StrS) and the dissimilarity-based structural diversity index (StrD) for the different structural diversity measures along the tundra and ecotone transects. Shades of gray indicate positions and scales for which the wavelet transform was significant (outside the 95% confidence interval). Light gray indicates negative wavelet transform values (gaps in structural diversity) whereas darker colors indicate positive values (patches). See Table 1 and caption for Figure 1 fore details.

Chapter 4 – Do anthropogenic edges and plant functional traits explain spatial variation in a savanna plant community?

Resumo

Bordas de distúrbios lineares podem afetar a composição de um comunidade vegetal, já que algumas espécies podem ocorrer predominantemente em bordas enquanto outras estariam restritas ao interior da floresta. Tais padrões, no entanto, podem ser menos conspícuos ou até mesmo ausentes em vegetação naturalmente heterogênea com um estrato arbóreo descontínuo. Portanto, é importante levar em conta a variação natural na composição de espécies ao estudar padrões relacionados a bordas em vegetação heterogênea. Nós estudamos a variação espacial e os padrões relacionados bordas em uma área de cerrado brasileiro com alguns aceiros e diferentes fitofisionomias, além de verificarmos se a distribuição espacial de diferentes espécies vegetais está relacionada às suas formas de vida e síndromes de dispersão. Para isso, nós amostramos a comunidade vegetal em parcelas contíguas de 1x1 m ao longo de um transecto de 1334 m de comprimento, e usamos transformações de *wavelet* e modelos autoregressivos para analisar o padrão espacial de diferentes aspectos da comunidade vegetal (altura da vegetação, número de espécies, e o número de espécies com diferentes formas de vida, síndromes de dispersão e classes de altura). Nós amostramos um total de 170 espécies pertencentes a 50 famílias. A maior parte dos aspectos da comunidade vegetal mostrou padrões significativos em escalas de 10-20 m a 150-170 m, sendo que as menores escalas foram observadas para o número de espécies de graminóides e de plantas anemocóricas. Embora nós observamos alguns padrões relacionados a bordas, eles não foram observados em todas as bordas de aceiro e não eram diferentes dos padrões observados longe de borda, e nós não encontramos espécies que preferem ou que evitam bordas. A variação na composição de espécies pareceu não estar relacionada às suas formas de vida e síndromes de dispersão. Assim, parece que a variação nesta comunidade vegetal é causada principalmente por interações inter-específicas e pelo histórico de perturbação, e que a influência de borda não necessariamente resulta em padrões diferentes da variação natural na composição de espécies.

Abstract

Linear disturbance edges may affect the composition of a plant community, as some species may occur predominantly at edges and others may be restricted to interior forest. Such patterns, however, may be less conspicuous or even absent in naturally heterogeneous vegetation with a discontinuous tree cover. It is therefore important to account for the natural variation in species composition when assessing edge-related patterns in patchy vegetation. We studied the spatial variation and edge-related patterns in species composition in a Brazilian cerrado area with several firebreak edges and different phytophysiognomies, and assessed whether the spatial distribution of different plant species is related to their lifeforms and dispersal syndromes. We sampled the plant community in contiguous 1x1 m quadrats along a 1334 m-long transect, and used wavelet transforms and autoregressive models to assess the spatial pattern of different aspects of the plant community (vegetation height, species richness, and number of species with different lifeforms, dispersal syndromes, and height classes). We sampled a total of 170 species belonging to 50 families. Most aspects of the plant community showed significant patterns at scales from 10-20 m to 150-170 m, the smallest scales being observed for the number of graminoid species and of wind-dispersed species. Although we observed some edge-related patterns, they were not observed at all firebreak edges and did not differ from the patterns observed far from edges, and we did not find any edge-preferring or edge-avoiding species. The variation in species composition appeared to be unrelated to species' lifeforms and dispersal syndromes. Thus, it appears that variation in this plant community is driven mostly by inter-specific interactions, and that edge influence does not necessarily result in patterns outside the natural variation in species composition.

4.1. Introduction

The composition of a plant community may vary at a different spatial scales due to numerous ecological factors. For example, the alternation between patches dominated by grasses and by woody plants in African savannas, at the scale of tens to hundreds of meters, may be driven both by inter-specific competition between woody species (Wiegand et al. 2005, 2006) and by competition between trees and grasses, as well as by browsing (Porensky and Veblen 2012). Disturbances have also been shown to alter the composition of plant communities at similar scales (Fischer et al. 2012). Floristic composition, species richness, and abundance of different species may also be related to soil characteristics (Dantas and

Batalha 2011), regeneration dynamics and the influence of the surrounding vegetation (Dodonov et al. 2014b). Treefall gaps caused by natural mortality or by disturbances are an important source of spatial variation in both tropical and temperate forests (Bradshaw and Spies 1992), and the spatial pattern of the forest canopy may affect that of the understory vegetation (Kembel and Dale 2006, Halpern and Lutz 2013).

This natural variation may be altered by anthropogenic disturbances, such as roads and trails, possibly because of microclimatic variation (Delgado et al. 2007, Pohlman et al. 2007) or differential dispersal by mammals (Suárez-Esteban et al. 2013). Such edge-related patterns are known as edge influence, and have been observed next to linear disturbances in a variety of environments. For example, in a temperate forest, species composition next to gravel forest roads was significantly different from sites further into the forest, as some species were only found at the road verge whereas others preferred interior forest habitat (Avon et al. 2010). In subtropical forests, an increase in the abundance of some pioneer species with a concomitant decrease in understory species was observed at the edges of forest roads (Enoki et al. 2014). Edge influence from paved and unpaved roads was also observed in grasslands and steppes in western Canada (Gieselman et al. 2013), and roads and railroads have been shown to affect species composition in African and Australian grasslands (Morgan 1998, Cillers et al. 2008). Even narrow forest trails may alter species composition, as their edges may harbor a larger number of exotic species than would otherwise be expected (LaPaix et al. 2012).

Plant responses to edges vary among species. Thus, different patterns of edge influence were observed for different species at natural edges in the Amazon rainforest (Santos et al. 2014) and in Canadian boreal forest (Harper and Macdonald 2001). Pioneer, generalist and/or exotic species are often favored by edges (Morgan 1998, Cilliers et al. 2008), but this is not always the case (Enoki et al. 2014). The spatial distribution and edge-related patterns may also be related to other traits of different plant species, e.g. their dispersal syndromes (Jardim and Batalha 2009, Suárez-Esteban et al. 2013, Dodonov et al. 2014b). Finally, patterns may vary between plant lifeforms, for example with vines being more common at the edge and epiphytic ferns in the interior of a tropical forest (Magrach et al. 2014). Thus, a better understanding of how plant traits are related to the plants’ spatial variation and responses to edges may aid in predicting the effects of disturbances and explaining part of the variation in spatial pattern.

Edge influence from linear disturbances may be harder to detect in heterogeneous vegetation with a large amount of natural variation (Harper et al. 2005a), such as savannas. However, there have been, to our knowledge, no studies relating edge-related changes in the plant community to its natural patterns (but see Porensky 2011 and Donihue et al. 2013). We performed a study on the natural variation and edge-related changes in the plant community in a Brazilian cerrado fragment with several firebreak edges and different plant communities. Our specific objectives were: 1) to assess the scale of spatial variation in the plant community for different aspects of the plant community , 2) to assess whether this natural variation is affected by firebreaks; and 3) to assess whether the distribution of different species is related to their lifeform and dispersal syndrome . We analyzed the following characteristics of the plant community: , namely vegetation height, the total number of species, the number of species with different life forms and dispersal syndromes, and the number of species in different height classes.

4.2. Methods

4.2.1 Study site

We performed this study in a Brazilian cerrado fragment in São Carlos[5], Sao Paulo State, Brazil (21°58'34"S, 47°52'31"W; Supplementary Material 1.1). The soil is acidic, with low nitrogen and high aluminium (Dantas and Batalha 2011), and the climate is subtropical with dry winters and wet summers (Oliveira and Batalha 2005). The vegetation in the study area ranges from open field with scattered shrubs and trees to a closed savanna with trees up to 15 m high. These formations represent part of the variation that exists in the cerrado domain, which is composed of vegetation ranging from open field to low-canopy forest (Ribeiro & Walter 2008). One characteristic of the cerrado is its high regeneration capacity by resprouting, an important adaptation after recurrent fires and harvesting for forestry or pastures (Hoffmann and Solbrig 2003, Dodonov et al. 2014a). Part of our study area was occupied by an eucalypt plantation until approx. two decades prior to our study and is currently in an advanced stage of regeneration.

4.2.2 Sampling

We sampled the vascular plant community (excluding epiphytes) between September 2011 and June 2012 along a 1334 m-long transect divided into contiguous 1x1-m quadrats.

---

[5] The transect used here was also sampled for invasive graminoids (Chapter 2).

The transect encompassed several firebreaks as well as different plant communities with varying land use and disturbance history (Table 1). We identified all plant species growing within each quadrat and recorded the maximum height of each species. We collected plants that we were unable to identify in the field and identified them afterwards, with the aid of identification guides and specialists. Plants that were too small or did not have any leaves or other characteristics to permit their identification were measured but excluded from the calculation of species richness. We also measured canopy height as the maximum height of vegetation above the quadrat. We did not include eucalypt trees in the regenerating cerrado because these trees had been planted and do not represent natural processes, whereas the other species represent either the natural distribution of the different plant species or natural regeneration. We used a foldable ruler to measure heights up to 4 m and, afterwards, a 15-m expandable ruler to measure the heights of the taller plants.

4.2.3 Data analysis

We analyzed the spatial pattern of several attributes related to vegetation structure and species composition along the study transect. For vegetation structure, we used canopy height, the maximum and average height of the species found within each quadrat, and a measure of height inequality (Gini’s coefficient) of these species. Gini’s index is greater in quadrats with more unequal height between species, i.e. in quadrats containing both very tall and very short species, than in quadrats where all species have more or less the same height (Silvertown and Lovett-Doust 1993). For species composition, we used different measures of species richness per quadrat: the total number of species, the number of species of different lifeforms, and the number of species with different dispersal syndromes. We also analyzed the number of species above 40 cm in height (hereafter “medium-tall plants”), as individuals of this size are less likely to suffer extensive mortality, and species above 130 cm in height (hereafter “tall plants”), which correspond mostly to shrubs, trees, tall herbaceous plants and vines. The lifeforms and dispersal syndromes of the different species were determined from the literature. We considered the lifeforms graminoids, herbaceous plants (including subshrubs, or low-growing woody plants), vines, and woody plants (including both trees and shrubs), and the dispersal syndromes animal, wind, and self dispersal. We combined herbaceous plants and subshrubs because they are often sampled together as the “herbaceous component” (e.g. Batalha et al. 2001).

We assessed the scales of the spatial patterns by calculating scale variance of a continuous wavelet transform (CWT) on scales from 1 to 330 m. We used the Mexican hat wavelet template for this analysis because it is symmetrical (does not depend on the direction of the transect) and may be interpreted in a more straightforward way than some other wavelet templates (Percival and Walden 2000). We also used discrete wavelet transforms (DWT) to perform a multi-resolution analysis to assess the spatial variation and edge-related patterns in the response variables (Keitt and Urban 2005), on scales of 2, 4, 8, 16, 32, 64, 128 and 256 m; an additional scale, of 512 m, is represented by the scaling coefficient of the discrete wavelet transform (Burrus et al. 1998). We used Daubechie's least-asymmetrical S16 wavelet template for this analysis because it is similar in shape to the Mexican hat wavelet, but is more appropriate for a discrete wavelet transform (Percival and Walden 2000).

We assessed the significance of the scale variance and the multiresolution analysis by comparing the results with 95% confidence intervals generated from 999 simulations of a second-order autoregressive (AR2) model. One difficulty in using this model is that autoregressive models are directional (James et al. 2010), whereas our data were not. We therefore calculated AR2 models both ways (towards the end and the beginning of the transect), and used the average of the two models to create a combined AR2 model. As the transect was composed of different plant communities, we created separate models for each plant community in the transect. We used one-tailed confidence intervals for scale variance and two-tailed confidence intervals for the multiresolution analysis. The confidence intervals account for both small-scale spatial autocorrelation and for differences among the plant communities, and deviations from them may be seen as representing edge influence or ecological processes such as intra- and inter-specific competition. For the multiresolution analysis, we assume that patterns close to edges represent edge influence.

We used two additional analyses to assess the distribution of different species along the study transect and whether this distribution may be related to the plants' lifeforms and dispersal syndromes. We first performed a seriation analysis (Brower and Kile 1988), which reorganizes the presence-absence matrix (with species in rows and quadrats in columns) so that presences are concentrated along the diagonal, thus putting into evidence the gradients in species composition. Significance of the gradient was assessed with a Monte Carlo test. We then made a visual assessment of whether there are in patterns in lifeforms and dispersal syndromes along the gradient. We then performed a similarity analysis between the spatial patterns shown by different species (Rouyer et al. 2008). This analysis calculates a similarity measure between pairs of wavelet transforms, and is explained in Chapter 1. We used the Mexican hat wavelet and a maximum scale of 160 m, as previous analyses showed scales up to 160 m to be significant. We used cluster analysis with complete linkage to analyze the dissimilarity matrix, and made a visual assessment to determine whether the clustering was related to lifeforms and dispersal syndromes. We also performed a multivariate permutational analysis of variance (PERMANOVA; Anderson 2001) on the distance matrix to assess whether lifeform and dispersal syndromes significantly affected dissimilarities between species.

All analyses were performed in R 2.15.3 (R Core Team 2013), except for the seriation analysis, performed in Past 2.17c (Hammer et al. 2001). Gini's coefficient for height was calculated with the *ineq* function of the *ineq* package (Zeileis 2013). All wavelet analyses were performed with the *wmtsa* library (Constantine and Percival 2012), with the functions *wavCWT*, *wavDWT*, *wavMRD* and *reconstruct*. Code for the autoregressive models is available in Supplementary Material 3.1. Code for the wavelet similarity analysis was provided by T. Rouyer (Rouyer et al. 2007). The PERMANOVA analysis was performed with the function *adonis* of the package *vegan* (Oksanen et al. 2013).

4.3. Results

We sampled 170 species belonging to 50 families (Supplementary Material 4.2), with a total of 9214 occurrences (one occurrence corresponding to one species occurring on one quadrat) in the 1334 quadrats. In addition, we were not able to identify 1234 of the collected individuals. The most frequent species were *Andropogon leucostachyus* (Poaceae, 605 occurrences), *Melinis minutiflora* (Poaceae, 605 occurrences), *Miconia albicans* (Melastomataceae, 375 occurrences), *Smilax cissoides* (Smilacaceae, 302 occurrences), *Diodia alata* (Rubiaceae, 294 occurrences), *Urochloa decumbens* (Poaceae, 261 occurrences), *Byrsonima intermedia* (Malpighiaceae, 222 occurrences), and *Schefflera vinosa* (Araliaceae, 208 occurrences). Of these, *M. minutiflora* and *U. decumbens* are invasive grasses native to Africa; *A. leucostachyus* is a native grass; *M. albicans*, *B. intermedia* and *S. vinosa* are common cerrado shrubs or trees; *D. alata* is a herbaceous species; and *S. cissoides* is a vine. The most frequent families were Poaceae (2162 occurrences), followed by Fabaceae (697 occurrences), Melastomataceae (697 occurrences), Myrtaceae (555 occurrences), Asteraceae (474 occurrences) and Rubiaceae (385 occurrences). Shrubs and trees were the most common life form, followed by graminoids, whereas vines were the least common (Table 2). Animal-dispersed and wind-dispersed plants were approximately equally common overall, with animal dispersal more common in woody plants and wind dispersal in graminoids, whereas a large part of the herbaceous plants were self-dispersed (Table 2). Animal and wind dispersal were more or less equally common in vines.

Scales of spatial pattern differed among the variables, but all response variables except for canopy height showed significant patterns at a variety of scales, ranging from a few meters to tens and hundreds of meters (Table 2). The smallest scales of variation were observed for canopy height, with significant patterns at a scale of 2 m, and for the number of herbaceous, self-dispersed and tall species, with significant patterns at scales of 1 m. The significance of these small scales is probably due to the existence of “spikes”, or single quadrats (sets of two quadrats for canopy height) with much greater values than the adjacent quadrats (Figures 2 and 3). Maximum and mean plant height varied at scales of roughly 10 to 20 m, whereas height inequality had patterns at scales of roughly 50 to 150 m. Total species richness and the species richness of vines, herbaceous, woody, animal-dispersed and self-dispersed plants had patterns at scales of 10-30 to 120-150 m. Species richness of graminoids and medium-tall plants varied at scales of approximately 10 to 60-70 m, and that of wind-dispersed plants had patterns at scales of approximately 30 to 60 m. In addition, all variables except for canopy height and the number of herbaceous and self-dispersed species had significant patterns at scales of 150 to 200-300 m.

Patterns along the transect were most conspicuous for canopy height and species richness (Figures 2 and 3). However, a large part of this variation was accounted for by either differences between plant communities or small-scale autocorrelation, as indicated by the confidence intervals (Figures 4 and 5 and Supplementary Material 4.3). We were able to detect only a small number of edge-related patterns. Thus, there were significant or marginally significant peaks in canopy height next to four edges at scales of 2 to 16 m. Height inequality showed a peak close to one edge and a trough next to another edge, at scales of 8 to 64 m, but similar variation was also observed far from edges. Species richness (except for graminoids and self-dispersed plants) showed significant peaks close to two or three edges at scales from 2 to 16-64 m, but similar peaks were also observed far from edges (Figure 5; Supplementary Material 4.3); these peaks usually occurred next to the firebreak between the two regenerating cerrado areas. Conspicuous edge-related patterns at scales of 2 to 16 m were observed for the number of vine species next to three edges (Figure 1). No variables showed edge-related patterns at all edges.

The seriation analysis showed a significant gradient along the transect ($p<0.001$; Figure 6 and Supplementary Material 4.4), with some species occurring closer to the typical cerrado and others more common in the regenerating cerrado. Still, many species occurred throughout the entire transect, and no patterns in the species' lifeforms or dispersal syndromes were evident. The similarity analysis showed similar results, showing some groups of species with different distributions along the transect. Thus, some species occurred mostly in the typical cerrado (e.g. *Anacardium humile* and *Tabebuia ochracea*), others in the regenerating cerrado (e.g. *Eriosema crinitum*, *Miconia fallax* and *Anemopaegma glaucum*), and others in the typical cerrado and in part of the regenerating cerrado (e.g. *Annona dioica*, *Miconia stenostachya* and *Psidium cinereum*). A large part of the species, however, were found in all parts of the transect, either homogeneously (e.g. *Aegiphila lhotzkiana*, *Stryphnodendron obovatum*) or in scattered patches (e.g *Stryphnodendron adstringens*, *Ocotea pulchella*), and we did not find any edge-preferring or edge-avoiding species (Supplementary material 4.5). Similar to the seriation analysis, we did not detect any patterns in species lifeforms or dispersal syndromes, and neither factor was significant in the PERMANOVA analysis ($p>0.2$).

4.4. Discussion

We assessed the variation in vegetation structure and species composition, including edge influence, at a variety of scales. Plant species richness found in our study is similar that observed in previous studies in this and other cerrado areas (Batalha and Martins 2004, Urbanetz et al. 2013, Dodonov et al. 2014b), and the predominant families were also the ones commonly reported as dominant in cerrado vegetation (Oliveira-Filho and Ratter 2002, Filgueiras 2002). The landscape configuration of the study site, with narrow firebreaks bisecting areas with different degrees of regeneration, is also common in the cerrado and in other types of savanna. Thus, even though we sampled only one transect, we believe that our study site may be considered representative and our results may be generalized to other cerrado areas.

The observed scales of spatial pattern may be related to a variety of ecological processes. Spatial patterns at scales of 1-2 m are localized "spikes", or small areas with greater values of the response variable than the adjacent vegetation. Such patterns were observed only for four variables: canopy height, probably reflecting the existence of sparse tall trees; species richness of tall plants, possibly indicating micropatches with favorable soil conditions for greater height growth in many species; and number of herbaceous and self-dispersed species. These two latter patterns may be related, as self-dispersal was dominant in the herbaceous component. However, this was unexpected, as self-dispersal is characterized by short dispersal distances and therefore the distribution of self-dispersed plants is expected to be highly autocorrelated, which would be accounted for by the autoregressive model. The significance of this small scale may also be related to micropatches with favorable conditions, e.g. soil fertility and texture (related to water availability), or to secondary dispersal, common in self-dispersing plants (Howe and Smallwood 1982).

Intermediate-scale patterns of tens of meters, observed for height inequality and species richness, may reflect competition, which has been proposed as an important structuring factor in savannas at these scales (Wiegand et al. 2005). Disturbance history may also explain some of the variation in height inequality, as part of the study area burned six years before the study (pers. obs). Fire severity has been shown to vary at the scale of tens of meters (Werner 2010), and fires in the cerrado may alter the height structure of different species due to topkill and resprouting (Hoffman and Solbrig 2003). Fire-related mortality, however, is not common in the cerrado (Dodonov et al. 2014a), and patterns in species richness are not likely to be explained by it. Thus, we believe that these scales of pattern in species richness are related mostly to competition between plants of different sizes, and possibly to variation in soil factors.

In addition, the species richness of plants in different height classes did not vary at the same scales as that of different lifeforms, indicating that the spatial structure of the plant community may be affected independently by these two factors. In turn, the scales of variation in vegetation structure, represented by maximum and mean plant height, were smaller than for species composition, indicating that patterns in species composition and vegetation structure are not necessarily related to each other. The scales for the number of animal- and wind-dispersed species are probably related to the dispersal distances of these plants, which is much greater when animals are the dispersing agents. Finally, patterns at the scale of hundreds of meters may be related to variation in soil fertility and topography (Ruggiero et al. 2002).

Some of the edge-related patterns observed here have also been observed in previous studies on edge influence from linear disturbances. Thus, variation in vegetation height has been previously observed at cerrado edges (Dodonov et al. 2013), and increases in species richness and woody cover have been observed in other forest and savanna areas (Smit and Asner 2012, Suárez-Esteban et al. 2013). Even so, in our study, these patterns were neither consistent among variables nor exclusive to edges. Thus, although canopy height and some measures of species richness were above average next to some edges, similarly high values were also observed far from edges. This may indicate that edge influence does not necessarily result in new habitat types, as patterns in vegetation structure and composition the edges may be similar to those observed outside the range of edge influence. It appears that, for example, areas with a greater quantity of vines or invasive grasses, commonly observed at the edge (Magrach et al. 2014, Otto et al. 2013), may also occur naturally in the cerrado, and edges simply increase their frequency.

Overall, species with similar spatial patterns tended to be of different lifeforms and have different dispersal syndromes. Once again, this may indicate that competition is an important factor structuring these communities, as species with different lifeforms and dispersal syndromes would occupy different niches, reducing the competition between them. However, a more detailed assessment of the species' functional traits would be needed to test this hypothesis. Still, the lack of a relationship between dispersal type and distribution was surprising, as other studies in the *cerrado* showed that animal- and wind-dispersed plants responded to edges in different manners (Jardim and Batalha 2009; Dodonov et al. 2014); these studies, however, were performed either next to high-contrast plantation edges or along a regeneration gradient. The lack of clear patterns in animal-dispersed species indicates that seed-dispersing animals use the entire study area, and their movements are neither favored nor hampered by firebreaks; whereas the lack of pattern in wind-dispersed species indicates that, in contrast to what is observed at high-contrast edges in tropical forests (Laurance and Curran 2008), firebreak edges in the cerrado do not affect the wind patterns in the cerrado enough to affect the distribution of wind-dispersed species.

We conclude that: 1) given the large range of significant scales of variation, the lack of conspicuous edge-related patterns in species composition, and the lack of a relationship between the spatial distribution of different species and their functional traits, competition appears to be the main driver of spatial variation in the studied community; and 2) edge influence from firebreaks does not result in patterns outside the natural range of variation in vegetation structure and composition in the cerrado.

Acknowledgments

We thank the many people who helped us in the field during this study, especially Cinthya C. Santos, Carolline Z. Fieker, and Viviane C. Pereira; Andreza L. Braga for aid in organizing the unidentified plant species prior to identification; and Cinthya C. Santos for aid in gathering information on species lifeforms and dispersal syndromes. We also thank Danilo M. Silva, Marcelo B. Leite, Marco A. Batalha, Rafael O. Xavier and Yoshio Tamashiro for help in identifying plant species, and Tristan Rouyer for providing code for the wavelet similarity analysis. Financial support for the first author was granted by the National Council for Scientific and Technological Development (CNPq grant 141623/2011-0).

Supplementary material description

SM 4.1 – R code used for generating the second-order autoregressive models

SM 4.2 – List of species found along the transect, with their abundances, life forms and dispersal syndromes

SM 4.3 – Full multiresolution analysis for all response variables along the study transect

SM 4.4 – Higher-resolution plot of the seriation analysis, with species names

SM 4.5 – Continuous wavelet transform plots for the 106 species used in the similarity analysis

Tables

Table 1. Different plant communities along the study transect.

Section	Plant community[1]	Starting distance (m)
1	Invaded grassland	1
2	Firebreak	33
3	Invaded grassland	36
4	Firebreak	105
5	Typical cerrado	109
6	Firebreak	332
7	Regenerating cerrado	337
8	Firebreak	546
9	Regenerating cerrado	550
10	Firebreak	1329

[1] Invaded grassland: grassland with sparse trees and shrubs, and largely dominated by the invasive grass *Urochloa decumbens*; firebreak: a dirt road with almost no vegetation; typical cerrado: savanna vegetation with an open canopy, and both woody and herbaceous strata; regenerating cerrado: an area of cerrado previously occupied by a Eucalypt plantation with some remaining eucalypt trees.

Table 2. Frequency / species richness for groups of species of different lifeforms and dispersal syndromes. Eucalypts (*Eucalyptus grandis*, with 53 occurrences) were not included into this table because they had been planted in the area. Unidentified individuals were not included.

	Graminoids	Herbaceous and subshrubs	Vines	Shrubs and trees	Total
Animal-dispersed	261 / 1	366 / 21	350 / 2	2376 / 55	3353 / 79
Wind-dispersed	2046 / 22	118 / 6	395 / 9	685 / 19	3244 / 56
Self-dispersed	187 / 1	863 / 24	27 /2	253 / 6	1330 / 33
Total	2494 / 24	1347 / 50	772 / 13	3367 / 81	9214 / 170

Table 3 Significant scales of spatial pattern in relation to a second-order autoregressive model.

Response variable	Significant scales (m)
Canopy height	2
Maximum height	9-22, 219-330
Mean height	8-17, 232-261
Height inequality	48-145
Species richness (species per quadrat)	
Total	28-129, 246-330
Graminoids	15-68, 154-195
Herbaceous/subshrubs	1, 11-129
Vines	10-122, 219-330
Shrubs/trees	38-145, 219-330
Animal-dispersed	24-154, 207-330
Wind-dispersed	36-64, 129-330
Self-dispersed	1, 22-129
Medium height(above 40 cm)	14-60, 246-330
Tall height (above 130 cm)	1-2, 8-64, 184-330

Figures

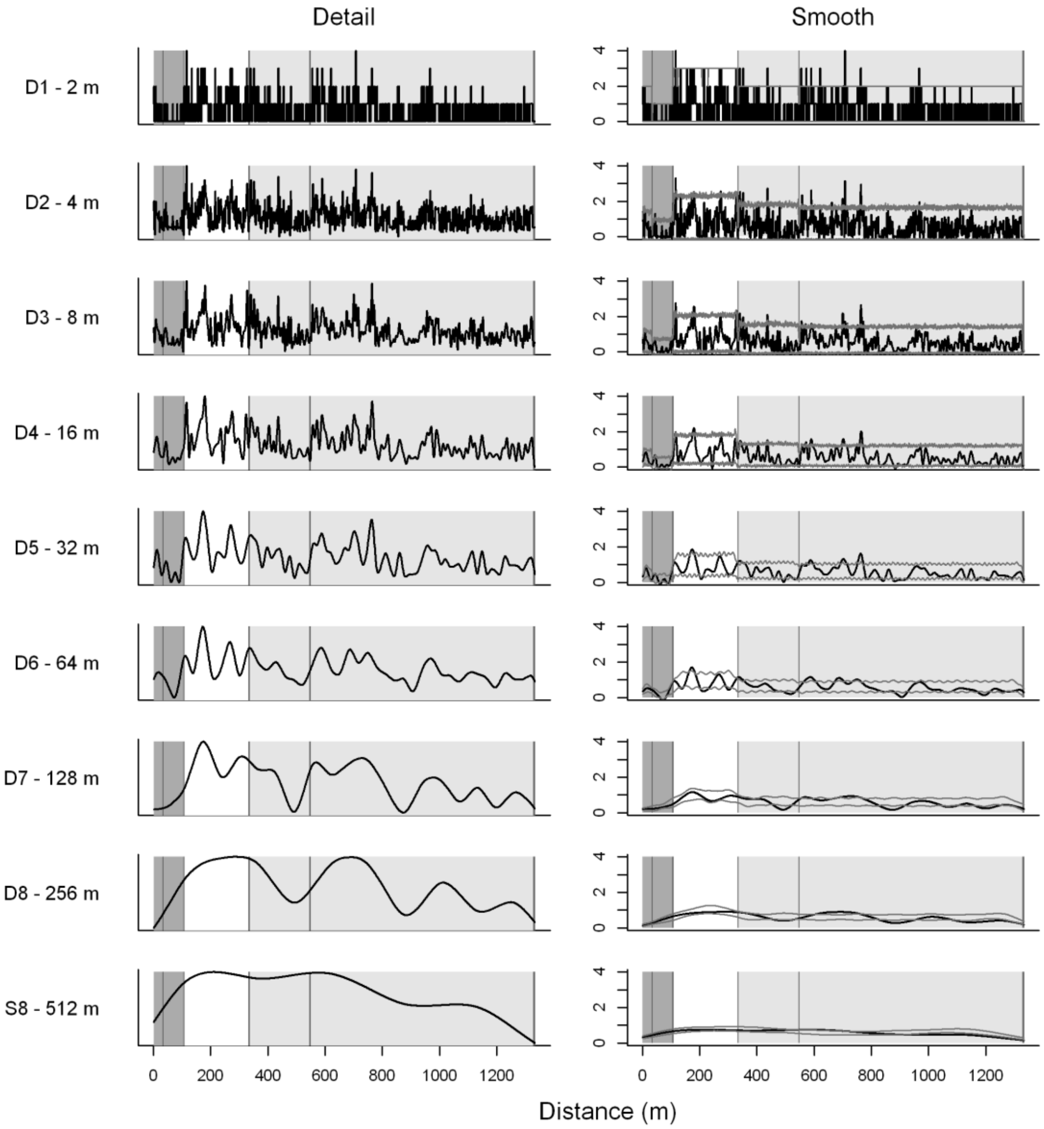

Figure 1. Example of a multi-resolution analysis with a discrete wavelet transform (Daubechie’s least-asymmetrical S16 wavelet) on the number of vine species found within the quadrats. The left panel shows the wavelet (D1 – D8) and scaling (S8) coefficients for each dyadic scale, whereas the right panel shows the reconstructed (smooth) signal for the corresponding scale. The gray line in the right panel shows the confidence intervals created from a second-order autoregressive model..

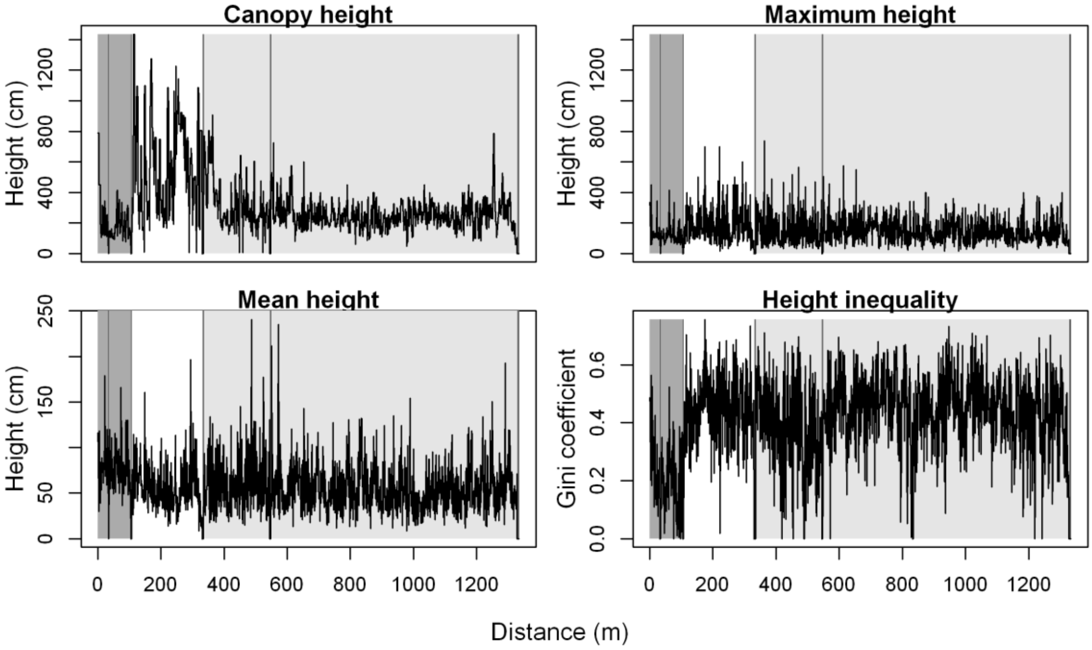

Figure 2. Variation in canopy height, maximum height, mean height, and height inequality along the transect. The background color represents the different plant communities: invaded grassland (dark gray), typical *cerrado* (white) and regenerating *cerrado* (light gray), and vertical lines represent the firebreaks. Note that mean height is not on the same scale as canopy and maximum height.

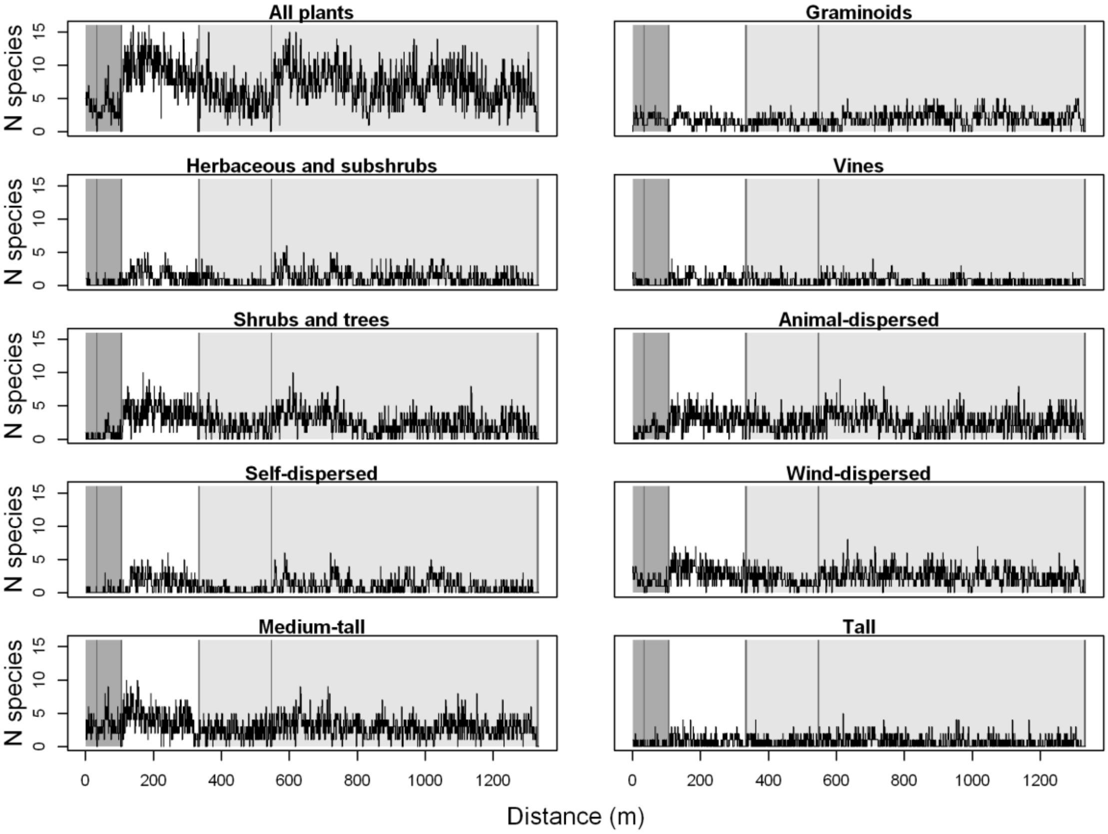

Figure 3. Variation in species richness (number of species per quadrat) along the transect, for all species, species with different lifeforms and dispersal syndromes, and medium-tall (above 40 cm) and tall (above 130 cm) species. Background color represents the different plant communities: invaded grassland (dark gray), typical *cerrado* (white) and regenerating *cerrado* (light gray), and vertical lines represent the firebreaks.

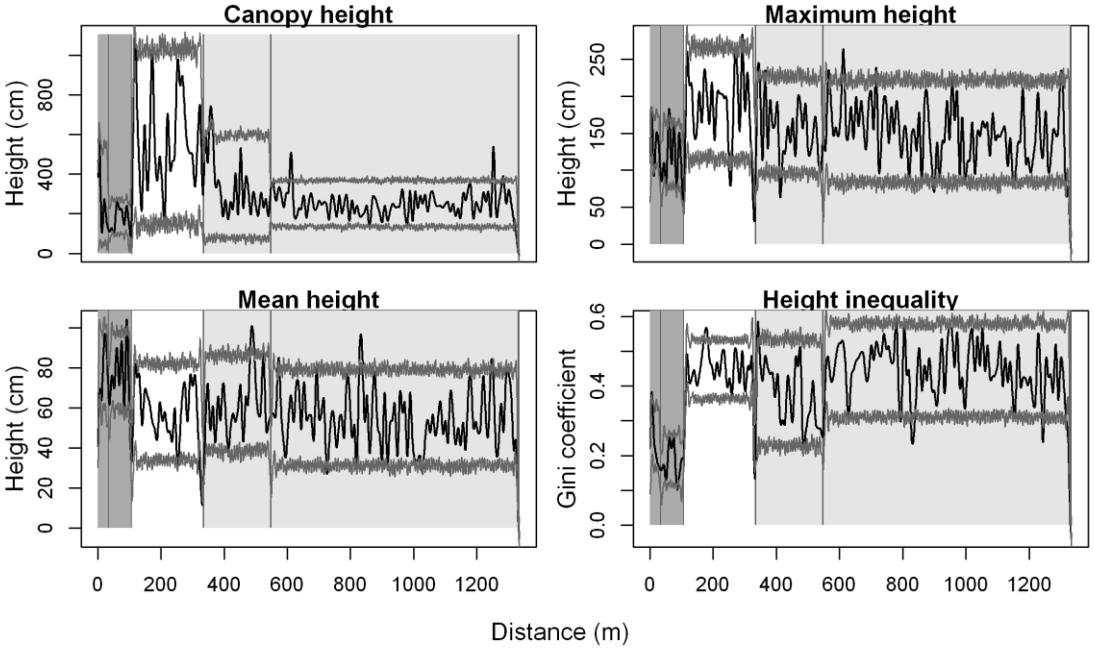

Figure 4. The smooth (reconstructed) signal for scale of 16 m for the variation in canopy height, maximum height, mean height, and height inequality along the transect. Background color represents the different plant communities: invaded grassland (dark gray), typical *cerrado* (white) and regenerating *cerrado* (light gray), and vertical lines represent the firebreaks. The smooth signal was reconstructed from a discrete wavelet transform with Daubechie’s least-asymmetrical S16 wavelet. Gray lines represent 95% confidence interval for a second-order autoregressive mode, simulated separately for each plant community.

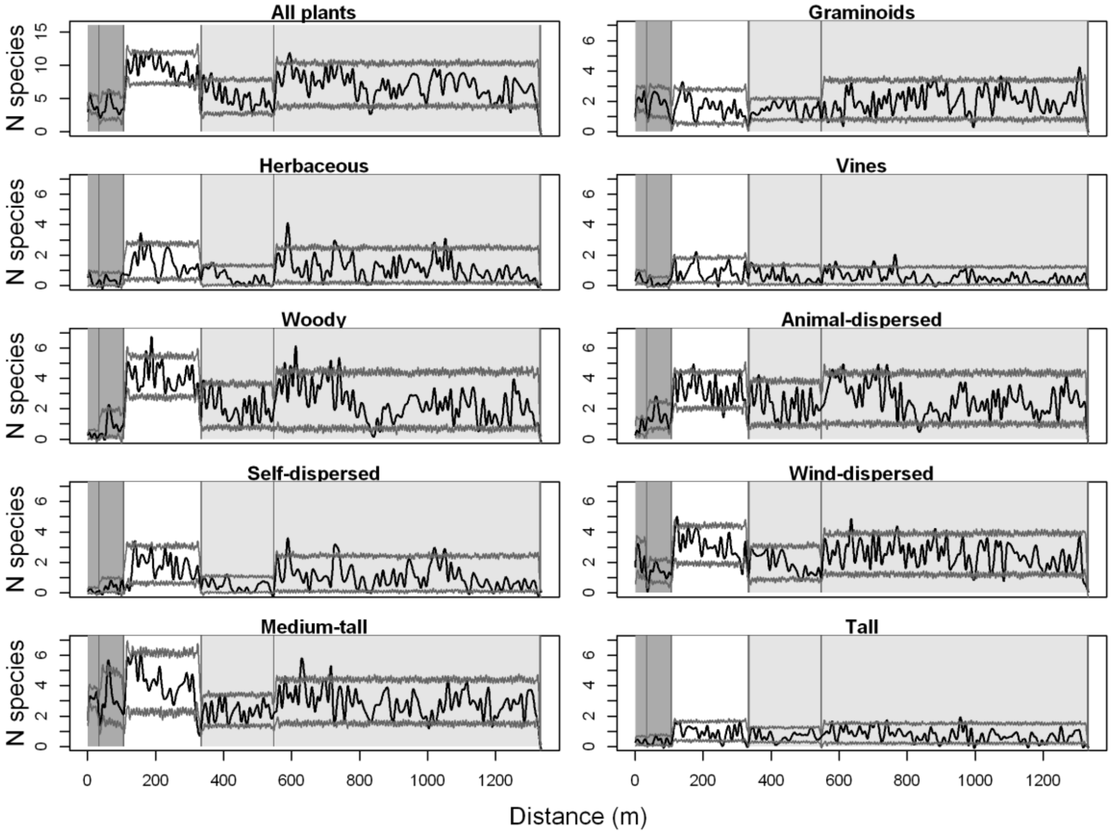

Figure 5. The smooth (reconstructed) signal for scale of 16 m for the variation in species richness (number of species per quadrat) along the transect, for all species, species with different lifeforms and dispersal syndromes, and medium-tall (above 40 cm) and tall (above 130 cm) species. The background color represents the different plant communities: invaded grassland (dark gray), typical *cerrado* (white) and regenerating *cerrado* (light gray), and vertical lines represent the firebreaks. The smooth signal was reconstructed from a discrete wavelet transform with Daubechie's least-asymmetrical S16 wavelet. Gray lines represent 95% confidence interval for a second-order autoregressive mode, simulated separately for each plant community.

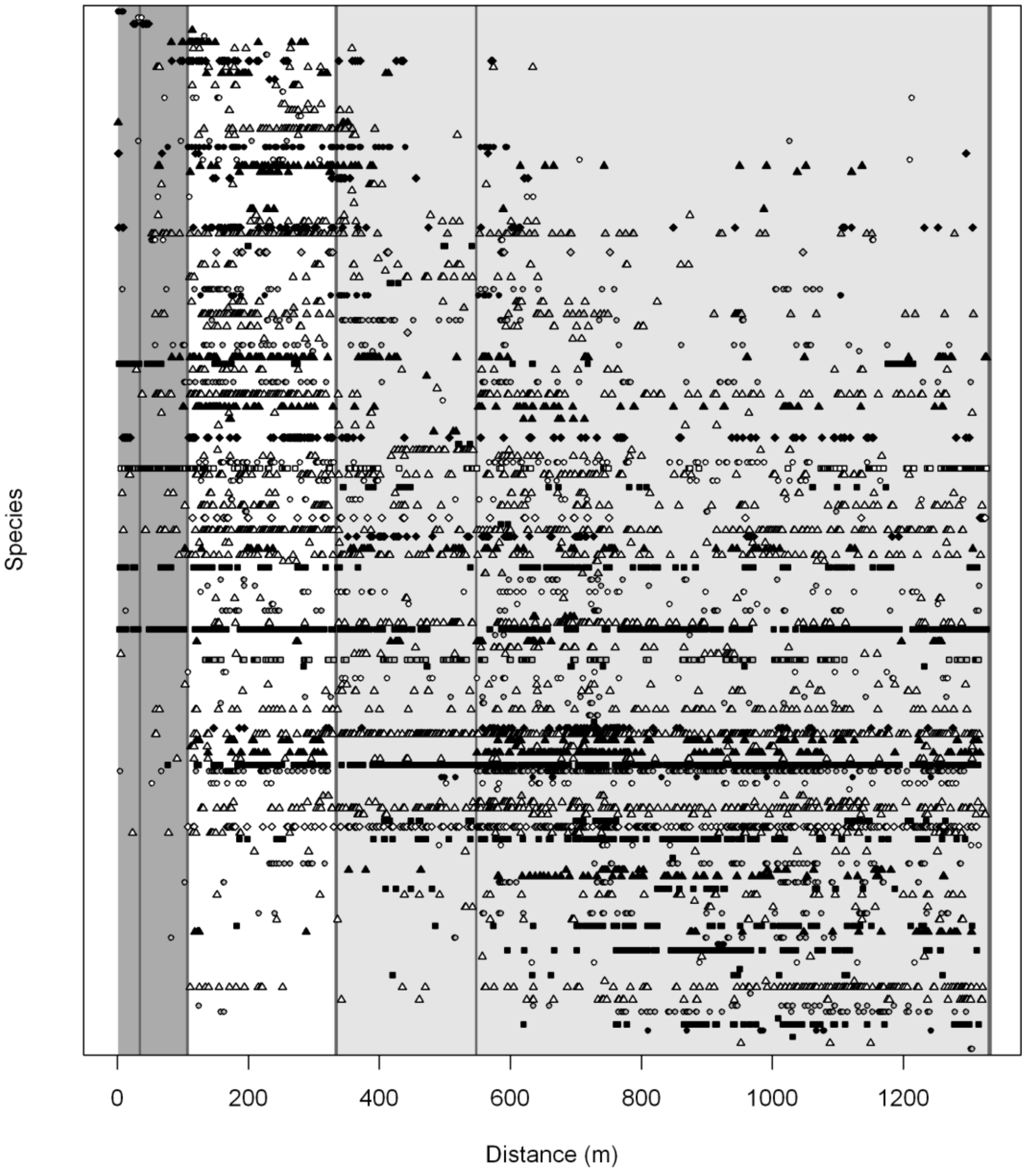

Figure 6. Seriation plot showing the variation in the plant community along the study transect. Each row corresponds to one species. Different symbol shapes represent different life forms and different colors represent different dispersal syndromes: herbaceous and subshrubs: circle; graminoids: square; liana: diamond; shrubs and trees: triangle; animal-dispersed: white symbols; wind-dispersed: black symbols; and self-dispersed: gray symbols. The background color represents the different plant communities: invaded grassland (dark gray), typical *cerrado* (white) and regenerating *cerrado* (light gray), and vertical lines represent firebreaks.

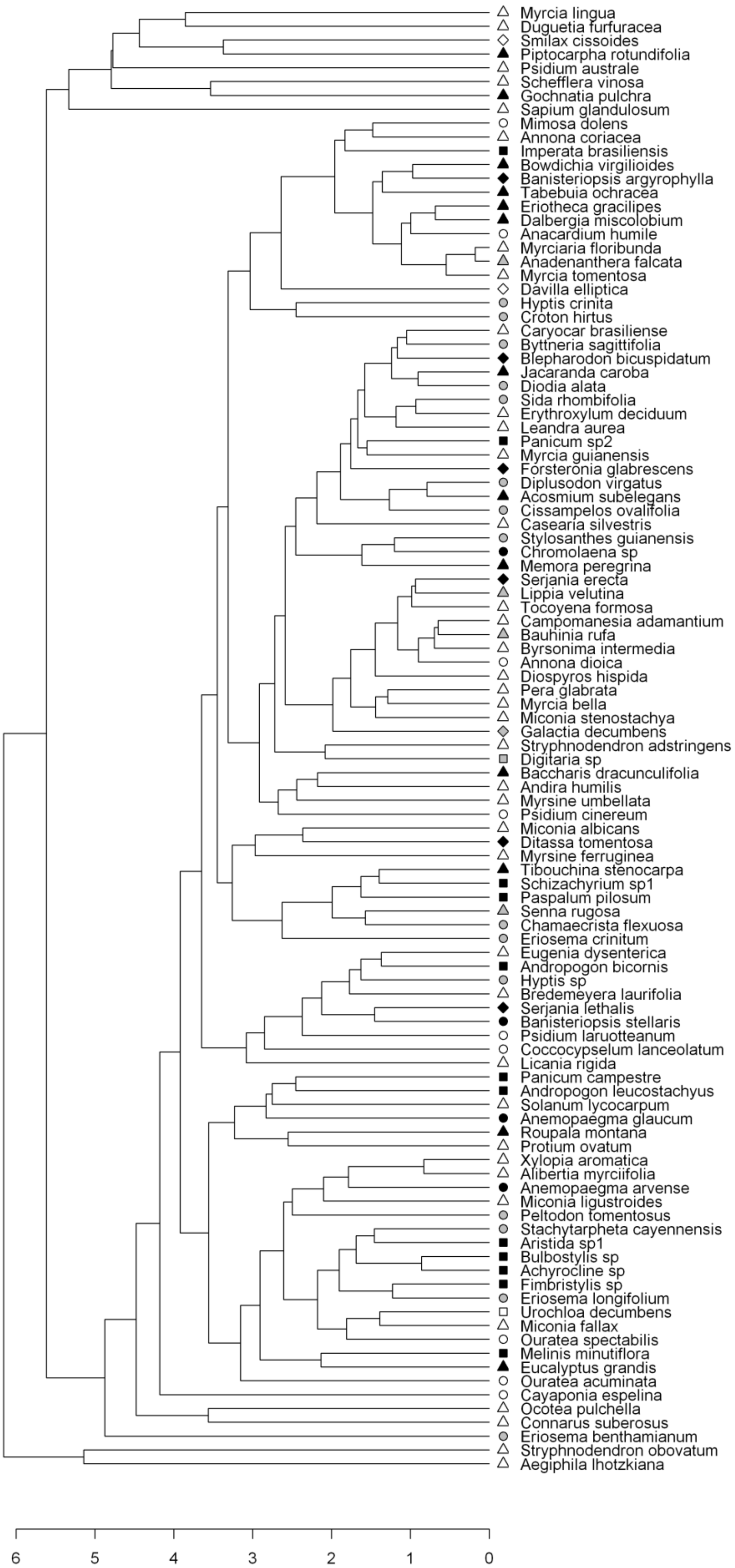

Figure 7.

Cluster analysis performed on the wavelet transform calculated for the 106 species found in at least 10 quadrats. The species are grouped according to their spatial distribution, i.e. species tending to occur in the same areas are placed closer in the cluster diagram. Symbols shapes represent lifeforms and symbols colors represent dispersal syndromes: herbaceous and subshrubs: circle; graminoids: square; lianas: diamond; shrubs and trees: triangle; animal-dispersed: white symbols; wind-dispersed: black symbols; and self-dispersed: gray symbols. See text for details on the analysis.

Final considerations

Overall, spatial pattern analysis coupled with wavelet transforms and null models is a powerful tool to assess variation in vegetation structure and make inferences on the effects of edges in heterogeneous vegetation. Further developments to the method may decrease the subjectivity present in the interpretation of some of the results. Such developments may include more complete null models, incorporating the various possible sources of variation in the spatial pattern (McIntire and Fajardo 2009) in addition to the small-scale autocorrelation and differences among plant communities. The confidence intervals may also be used to calculate effect sizes and significance of edge-related patterns.

Studies on spatial pattern usually have a small number of replicate transects with intensive sampling. In fact, some studies (Brosofske et al. 1999, James et al. 2010) used one single very long transect, as we used in Chapter 4. We sampled a total of five transects, but, as they all had different characteristics, it was not possible to use them as replicates. The solution employed in this study was to look for consistent patterns at different edges along each transect. One alternative would be to treat the edges as replicates in a statistical treatment, and we intend to work on such approach in the future.

Still, we were able to detect some consistent edge-related patterns across response variables and study sites. It is therefore apparent that low-contrast edges, such as firebreaks and low-traffic roads, may affect vegetation structure in areas as different as the Brazilian cerrado and the Canadian forest-tundra ecotone. However, these patterns were usually not outside the range of natural variation in the response variables, indicating that edges do not create new habitats but simply modify the distribution and frequency of naturally occurring patterns of vegetation. Conversely, high-contrast lake edges appeared to affect the adjacent vegetation on a larger scale. Thus, it is likely that high-contrast anthropogenic edges, such as maintained plantations and high-traffic roads, may also have large scale effects, and this should be explored in future studies.

References

Almeida-Neto, M., Prado, P. I., Kubota, U., Bariani, J. M., Aguirre, G. H., and Lewinsohn, T. M. 2010. Invasive grasses and native Asteraceae in Brazilian Cerrado. – Plant Ecol 209: 109-122.

Anderson, M. J. 2001. A new method for non-parametric multivariate analysis of variance. Austral Ecol 26: 32-46.

Asner, G. P., Levick, S. R., Kennedy-Bowdoin, T., Knapp, D. E., Emerson, R., Jacobson, J., Colgan, M. S., and Martin, R. E. 2009. Large-scale impacts of herbivores on the structural diversity of African savannas. Proc Natl Acad Sci 106: 4947-4952.

Avon, C., Bergès, L., Dumas, Y. and Dupouey, J. L. 2010. Does the effect of forest roads extend a few meters or more into the adjacent forest? A study on understorey plant diversity in managed oak stands. – For Ecol Manag 259: 1546-1555.

Ballantyne, M., Gudes, O., and Pickering, C. M. 2014. Recreational trails are an important cause of fragmentation in endangered urban forests: A case-study from Australia. Landscape Urban Plan 130: 112-124.

Batalha, M. A. and Martins, F. R. 2001. Floristics, frequency, and vegetation life-form spectra of a cerrado site. Braz J Biol 62: 203-209.

Batalha, M. A., Mantovani, W., and Mesquita Júnior, H. N. 2001. Vegetation structure in cerrado physiognomies in South-Eastern Brazil. Braz J Biol 61: 475-483.

Batllori, E., Blanco-Moreno, J. M., Ninot, J. M., Gutiérrez, E., and Carrillo, E. 2009. Vegetation patterns at the alpine treeline ecotone: the influence of tree cover on abrupt change in species composition of alpine communities. J Veg Sci 20: 814-825.

Bettez, N. D., Marino, R., Howarth, R. W., and Davidson, E. A. 2013. Roads as nitrogen deposition hot spots. Biogeochem 114: 149-163.

Bowering, M., LeMay, V., and Marshall, P. 2006 Effects of forest roads on the growth of adjacent lodgepole pine trees. Can J For Res 36:919–929.

Bradshaw, G. A. and Spies, T. A. 1992. Characterizing canopy gap structure in forests using wavelet analysis. – J Ecol 80: 205-215.

Brosofske, K. D., Chen, J., Crow, T. R., and Saunders, S. C. 1999. Vegetation responses to landscape structure at multiple scales across a Northern Wisconsin, USA, pine barrens landscape. – Plant Ecol 143: 203-218.

Brower, J.C. and Kile, M. M. 1988. Seriation of an original data matrix as applied to palaeoecology. Lethaia 21:79-93.

Burrus, C. S., Gopinath, R. A. and Guo, H. 1998.Introduction to wavelets and wavelet transforms: a primer. – Prentice Hall.

Cilliers, S. S., Williams, N. S. G. and Barnard, F. J. 2008. Patterns of invasive plant invasions in fragmented urban and rural grasslands across continents. – Landscape Ecol 23: 1243-1256.

Constantine, W. and Percival, D. 2012. wmtsa: Wavelet methods for time series analysis. R package version 1.1-1. Available from http://CRAN.R-project.org/package=wmtsa

Coppedge, B. R., Fuhlendorf, S. D., Harrel, W. C., and Engle, D. M. 2008. Avian community response to vegetation and structural features in grasslands managed with fire and grazing. Biol Conserv 141: 1196-1203.

Coutinho, L. M. 1978. O conceito de cerrado. – Revista Brasileira de Botânica 1: 17-23.

Coutinho, L. M. 1982. Aspectos ecológicos da saúva no cerrado. Os murundus de terra, as características psamofíticas das espécies de sua vegetação e a sua invasão pelo capim gordura. Revista Brasileira de Biologia 42: 147-153.

Dale, M. R. T. 1999. Spatial pattern analysis in plant ecology. – Cambridge Univ. Press.

Dale, M. R. T. and Mah, M. 1998. The use of wavelets for spatial pattern analysis in ecology. – J Veg Sci 9: 805-814.

Dantas, V. L. and Batalha, M. A. 2011. Vegetation structure: fine scale relationships with soil in a cerrado site. – Flora 206: 341-346.

Delgado, J. D., Arroyo, N. L., Arévalo, J. R., and Fernández-Palacios, J. M. 2007. Edge effects of roads on temperature, light, canopy cover, and canopy height in laurel and pine forests (Tenerife, Canary Islands). Landscape Urban Plan 81: 328-340.

Dias-Filho, M. B. and Carvalho, C. J. R. 2000. Physiological and morphological responses of *Brachiaria* spp. to flooding. – Pesquisa Agropecuária Brasileira 35: 1959-1966.

Didham, R. K. and Lawton, J. H. 1999. Edge structure determines the magnitude of changes in microclimate and vegetation structure in tropical forest fragments. Biotropica 31: 17-30.

Dodonov, P., Harper, K. A., Silva-Matos, D. M. 2013. The role of edge contrast and forest structure in edge influence: vegetation and microclimate at edges in the Brazilian cerrado. – Plant Ecol 214: 1345-1359.

Dodonov, P., Xavier, R. O., Tiberio, F. C. S., Lucena, I. C., Zanelli, C. B., and Silva-Matos, D. M. 2014a. Driving factors of small-scale variability in a savanna plant population after a fire. Acta Oecologica 56: 47-55.

Dodonov, P., Silva, D. M., and Rosatti, N. B. 2014b. Understorey vegetation gradient in a *Eucalyptus grandis* plantation between a savanna and a semideciduous forest. N Z J For Sci 44: 10.

Dong, X., Nyren, P., Patton, B., Nyren, A., Richardson, J., and Maresca, T. 2008. Wavelets for agriculture and biology: a tutorial with applications and outlook. BioScience 58: 445-453.

Donihue, C. M., Porensky, K. M., Foufopoulos, J., Riginos, C, and Pringle, R. M. 2013. Glade cascades: indirect legacy effects of pastoralism enhance the abundance and spatial structuring of arboreal fauna. Ecol 94: 827-837.

Eigenbrod, F., Hecnar, S. J., and Fahrig, L. 2009. Quantifying the road-effect zone: threshold effects of a motorway on anuran populations in Ontario, Canada. Ecol Soc 14: 24.

Enoki, T., Kusumoto, B., Igarashi, S., and Tsuji, K. 2014. Stand structure and plant species occurrence in forest edge habitat along different aged roads in Okinawa Island, southwestern Japan. J For Res 19: 97-104.

Fahrig, L. 2003. Effects of habitat fragmentation on biodiversity. Annu Rev Ecol Evol Syst 34: 487-515.

Falcão, P. F., Pinto, S. R. R., Wirth, R., and Leal, I. R. 2011. Edge-induced narrowing of dietary diversity of leaf-cutting ants. Bull Entomol Res 101: 305-311.

Filgueiras, T. S. 2002. Herbaceous plant communities. In: Oliveira, P. S. and Marquis, R. J. The cerrados of Brazil: ecology and natural history of a Neotropical savanna. Colombia University Press, New York.

Fischer, A., Fischer, H. S., and Lehnert, U. 2012. Avalanches creating high structural and floristic diversity in mountain mixed forests in the Alps. Biodivers Conser 21: 643-654.

Gamon, J. A., Kershaw, G. P., Williamson, S., and Hik, D. S. 2012. Microtopographic patterns in an arctic baydjarakh field: do fine-grain patterns enforce landscape stability? Environ Res Lett 7: 015502.

Gelbard, J. L. and Belnap, J. 2003. Roads as conduits for invasive plant invasions in a semiarid landscape. – Cons Biol 17: 420-432.

Gieselman, T. M., Hodges, K. E., and Vellend, M. 2013. Human-induced edges alter grassland community composition. – Biol Cons 158: 384-392.

Gorchov, D. L., Rondon, X. J., Cornejo, F., Schaefer, R. L., Janosko, J. M., and Slutz, G. 2013. Edge effects in recruitment of trees, and relationship to seed dispersal patterns, in cleared strips in the Peruvian Amazon. Ecol Res 28: 53-65.

Gray, A. N., Spies, T. A., and Pabst, R. J. 2012. Canopy gaps affect long-term patterns of tree growth and mortality in mature and old-growth forests in the Pacific Northwest. For Ecol Manag 281: 111-120.

Guerra, T. N. F., Rodal, M. J. N., Silva, A. C. B. L., Alves, M., Silva, M. A. M., and Mendes, P. G. A. 2013. Influence of edge and topography on the vegetation in an Atlantic Forest remnant in northeastern Brazil. J For Res 18: 200-208.

Halpern, C. B. and Lutz, J. A. 2013. Canopy closure exerts weak controls on understory dynamics: a 30-year study of overstory-understory interactions. Ecol Monogr 82: 221-237.

Hammer, Ø, Harper, D. A. T., and Ryan, P.D. 2001. PAST: Paleontological Statistics Software Package for Education and Data Analysis. Palaeontologia Electronica 4, 9 pp.

Harper, K. A. and Macdonald, S. E. 2001. Structure and composition of riparian boreal forest: new methods for analyzing edge influence. Ecol 82: 649-659.

Harper, K. A., Lesieur, D., Bergeron, Y., and Drapeau, P. 2004. Forest structure and composition at young fire and cut edges in black spruce boreal forest. Can J For Res 34: 289-302.

Harper, K. A., Macdonald, S. E., Burton, P. J., Chen, J., Brosofske, K. D., Saunders, S. C., Euskirchen, E. S., Roberts, D, Jaiteh, M. S., and Esseen, P. A. 2005a. Edge influence on forest structure and composition in fragmented landscapes. – Conserv Biol 19: 768-782.

Harper, K. A., Bergeron, Y., Drapeau, P., Gauthier, S., and Grandpré, L. 2005b. Structural development following fire in black spruce boreal forest. For Ecol Manag 206: 293-306.

Harper, K. A., Drapeau, P., Lesieur, D., and Bergeron, Y. 2014. Forest structure and composition at fire edges of different ages: evidence of persistent structural features on the landscape. For Ecol Manag 314: 131-140.

Hengeveld, R. 1989. Dynamics of biological invasions. – Chapman and Hall.

Hoffman, W. A. and Haridasan, M. 2008. The invasive grass, *Melinis minutiflora*, inhibits tree regeneration in a Neotropical savanna. – Austral Ecol 33: 29-36.

Hoffman, W. A., Jaconis, S., McKinley, K. L., Geiger, E. L., Gotsch, S. G and Franco, A. C. 2012. Fuels or microclimate? Understanding the drivers of fire feedbacks at savanna-forest boundaries. – Austral Ecol 37: 634-643.

Hoffmann, W. A. and Solbrig, O. T. 2003. The role of topkill in the differential response of savanna woody species to fire. For Ecol Manag 180: 273-286.

Hoffmann, W. A., Jaconis, S. Y., McKinley, K. L., Geiger, E. L., Gotsch, S. G., and Franco, A. C. 2012. Fuels or microclimate? Understanding the drivers of fire feedbacks at savanna-forest boundaries. Austral Ecol 37: 634-643.

Hofmeister, J., Hosek, J., Brabec, M., Hédi, R., and Modrý, M. 2013. Strong influence of long-distance edge effect on herb-layer vegetation in forest fragments in an agricultural landscape. Persp Plant Ecol Evol Syst 15: 293-303.

Honnay, O., Verheyen, K. and Hermy, M. 2002. Permeability of ancient forest edges for weedy plant species invasion. – For Ecol Manag 161: 109-122.

Howe, H. F. and Smallwood, J. 1982. Ecology of seed dispersal. Annu Rev Ecol Evol Syst 13: 201-228.

Huang, B. Q., Sun, Y. N., Yu, X. H., Luo, Y. B., Hutchings, M. J., and Tang, S. Y. 2009. Impact of proximity to a pathway on orchid pollination success in Huanglong National Park, South-West China.

Hudgins, L. and Huang, J. 1996. Bivariate wavelet analysis of Asia Monsoon and ENSO. – Adv Atm Sci 13: 299-312.

James, P. M. A., Fleming, R. A. and Fortin, M. J. 2010. Identifying scale-specific spatial boundaries using wavelets and null models: spruce worm defoliation in Ontario, Canada as a case study. – Landscape Ecol 25: 873-887.

James, P. M. A., Sturtevant, B. R., Townsend, P., Wolter, P., and Fortin, M. J. 2011. Two-dimensional wavelet analysis of spruce budworm host basal area in the Border Lakes landscape. Ecol Appl 21: 2197-2209.

Jardim, A. V. F. and Batalha, M. A. 2009. Dispersal syndromes related to edge distance in cerrado *sensu stricto* fragments of Central-Western Brazil. Braz Arch Biol Technol 52: 1167-1177

Jimu, L., Ngoroyemoto, N., and Mujuru, L. 2012. Structural diversity and regeneration of the endangered *Prunus africana* (Rosaceae) in Zimbabwe. Afr J Ecol 51: 102-110.

Jung, K., Kaiser, S., Böhm, S., Nieschulze, J., and Kalko, E. K. V. 2012. Moving in three dimensions: effects of structural complexity on occurrence and activity of insectivorous bats in managed forest stands. J App Ecol 49: 523-531.

Kauffman, J. B., Cummings, D. L. and Ward, D. E. 1994. Relationships of fire, biomass and nutrient dynamics along a vegetation gradient in the Brazilian cerrado. – J Ecol 82: 519-531.

Keitt, T. H. and Urban, D. L. 2005. Scale-specific inference using wavelets. Ecol 2497-2504.

Kembel, S. W. and Dale, M. R. T. 2006. Within-stand spatial structure and relation of boreal canopy and understorey vegetation. J Veg Sci 17: 783-790.

Klink, C. A. and Joly, C. A. 1989. Identification and distribution of C3 and C4 grasses in open and shaded habitats in Sao Paulo State, Brazil. – Biotropica 21: 30-34.

LaPaix, R., Harper, K. and Freedman, B. 2012. Patterns of invasive plants in relation to anthropogenic edges within urban forest remnants. – App Veg Sci 15: 525-535.

Laurance, W. F. and Curran, T. J. 2008. Impacts of wind disturbance on fragmented tropical forests: a review and synthesis. Austral Ecol 33: 399-408.

Laurance, W. F., Goosem, M., and Laurance, S. G. W. Impacts of roads and linear clearings on tropical forests. Trends Ecol Evol 24: 659-669.

Legendre, P. and Legendre, L. 1998. Numerical ecology. 2 ed. Elsevier Science B. V., Amsterdam.

Leise, T.L., Premananda, I., Paul, M.J., and Schwartz, W. J. 2013. Wavelet meets actogram. J Biol Rhythms 28: 6-68

Lima-Ribeiro, M. S. 2008. Efeitos de borda sobre a vegetação e estruturação populacional em fragmentos de Cerradão no Sudoeste Goiano, Brasil. Acta Bot Bras 22: 535-545.

Lippok, D., Walter, F., Hensen, I., Beck, S. G., and Schleuning, M. 2013. Effects of disturbance and altitude on soil seed banks of tropical montane forests. J Trop Ecol 29: 523-529.

Lippok, D., Beck, S. G., Renison, D., Hensen, I., Apaza, A. E., and Schleuning, M. 2014. Topography and edge effects are more important than elevation as drivers of vegetation patterns in a neotropical montane forest. J Veg Sci 25: 724-733.

Maechler, M., Rousseeuw, P., Struyf, A., Hubert, M., and Hornik, K.(2012). cluster: Cluster Analysis Basics and Extensions. R package version 1.14.3.

Magrach, A., Santamaría, L., and Larrinaga, A. R. 2013. Edge effects in a three-dimensional world: height in the canopy modulates edge effects on the epiphyte *Sarmienta repens* (Gesneriaceae). Plant Ecol 214: 965-973.

Magrach, A., Rodríguez-Pérez, J., Campbell, M., and Laurance, W. F. 2014. Edge effects shape the spatial distribution of lianas and epiphytic ferns in Australian tropical rain forest fragments. App Veg Sci 17: 754-764.

Manly, B. F. J.2007. Randomizations, bootstrap and Monte Carlo methods in biology. 3 ed. – Chapman and Hall/CRC.

Marchand, P. and Houle, G. 2006. Spatial patterns of plant species richness along a forest edge: what are their determinants? – For Ecol Manag 223: 113-124.

McElhinny, C., Gibbons, P., Brack, C., and Bauhus, J. 2005. Forest and woodland structural complexity: its definition and measurement. For Ecol Manag 218: 1-24.

McIntire, E. J. B. and Fajardo, A. 2009. Beyond description: the active and effective way to infer processes from spatial patterns. Ecol 90: 46-56.

Miatto, R. C. et al. 2011. Woody vegetation structure of Brazilian Cerrado invaded by *Pteridium arachnoideum* (Kaulf.) Maxon (Dennstaedtiaceae). – Flora 206: 757-762.

Miranda, H. S., Bustamante, M. C. M., and Miranda, A. C. 2002. The fire factor. In: Oliveira, P. S. and Marquis, R. J. The cerrados of Brazil: ecology and natural history of a Neotropical savanna. Colombia University Press, New York.

Molinari, N. A. and D’Antonio, C. 2014. Structural, compositional and trait differences between native- and non-native-dominated grassland patches. Funct Ecol 28: 745-754.

Morgan, J. W. 1998. Patterns of invasion of an urban remnant of a species-rich grassland in Southeastern Australia by non-native plant species. J Veg Sci 9: 181-190.

Oksanen, J., Blanchet, F. G., Kindt, R., Legendre, P., Minchin, P. R, O'Hara, R. B., Simpson, G. L., Solymos, P., Stevens, M. H. H., and Wagner, H. 2013. vegan: Community Ecology Package. R package version 2.0-8.

Oliveira, F. F. and Batalha, M. A. 2005. Lognormal abundance distribution of woody species in a cerrado fragment (São Carlos, southeastern Brazil). Revista Brasileira de Botânica 28: 39-45.

Oliveira-Filho, A. R. and Ratter, J. A. 2002. Vegetation physiognomies and woody flora of the Cerrado biome. In: Oliveira, P. S. and Marquis, R. J. The cerrados of Brazil: ecology and natural history of a Neotropical savanna. Colombia University Press, New York.

Ozdemir, I. and Donoghue, D. N. M. 2013. Modelling tree size diversity from airborne laser scanning using canopy height models with image texture measures. For Ecol Manag 295: 28-37.

Penone, C., Machon, N., Julliard, R. and Le Viol, I. 2012. Do railway edges provide functional connectivity for plant communities in an urban context? – Biol Cons 148: 126-133.

Percival, D. B. and Walden, A. T. 2000. Wavelet methods for time series analysis. – Cambridge Univ. Press.

Petchey, O. L. and Gaston, K. J. 2006. Functiona diversity: back to basics and looking forward. Ecol Lett 9: 741-758.

Petraitis, P. 2013. Multiple stable states in natural ecosystems. – Oxford Univ. Press.

Pires, J. P. A., Silva, A. G., and Freitas, L. 2014. Plant size, flowering synchrony and edge effects: what, how and where they affect the reproductive success of a Neotropical tree species. Austral Ecol 39: 328-336.

Pivello, V. R., Shida, C. N. and Meirelles, S. T. 1999a. Alien grasses in Brazilian savannas: a threat to the biodiversity. – Biodiv Conserv 8: 1281-1294.

Pivello, V. R., Carvalho, V. M. C., Lopes, P. F., Peccinini, A. A. and Rosso, S. 1999b. Abundance and distribution of native and alien grasses in a “cerrado” (Brazilian savanna) ecological reserve. – Biotropica 31: 71-82.

Pohlman, C. L., Turton, S. M. and Goosem, M. 2007 Edge effects of linear canopy openings on tropical rain forest understory climate. – Biotropica 39: 62-71.

Porensky, L. M. 2011. When edges meet: interacting edge effects in an African savanna. J Ecol 99: 923-934.

Porensky, L. M. and Veblen, K. E. 2012. Grasses and browsers reinforce landscape heterogeneity by excluding trees from ecosystem hotspots. Oecologia 168: 749-759.

Porensky, L. M. and Young, T. P. 2013. Edge-effect interactions in fragmented and patchy landscapes. Conserv Biol 27: 509-519.

R Core Team. 2013. R: A language and environment for statistical computing. - R Foundation for Statistical Computing.

Reis, C. M. and Zanchetta, D. 2006. Plano de manejo integrado das Unidades de Itirapina. – Secretaria do Meio Ambiente, São Paulo.

Ribeiro, J. F. and Walter, B. M. T. 2008. As principais fitofisionomias do bioma cerrado. – In: Sano, S. S., Almeida, S. P. and Ribeiro, J. F. Cerrado: ecologia e flora. Embrapa, pp. 151-212.

Ries, L., Fletcher, R. J., Battin, J., and Sisk, T. D. 2004. Ecological responses to habitat edges: mechanisms, models, and variability explained. Annu Rev Ecol Evol Syst 35: 491-522.

Rosenberg, M.S. and Anderson, C. D. 2011a. PASSaGE: Pattern Analysis, Spatial Statistics and Geographic Exegesis. Version 2 – User mannual. Met Ecol Evol 2: 229-232.

Rosenberg, M.S. and Anderson, C. D. 2011b. PASSaGE: Pattern Analysis, Spatial Statistics and Geographic Exegesis. Version 2. Met Ecol Evol 2: 229-232.

Rotholz, E. and Mandelik, Y. 2013. Roadside habitats: effects on diversity and composition of plant, arthropod, and small mammal communities. Biodivers Conserv 22: 1017-1031.

Rouyer, T., Fromentin, J. M., Stenseth, N. C. and Cazelles, B. 2008. Analysing multiple time scales and extending significance testing in wavelet analysis. – Mar Ecol Prog Series 359: 11-23.

Ruggiero, P. G. C., Batalha, M. A., Pivello, V. R., and Meirelles, S. T. 2002. Soil-vegetation relationships in cerrado (Brazilian savanna) and semideciduous forest, Southeastern Brazil. Plant Ecol 160: 1-16.

Sage, R. F., Christin, P. A. and Edwards, E. J. 2011. The C4 plant lineages of planet Earth. – J Exp Bot 62: 3155-3169.

Santos, L. O., Santos, L. O., Menezes, M. P. M., Beasley, C. R., and Mehlig, U. 2014. Composition and structure of a diverse tree community at the edges of a Brazilian Amazon rainforest island surrounded by marshes and mangrooves. Plant Ecol 215: 1469-1481.

Saunders, D. A., Hobbs, R. J., and Margules, C. R. 1991. Biological consequences of ecosystem fragmentation: a review. Conserv Biol 5: 18-32.

Schimmel, J., and Granström, A. 1997. Fuel succession and fire behavior in the Swedish boreal forest. Stand 1216: 1207-1216.

Silva, I. A., Cianciaruso, M. V., and Batalha, M. A. 2010. Abundance distribution of common and rare plant species of Brazilian savannas along a seasonality gradient. Acta Bot Bras 24: 407-413.

Silvertown, J. W. and Lovett-Doust, J. 1993. Introduction to Plant Population Biology. Blackwell Scientific Publications, London.

Smit, I. P. J. and Asner, G. P. 2012. Roads increase woody cover under varying geological rainfall and fire regimes in African savanna. – J Arid Envir 80: 74-80.

Strand, E. K., Robinson, A. P., and Bunting, S. C. 2007. Spatial patterns on the sagebrush steppe/Western juniper ecotone. Plant Ecol 190: 159-173.

Suárez-Esteban, A., Delibes, M., and Fedriani, J. M. 2013. Unpaved road verges as hotspots of fleshy-fruited shrub recruitment and establishment. Biol Conserv 167: 50-56.

Tews, J., Brose, U., Tielbörger, K., Wichmann, M. C., Schwager, M., and Jeltsch, F. 2004. Animal species diversity driven by habitat heterogeneity/diversity: the importance of keystone structures. J Biogeogr 31: 79-92.

Urbanetz, C., Shimizu, G. H. and Lima, M. I. S. 2013. An illustrated angiosperm flora of cerrado and riparian forest, São Carlos, Brazil. Check List 9: 275-293.

Vaughn, N. R., Asner, G. P., and Giardina, C. P. 2014. Centennial impacts of fragmentation on the canopy structure of tropical montane forest. Ecol App 24: 1638-1650.

Werner, P. A. 2010. Fine-scale patchiness of burns in a mesic eucalypt savanna differs with fire season and Sorghum abundance. Northern Terr Nat 22: 31-44.

Wiegand, K., Ward, D. and Saltz, D. 2005. Multi-scale patterns and bush encroachment in an arid savanna with a shallow soil layer. J Veg Sci 16: 311-320.

Wiegand, K., Saltz, D., and Ward, D. 2006.A patch-dynamics approach to savanna dynamics and woody plant encroachment – insights from an arid savanna. Persp Plant Ecol Evol Syst 7: 229-242.

Zeileis, A. 2013. ineq: Measuring inequality, concentration, and poverty. R package version 0.2-11.

Citation index

Supplementary material

SM 1.1 – Photos of the 1334 m-long transect in São Carlos, used for chapters 2 and 4

The invaded grassland, dominated by *U. decumbens* and *M. minutiflora*

The typical cerrado, with a denser tree cover

A firebreak between two regenearing cerrado areas

The regenearing cerrado area

SM 1.2 – Photos of the 301 m-long transect in São Carlos (“woodland transect”), used for chapter 3

The regenerating cerrado area

Firebreak separating the regenerating cerrado from the cerrado-forest transition

Riparian gallery forest

The edge between the riparian forest and the typical cerrado

SM 1.3 – Photos of the transect in Itirapina (“savanna transect”), used in chapters 2 and 3

Invaded grassland, dominated by *U. decumbens*

Campo sujo with the riparian gallery forest at the end

Transition area between the *campo sujo* and the riparian forest

Riparian gallery forest

SM 1.4 – Photos of the tundra transect near the Churchill Northern Studies Centre, used for chapter 3

Tundra, with numerous hummocks (micro-elevations)

Tundra dominated by fruticose lichens

A prostrate shrub patch

Edge of the lake at the end of the transect

SM 1.5 – Photos of the ecotone transect near the Churchill Northern Studies Center, used for chapter 3

A more open part of the ecotone transect, with large microtopographic variation

Willow (*Salix* aff *planifolia*) shrubs in the ecotone transect

The edge of the lake and a small pond next to it in the ecotone transect

Spruce forest, similar to the one in the ecotone transect

SM 2.1 - Pseudocode for generating the null models

Dodonov, P., Harper, K. A. and Silva-Matos, D. M. Spatial heterogeneity and edge influence on native and invasive graminoids in Brazilian cerrado.

These models are simulated from a vector of the values of the response variable for each quadrat.

The models MC1$_d$, CSR$_s$ and MC1$_s$ also require a second object with the type and the first and last distances corresponding to each of the sections composing a transect.

N: number of quadrats

S: number of sections

CSRh:

```
Reorder the quadrats, without replacement, along the transect (shuffle (transect, replace=F))
```

CSRs:

```
1) Create one dataset for each section of the transect. Firebreaks are considered as one type of section.
2) Create an object with the data corresponding to the first section in a random order
3) Randomize the datasets corresponding to sequence 2, 3... S, in sequence, and add them to the object created in 2).
```

MC1h:

```
1) Create three objects:
    a. Object 1 – the transect values, unchanged
    b. Object 2 – transect values from 2 to N followed by NA
    c. Object 3 – NA followed transect values from 1 to N-1
2) Make transition matrix:
    a. Create Object 4 with two repetitions of Object 1
    b. Create Object 5 combining Object 2 and Object 3
```

```
    c. Make a contingency table between these two new objects (table). The rows containing NA are ignored.
    d. Calculate the row sums of this contingency table (apply(MARGIN=1, FUN=sum))
    e. Divide each value of the contingency table by the corresponding row sum to create the transition matrix whose values vary from 0 to 1
3)  Set the first value of the simulated transect:
        i. Select a random position, t, along the transect (sample(1,1:N))
        ii. Assign a random value from the transect, $x_t$, to this position (sample)
4)  Simulate the rest of the simulated transect:
        i. Determine $x_{t-1}$ from the transition matrix:
        ii. Select row of the transition matrix corresponding to $x_t$
        iii. Create an object with the cumulative sum for the elements of this object (cumsum)
        iv. Generate a random number between 0 and 1 (runif(1))
        v. Test if each element of the cumulative sum object is greater than this random number
        vi. Select the first column of the transition matrix for which this test is true
        vii. Set $x_{t-1}$ as the cover class corresponding to this column
        viii. Repeat these steps for every $x_{t-j}$ using the row of the transition matrix corresponding to $x_{t-j+1}$, until t=1
        ix. Determine $x_{t+1}$ in the same manner, from the row of the transition matrix corresponding to $x_t$
        x. Repeat for every $x_{t+j}$ using the transition matrix for $x_{t+j-1}$, until t=N.
```

```
MC1d:
  1) Divide the transect into sections, based information in
     the Sections object:
       a. Create an object with the first and last distance of
          each section located between two firebreaks or
          between a firebreak and the beginning or end of the
          transect by combining sections that are not
          separated by a firebreak
       b. Create a second object with the first and last
          distance corresponding to each of the firebreaks
       c. Create an object, of length N, with TRUE for
          quadrats corresponding to firebreaks and FALSE for
          the other quadrats
  2) Create the overall transition matrix:
       a. Create the Objects 1, 2 and 3 from step 1) of MC1
       b. Modify these objects so that only adjacent quadrats,
          and not those separated by firebreaks, are used to
          calculate the transition matrix:
            i. Replace the values of Object 2 at positions
               corresponding to the last distances of each
               section by NA
           ii. Replace the values of Object 3 at positions
               corresponding to the first distance of each
               section by NA
       c. Remove the quadrats corresponding to the firebreaks
          from the three objects
       d. Create the transition matrix as in step 2) of MC1
  3) Simulate the data:
       a. Use the same simulation procedure as in MC1, for
          quadrats 1 to N
       b. Replace the quadrats corresponding to each of the F
          firebreaks by a random sample of the corresponding
          firebreak:
            i. Select, from the original data, the quadrats
               corresponding to firebreak F
           ii. Create an object with a random reordering of
               these quadrats (sample)
```

```
            iii. Add to this object the quadrats corresponding
                 to the next firebreak, also in a random order,
                 until all the firebreaks have been included
             iv. Use the object created in 1c) to select the
                 quadrats of the simulated dataset
                 corresponding to the firebreaks
              v. Replace these quadrats by the random sample of
                 the firebreaks created above.
```

MC1s:

```
1) Create the objects that will be used to calculate all
   the transition matrices:
      a. Create the Objects 1, 2 and 3 from step 1 of MC1
      b. Modify these objects so that only adjacent
         quadrats, and not those separated by firebreaks,
         are used to calculate the transition matrix:
            i. Replace the values of Object 2 at positions
               corresponding to the last distances of the
               different sections by NA
           ii. Replace the values of Object 3 at positions
               corresponding to the first distance the
               different sections by NA
2) Create the transition matrices for the different
   section types (e.g. grassland, forest, firebreak,
   regenerating firebreak):
      a. Select all the quadrats of Objects 1, 2 and 3
         corresponding to a given section type
      b. Create the transition matrix as in step 2 of MC1
3) Simulate the data:
      a. Simulate the data the first section, as in step 3
         of MC1, with the number of quadrats corresponding
         to this section and the transition matrix
         corresponding to this section type (so all
         sections occupied by, e.g. grassland will use the
         same transition matrix)
```

5) *Simulate the data for the other sections in the same way and add to the object created in 3a.*

SM 2.2 - R code for generating the null models

Dodonov, P., Harper, K. A. and Silva-Matos, D. M. Spatial heterogeneity and edge influence on native and invasive graminoids in Brazilian cerrado.

CSRh

```
setwd(choose.dir())
Itirapina = read.table(file.choose(), header=T) #First column
 for distance along the transect, then one column for each
 variable
Patches.Itir = read.table(file.choose(), header=T) #Three
 columns: section type, first quadrat of the section, last
 quadrat of the section
Nperm=4999
Nquad = nrow(Itirapina)
Nvar = ncol(Itirapina)-1
Vars = names(Itirapina)[2:(Nvar+1)]
for(l in 1:Nvar) {
 nome=Vars[l]
 dados=Itirapina[,nome]
 for(i in 1:Nperm) {
  foobar=sample(dados)
  if(i%%10 == 0) plot(foobar, type="l", main=c(nome,l,i))
  write.table(x=t(foobar), file=paste(nome,"_CSRh.txt"),
  sep=" ", append=T, row.names=F, col.names=F)
 }
import=as.matrix(read.table(paste(nome,"_CSRh.txt"), sep="",
 header=F))
dimnames(import) = NULL
import=t(import)
ncol(import)
nrow(import)
str(import)
import=cbind(dados, import)
```

```
 write.table(x=import, file=paste(nome,"_CSRh.txt"), sep=" ",
  row.names = F, col.names=F)
 }
```

CSRs

```
Itirapina = read.table(file.choose(), header=T)
Patches.Itir = read.table(file.choose(), header=T)
Nvar = ncol(Itirapina)-1
Vars = names(Itirapina)[2:(Nvar+1)]
patches=Patches.Itir
for(l in 1:Nvar) {
 nome=Vars[l]
 coisa=Itirapina[,nome]
 Nperm = 4999
 for (i in 1:Nperm) {
   for (j in 1:nrow(patches)) {
     foo = sample(coisa[(patches$Start[j]:patches$End[j])])
     if (j == 1) bar = foo else bar = c(bar,foo)
     }
   if(i<1000) plot(bar, type="l", main=c(nome,i))
   if(i>1000) print(c(nome,i))
   if(i==1000) plot(coisa, type="l", main=nome)
   write.table(x=t(bar),
 file=paste(nome,"_RestRand.txt",sep=""), sep=" ", append=T,
 row.names=F, col.names=F)
   }
 import=as.matrix(read.table(paste(nome,"_RestRand.txt",
 sep=""), sep="", header=F))
 dimnames(import) = NULL
 import=t(import)
 ncol(import)
 nrow(import)
 str(import)
 import=cbind(coisa, import)
 write.table(import, file=paste(nome,"_RestRand",".txt",
 sep=""), sep=" ", row.names = F, col.names=F)
```

```
  }
```

MC1h

```
Itirapina = read.table(file.choose(), header=T)
Patches.Itir = read.table(file.choose(), header=T)
Nperm=4999
Nquad = nrow(Itirapina)
Nvar = ncol(Itirapina)-1
Vars = names(Itirapina)[2:(Nvar+1)]
for(l in 1:Nvar) {
  nome=Vars[l]
  dados=Itirapina[,nome]
  foo = c(dados[2:length(dados)], NA)
  bar = c(NA, dados[1:(length(dados)-1)])
  dados.trans = data.frame(dados, foo, bar)
  foo = c(dados.trans$dados, dados.trans$dados)
  bar = c(dados.trans$foo, dados.trans$bar)
  transmatrix = table(foo,bar)
  sums = apply(transmatrix, 1, sum)
  transmatrix = transmatrix / sums
for (i in 1:Nperm) {
    foo=numeric(Nquad)
    foo.patch = dados.trans$dados
    foo.trans = transmatrix
    foo.classes = colnames(foo.trans)
    first = sample(length(foo),1)
    foo[first] = sample(foo.patch,1)
    #Going backward
      if (first != 1 ) {
      for(k in first:2) {
        ref = as.character(foo[k])
        trans.row = foo.trans[ref,]
        trans.row = cumsum(trans.row)
        random = runif(1)
        test = random > trans.row
```

```
        foo[k-1] = foo.classes[sum(test)+1]
        if (i<10) plot(foo, type="l", main=c(nome,l,i,k))
        if (i>10) print(c(nome,l,i,k))
        }
      }
      if (first != length(foo)) {
      for(k in first:(length(foo)-1)) {
        ref = as.character(foo[k])
        trans.row = foo.trans[ref,]
        trans.row = cumsum(trans.row)
        random = runif(1)
        test = random > trans.row
        foo[k+1] = foo.classes[sum(test)+1]
        if (i<10) plot(foo, type="l", main=c(nome,l,i,k))
        if (i>10) print(c(nome,l,i,k))
        }
      }


    foobar=as.numeric(foo)
    if(i%%10 == 0) plot(foobar, type="l", main=c(nome,i))
    write.table(x=t(foobar), file=paste(nome,"_MC1h.txt"),
      sep=" ", append=T, row.names=F, col.names=F)
  }
import=as.matrix(read.table(paste(nome,"_MC1h.txt"), sep="",
 header=F))
dimnames(import) = NULL
import=t(import)
ncol(import)
nrow(import)
str(import)
import=cbind(dados, import)
write.table(x=import, file=paste(nome,"_MC1h.txt"), sep=" ",
 row.names = F, col.names=F)
}
```

MC1d

```
Itirapina = read.table(file.choose(), header=T)
Patches.Itir = read.table(file.choose(), header=T)
Nperm=4999
Nquad = nrow(Itirapina)
patches = Patches.Itir
patches.veg = patches[patches$Patch != "firebreak" &
 patches$Patch != "firebreak_regrowth" & patches$Patch !=
 "railroad",]
section = numeric(nrow(patches.veg) )
section[1] = 1
for (i in 2: nrow(patches.veg) ) {
 section[i] = ifelse(patches.veg$Start[i]==(patches.veg$End[i-
 1]+1),section[i-1],section[i-1]+1)
 }
foo=aggregate(patches.veg$Start,by=list(section),FUN=min)$x
bar=aggregate(patches.veg$End,by=list(section),FUN=max)$x
patches.veg=data.frame(unique(section),foo,bar)
names(patches.veg)=c("Patch","Start","End")
patches.disturb = patches[patches$Patch == "firebreak" |
 patches$Patch == "firebreak_regrowth" | patches$Patch ==
 "railroad",]
quad.disturb = numeric(Nquad)
quad.dist = 1:Nquad
for(i in 1:nrow(patches.disturb)) {
 quad.disturb = quad.disturb + (quad.dist >=
 patches.disturb$Start[i] & quad.dist <=
 patches.disturb$End[i])
 }
quad.disturb = as.logical(quad.disturb)
Nvar = ncol(Itirapina)-1
Vars = names(Itirapina)[2:(Nvar+1)]
patches=Patches.Itir
for(l in 1:Nvar) {
 nome=Vars[l]
 dados=Itirapina[,nome]
```

```
 foo = c(dados[2:length(dados)], NA)
 bar = c(NA, dados[1:(length(dados)-1)])
 foo[patches.veg$End] = NA
 bar[patches.veg$Start] = NA
 dados.trans = data.frame(dados, foo, bar)
 dados.trans = dados.trans[quad.disturb==F,]
 foo = c(dados.trans$dados, dados.trans$dados)
 bar = c(dados.trans$foo, dados.trans$bar)
 transmatrix = table(foo,bar)
 sums = apply(transmatrix, 1, sum)
 transmatrix = transmatrix / sums
for (i in 1:Nperm) {
   foo=numeric(Nquad)
   foo.patch = dados.trans$dados
   foo.trans = transmatrix
   foo.classes = colnames(foo.trans)
   first = sample(length(foo),1)
   foo[first] = sample(foo.patch,1)
   #Going backward
     if (first != 1 ) {
     for(k in first:2) {
       ref = as.character(foo[k])
       trans.row = foo.trans[ref,]
       trans.row = cumsum(trans.row)
       random = runif(1)
       test = random > trans.row
       foo[k-1] = foo.classes[sum(test)+1]
       if (i<10) plot(foo, type="l", main=c(nome,l,i,k))
       if (i>10) print(c(nome,l,i,k))
       }
     }
     if (first != length(foo)) {
     for(k in first:(length(foo)-1)) {
       ref = as.character(foo[k])
       trans.row = foo.trans[ref,]
       trans.row = cumsum(trans.row)
       random = runif(1)
```

```
       test = random > trans.row
       foo[k+1] = foo.classes[sum(test)+1]
       if (i<10) plot(foo, type="l", main=c(nome,l,i,k))
       if (i>10) print(c(nome,l,i,k))
       }
     }
   foobar=as.numeric(foo)
   for(k in 1:nrow(patches.disturb) ) {
     if(k == 1){
      foo.disturb = sample (dados[patches.disturb$Start[k]:
 patches.disturb$End[k]])
     next }
   foo.disturb=c(foo.disturb,sample(dados[patches.disturb$Start[
 k]:patches.disturb$End[k]]))
     }
   foobar[quad.disturb] = foo.disturb
   foobar=as.numeric(foobar)
   if(i%%10 == 0) plot(foobar, type="l", main=c(nome,i))
   write.table(x=t(foobar), file=paste(nome,"_MC1d_not.txt"),
     sep=" ", append=T, row.names=F, col.names=F)
 }
import=as.matrix(read.table(paste(nome,"_MC1d_not.txt"), sep="",
 header=F))
dimnames(import) = NULL
import=t(import)
ncol(import)
nrow(import)
str(import)
import=cbind(dados, import)
write.table(x=import, file=paste(nome,"_MC1d.txt"), sep=" ",
 row.names = F, col.names=F)
}
```

MC1s

```
Itirapina = read.table(file.choose(), header=T)
```

```
Patches.Itir = read.table(file.choose(), header=T)
patches = Patches.Itir
patch.col=factor()
lengths=patches$End-patches$Start+1
patch.col=rep(as.character(patches[1,1]), lengths[1] )
for (i in 2:nrow(patches)) {
 patch.col=c(patch.col, rep(as.character(patches[i,1]),
 lengths[i] ) )
 }
patch.col=as.factor(patch.col)
patches.quad = as.character(patch.col)
Nvar = ncol(Itirapina)-1
Vars = names(Itirapina)[2:(Nvar+1)]
patches=Patches.Itir
 for(l in 2:Nvar) {
 nome=Vars[l]
 dados=Itirapina[,nome]
 Nquad = length(dados)
 foo = c(dados[2:Nquad], NA)
 bar = c(NA, dados[1:(Nquad-1)])
 dados.trans = data.frame(dados, foo, bar)
 Npatches = nrow(patches)
 patchtypes = unique(patches.quad)
 Npatchtypes = length(patchtypes)
 dados.trans$loc = character(Nquad)
 patches.quad.next = c(patches.quad[2:Nquad],NA)
 patches.quad.prev = c(NA, patches.quad[1:Nquad-1])
 dados.trans$loc = ifelse(patches.quad == patches.quad.next &
   patches.quad == patches.quad.prev, "middle",
   ifelse(patches.quad != patches.quad.prev, "first",
   ifelse(patches.quad != patches.quad.next, "last", "error")))
 dados.trans$loc[1] = "first"
 dados.trans$loc[Nquad] = "last"
 #Make a transition matrix per patch type
 trans.matrices = list()
 for(i in 1:Npatchtypes) {
   patchtype = patchtypes[i]
```

```
  foobar.lines = (1:Nquad)[patches.quad == patchtype]
  foobar = dados.trans[foobar.lines,]
  foobar [foobar$loc == "last", 2] = NA
  foobar[foobar$loc == "first", 3] = NA
  foo = c(foobar$dados, foobar$dados)
  bar = c(foobar$foo, foobar$bar)
  trans.matrices[[i]] = table(foo,bar)
  sums = apply(trans.matrices[[i]], 1, sum)
  trans.matrices[[i]] = trans.matrices[[i]] / sums
  }
names(trans.matrices) = patchtypes
#Create random dataset
Nperm = 4999
time.start = date()
for (i in 1:Nperm) {
  foobar = numeric()
  for (j in 1:Npatches) {
    foo.patch = as.character(patches[j,1])
    foo.trans = trans.matrices[[foo.patch]]
    foo.classes = colnames(foo.trans)
    foo = numeric( (patches[j,3]-patches[j,2]+1) )
    first = sample(length(foo),1)
    foo[first] = sample(dados[patches[j,2]:patches[j,3]],1)
    #Going backward
      if (first != 1 ) {
      for(k in first:2) {
        ref = as.character(foo[k])
        trans.row = foo.trans[ref,]
        trans.row = cumsum(trans.row)
        random = runif(1)
        test = random > trans.row
        foo[k-1] = foo.classes[sum(test)+1]
        if (i<1000) plot(foo, type="l", main=c(nome,l,i,j,k))
        if (i>1000) print(c(nome,l,i,j,k))
        }
      }
      if (first != length(foo)) {
```

```
       for(k in first:(length(foo)-1)) {
         ref = as.character(foo[k])
         trans.row = foo.trans[ref,]
         trans.row = cumsum(trans.row)
         random = runif(1)
         test = random > trans.row
         foo[k+1] = foo.classes[sum(test)+1]
         if (i<1000) plot(foo, type="l", main=c(nome,l,i,j,k))
         if (i>1000) print(c(nome,l,i,j,k))
         }
       }
     if (j == 1) foobar = foo else foobar = c(foobar,foo)
     }
foobar=as.numeric(foobar)
if (i==1000) plot(foobar, type="l", name=nome)
write.table(x=t(foobar), file=paste(nome,"_MC1.txt"),
  sep=" ", append=T, row.names=F, col.names=F)
}
import=as.matrix(read.table(paste(nome,"_MC1.txt"), sep="",
header=F))
dimnames(import) = NULL
import=t(import)
ncol(import)
nrow(import)
str(import)
import=cbind(dados, import)
write.table(x=import, file=paste(nome,"_MC1_t.txt"), sep=" ",
row.names = F, col.names=F)
}
```

SM 2.3 – Univariate and bivariate confidence intervals for the five null models used in the study

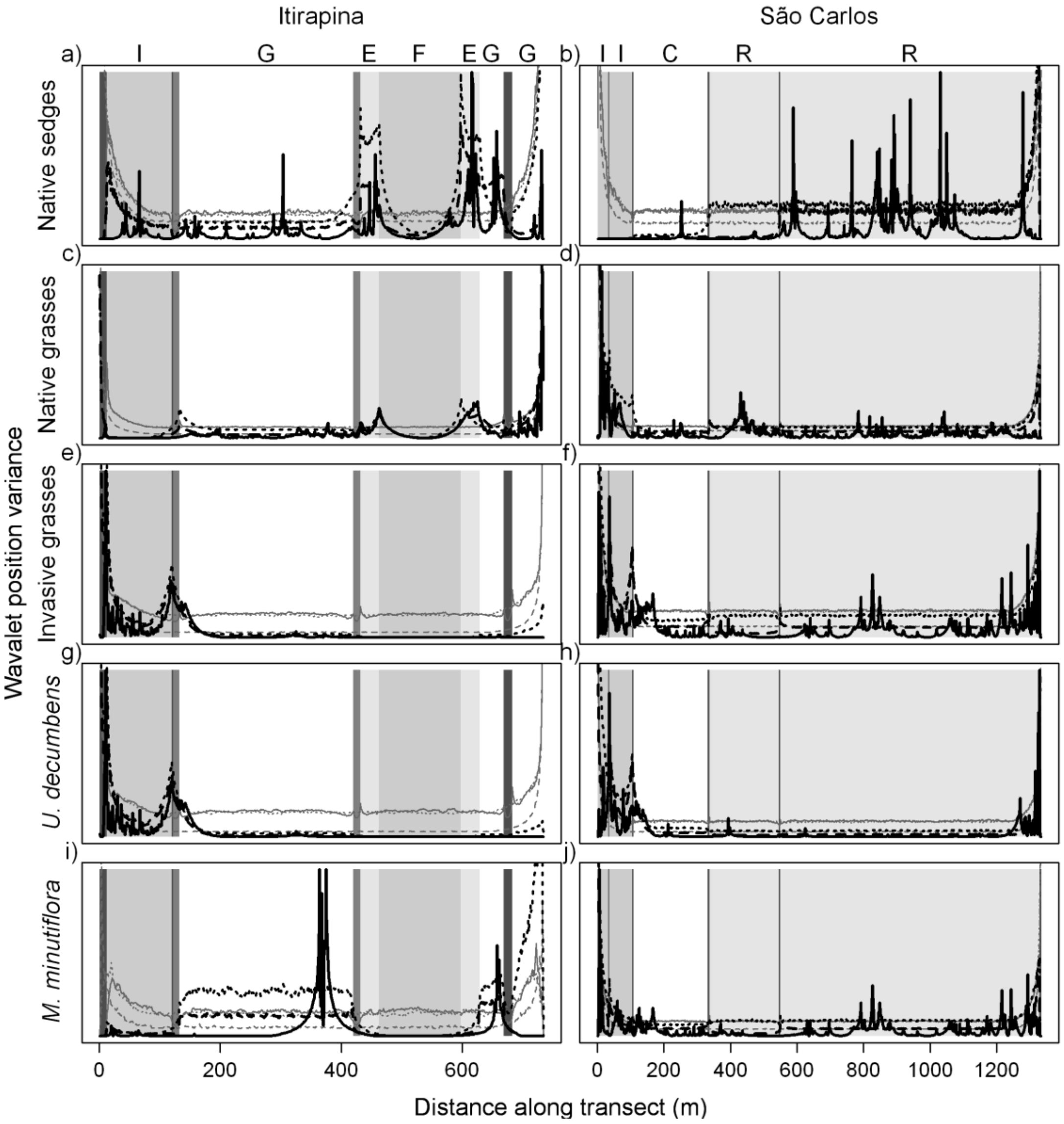

Figure A1. Wavelet position variance (solid black line) and confidence intervals calculated using different null models for native sedges, native grasses, combined invasive grasses, and the invasive grass species *Urochloa decumbens* and *Melinis minutiflora* along the two transects. We used the Haar wavelet template for scales 1 to 176 m in Itirapina and 1 to 173 m in São Carlos. The following null models were used: complete spatial randomness (CSRh, dashed gray line), complete spatial randomness accounting for differences between sections of the transect (CSRs, dashed black line), first-order Markov chain model (MC1h, dotted gray line), first-order Markov chain model accounting for linear disturbances (MC1d, solid gray line), and first-order Markov chain model accounting for differences between sections (MC1s, dotted black line). See Table 1 and Figure 2 for more details.

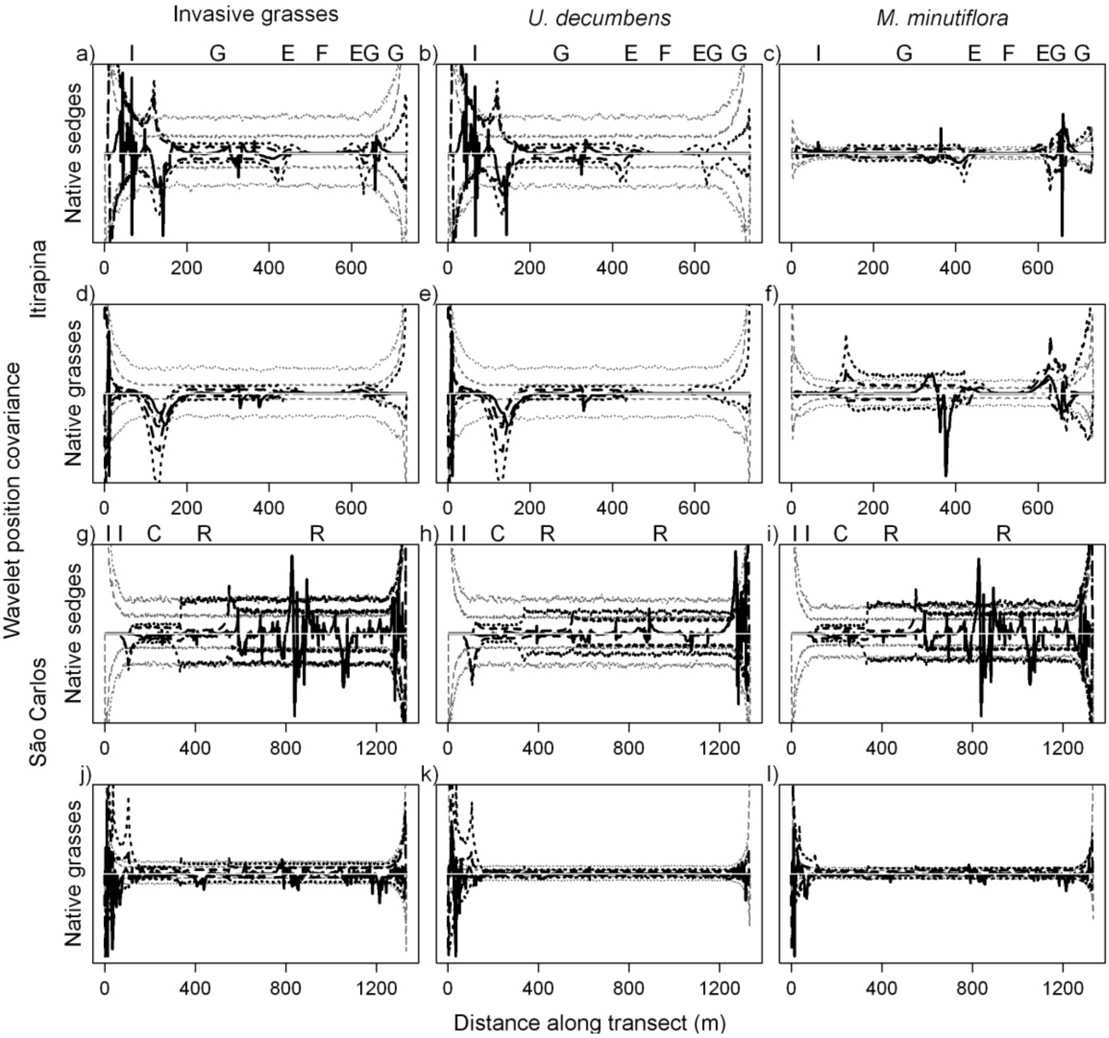

Figure A2. Confidence intervals for the bivariate position covariance (black solid line) between the native graminoids (sedges and grasses) and the invasive grasses, *Urochloa decumbens* and *Melinis minutiflora*), for the two study transects. We used the Haar wavelet template for scales 1 to 176 m in Itirapina and 1 to 173 m in São Carlos. The following null models were used to calculate the confidence intervals: complete spatial randomness (CSRh, dashed gray line), complete spatial randomness accounting for differences between sections of the transect (CSRs, dashed black line), first-order Markov chain model (MC1h, dotted gray line), first-order Markov chain model accounting for linear disturbances (MC1d, solid gray line), and first-order Markov chain model accounting for differences between sections (MC1s, dotted black line. The white line represents covariance equal to zero.

SM 3.1 – R code used to calculate the structural diversity, perform the wavelet transforms and calculate their significance

###This script requires two objects, one with the original data (“dados”) and one with the weights used for each descriptor (“weights”). Descriptors not used to calculate a measure must be excluded from the first object before the analysis.

###Both files from which the objects will be created must have named column names. The data file must have a column with the distance along the transect, optional columns with the names of the structural elements and their quantities (not used), and the values (numeric or 0/1) corresponding to each descriptor. The weights file must have the descriptors as column names, in the same order as the data file, and the weights corresponding to each descriptor as a single row.

```
####Calculating structural diversity
library(vegan)
library(cluster)
dados=read.table(files.choose(),header=T,sep="")
weights=read.table(file.choose(),header=T,sep="",dec=".")
#Calculating StrS
foo=unique(dados,margin=1)
StrS=aggregate(foo$Distance,by=list(foo$Distance),FUN=length)
foo=max(dados$Distance)
#adding quadrats with zero diversity (not present in the data)
Nquad=max(foo)
StrS.old=StrS
StrS=numeric(Nquad)
values=StrS.old[,1]
StrS[values]=StrS.old[,2]
#calculating StrD
data.temp=dados
distances=unique(data.temp$Distance)
Ndist=length(distances)
StrD[[i]]=numeric(Nquad)
varranges=matrix(nrow=2,ncol=ncol(data.temp)-3)
#Calculating the range of variation for each variable
for (j in 4:ncol(data.temp)) {
```

```
    varranges[1,j-3] = ifelse (is.factor(data.temp[,j]),
   NA,min(data.temp[,j],na.rm=T))
    varranges[2,j-3] = ifelse (is.factor(data.temp[,j]),
   NA,max(data.temp[,j],na.rm=T))
    }
colnames(varranges)=colnames(data.temp)[-(1:3)]
weights.temp=as.numeric(weights)
for(j in distances) {
   foo=subset(data.temp,Distance==j,4:ncol(data.temp))
   Nelements=nrow(foo)
   if(Nelements==1) StrD[[i]][j]=0 else {
    foo=rbind(foo,varranges)
    foo.dist=daisy(foo, metric="gower", weights=weights.temp)
    foo.dist=as.matrix(foo.dist)
    foo.dist=foo.dist[1:Nelements,1:Nelements]
    foo.dist=as.dist(foo.dist)
    foo.clust=agnes(foo.dist, diss=1, method="average", keep.diss=F,
   keep.data=F)
    foo.sum=treeheight(as.hclust(foo.clust))
    StrD[[i]][j]=foo.sum
    print(c(i,j))
    }
   }
names(StrD)=types
setwd("../..")
#Saving the values
setwd("forR/Results_1")
for(i in 1:5) {
   name.StrS=paste("StrS_",types[i],".txt",sep="")
   name.StrD=paste("StrD_",types[i],".txt",sep="")
   write.table(StrS[[i]],file=name.StrS, sep="\t",
   row.names=F,col.names=F)
   write.table(StrD[[i]],file=name.StrD, sep="\t",
   row.names=F,col.names=F)
   }
setwd("../..")
####Wavelet transforms and scale variance
```

```
library(wmtsa)
for(m in 1:4) {
setwd(“your_working_directory_here”)
current=c("ecotone","tundra","itirapina","ufscar")[m]
setwd("forR/randomized")
setwd(current)
files=list.files()
types=files
types=gsub(".txt","",types)
make.plot=F #Make a plot for each randomization?
zero.padding=T #Add zeroes to extremities?
remove.COI=T #Remove boundary effects (cone of influence)?
data.scale=list()
for (i in 1:length(files)) {
  data.main=as.matrix(read.table(files[i],header=F,sep=""))
  dimnames(data.main)=NULL
  setwd("../../wavelets")
  setwd(current)
  try(dir.create(types[i]))
  setwd(types[i])
  data.foo=data.main[,1]
  full.length=length(data.foo)
  half.length=round(length(data.foo)/2)
  if(zero.padding)
  data.foo=c(rep(0,half.length),data.foo,rep(0,half.length/2))
  wav.orig=wavCWT(data.foo,scale.range=c(1,75),wavelet="gaussian2")
  scales=attr(wav.orig,"scale")
  if(zero.padding) {
   wav.scale=attr(wav.orig,"scale")
   wav.time=1:full.length
   wav.wavelet=attr(wav.orig,"wavelet")
   wav.series=attr(wav.orig,"series")
   wav.sampling.interval=attr(wav.orig,"sampling.interval")
   wav.series.name=attr(wav.orig,"series.name")
   wav.n.sample=length(wav.time)
   wav.n.scale=attr(wav.orig,"n.scale")
   wav.filter.arg=attr(wav.orig,"filter.arg")
```

```
  wav.orig=wav.orig[(half.length+1):(half.length+full.length),]
  class(wav.orig)="wavCWT"
  attr(wav.orig,"scale")=wav.scale
  attr(wav.orig,"time")=wav.time
  attr(wav.orig,"wavelet")=wav.wavelet
  attr(wav.orig,"series")=wav.series
  attr(wav.orig,"sampling.interval")=wav.sampling.interval
  attr(wav.orig,"series.names")=wav.series.name
  attr(wav.orig,"n.sample")=wav.n.sample
  attr(wav.orig,"n.scale")=wav.n.scale
  attr(wav.orig,"filter.arg")=wav.filter.arg
  }
if(remove.COI) {
  for(k in 1:length(scales)) {
    index1=1:(scales[k]*2)
    index2=nrow(wav.orig)-index1+1
    indices=c(index1,index2)
    wav.orig[indices,k]=NA
    }
  }
wav.orig.scale=apply(as.matrix(wav.orig)^2,2,mean, na.rm=T)
png(paste("wavCWT_MH_",types[i],"_wav_0001",".png",sep=""),res=96,
width=20,height=20,unit="cm")
plot(wav.orig)
dev.off()
data.scale[[i]]=matrix(ncol=ncol(data.main),nrow=length(wav.orig.s
cale))
data.scale[[i]][,1]=wav.orig.scale
rownames(data.scale[[i]])=scales
file.title=paste("wavCWT_MH_",types[i],"_wav_0001",".txt",sep="")
write.table(wav.orig,file.title,sep=" ", dec=".", row.names=F,
col.names=F)
for(j in 2:ncol(data.main)) {
  foo=data.main[,j]
  full.length=length(foo)
  half.length=round(length(foo)/2)
```

```
  if(zero.padding)
foo=c(rep(0,half.length),foo,rep(0,half.length/2))
  foo.wav=wavCWT(foo, scale.range=c(1,75), wavelet="gaussian2")
  if(zero.padding) {
    wav.scale=attr(foo.wav,"scale")
    wav.time=1:full.length
    wav.wavelet=attr(foo.wav,"wavelet")
    wav.series=attr(foo.wav,"series")
    wav.sampling.interval=attr(foo.wav,"sampling.interval")
    wav.series.name=attr(foo.wav,"series.name")
    wav.n.sample=length(wav.time)
    wav.n.scale=attr(foo.wav,"n.scale")
    wav.filter.arg=attr(foo.wav,"filter.arg")
  foo.wav=foo.wav[(half.length+1):(half.length+full.length),]
    class(foo.wav)="wavCWT"
    attr(foo.wav,"scale")=wav.scale
    attr(foo.wav,"time")=wav.time
    attr(foo.wav,"wavelet")=wav.wavelet
    attr(foo.wav,"series")=wav.series
    attr(foo.wav,"sampling.interval")=wav.sampling.interval
    attr(foo.wav,"series.names")=wav.series.name
    attr(foo.wav,"n.sample")=wav.n.sample
    attr(foo.wav,"n.scale")=wav.n.scale
    attr(foo.wav,"filter.arg")=wav.filter.arg
    }
  if(remove.COI) {
    for(k in 1:length(scales)) {
      index1=1:(scales[k]*2)
      index2=nrow(wav.orig)-index1+1
      indices=c(index1,index2)
      foo.wav[indices,k]=NA
      }
    }
  file.title=paste("wavCWT_MH_",types[i],"_wav_",formatC(j,digits=
3,format="d",flag=0),sep="")
  if(make.plot) {
```

```
   png(paste(file.title,".png",sep=""),res=96,width=20,height=20,un
  it="cm")
    plot(foo.wav)
    dev.off()
    }
   foo.scale=apply(as.matrix(foo.wav)^2,2,mean,na.rm=T)
   data.scale[[i]][,j]=foo.scale
   write.table(foo.wav,paste(file.title,".txt",sep=""),sep=" ",
  dec=".", row.names=F, col.names=F)
   print(c(current,i,j))
   }
  setwd("../../../randomized")
  setwd(current)
  }
setwd("../../../figures")
names(data.scale)=types
CIs=list()
for (i in 1:length(types)) {
  CIs[[i]]=apply(data.scale[[i]],1,quantile,0.95,na.rm=T)
  }
names(CIs)=types
png.title=paste("scale_",current,".png",sep="")
png(png.title, res=96, height=30, width=30, unit="cm")
par(mfcol=c(5,2), mar=c(2,2,4,4))
for (i in c(3,2,5,1,4,8,7,10,6,9)) {
  plot(data.scale[[i]][,1]~as.numeric(rownames(data.scale[[i]])),
  main=types[i], xlab="scale (m)", ylab="wavelet variance",
  type="l", lwd=2)
  points(CIs[[i]]~as.numeric(names(CIs[[i]])), type="l", col="red")
  }
dev.off()
setwd("../forR/scale_variance")
for (i in 1:length(types)) {
  file.title=paste("scale_all_",types[i],".txt")
  write.table(data.scale[[i]], file.title, sep=" ", dec=".",
  row.names=F, col.names=F)
```

```
  file.title=paste("scale_CI_",types[i],".txt")
  write.table(CIs[[i]], file.title, sep=" ", dec=".", row.names=F,
  col.names=F)
  }
}
####Calculate significant wavelets
library(wmtsa)
scales=c(1,2,3,4,5,6,7,8,9,10,11,12,13,14,15,16,17,18,19,20,21,22,23
  ,24,25,26,
  28,29,30,31,33,34,36,37,39,41,43,44,46,48,51,53,55,58,60,63,66,69,
  72,75) #Scales for which the CWT was calculated
as.wavCWT=function(x,
  scale,time,wavelet,series,sampling.interval,series.name,
  n.sample,n.scale,filter.arg) {
  class(x)="wavCWT"
  attr(x,"scale")=scale
  attr(x,"time")=time
  attr(x,"wavelet")=wavelet
  attr(x,"series")=series
  attr(x,"sampling.interval")=sampling.interval
  attr(x,"series.name")=series.name
  attr(x,"n.sample")=n.sample
  attr(x,"n.scale")=n.scale
  attr(x,"filter.arg")=filter.arg
  return(x)
  }
for(m in 1:4) {
setwd(“your_working_directory_here”)
current=c("ecotone","tundra","itirapina","ufscar")[m]
setwd("ForR/wavelets")
setwd(current)
types=list.files()
wav.orig=list()
CIs.inf=list()
CIs.sup=list()
wav.signif=list()
```

```
for(i in 1:length(types)) {
  setwd(types[i])
  files=list.files()
  orig=as.matrix(read.table(files[1],sep="",dec="."))
  CI.inf=matrix(nrow=nrow(orig),ncol=ncol(orig))
  CI.sup=matrix(nrow=nrow(orig),ncol=ncol(orig))
  foo=array(dim=c(nrow(orig),ncol(orig),length(files)))
  for(j in 1:length(files)) {
   foo[,,j]=as.matrix(read.table(files[j],sep="",dec=".",
  header=F))
   print(c(current,i,j))
   }
  CI.inf[,]=apply(foo,c(1,2),quantile,0.025,na.rm=T)
  CI.sup[,]=apply(foo,c(1,2),quantile,0.975,na.rm=T)
  CI.inf=as.wavCWT(CI.inf,scale=scales,time=1:nrow(orig),wavelet="ga
  ussian2",series=NULL,
   sampling.interval=1,series.name=types[i],
  n.sample=nrow(orig),n.scale=50,filter.arg=1)
  CI.sup=as.wavCWT(CI.sup,scale=scales,time=1:nrow(orig),wavelet="ga
  ussian2",series=NULL,
   sampling.interval=1,series.name=types[i],
  n.sample=nrow(orig),n.scale=50,filter.arg=1)
  indices=which(orig >= CI.inf & orig <= CI.sup)
  signif=orig
  signif[indices]=NA
  CIs.inf[[i]]=CI.inf
  CIs.sup[[i]]=CI.sup
  wav.orig[[i]]=as.wavCWT(orig,scale=scales,time=1:nrow(orig),wavele
  t="gaussian2",series=NULL,
   sampling.interval=1,series.name=types[i],
  n.sample=nrow(orig),n.scale=50,filter.arg=1)
  wav.signif[[i]]=as.wavCWT(signif,scale=scales,time=1:nrow(orig),wa
  velet="gaussian2",series=NULL,
   sampling.interval=1,series.name=types[i],
  n.sample=nrow(orig),n.scale=50,filter.arg=1)
  setwd("..")
```

```
  }
setwd("../../wav_full")
setwd(current)
for(i in 1:length(wav.orig)) {
  write.table(wav.orig[[i]],
  file=paste("wav_full_",types[i],".txt"),
  row.names=F,col.names=F,sep=" ")
  }
setwd("../../wav_signif")
setwd(current)
for(i in 1:length(wav.orig)) {
  write.table(wav.signif[[i]],
  file=paste("wav_signif_",types[i],".txt"),
  row.names=F,col.names=F,sep=" ")
  }
setwd("../../patches")
patches=read.table(paste(current,".txt",sep=""),header=T,sep="")
setwd("../../figures")
png.title=paste("wav_",current,"_full.png",sep="")
png(png.title, res=300, height=30, width=30, unit="cm")
par(mfcol=c(5,2), mar=c(2,2,4,4))
for (i in c(3,2,5,1,4,8,7,10,6,9)) {
  plot(wav.orig[[i]], main=types[i], add=T,
  col=gray.colors(12,start=0.3))
  abline(v=patches$Start,lwd=2)
  }
dev.off()
png.title=paste("wav_",current,"_signif.png",sep="")
png(png.title, res=300, height=30, width=30, unit="cm")
par(mfcol=c(5,2), mar=c(2,2,4,4))
for (i in c(3,2,5,1,4,8,7,10,6,9)) {
  plot(wav.signif[[i]], main=types[i], add=T,
  col=gray.colors(12,start=0.3))
  abline(v=patches$Start,lwd=2)
  }
dev.off()
}
```

SM 3.2 – Colored high-resolution Figures of the wavelet results

Below are the higher-resolution Figures for the significant wavelet results for Chapter 3. Letters above each plot indicate the plant communities and disturbances: railroad and gravel road (r), invaded grassland (I), firebreak (f), regenerating firebreak with grass (g), savanna vegetation - campo sujo in Itirapina and typical cerrado in São Carlos (C), savanna-forest or tundra-forest transitions (E), riparian or boreal forest (F), regenerating cerrado with eucalypt trees (R), tundra (T), lakes (L), wet grassland (W), and pond (P). Refer to Table 1 for details. Red color indicates low wavelet variance.

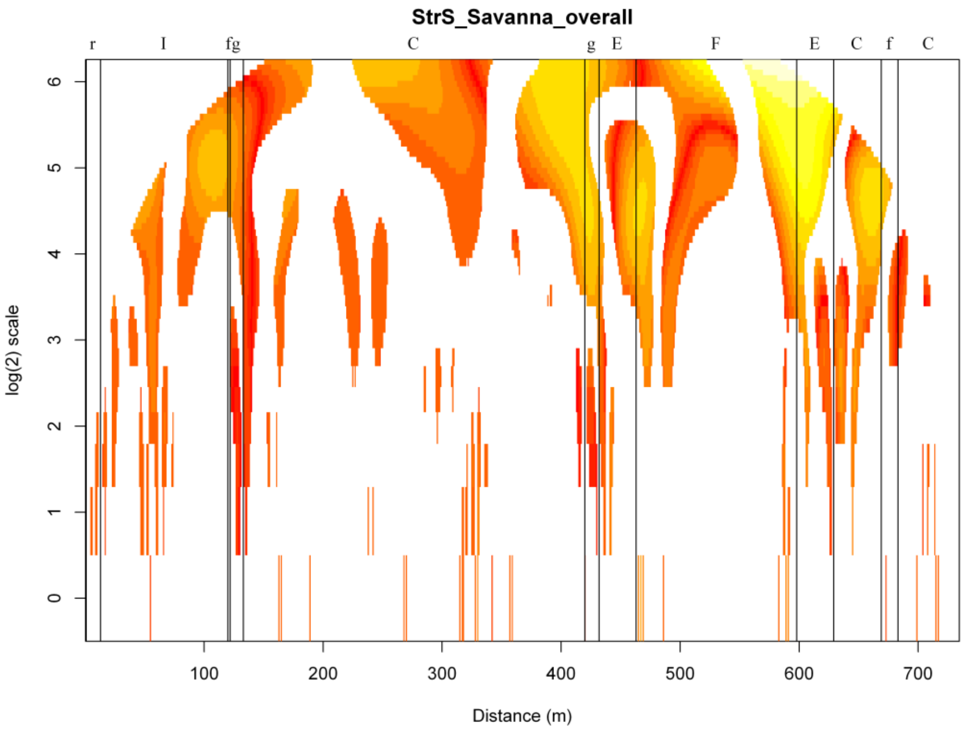

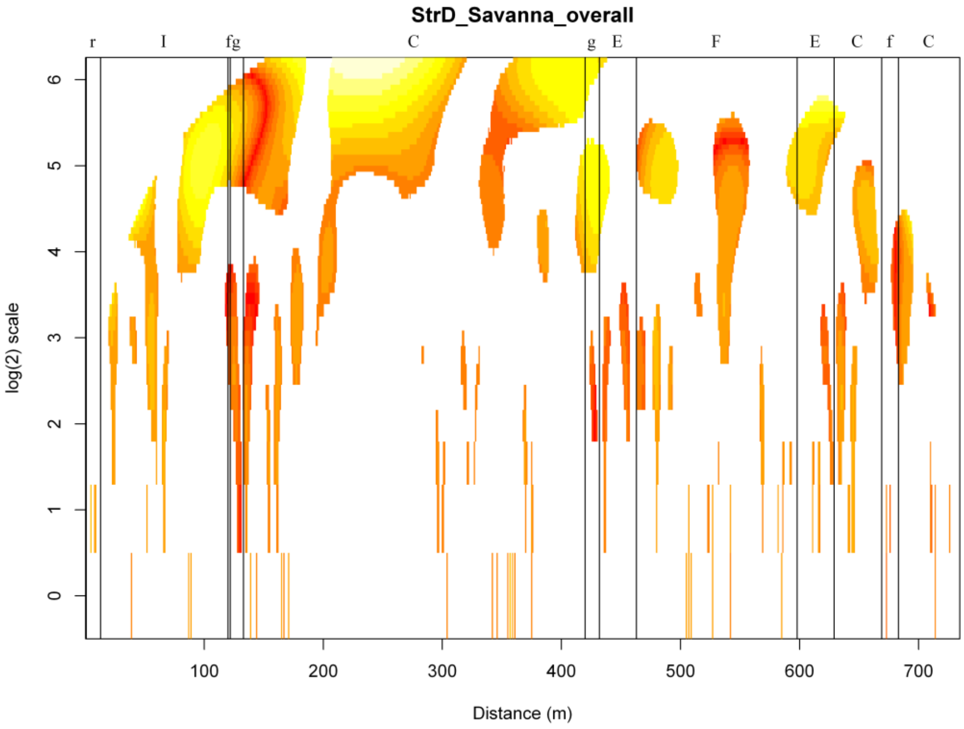
StrD_Savanna_overall
r
I
fg
C
g
E
F
E
C
f
C
log(2) scale
0
1
2
3
4
5
6
100
200
300
400
500
600
700
Distance (m)

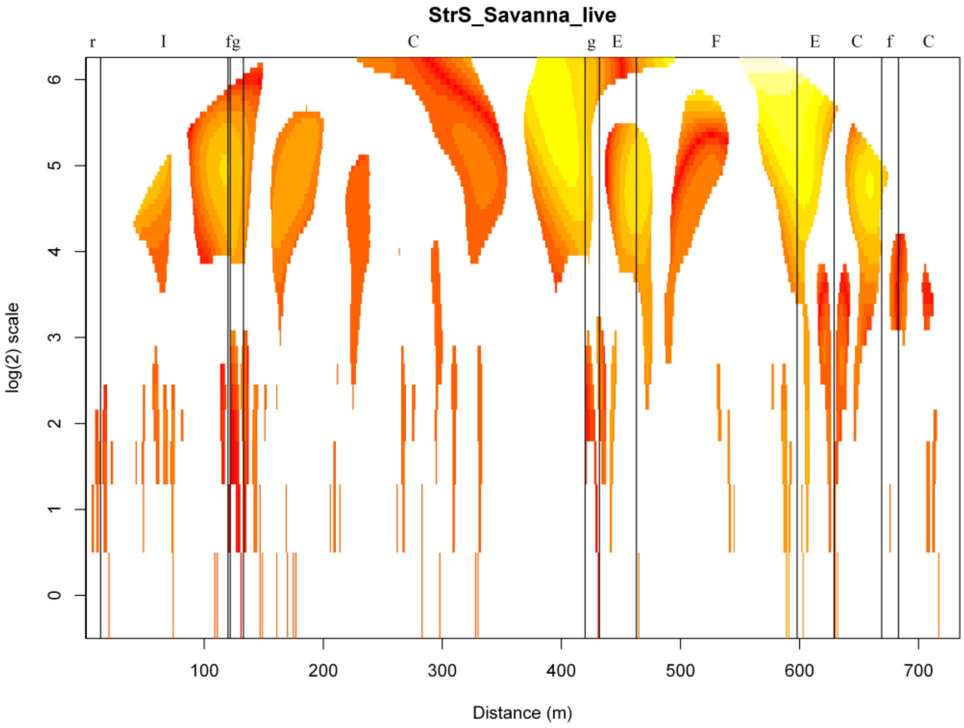
StrS_Savanna_live
r
I
fg
C
g
E
F
E
C
f
C
log(2) scale
0
1
2
3
4
5
6
100
200
300
400
500
600
700
Distance (m)

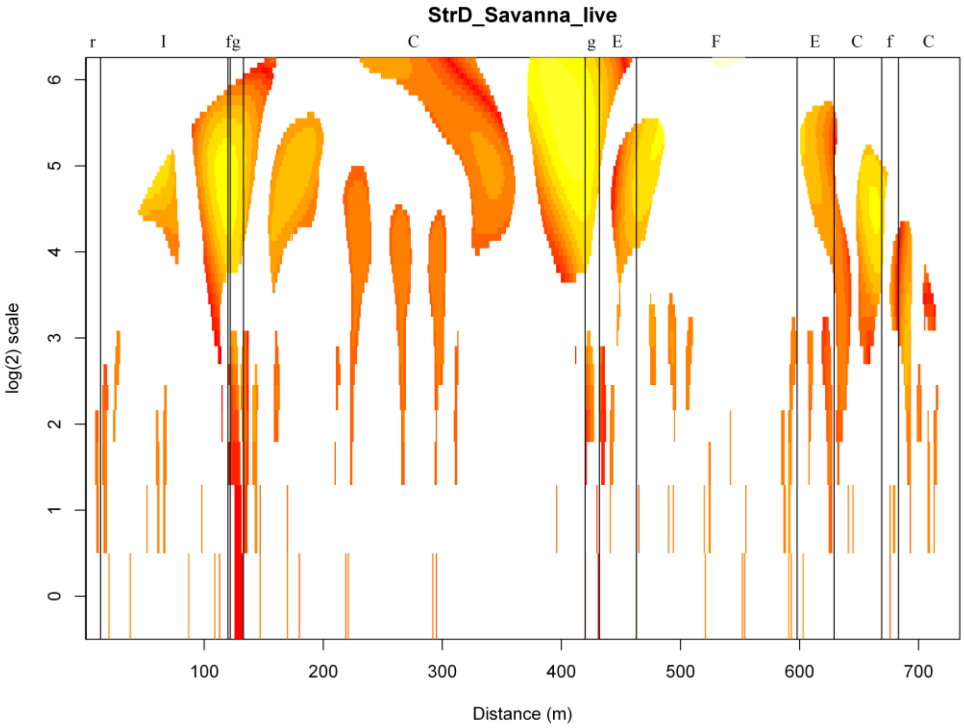
StrD_Savanna_live
r
I
fg
C
g
E
F
E
C
f
C
log(2) scale
0
1
2
3
4
5
6
100
200
300
400
500
600
700
Distance (m)

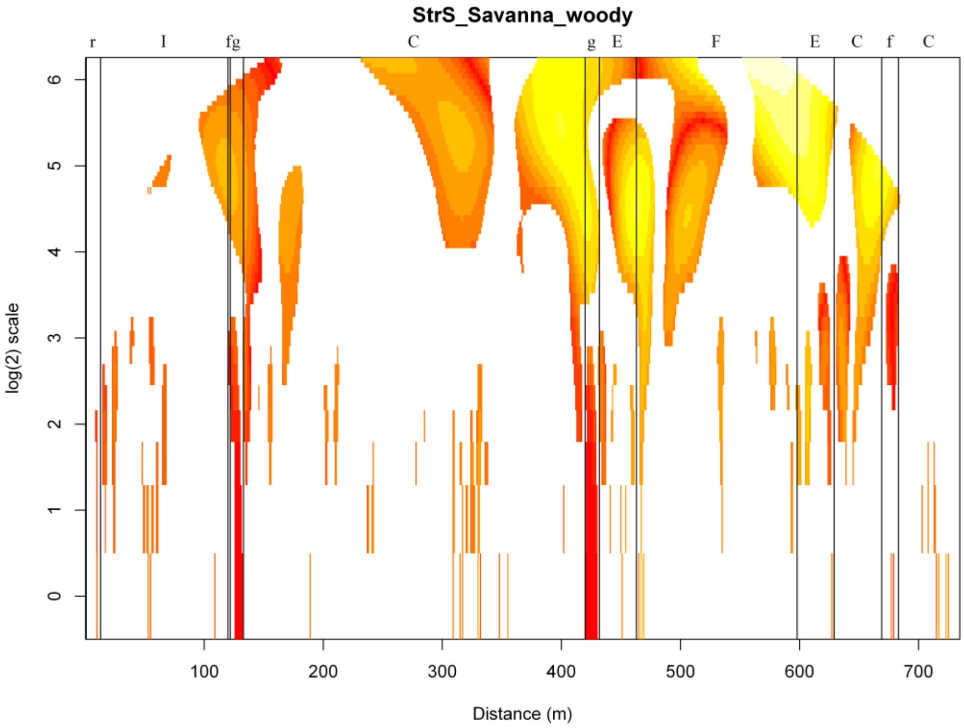
StrS_Savanna_woody
r
I
fg
C
g
E
F
E
C
f
C
log(2) scale
0
1
2
3
4
5
6
100
200
300
400
500
600
700
Distance (m)

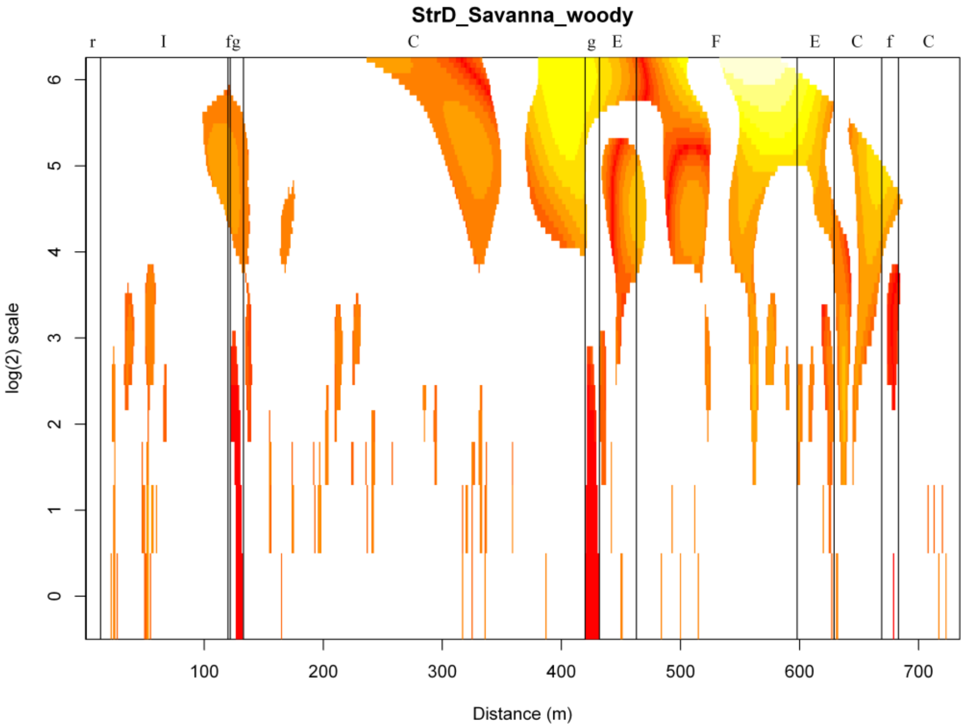
StrD_Savanna_woody
r
I
fg
C
g
E
F
E
C
f
C
log(2) scale
0
1
2
3
4
5
6
100
200
300
400
500
600
700
Distance (m)

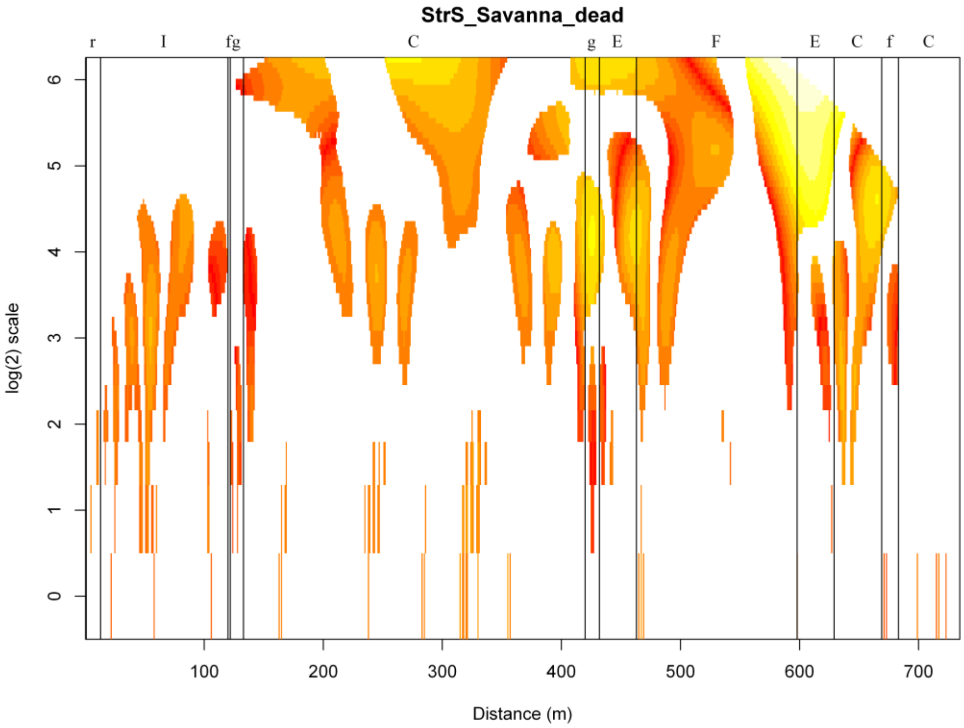
StrS_Savanna_dead
r
I
fg
C
g
E
F
E
C
f
C
log(2) scale
0
1
2
3
4
5
6
100
200
300
400
500
600
700
Distance (m)

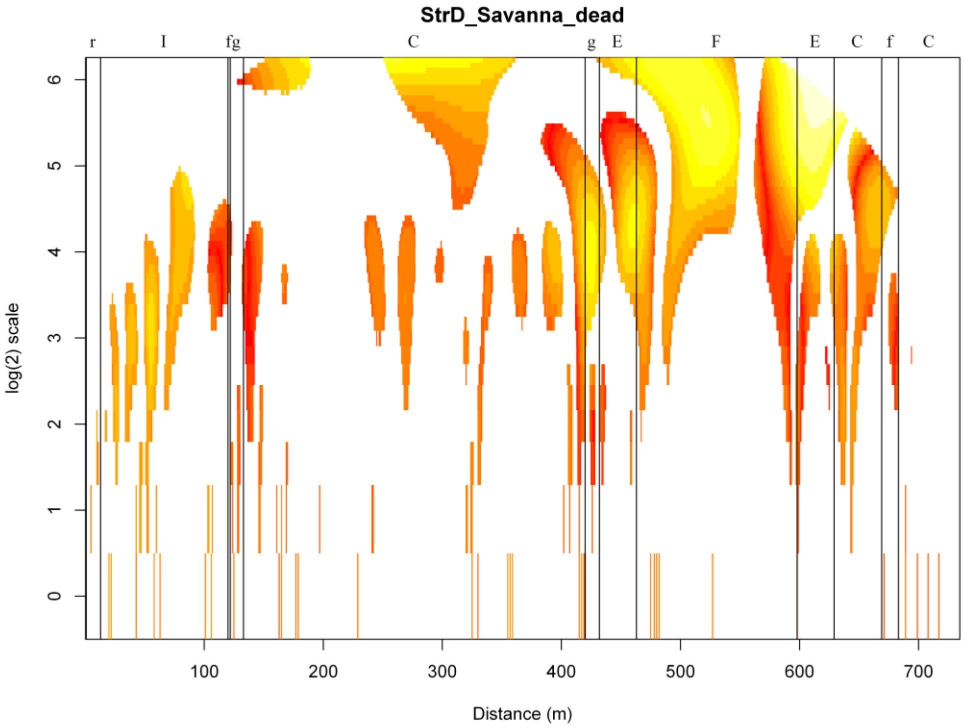
StrD_Savanna_dead
r
I
fg
C
g
E
F
E
C
f
C
log(2) scale
0
1
2
3
4
5
6
100
200
300
400
500
600
700
Distance (m)

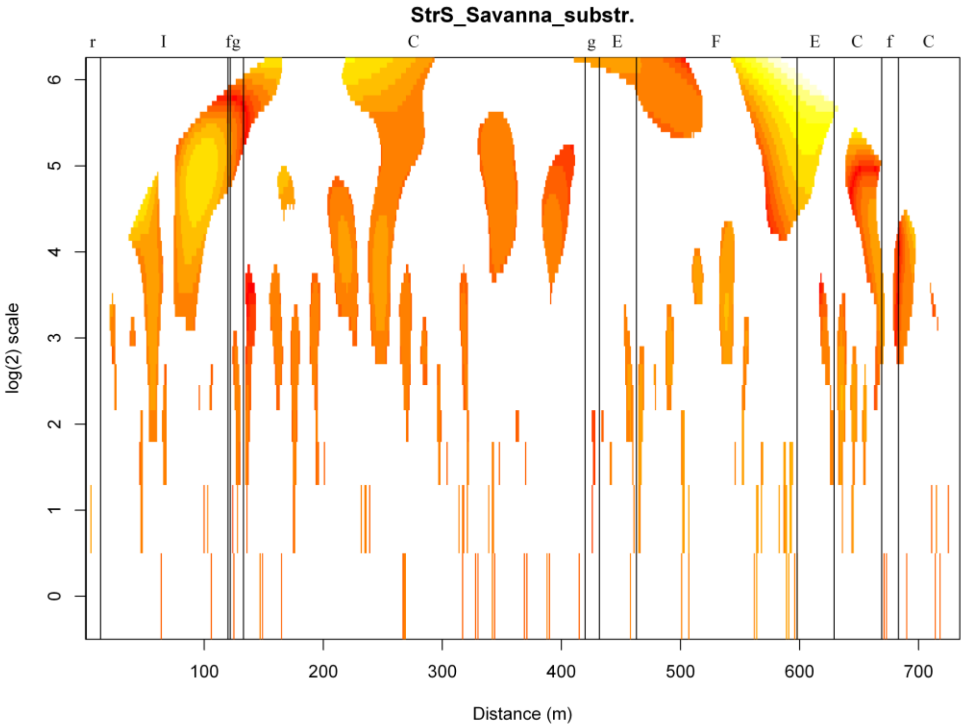
StrS_Savanna_substr.
r
I
fg
C
g
E
F
E
C
f
C
log(2) scale
0
1
2
3
4
5
6
100
200
300
400
500
600
700
Distance (m)

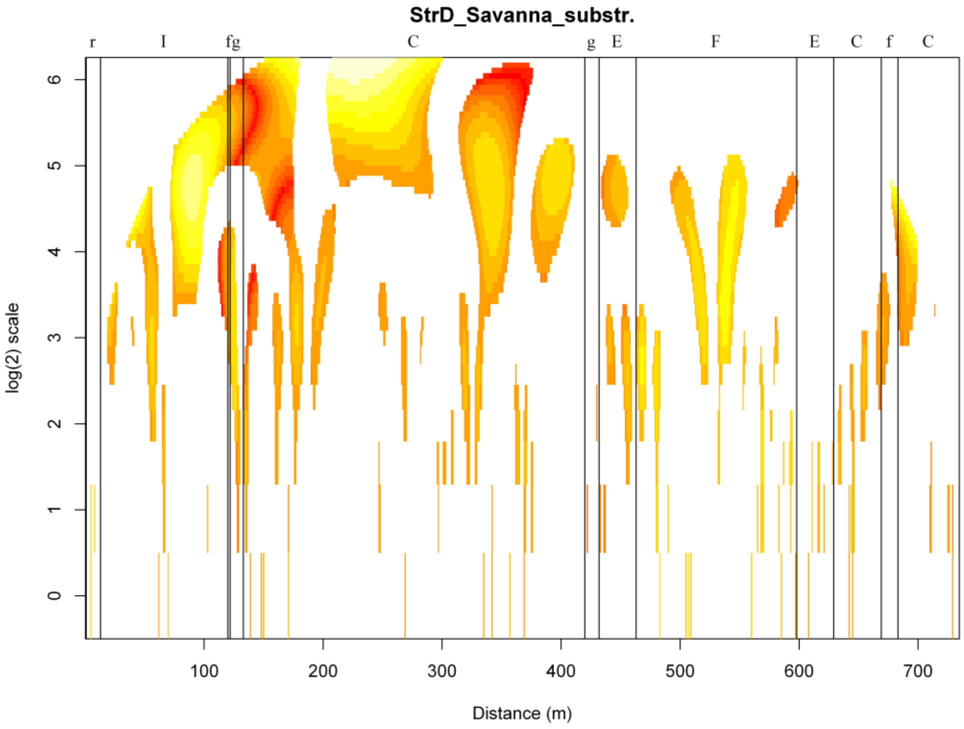
StrD_Savanna_substr.
r
I
fg
C
g
E
F
E
C
f
C
log(2) scale
0
1
2
3
4
5
6
100
200
300
400
500
600
700
Distance (m)

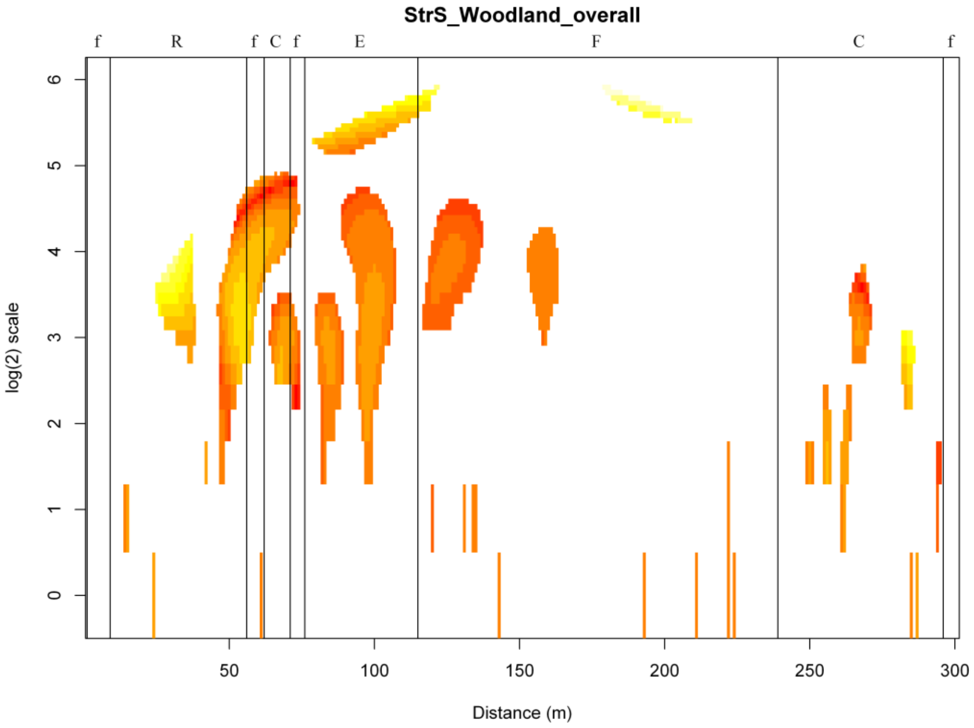
StrS_Woodland_overall
f
R
f
C
f
E
F
C
f
log(2) scale
0
1
2
3
4
5
6
50
100
150
200
250
300
Distance (m)


StrD_Woodland_overall
f
R
f
C
f
E
F
C
f
log(2) scale
0
1
2
3
4
5
6
50
100
150
200
250
300
Distance (m)

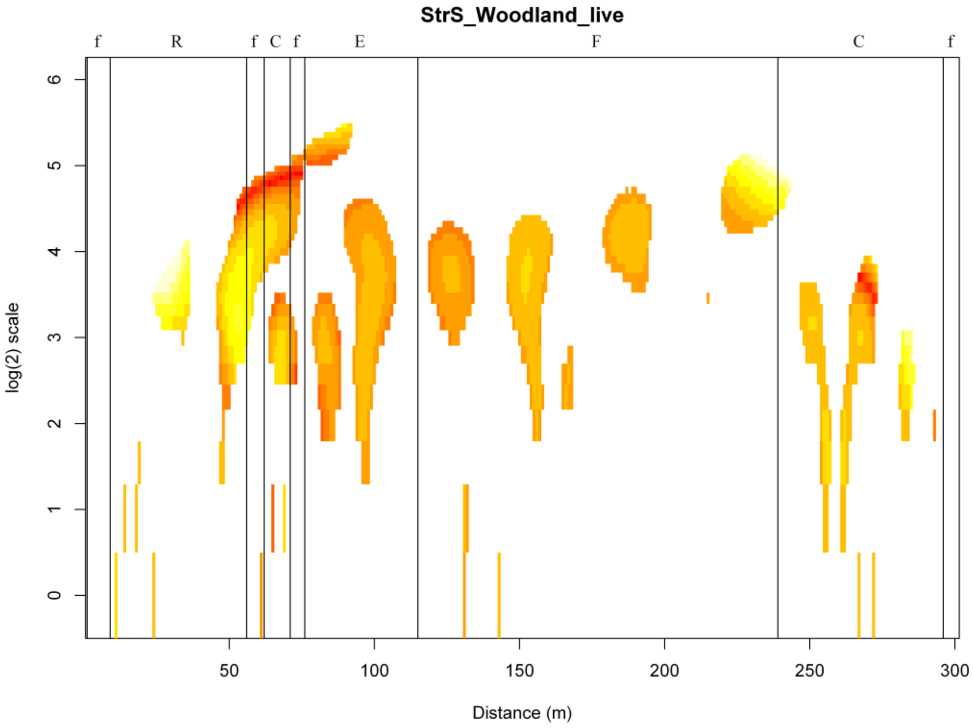
StrS_Woodland_live
f
R
f
C
f
E
F
C
f
log(2) scale
0
1
2
3
4
5
6
50
100
150
200
250
300
Distance (m)

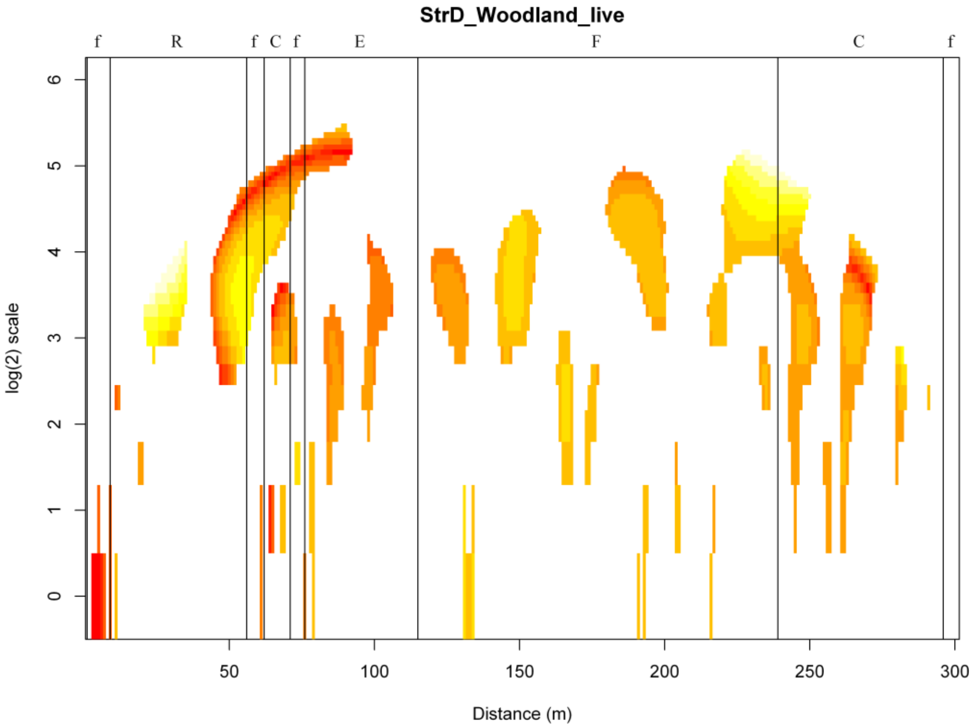
StrD_Woodland_live
f
R
f
C
f
E
F
C
f
log(2) scale
0
1
2
3
4
5
6
50
100
150
200
250
300
Distance (m)

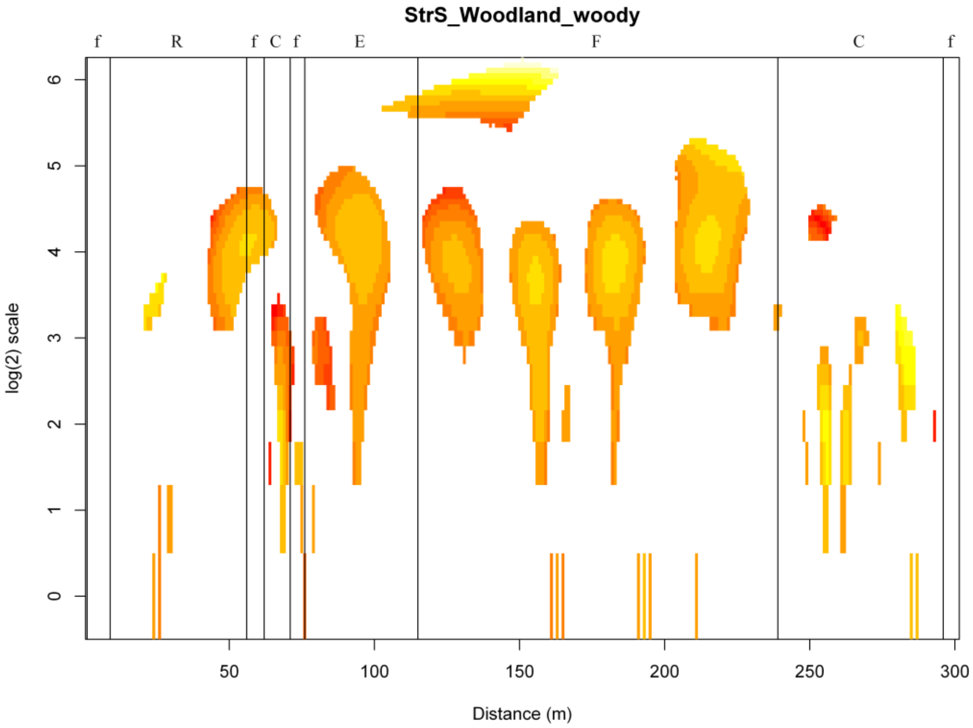
StrS_Woodland_woody
f
R
f
C
f
E
F
C
f
log(2) scale
0
1
2
3
4
5
6
50
100
150
200
250
300
Distance (m)

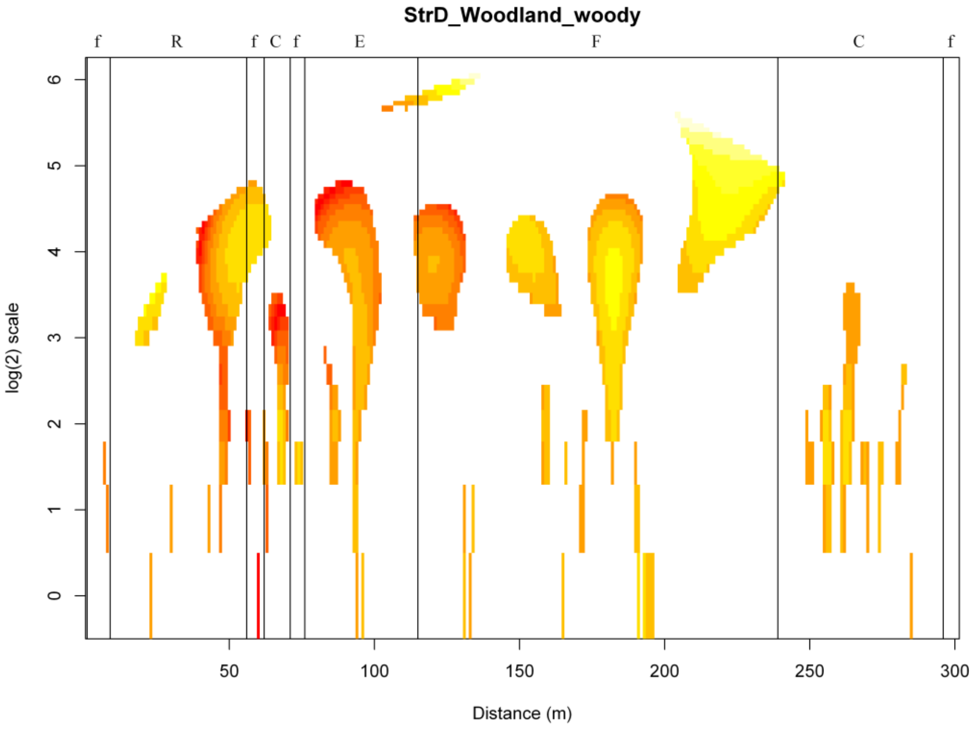
StrD_Woodland_woody
f
R
f
C
f
E
F
C
f
log(2) scale
0
1
2
3
4
5
6
50
100
150
200
250
300
Distance (m)

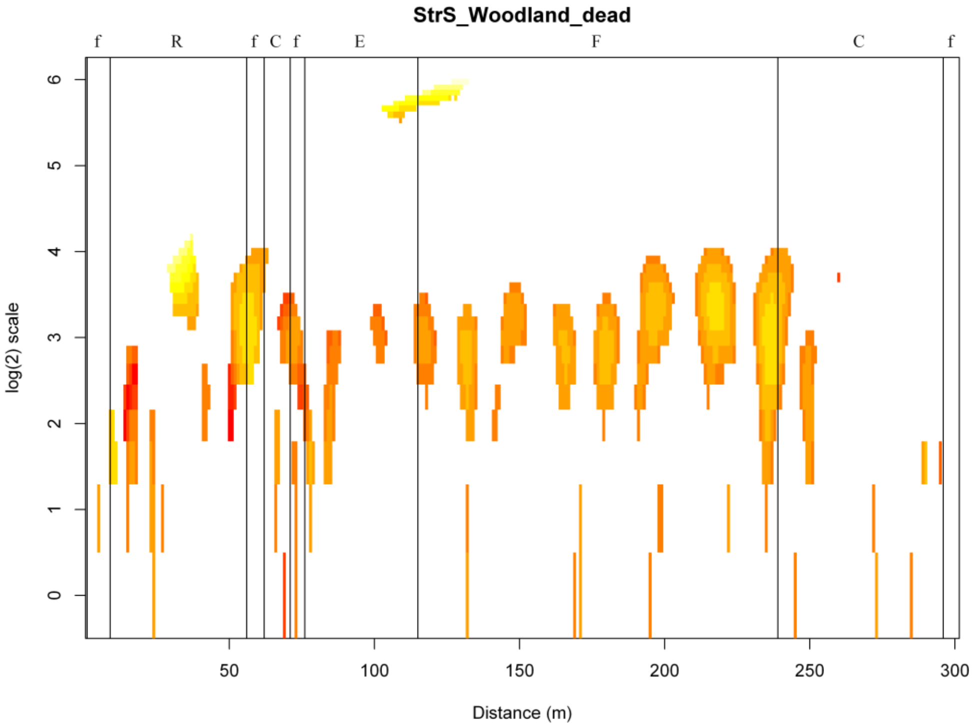
StrS_Woodland_dead
f
R
f
C
f
E
F
C
f
log(2) scale
0
1
2
3
4
5
6
50
100
150
200
250
300
Distance (m)

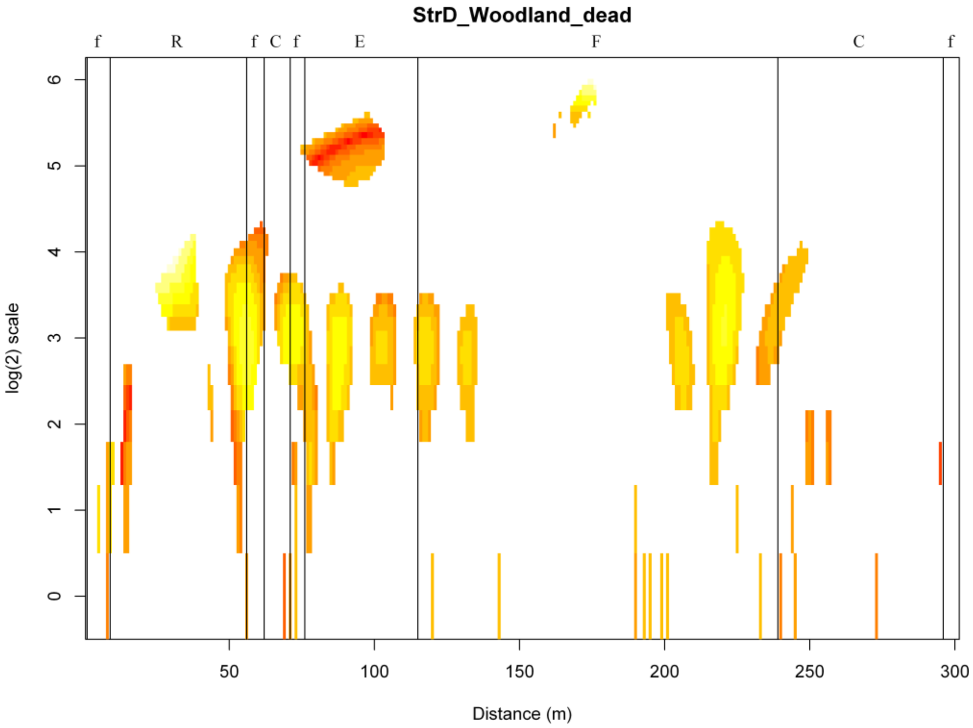
StrD_Woodland_dead
f
R
f
C
f
E
F
C
f
log(2) scale
0
1
2
3
4
5
6
50
100
150
200
250
300
Distance (m)

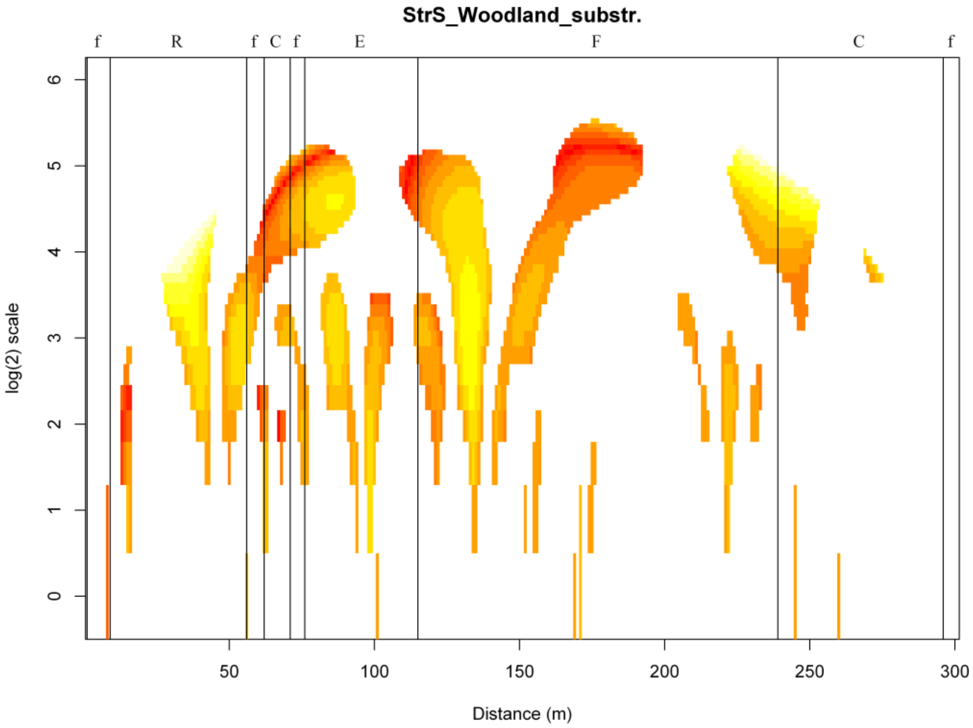
StrS_Woodland_substr.
f
R
f
C
f
E
F
C
f
log(2) scale
0
1
2
3
4
5
6
50
100
150
200
250
300
Distance (m)

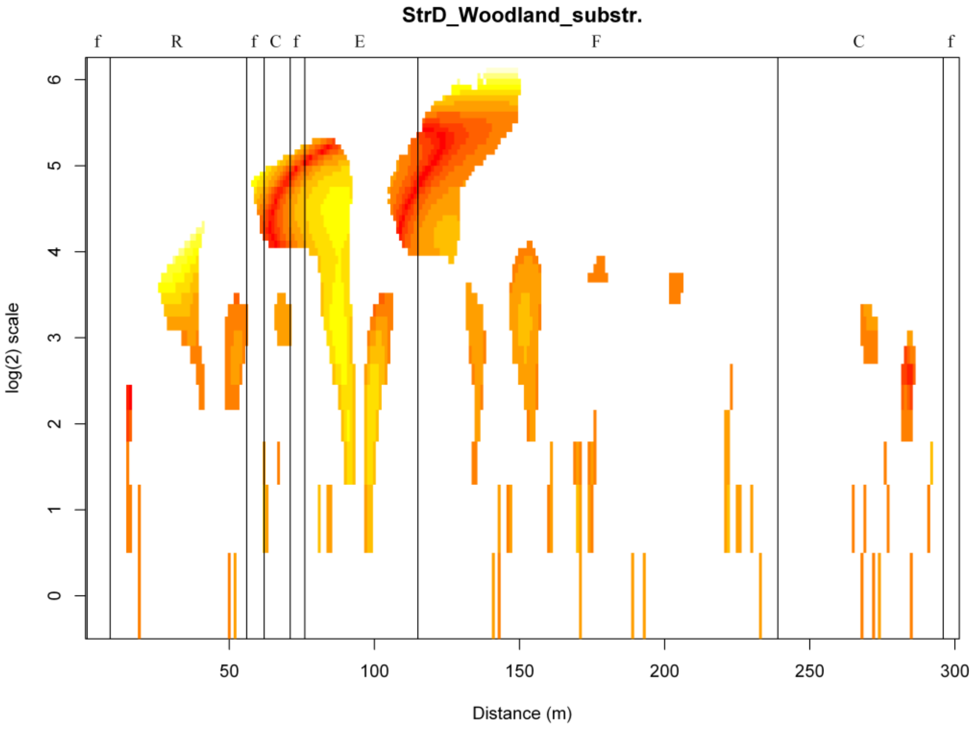
StrD_Woodland_substr.
f
R
f
C
f
E
F
C
f
log(2) scale
0
1
2
3
4
5
6
50
100
150
200
250
300
Distance (m)

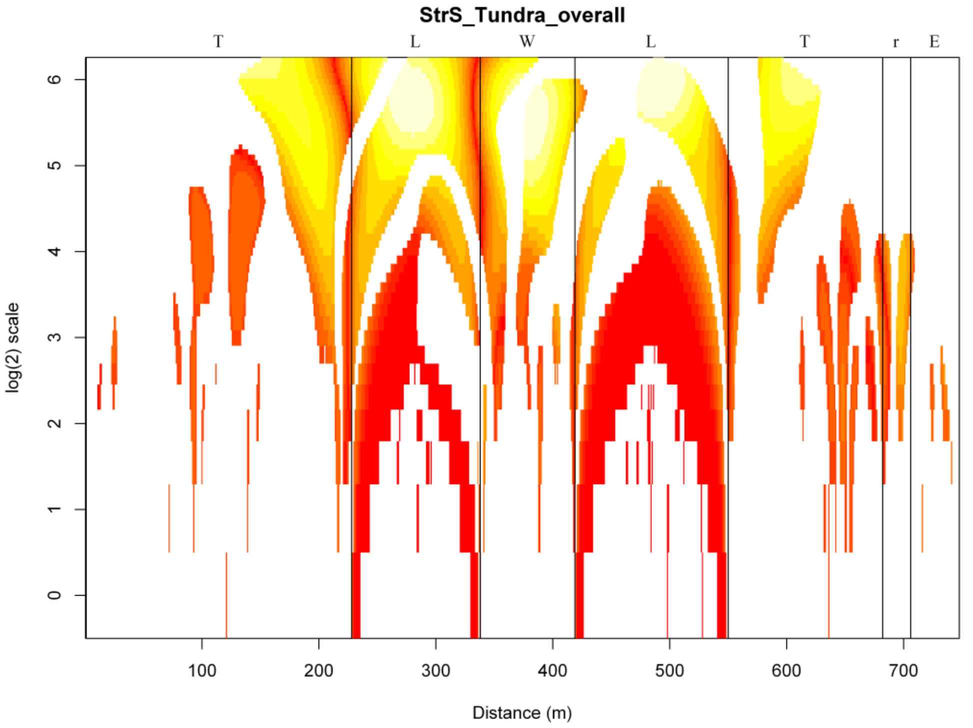
StrS_Tundra_overall
T
L
W
L
T
r
E
log(2) scale
0
1
2
3
4
5
6
100
200
300
400
500
600
700
Distance (m)

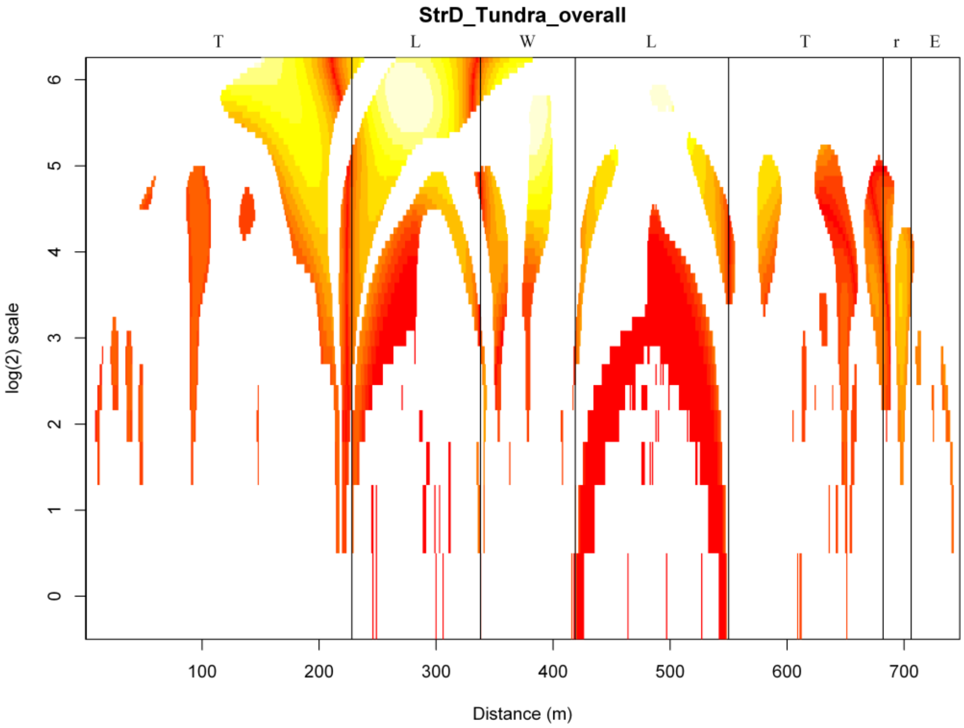
StrD_Tundra_overall
T
L
W
L
T
r
E
log(2) scale
0
1
2
3
4
5
6
100
200
300
400
500
600
700
Distance (m)

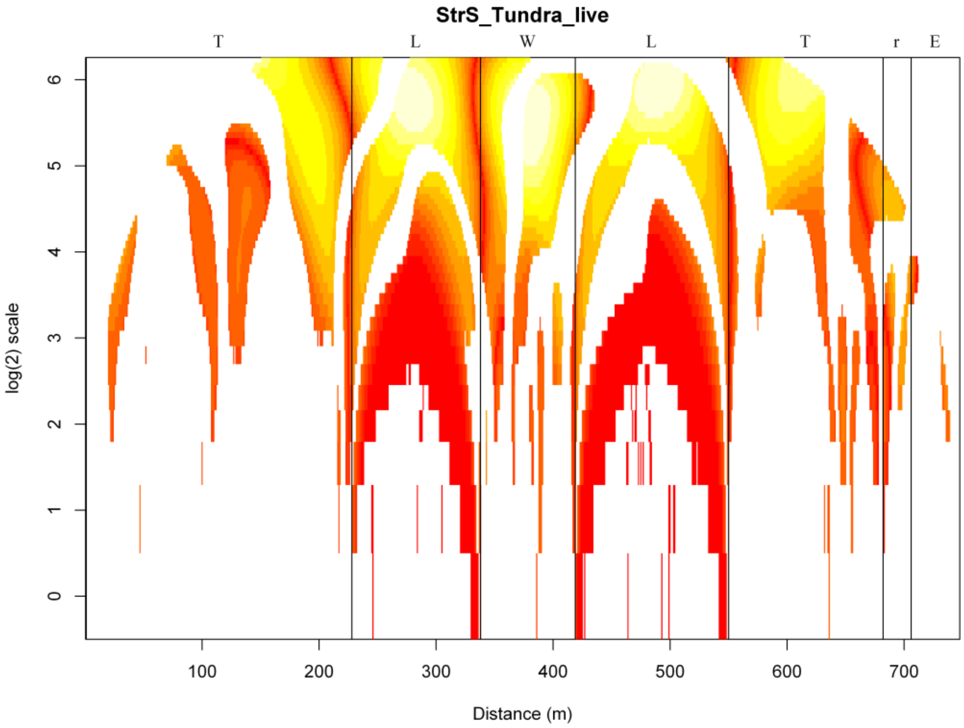
StrS_Tundra_live
T
L
W
L
T
r
E
log(2) scale
0
1
2
3
4
5
6
100
200
300
400
500
600
700
Distance (m)

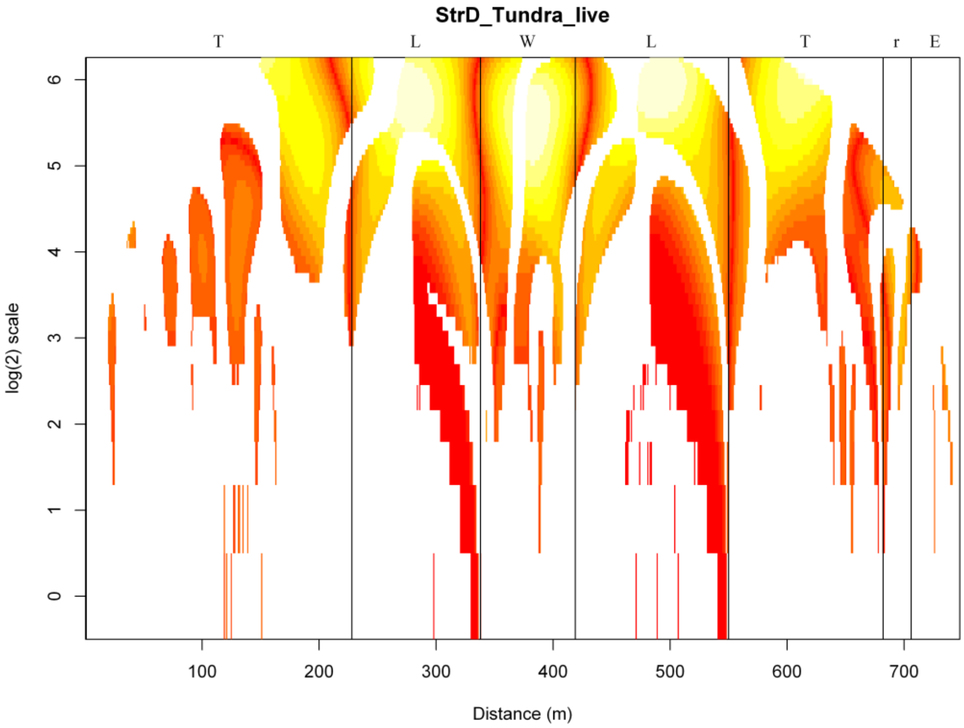
StrD_Tundra_live
T
L
W
L
T
r
E
log(2) scale
0
1
2
3
4
5
6
100
200
300
400
500
600
700
Distance (m)

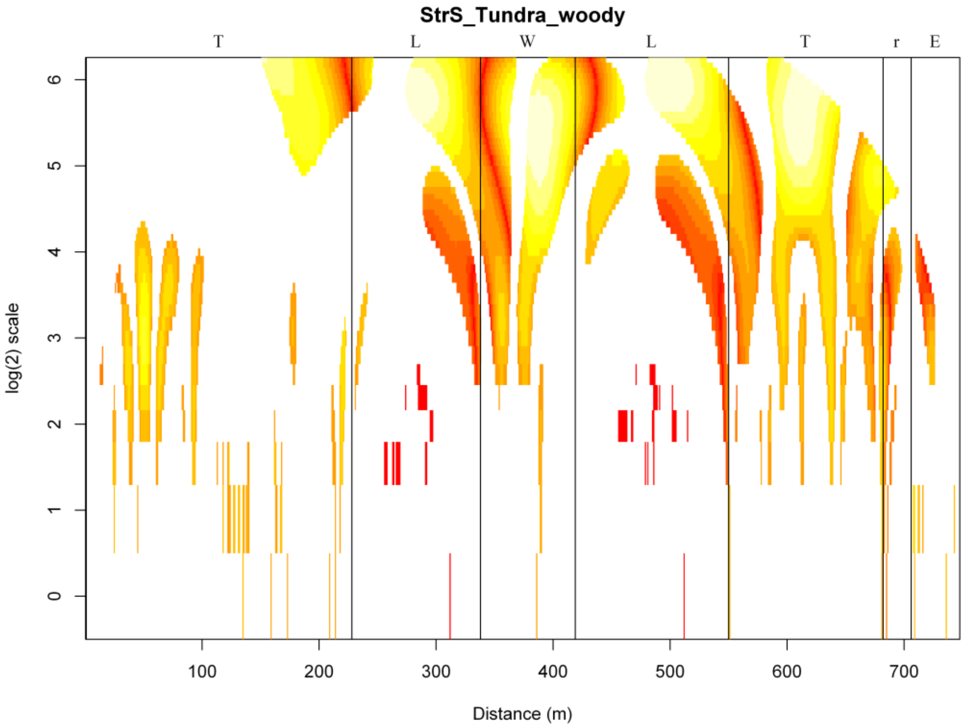
StrS_Tundra_woody
T
L
W
L
T
r
E
log(2) scale
0
1
2
3
4
5
6
100
200
300
400
500
600
700
Distance (m)

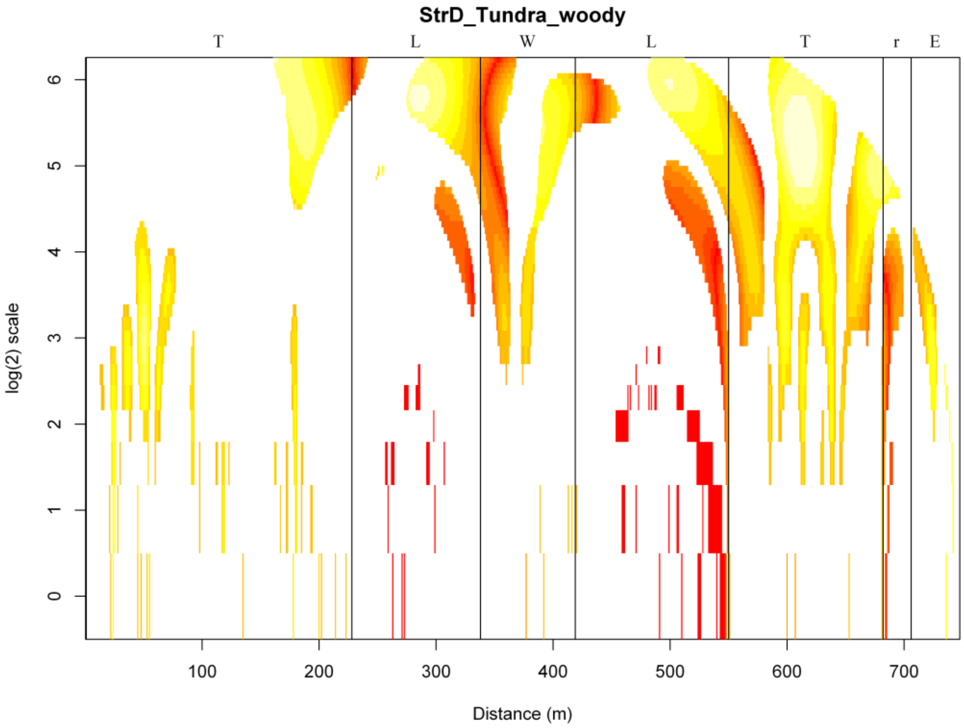
StrD_Tundra_woody
T
L
W
L
T
r
E
log(2) scale
0
1
2
3
4
5
6
100
200
300
400
500
600
700
Distance (m)

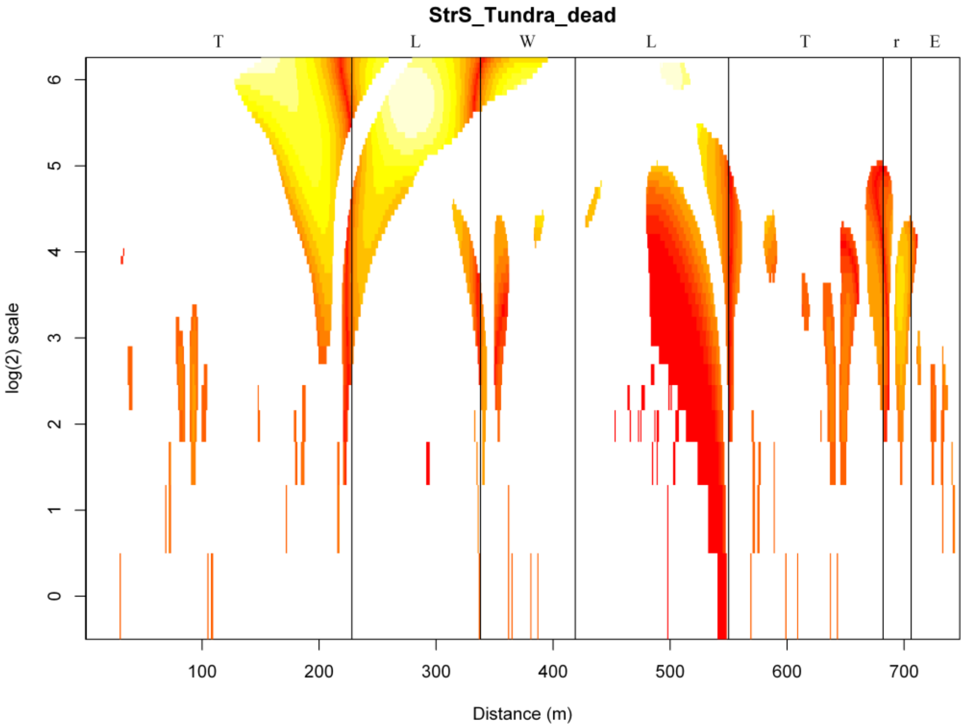
StrS_Tundra_dead
T
L
W
L
T
r
E
log(2) scale
0
1
2
3
4
5
6
100
200
300
400
500
600
700
Distance (m)

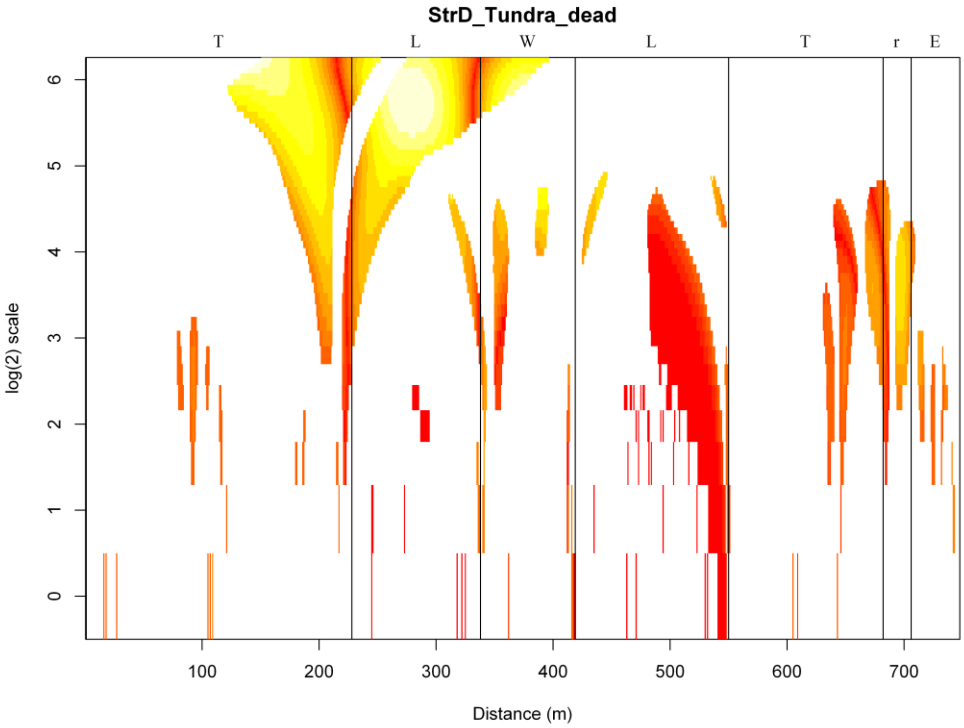
StrD_Tundra_dead
T
L
W
L
T
r
E
log(2) scale
0
1
2
3
4
5
6
100
200
300
400
500
600
700
Distance (m)

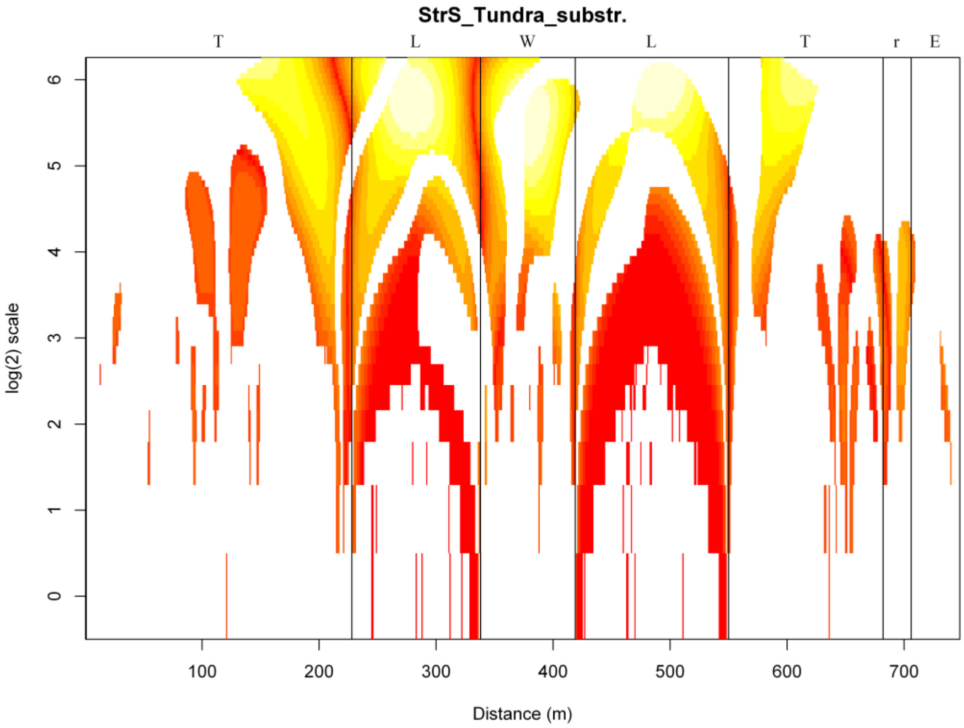
StrS_Tundra_substr.
T
L
W
L
T
r
E
log(2) scale
0
1
2
3
4
5
6
100
200
300
400
500
600
700
Distance (m)

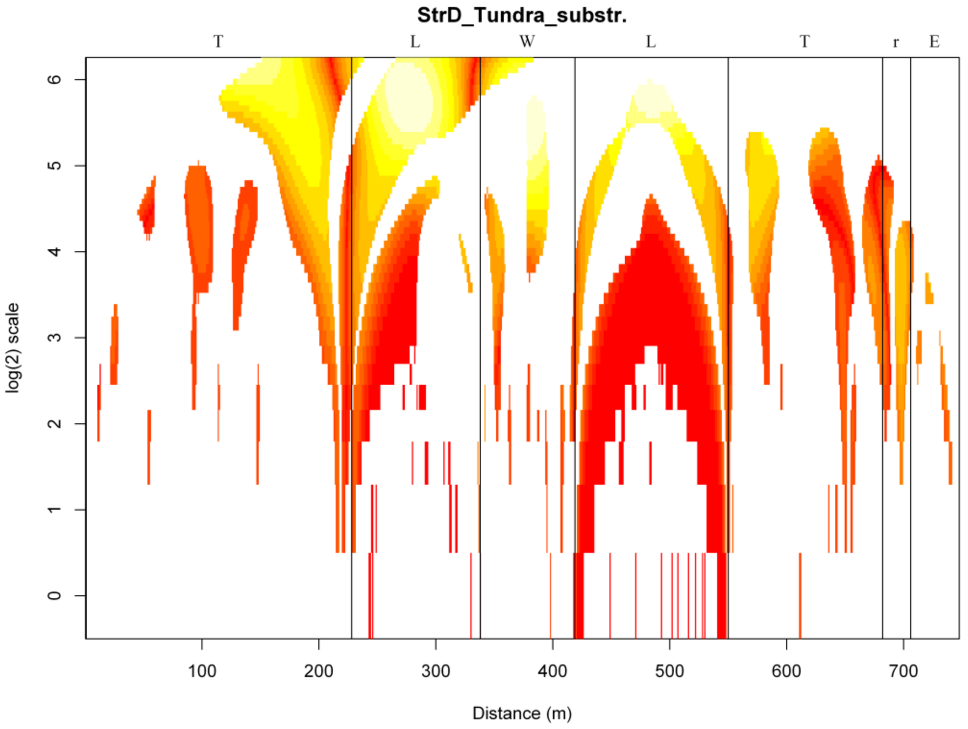
StrD_Tundra_substr.
T
L
W
L
T
r
E
log(2) scale
0
1
2
3
4
5
6
100
200
300
400
500
600
700
Distance (m)

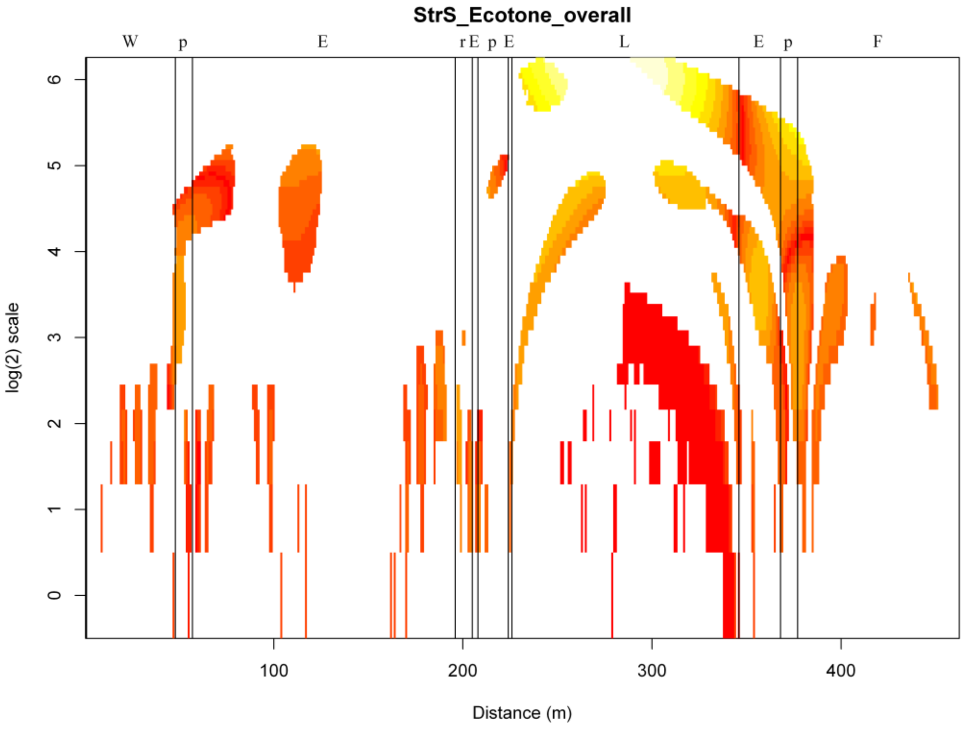
StrS_Ecotone_overall
W
p
E
r E
p
E
L
E
p
F
log(2) scale
0
1
2
3
4
5
6
100
200
300
400
Distance (m)

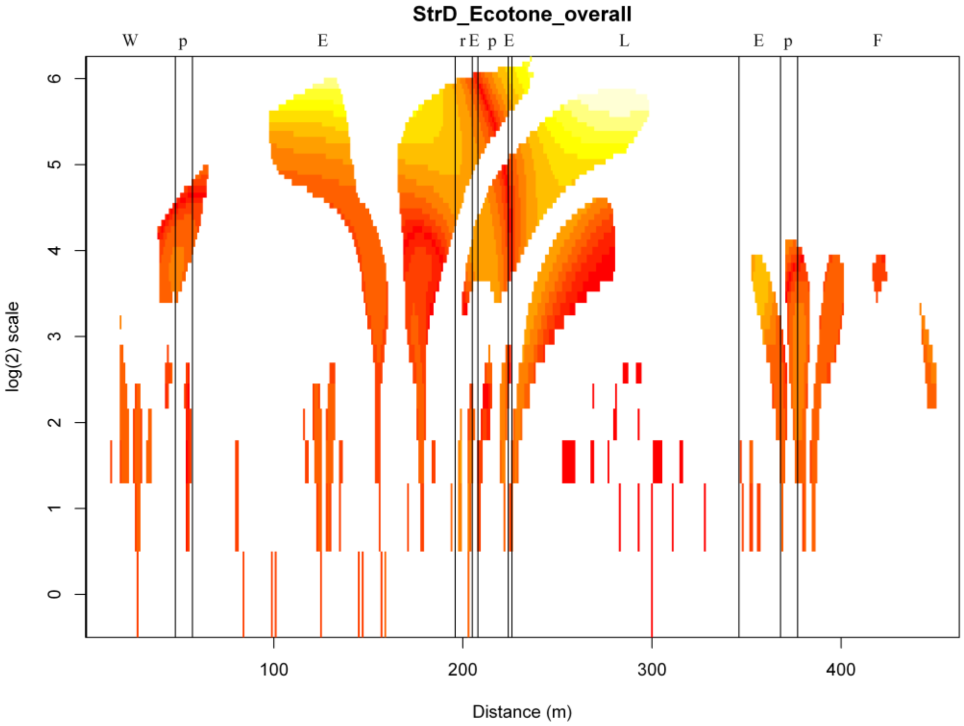
StrD_Ecotone_overall
W
p
E
r E
p
E
L
E
p
F
log(2) scale
0
1
2
3
4
5
6
100
200
300
400
Distance (m)

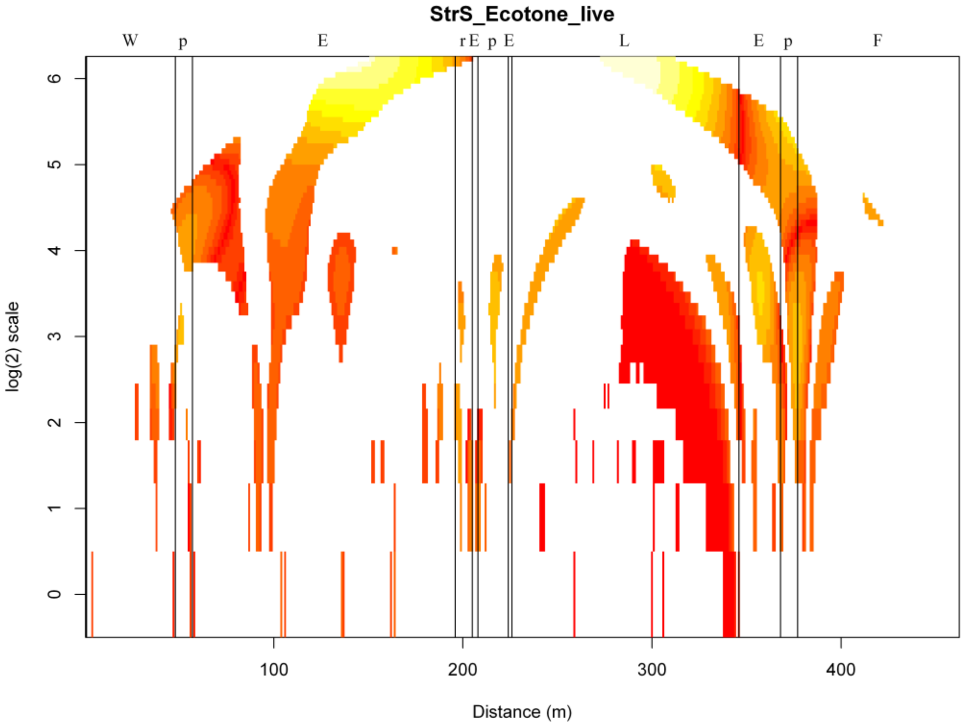
StrS_Ecotone_live
W
p
E
r E
p
E
L
E
p
F
log(2) scale
0
1
2
3
4
5
6
100
200
300
400
Distance (m)

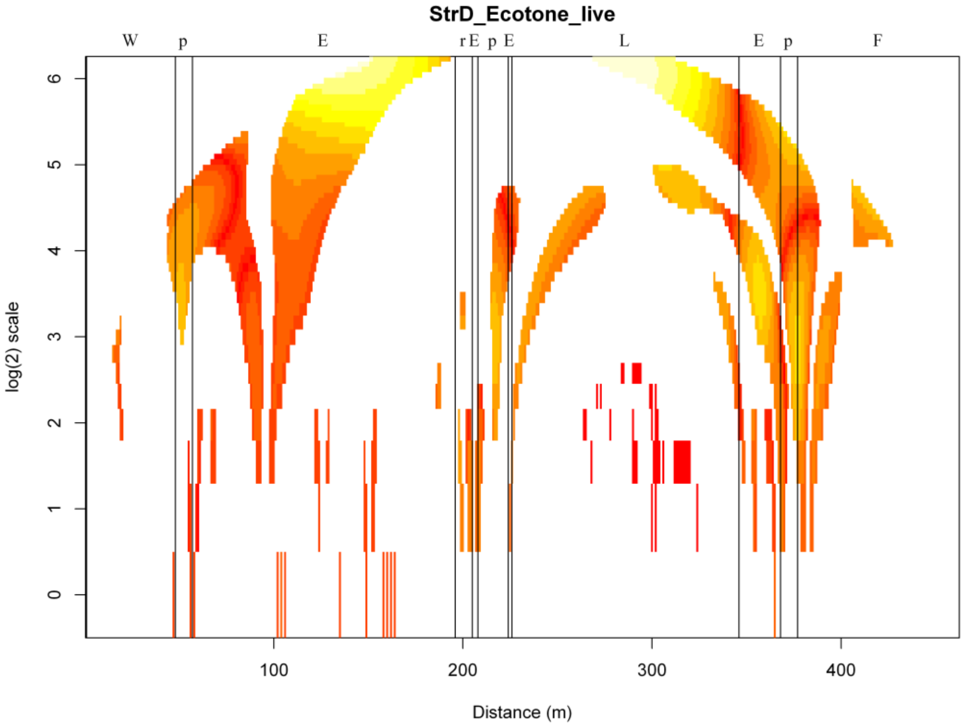
StrD_Ecotone_live
W
p
E
r
E
p
E
L
E
p
F
log(2) scale
0
1
2
3
4
5
6
100
200
300
400
Distance (m)

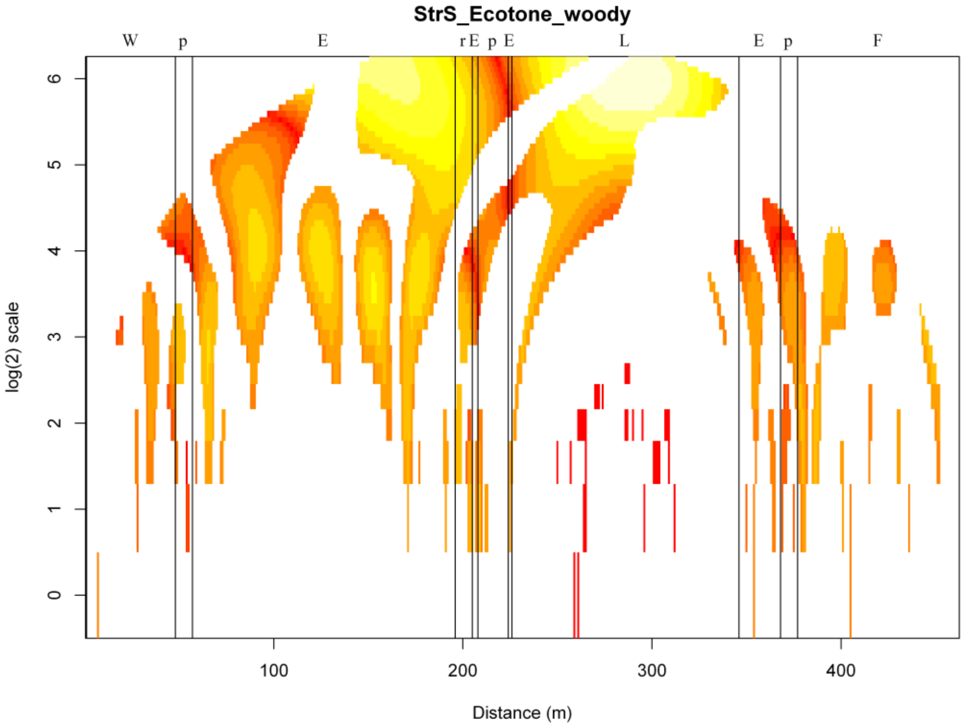
StrS_Ecotone_woody
W
p
E
r
E
p
E
L
E
p
F
log(2) scale
0
1
2
3
4
5
6
100
200
300
400
Distance (m)

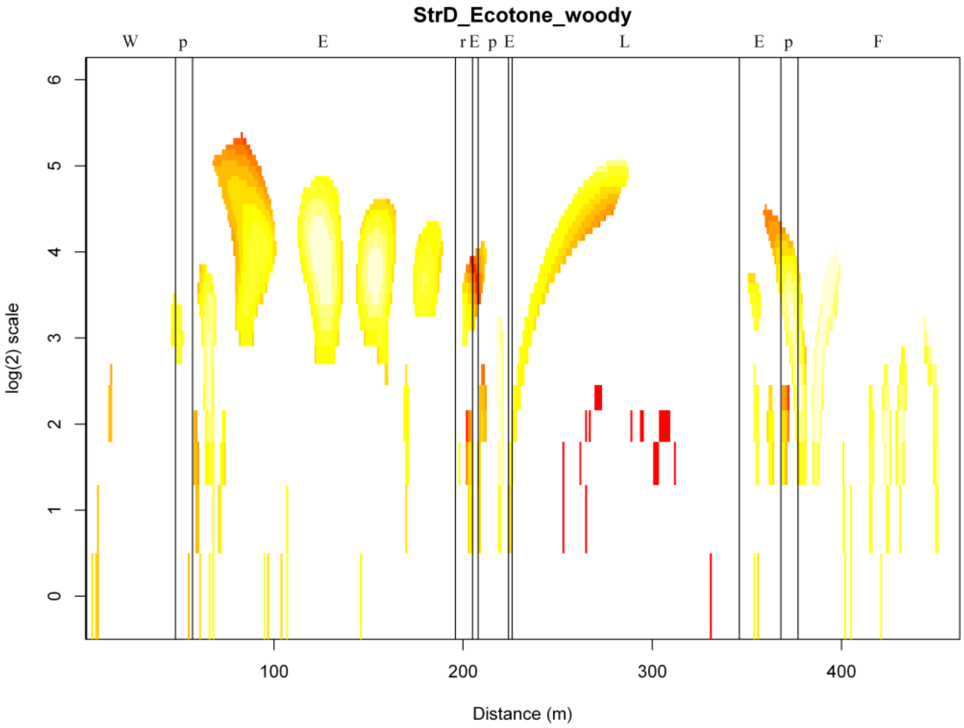
StrD_Ecotone_woody
W
p
E
r E
p
E
L
E
p
F
log(2) scale
0
1
2
3
4
5
6
100
200
300
400
Distance (m)

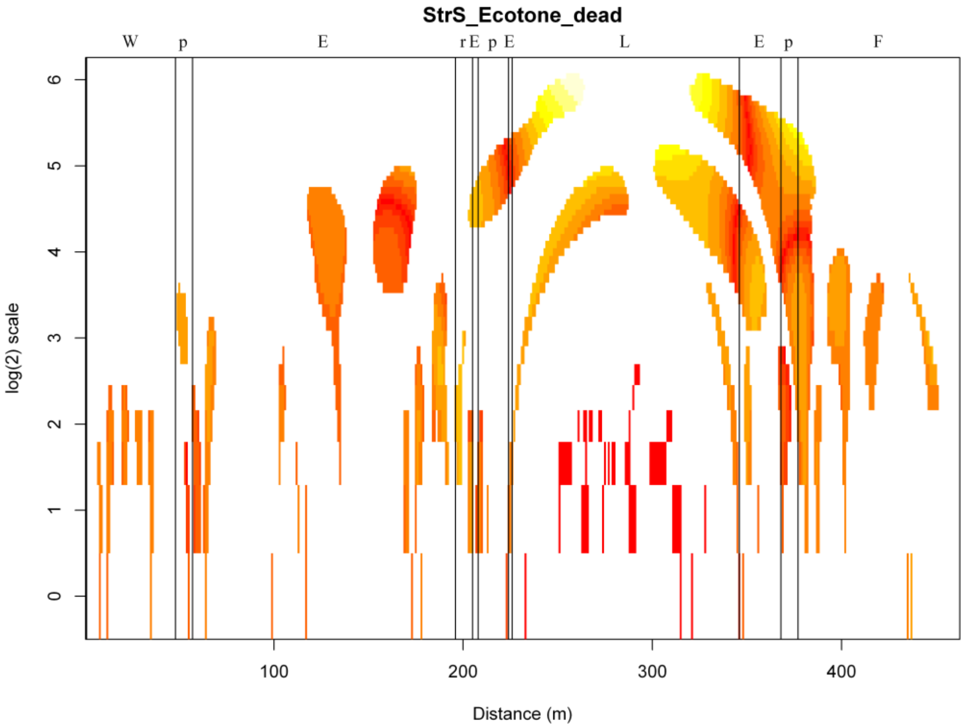
StrS_Ecotone_dead
W
p
E
r E
p
E
L
E
p
F
log(2) scale
0
1
2
3
4
5
6
100
200
300
400
Distance (m)

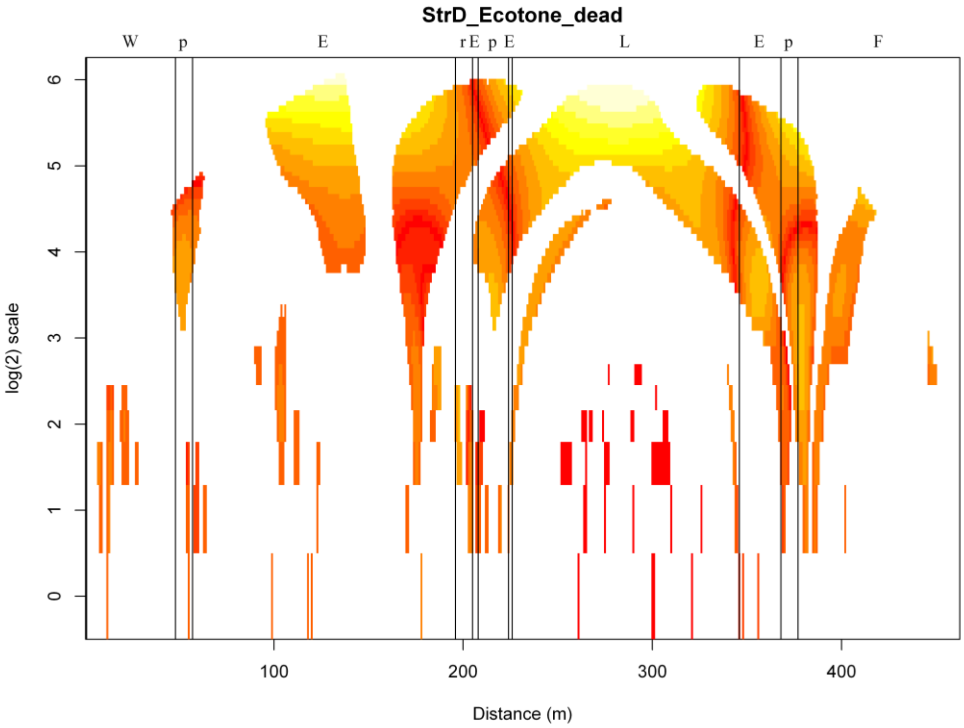
StrD_Ecotone_dead
W
p
E
r
E
p
E
L
E
p
F
log(2) scale
0
1
2
3
4
5
6
100
200
300
400
Distance (m)

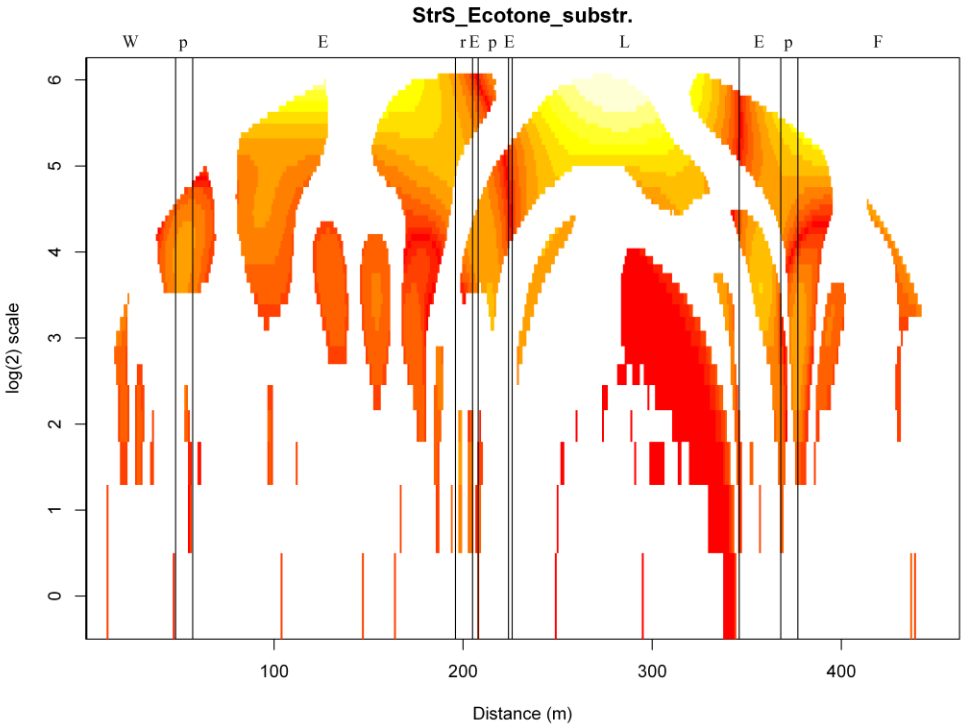
StrS_Ecotone_substr.
W
p
E
r
E
p
E
L
E
p
F
log(2) scale
0
1
2
3
4
5
6
100
200
300
400
Distance (m)

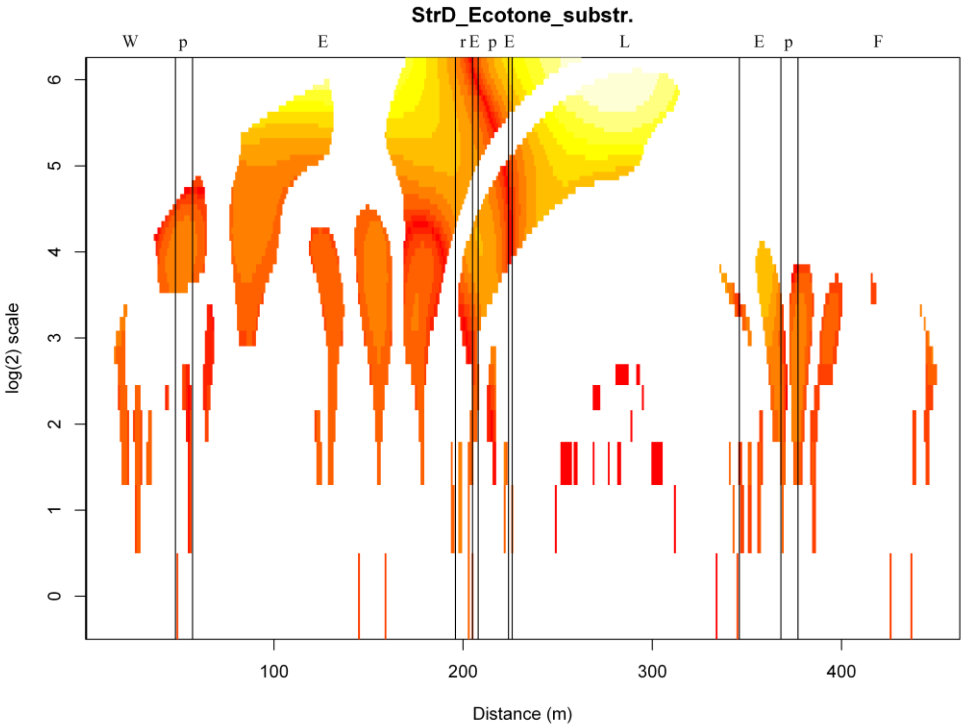
StrD_Ecotone_substr.
W
p
E
r E
p
E
L
E
p
F
log(2) scale
0
1
2
3
4
5
6
100
200
300
400
Distance (m)

SM 4.1 – R code used for generating the second-order autoregressive models

```
data.full = read.table(file.choose(), header=T, sep="\t") #A dataset
#with the variables to be analyzed in columns, each row
corresponding #to one quadrat. No column with the distance data,
only the variables #to be randomized.
patches = read.table("patches.txt", header=T) #A dataset with the
#patch type, starting and ending distances, same as in other
chapters
lengths=patches$End-patches$Start+1
patch.col=rep(as.character(patches[1,1]), lengths[1] )
for (i in 2:nrow(patches)) {
  patch.col=c(patch.col,
             rep(as.character(patches[i,1]), lengths[i] ) )
  }
patch.col=as.factor(patch.col)
patches.quad = as.character(patch.col)
Nvar = ncol(data.full)
Vars = names(data.full)
patches.use=subset(patches,Patch!="firebreak")
setwd("randomized") #The directory where the randomized datasets
will #be saved
make.plot=T #Whether plots of the dataset are to be shown in R when
#they are created
data.write=list()
Nperm=999 #Number of randomized datasets to be created
for(l in 1:Nvar) {
  nome=Vars[l]
  dados=data.full[,nome]
  Nquad = length(dados)
  data.write.temp=matrix(nrow=Nquad, ncol=Nperm+1)
  Npatches = nrow(patches)
  patchtypes = unique(patches.quad)
  Npatchtypes = length(patchtypes)
  regr.patches=list()
  for(i in 1:nrow(patches.use)) {
    indices=patches.use$Start[i]:patches.use$End[i]
```

```
    data.temp=dados[indices]
    Nquad=length(data.temp)
    #forward regression
    data.regr=data.frame(orig=data.temp)
    data.regr$second=c(NA,data.temp[-Nquad])
    data.regr$third=c(NA,NA,data.temp[-c(Nquad-1,Nquad)])
    regr.forward=lm(orig~second+third,data=data.regr)
    data.regr=data.frame(orig=data.temp)
    data.regr$second=c(data.temp[-1],NA)
    data.regr$third=c(data.temp[-c(1,2)],NA,NA)
    regr.backward=lm(orig~second+third,data=data.regr)
    coefs.forward=numeric(4)
    names(coefs.forward)=c("intercept", "second", "third", "sigma")

  coefs.forward["intercept"]=regr.forward$coefficients["(Intercept)"
]
    coefs.forward["second"]=regr.forward$coefficients["second"]
    coefs.forward["third"]=regr.forward$coefficients["third"]
    coefs.forward["sigma"]=summary(regr.forward)$sigma
    coefs.backward=numeric(4)
    names(coefs.backward)=c("intercept", "second", "third", "sigma")

  coefs.backward["intercept"]=regr.backward$coefficients["(Intercept
)"]
    coefs.backward["second"]=regr.backward$coefficients["second"]
    coefs.backward["third"]=regr.backward$coefficients["third"]
    coefs.backward["sigma"]=summary(regr.backward)$sigma
    coefs.regr=(coefs.forward+coefs.backward)/2
    regr.patches[[i]]=coefs.regr
    }
  for (i in 1:Nperm) {
    index=1
    for (j in 1:nrow(patches)) {
      indices=patches$Start[j]:patches$End[j]
      data.temp=dados[indices]
      Nquad=length(data.temp)
      if(patches$Patch[j] == "firebreak") {
```

```
        data.sim=sample(data.temp)
        } else {
        first=sample(1:(Nquad-2),1)
        data.sim=numeric(Nquad)
        data.sim[c(first,first+1)]=data.temp[c(first,first+1)]
        coefs.regr=regr.patches[[index]]
        for(k in (first+2):Nquad) {
          data.sim[k]=coefs.regr["intercept"]+
            data.sim[k-1]*coefs.regr["second"]+
            data.sim[k-2]*coefs.regr["third"]+
            rnorm(1,0,coefs.regr["sigma"])
          }
        for(k in (first-1):1) {
          data.sim[k]=coefs.regr["intercept"]+
            data.sim[k+1]*coefs.regr["second"]+
            data.sim[k+2]*coefs.regr["third"]+
            rnorm(1,0,coefs.regr["sigma"])
          }
        data.sim[data.sim<0]=0
        index=index+1
        }
      if(j==1) foobar = data.sim else foobar = c(foobar,data.sim)
      }
    if(l>4) foobar=round(foobar)
    data.write.temp[,i+1]=foobar
    print(c(l,i))
    if(make.plot) plot(foobar, type="l",
col=sample(colors(),1),main=c(l,i,nome), ylim=c(0,max(dados)))
    }
  data.write.temp[,1]=dados
  data.write[[l]]=data.write.temp
  write.table(data.write.temp, file=paste(nome,".txt",sep=""),
row.names=F, col.names=F, sep=" ")
  }
```

SM 4.1 – R code used for generating the second-order autoregressive models

```
transects
setwd("F:/Pavel/0-Research/MyPapers-Thesis/03-SpeciesComposition-JVegSci/")
setwd("forR")
data.full = read.table("data_within.txt", header=T, sep="\t")
patches = read.table("patches.txt", header=T)
lengths=patches$End-patches$Start+1
patch.col=rep(as.character(patches[1,1]), lengths[1] )
for (i in 2:nrow(patches)) {
 patch.col=c(patch.col, rep(as.character(patches[i,1]), lengths[i] ) )
  }
patch.col=as.factor(patch.col)
patches.quad = as.character(patch.col)
Nvar = ncol(data.full)
Vars = names(data.full)
patches.use=subset(patches,Patch!="firebreak")
setwd("randomized")

make.plot=T
data.write=list()
Nperm=999
for(l in 1:Nvar) {
 nome=Vars[l]
 dados=data.full[,nome]
 Nquad = length(dados)
 data.write.temp=matrix(nrow=Nquad, ncol=Nperm+1)
 Npatches = nrow(patches)
 patchtypes = unique(patches.quad)
 Npatchtypes = length(patchtypes)
 regr.patches=list()
 for(i in 1:nrow(patches.use)) {
   indices=patches.use$Start[i]:patches.use$End[i]
```

```
        data.temp=dados[indices]
        Nquad=length(data.temp)
        #forward regression
        data.regr=data.frame(orig=data.temp)
        data.regr$second=c(NA,data.temp[-Nquad])
        data.regr$third=c(NA,NA,data.temp[-c(Nquad-1,Nquad)])
        regr.forward=lm(orig~second+third,data=data.regr)
        data.regr=data.frame(orig=data.temp)
        data.regr$second=c(data.temp[-1],NA)
        data.regr$third=c(data.temp[-c(1,2)],NA,NA)
        regr.backward=lm(orig~second+third,data=data.regr)
        coefs.forward=numeric(4)
        names(coefs.forward)=c("intercept", "second", "third",
"sigma")

  coefs.forward["intercept"]=regr.forward$coefficients["(Intercept)"
]
        coefs.forward["second"]=regr.forward$coefficients["second"]
        coefs.forward["third"]=regr.forward$coefficients["third"]
        coefs.forward["sigma"]=summary(regr.forward)$sigma
        coefs.backward=numeric(4)
        names(coefs.backward)=c("intercept", "second", "third",
"sigma")

  coefs.backward["intercept"]=regr.backward$coefficients["(Intercept
)"]

  coefs.backward["second"]=regr.backward$coefficients["second"]
        coefs.backward["third"]=regr.backward$coefficients["third"]
        coefs.backward["sigma"]=summary(regr.backward)$sigma
        coefs.regr=(coefs.forward+coefs.backward)/2
        regr.patches[[i]]=coefs.regr
        }
      for (i in 1:Nperm) {
        index=1
        for (j in 1:nrow(patches)) {
          indices=patches$Start[j]:patches$End[j]
```

```
            data.temp=dados[indices]
            Nquad=length(data.temp)
            if(patches$Patch[j] == "firebreak") {
              data.sim=sample(data.temp)
              } else {
              first=sample(1:(Nquad-2),1)
              data.sim=numeric(Nquad)
              data.sim[c(first,first+1)]=data.temp[c(first,first+1)]
              coefs.regr=regr.patches[[index]]
              for(k in (first+2):Nquad) {
                data.sim[k]=coefs.regr["intercept"]+
                  data.sim[k-1]*coefs.regr["second"]+
                  data.sim[k-2]*coefs.regr["third"]+
                  rnorm(1,0,coefs.regr["sigma"])
                }
              for(k in (first-1):1) {
                data.sim[k]=coefs.regr["intercept"]+
                  data.sim[k+1]*coefs.regr["second"]+
                  data.sim[k+2]*coefs.regr["third"]+
                  rnorm(1,0,coefs.regr["sigma"])
                }
              data.sim[data.sim<0]=0
              index=index+1
              }
            if(j==1) foobar = data.sim else foobar =
c(foobar,data.sim)
            }
          if(l>4) foobar=round(foobar)
          data.write.temp[,i+1]=foobar
          print(c(l,i))
          if(make.plot) plot(foobar, type="l",
col=sample(colors(),1),main=c(l,i,nome), ylim=c(0,max(dados)))
          }
        data.write.temp[,1]=dados
        data.write[[l]]=data.write.temp
        write.table(data.write.temp, file=paste(nome,".txt",sep=""),
row.names=F, col.names=F, sep=" ")
```

```
}
```

SM 4.2 – List of species found along the transect, with their abundances, life forms and dispersal syndromes

Table SM 4.2. The species, with their corresponding lifeforms, dispersal syndromes, abundances (number of quadrats in which they were found), and abundance ranks (with the most abundant species corresponding to rank 1).

Family	Species	Lifeform	Dispersal	Abundance	Rank
Anacardiaceae					
	Anacardium humile	Herbaceous	Animal	13	66
Annonaceae					
	Annona coriacea	Woody	Animal	12	68
	Annona crassiflora	Woody	Animal	1	79
	Annona dioica	Herbaceous	Animal	85	22
	Duguetia furfuracea	Woody	Animal	31	54
	Xylopia aromatica	Woody	Animal	21	61
Apocynaceae					
	Aspidosperma tomentosum	Woody	Wind	9	71
	Blepharodon cf bicuspidatum	Vine	Wind	59	34
	Ditassa cf tomentosa	Vine	Wind	60	33
	Forsteronia glabrescens	Vine	Wind	122	14
	Oxypetalum cf *appendiculatum*	Vine	Wind	2	78
	Oxypetalum sp	Vine	Wind	7	73
Araliaceae					
	Schefflera vinosa	Woody	Animal	208	7
Arecaceae					
	Attalea geraensis	Herbaceous	Animal	1	79
Asteraceae					
	Achyrocline sp	Graminoid	Wind	115	16
	Baccharis dracunculifolia	Woody	Wind	26	58
	Bulbostylis sp	Graminoid	Wind	139	11
	Bulbostylis sp2	Graminoid	Wind	3	77
	Chromolaena sp	Herbaceous	Wind	63	31
	Gochnatia pulchra	Woody	Wind	70	26
	Piptocarpha rotundifolia	Woody	Wind	58	35
Bignoniaceae					
	Anemopaegma arvense	Herbaceous	Wind	12	67
	Anemopaegma glaucum	Herbaceous	Wind	10	70
	Jacaranda caroba	Woody	Wind	128	12
	Memora peregrina	Woody	Wind	104	20
	Pyrostegia venusta	Vine	Wind	9	71

Family	Species	Lifeform	Dispersal	Abundance	Rank
	Tabebuia ochracea	Woody	Wind	16	63
Bromeliaceae					
	Ananas ananassoides	Herbaceous	Animal	3	77
Burseraceae					
	Protium ovatum	Woody	Animal	11	69
Calophyllaceae					
	Kielmeyera coriacea	Woody	Wind	8	72
Caryocaraceae					
	Caryocar brasiliense	Woody	Animal	30	55
Celastraceae					
	Peritassa campestris	Herbaceous	Animal	8	72
Chrysobalanaceae					
	Licania rigida	Woody	Animal	33	52
Connaraceae					
	Connarus suberosus	Woody	Animal	28	56
	Rourea induta	Woody	Animal	1	79
Cucurbitaceae					
	Cayaponia espelina	Herbaceous	Animal	23	59
Cyperaceae					
	Cyperus sp	Graminoid	Wind	2	78
	Fimbristylis sp	Graminoid	Wind	65	29
	Rhynchospora cf *aurea*	Graminoid	Wind	8	72
Dilleniaceae					
	Davilla elliptica	Vine	Animal	48	41
	Doliocarpus sp	Vine	Self	1	79
Ebenaceae					
	Diospyros hispida	Woody	Animal	88	21
Erythroxylaceae					
	Erythroxylum cuneifolium	Woody	Animal	7	73
	Erythroxylum deciduum	Woody	Animal	127	13
	Erythroxylum suberosum	Woody	Animal	9	71
	Erythroxylum tortuosum	Woody	Animal	6	74
Euphorbiaceae					
	Croton antisyphiliticus	Herbaceous	Self	5	75
	Croton cf *hirtus*	Herbaceous	Self	12	68
	Croton sp	Herbaceous	Self	6	74
	Maprounea guianensis	Woody	Animal	2	78
	Sapium glandulosum	Woody	Animal	14	65
Fabaceae					
	Acosmium subelegans	Woody	Wind	83	23
	Anadenanthera falcata	Woody	Self	50	39

SM 4.2 – List of species found along the transect, with their abundances, life forms and dispersal syndromes

Family	Species	Lifeform	Dispersal	Abundance	Rank
	Andira humilis	Woody	Animal	56	37
	Bauhinia rufa	Woody	Self	109	19
	Bowdichia virgilioides	Woody	Wind	26	58
	Chamaecrista cf *cathartica*	Herbaceous	Self	5	75
	Chamaecrista desvauxii	Herbaceous	Self	3	77
	Chamaecrista flexuosa	Herbaceous	Self	46	43
	Chamaecrista sp	Herbaceous	Self	2	78
	Copaifera langsdorffii	Woody	Animal	1	79
	Dalbergia miscolobium	Woody	Wind	57	36
	Dimorphandra mollis	Woody	Animal	7	73
	Eriosema cf *benthamianum*	Herbaceous	Self	10	70
	Eriosema crinitum	Herbaceous	Self	37	50
	Eriosema longifolium	Herbaceous	Self	20	62
	Galactia decumbens	Vine	Self	26	58
	Inga sp	Woody	Animal	1	79
	Mimosa dolens	Herbaceous	Animal	10	70
	Mimosa nuda	Herbaceous	Self	6	74
	Mimosa sp	Herbaceous	Self	3	77
	Mimosa velloziana	Herbaceous	Self	2	78
	Mimosa xanthocentra	Herbaceous	Wind	5	75
	Plathymenia reticulata	Woody	Wind	1	79
	Sclerolobium paniculatum	Woody	Wind	5	75
	Senna rugosa	Woody	Self	10	70
	Stryphnodendron adstringens	Woody	Animal	27	57
	Stryphnodendron obovatum	Woody	Animal	36	51
	Stylosanthes guianensis	Herbaceous	Self	45	44
	Zornia diphylla	Herbaceous	Animal	8	72
Gleicheniaceae					
	Gleichenia sp.	Fern (herbaceous)	Wind	6	74
Lamiaceae					
	Aegiphila lhotzkiana	Woody	Animal	82	24
	Hyptis crinita	Herbaceous	Self	47	42
	Hyptis marrubioides	Herbaceous	Self	7	73
	Hyptis sp	Herbaceous	Self	48	41
	Peltodon tomentosus	Herbaceous	Self	62	32
Lauraceae					
	Ocotea pulchella	Woody	Animal	12	68
Lythraceae					
	Diplusodon virgatus	herbaceous	Self	45	44
Malpighiaceae					

SM 4.2 – List of species found along the transect, with their abundances, life forms and dispersal syndromes

Family	Species	Lifeform	Dispersal	Abundance	Rank
	Banisteriopsis argyrophylla	Vine	Wind	49	40
	Banisteriopsis stellaris	Herbaceous	Wind	22	60
	Byrsonima intermedia	Woody	Animal	222	6
	Byrsonima pachyphylla	Woody	Animal	4	76
Malvaceae					
	Byttneria sagittifolia	Herbaceous	Self	20	62
	Eriotheca gracilipes	Woody	Wind	15	64
	Sida cf *rhombifolia*	Herbaceous	Self	21	61
Melastomataceae					
	Leandra aurea	Woody	Animal	63	31
	Miconia albicans	Woody	Animal	375	2
	Miconia fallax	Woody	Animal	36	51
	Miconia ligustroides	Woody	Animal	112	18
	Miconia rubiginosa	Woody	Animal	1	79
	Miconia stenostachya	Woody	Animal	27	57
	Tibouchina stenocarpa	Woody	Wind	31	54
Menispermaceae					
	Cissampelos ovalifolia	Herbaceous	Self	64	30
Myrtaceae					
	Campomanesia adamantium	Woody	Animal	160	10
	Eucalyptus grandis	Woody	Planted	53	38
	Eugenia aff bimarginata	Woody	Animal	3	77
	Eugenia dysenterica	Woody	Animal	10	70
	Eugenia punicifolia	Woody	Animal	3	77
	Myrcia bella	Woody	Animal	22	60
	Myrcia guianesis	Woody	Animal	28	56
	Myrcia lingua	Woody	Animal	114	17
	Myrcia tomentosa	Woody	Animal	14	65
	Myrciaria cf floribunda	Woody	Animal	14	65
	Psidium australe	Woody	Animal	44	45
	Psidium cinereum	herbaceous	Animal	41	47
	Psidium laruotteanum	herbaceous	Animal	43	46
	Psidium suffruticosum	herbaceous	Animal	6	74
Nyctaginaceae					
	Guapira noxia	Woody	Animal	5	75
Ochnaceae					
	Ouratea acuminata	Herbaceous	Animal	31	54
	Ouratea spectabilis	Herbaceous	Animal	10	70
Peraceae					
	Pera glabrata	Woody	Animal	22	60
Phyllanthaceae					

Family	Species	Lifeform	Dispersal	Abundance	Rank
	Phyllanthus acuminatus	Woody	Self	5	75
Poaceae					
	Andropogon bicornis	Graminoid	Wind	32	53
	Andropogon cf *leucostachyus*	Graminoid	Wind	605	1
	Aristida sp1	Graminoid	Wind	28	56
	Aristida sp2	Graminoid	Wind	5	75
	Chloris cf orthonoton	Graminoid	Wind	3	77
	Digitaria sp	Graminoid	Self	187	8
	Imperata brasiliensis	Graminoid	Wind	122	14
	Melinis minutiflora	Graminoid	Wind	605	1
	Melinis repens	Graminoid	Wind	1	79
	Panicum cf campestre	Graminoid	Wind	12	68
	Panicum sp2	Graminoid	Wind	168	9
	Panicum sp3	Graminoid	Wind	1	79
	Paspalum cf pilosum	Graminoid	Wind	66	28
	Paspalum sp2	Graminoid	Wind	1	79
	Paspalum sp3	Graminoid	Wind	1	79
	Schizachyrium sp1	Graminoid	Wind	63	31
	Schizachyrium sp2	Graminoid	Wind	1	79
	Urochloa decumbens	Graminoid	Animal	261	5
Polygalaceae					
	Bredemeyera laurifolia	Woody	Animal	22	60
Primulaceae					
	Myrsine ferruginea	Woody	Animal	16	63
	Myrsine umbellata	Woody	Animal	40	48
Proteaceae					
	Roupala montana	Woody	Wind	37	50
Rosaceae					
	Rubus sp	Herbaceous	Animal	8	72
Rubiaceae					
	Alibertia myrciifolia	Woody	Animal	38	49
	Chomelia cf ribesioides	Woody	Animal	7	73
	Coccocypselum cf *lanceolatum*	Herbaceous	Animal	21	61
	Diodia cf *alata*	Herbaceous	Self	294	4
	Psychotria sp.	Herbaceous	Animal	2	78
	Tocoyena formosa	Woody	Animal	23	59
Rutaceae					
	Zanthoxylum rhoifolium	Woody	Animal	6	74
Salicaceae					
	Casearia silvestris	Woody	Animal	117	15

SM 4.2 – List of species found along the transect, with their abundances, life forms and dispersal syndromes

Family	Species	Lifeform	Dispersal	Abundance	Rank
Sapindaceae					
	Serjania erecta	Vine	Wind	67	27
	Serjania lethalis	Vine	Wind	20	62
Sapotaceae					
	Pouteria torta	Woody	Animal	5	75
Smilacaceae					
	Smilax cissoides	Vine	Animal	302	3
Solanaceae					
	Solanum cf robustum	Herbaceous	Animal	10	70
	Solanum lycocarpum	Woody	Animal	2	78
	Solanum megalochiton	Herbaceous	Animal	1	79
	Solanum paniculatum	Herbaceous	Animal	2	78
	Solanum sp	Herbaceous	Animal	4	76
Styracaceae					
	Styrax ferrugineus	Woody	Animal	6	74
Verbenaceae					
	Lippia sp1	Woody	Self	5	75
	Lippia velutina	Woody	Self	74	25
	Stachytarpheta cayennensis	Herbaceous	Self	53	38
Vochysiaceae					
	Qualea cordata	Woody	Wind	1	79
	Qualea multiflora	Woody	Wind	7	73
	Vochysia tucanorum	Woody	Wind	3	77

SM 4.2 – List of species found along the transect, with their abundances, life forms and dispersal syndromes

SM 4.3 – Full multiresolution analysis for all response variables along the study transect

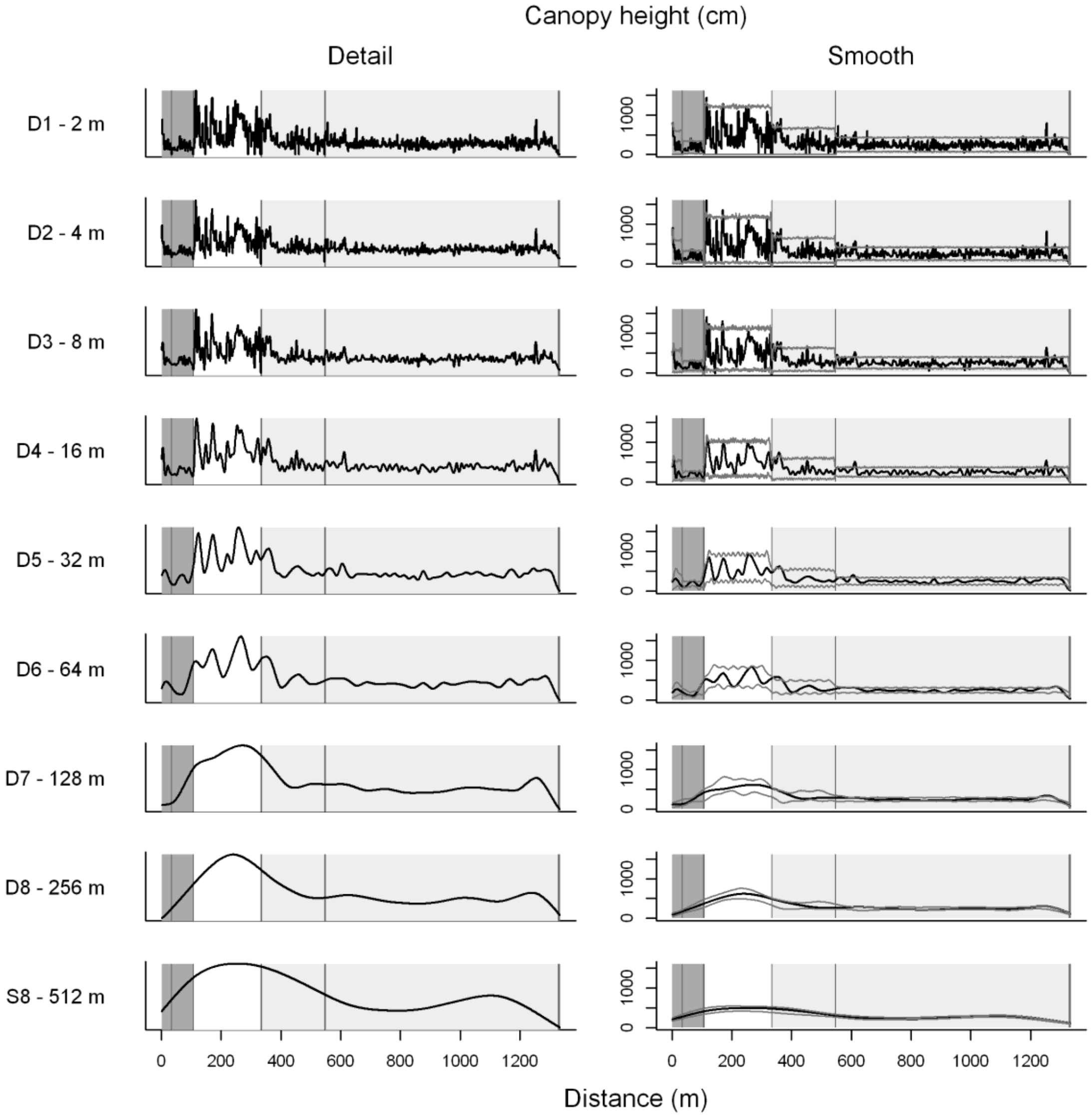

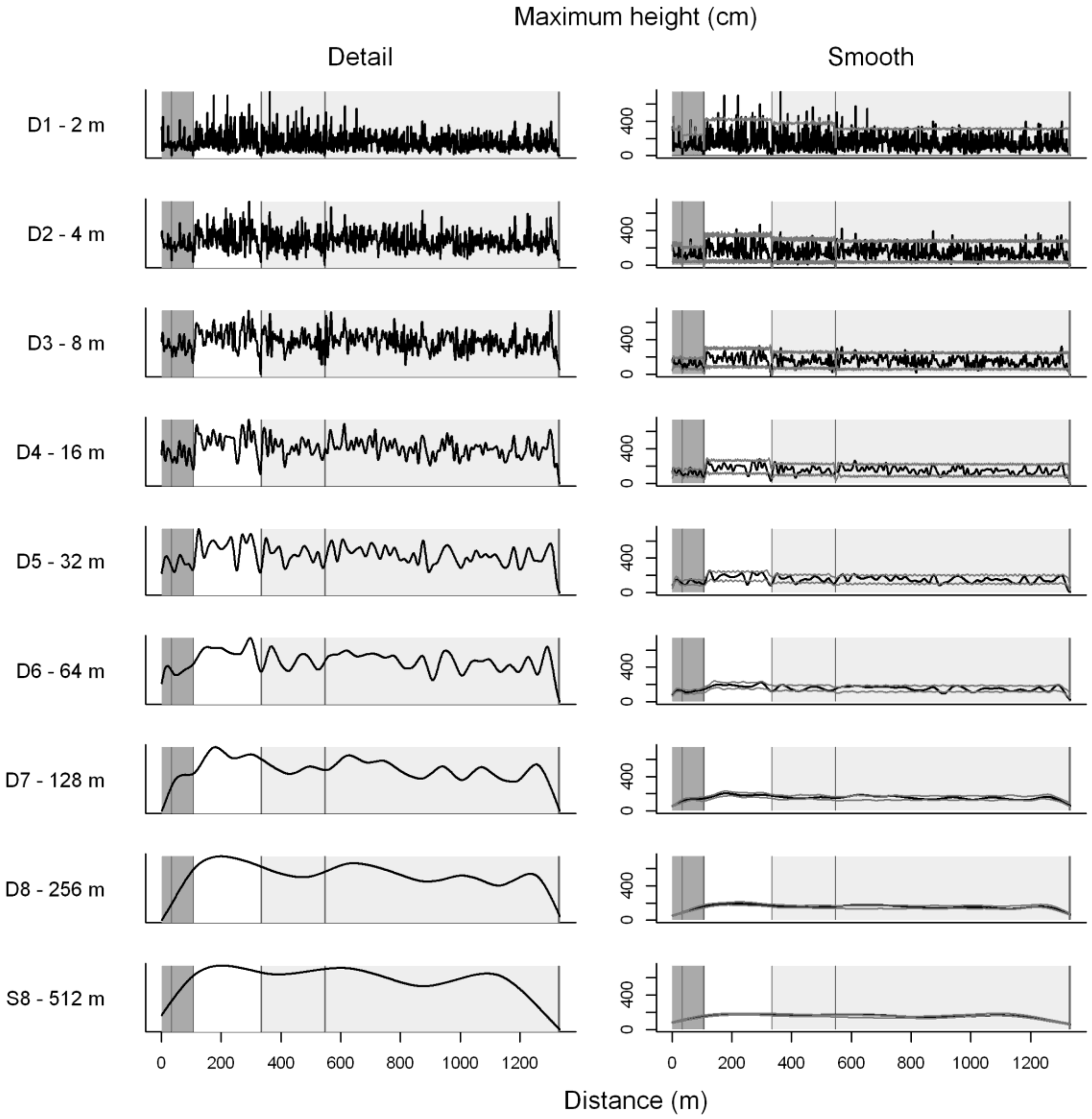

SM 4.3 – Full multiresolution analysis for all response variables along the study transect

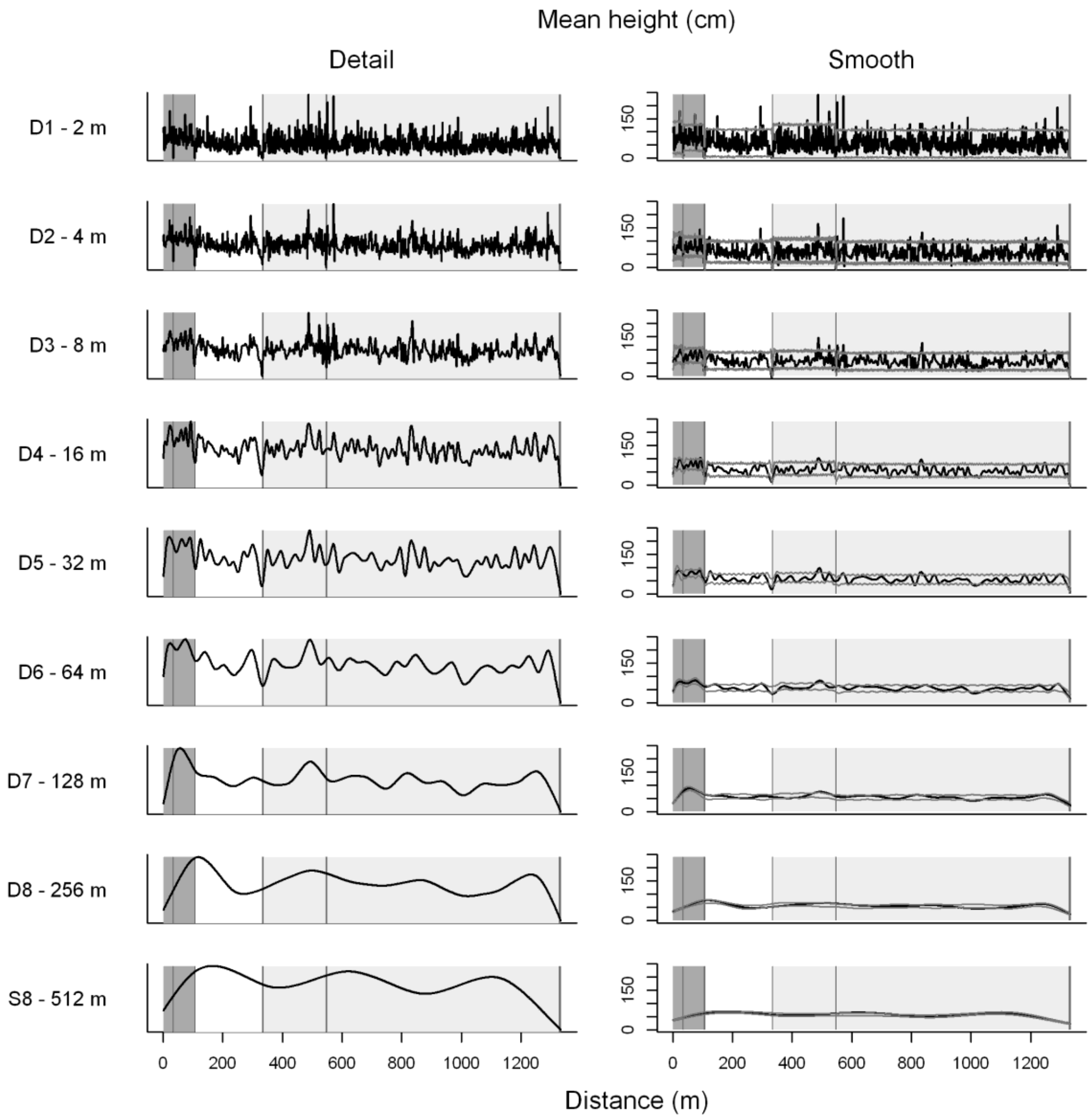
Mean height (cm)
Detail
Smooth
D1 - 2 m
D2 - 4 m
D3 - 8 m
D4 - 16 m
D5 - 32 m
D6 - 64 m
D7 - 128 m
D8 - 256 m
S8 - 512 m
0
150
0
200
400
600
800
1000
1200
Distance (m)

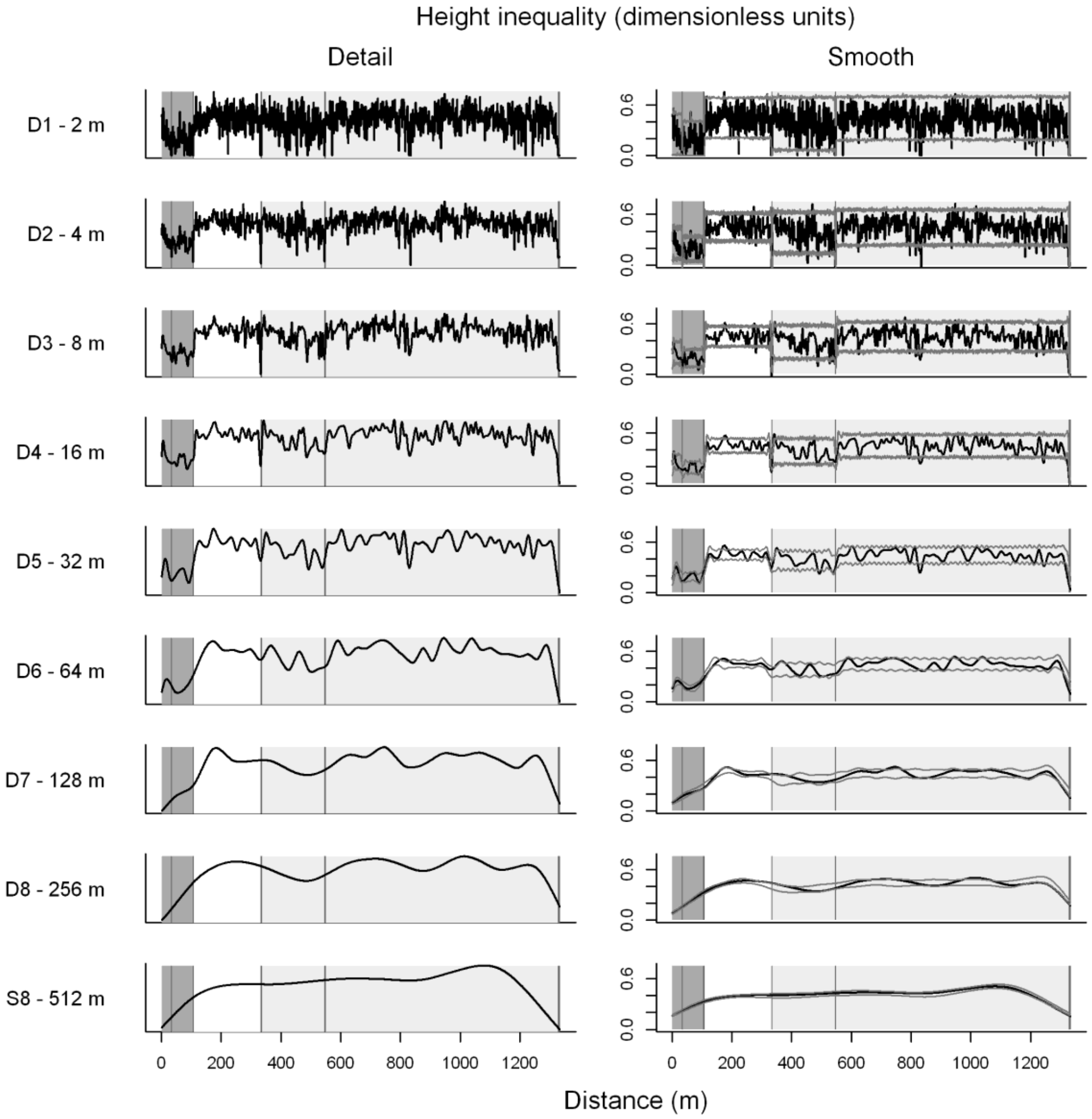

SM 4.3 – Full multiresolution analysis for all response variables along the study transect

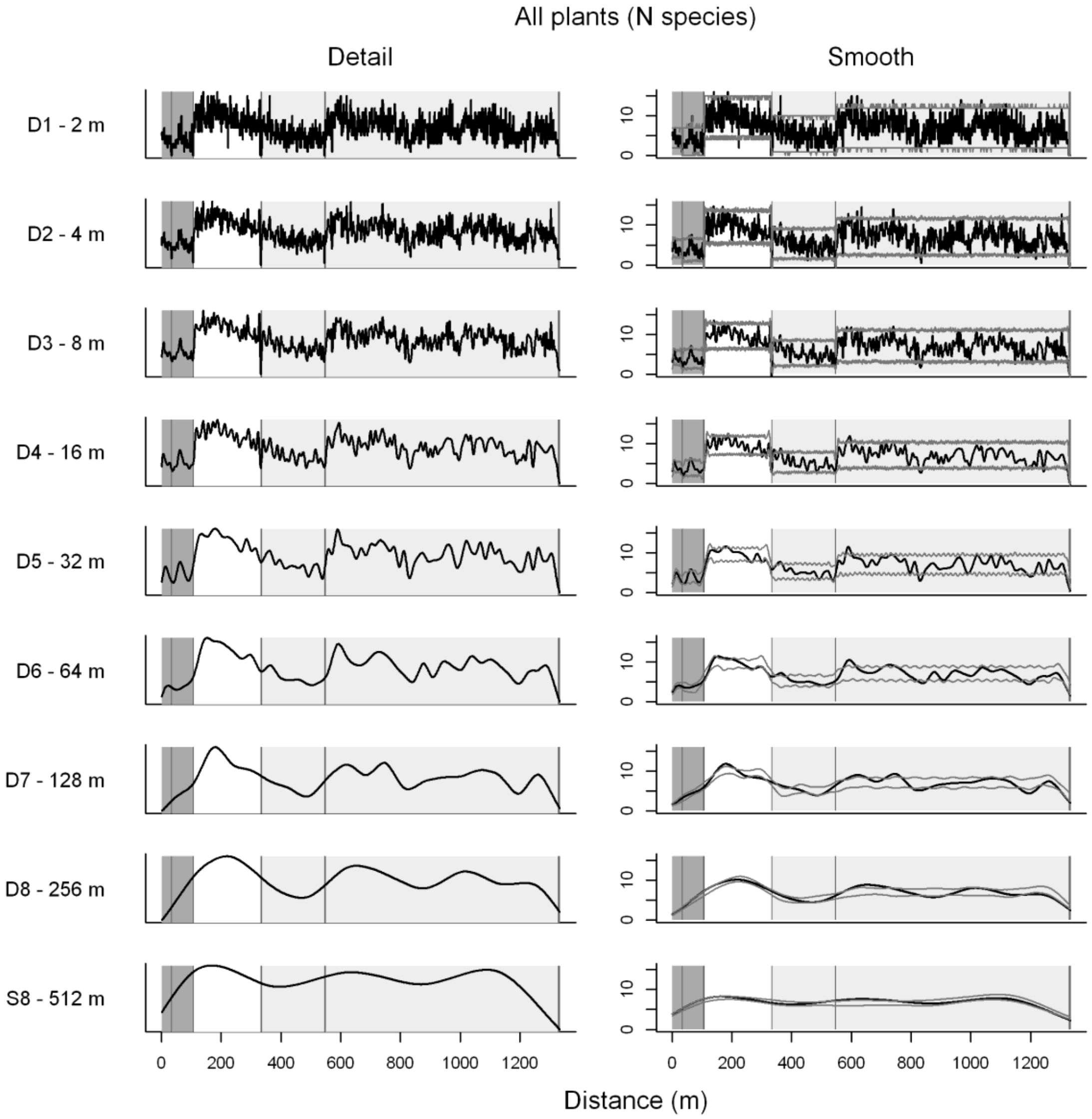
All plants (N species)
Detail
Smooth
D1 - 2 m
D2 - 4 m
D3 - 8 m
D4 - 16 m
D5 - 32 m
D6 - 64 m
D7 - 128 m
D8 - 256 m
S8 - 512 m
0
10
0
200
400
600
800
1000
1200
Distance (m)

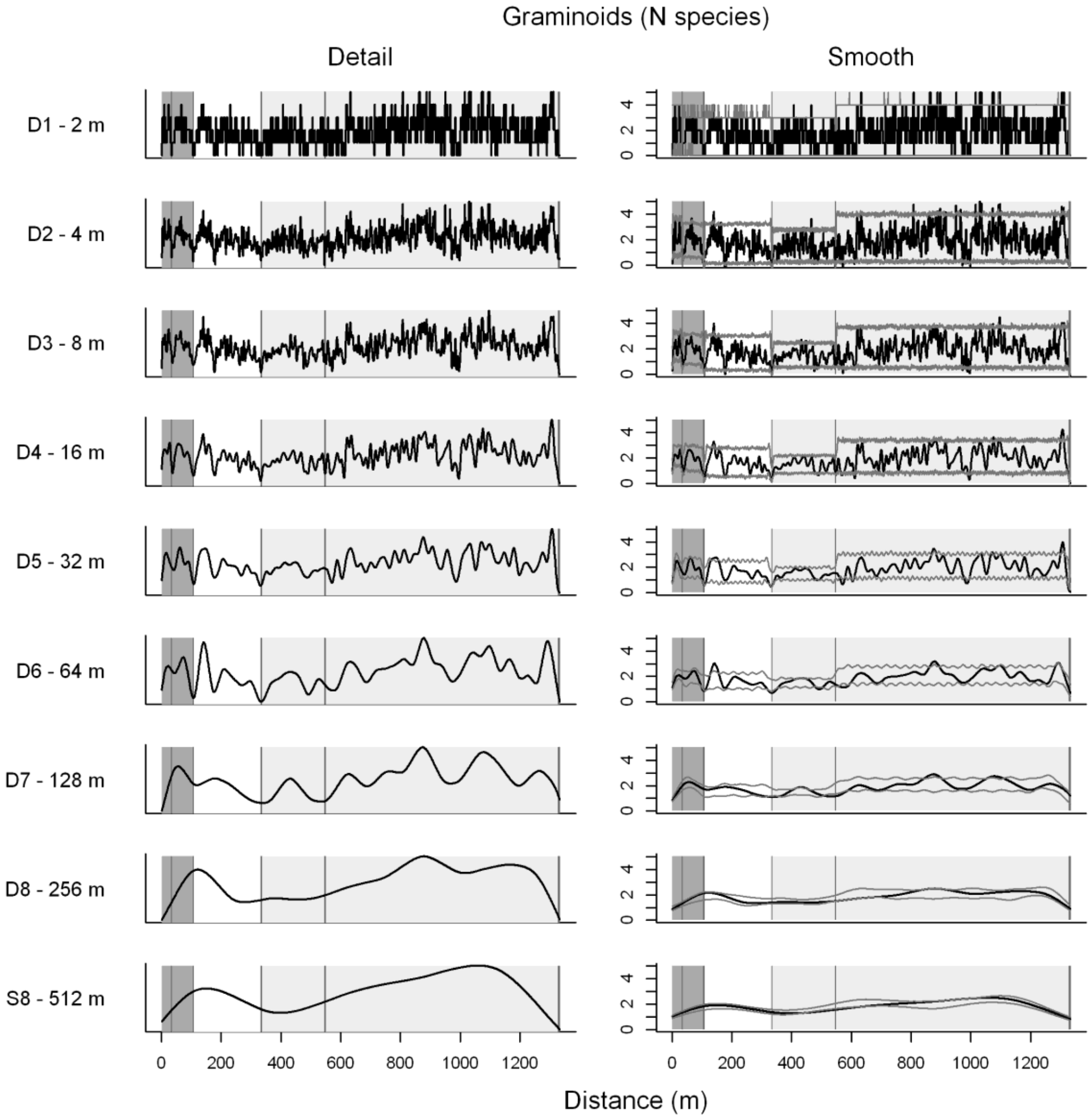
Graminoids (N species)
Detail
Smooth
D1 - 2 m
D2 - 4 m
D3 - 8 m
D4 - 16 m
D5 - 32 m
D6 - 64 m
D7 - 128 m
D8 - 256 m
S8 - 512 m
0
2
4
0
200
400
600
800
1000
1200
Distance (m)

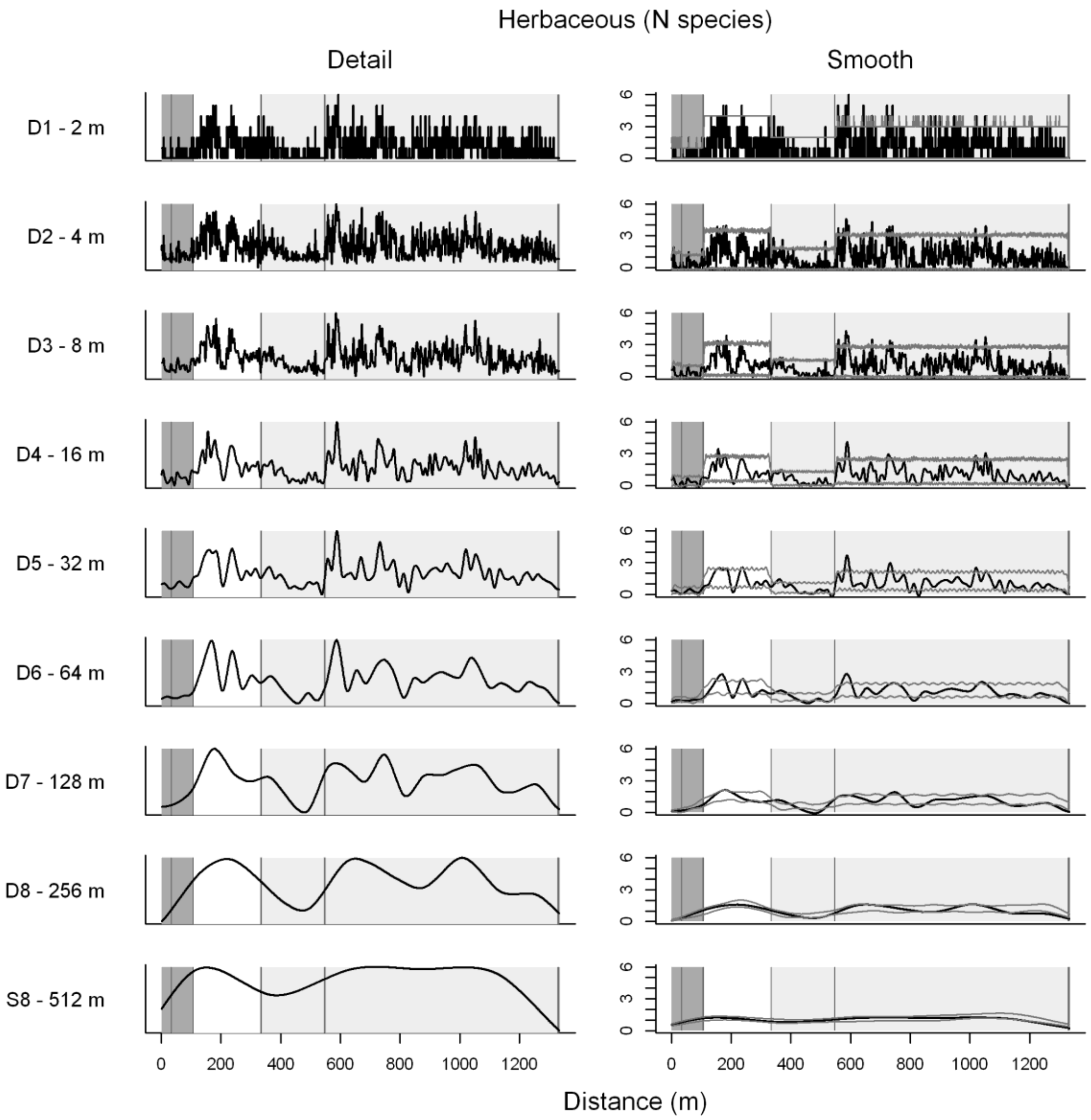
Herbaceous (N species)
Detail
Smooth
D1 - 2 m
D2 - 4 m
D3 - 8 m
D4 - 16 m
D5 - 32 m
D6 - 64 m
D7 - 128 m
D8 - 256 m
S8 - 512 m
0
3
6
0
200
400
600
800
1000
1200
Distance (m)

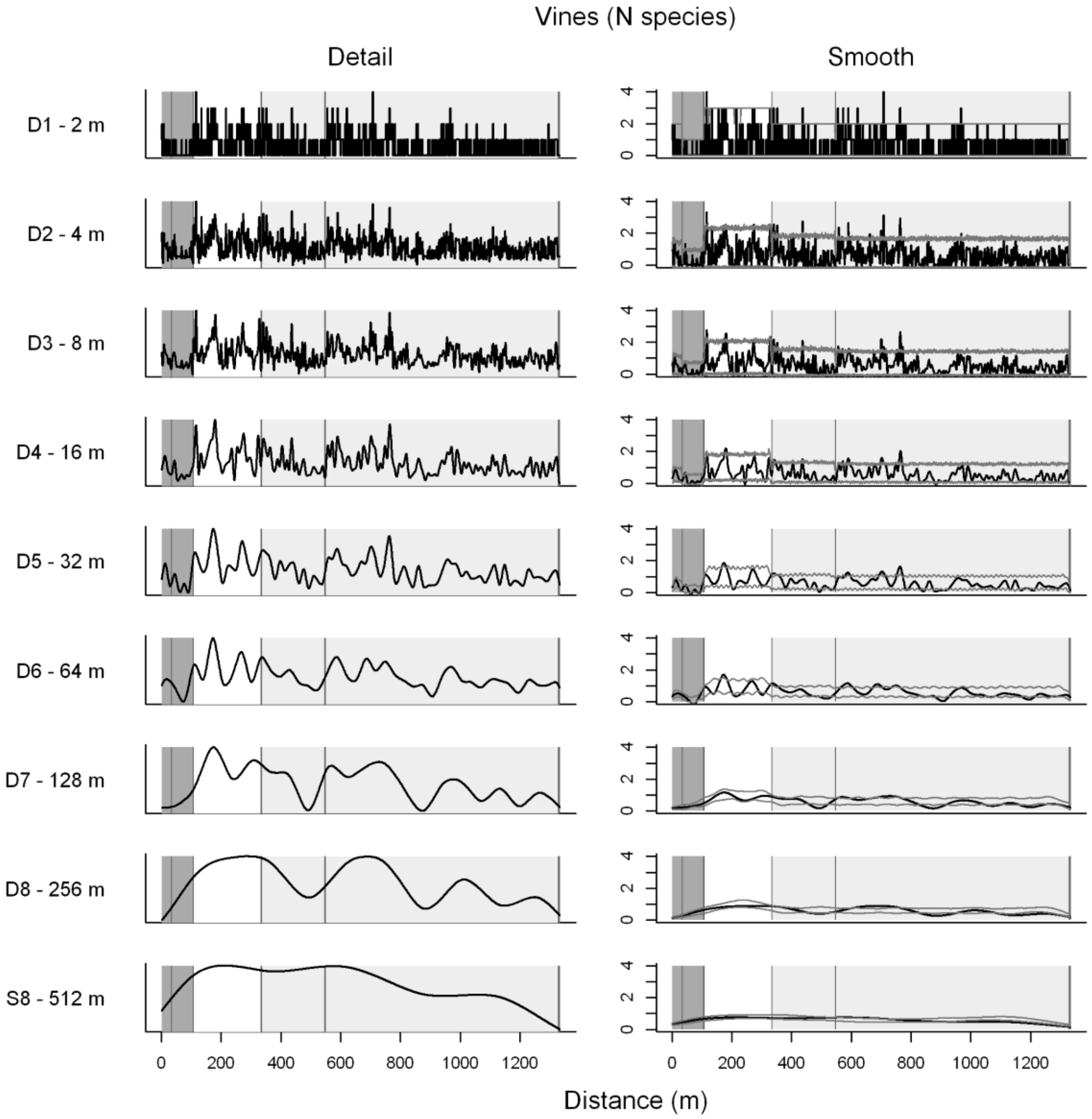
Vines (N species)
Detail
Smooth
D1 - 2 m
D2 - 4 m
D3 - 8 m
D4 - 16 m
D5 - 32 m
D6 - 64 m
D7 - 128 m
D8 - 256 m
S8 - 512 m
0
2
4
0
200
400
600
800
1000
1200
Distance (m)

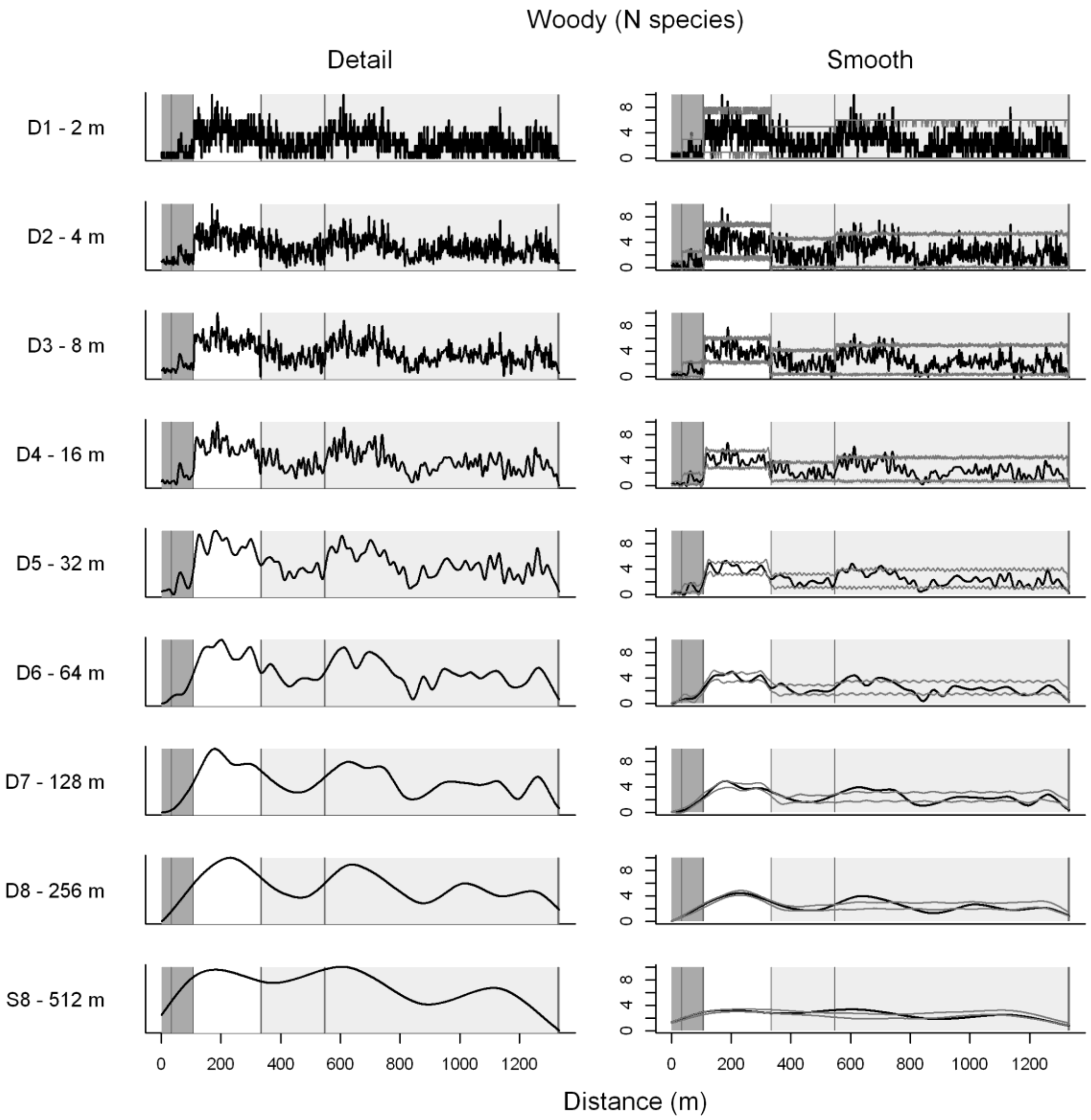
Woody (N species)
Detail
Smooth
D1 - 2 m
D2 - 4 m
D3 - 8 m
D4 - 16 m
D5 - 32 m
D6 - 64 m
D7 - 128 m
D8 - 256 m
S8 - 512 m
0
4
8
0
200
400
600
800
1000
1200
Distance (m)

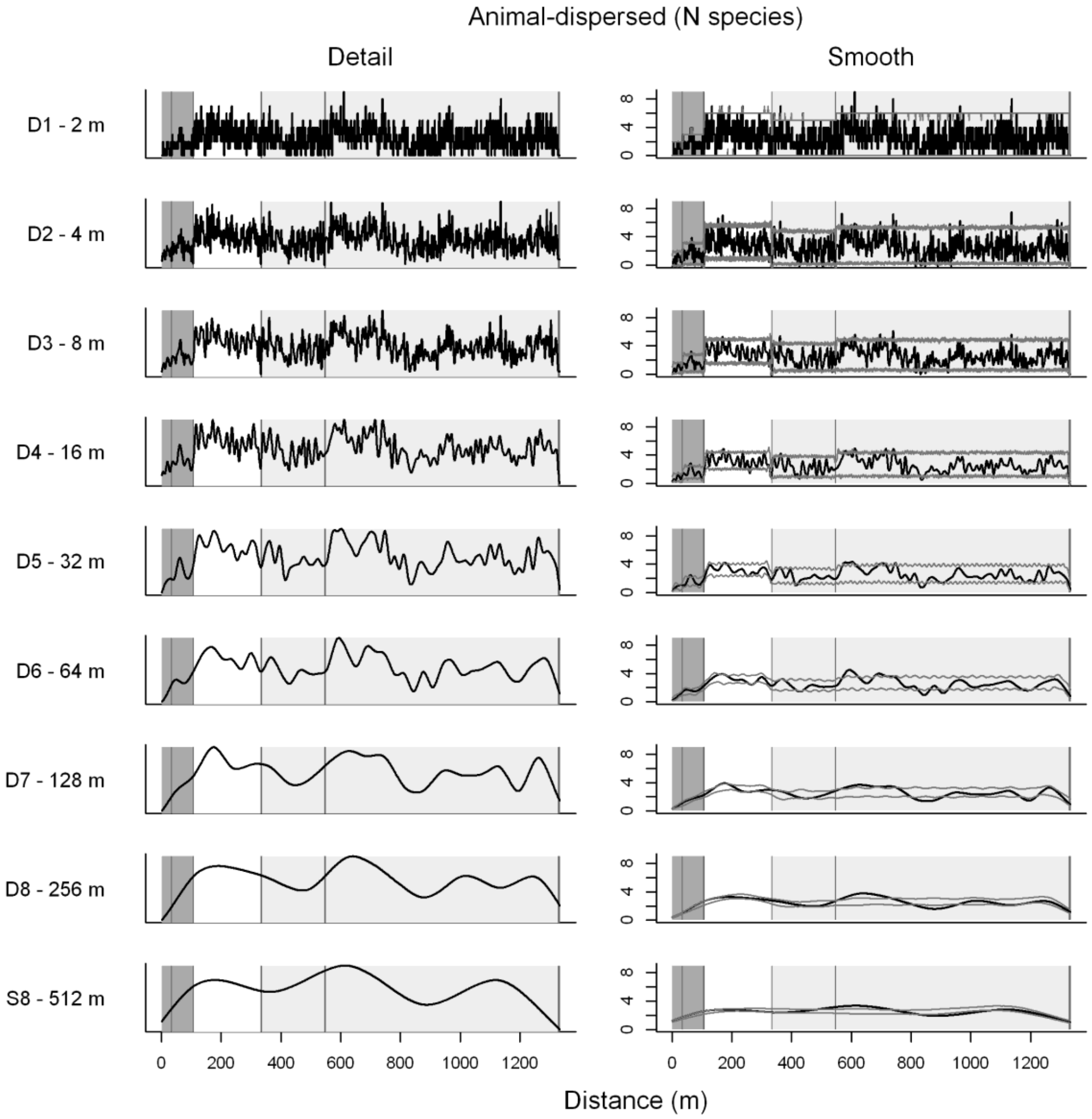
Animal-dispersed (N species)
Detail
Smooth
D1 - 2 m
D2 - 4 m
D3 - 8 m
D4 - 16 m
D5 - 32 m
D6 - 64 m
D7 - 128 m
D8 - 256 m
S8 - 512 m
0
4
8
0
200
400
600
800
1000
1200
Distance (m)

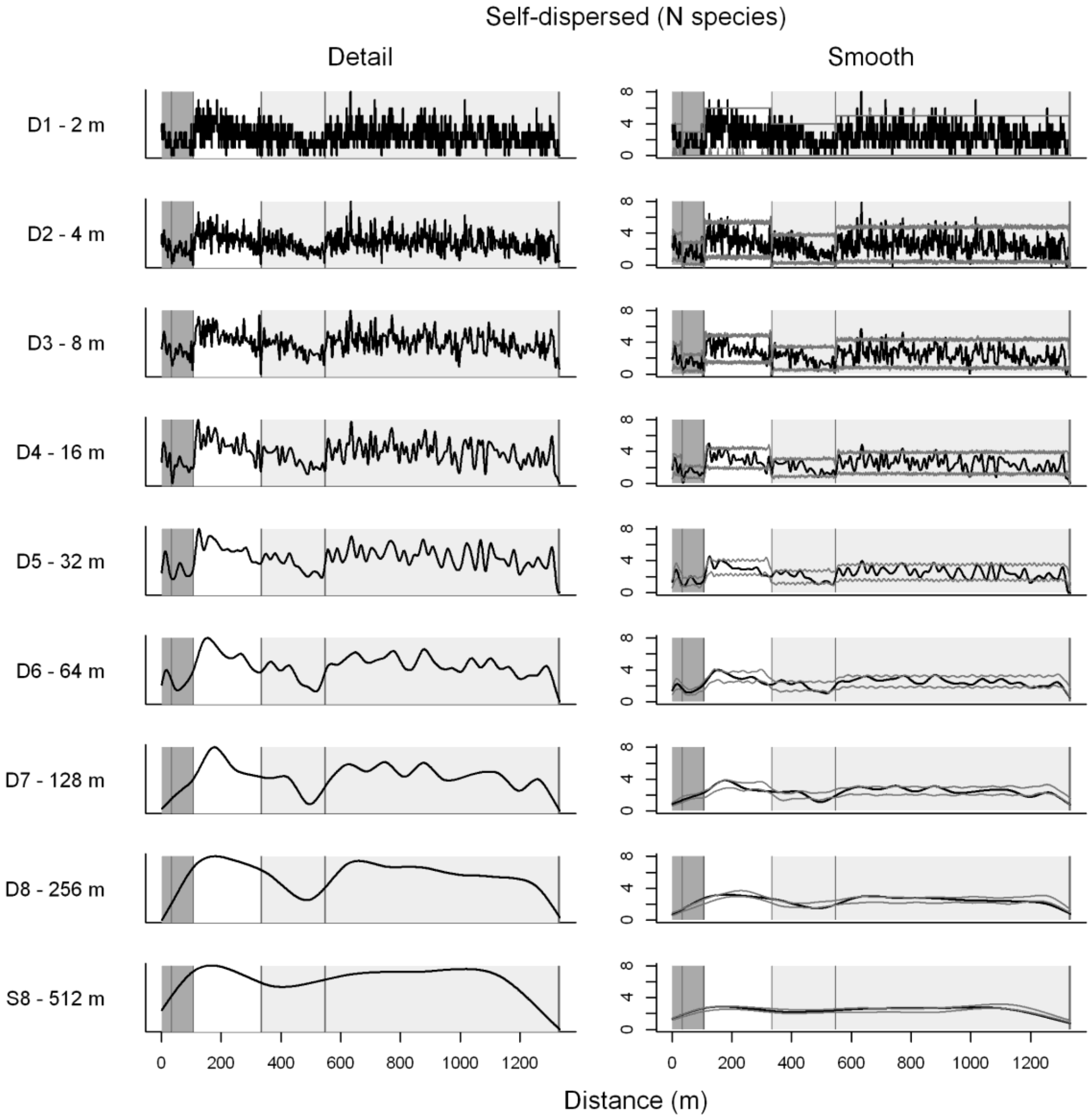
Self-dispersed (N species)
Detail
Smooth
D1 - 2 m
D2 - 4 m
D3 - 8 m
D4 - 16 m
D5 - 32 m
D6 - 64 m
D7 - 128 m
D8 - 256 m
S8 - 512 m
0
4
8
0
200
400
600
800
1000
1200
Distance (m)

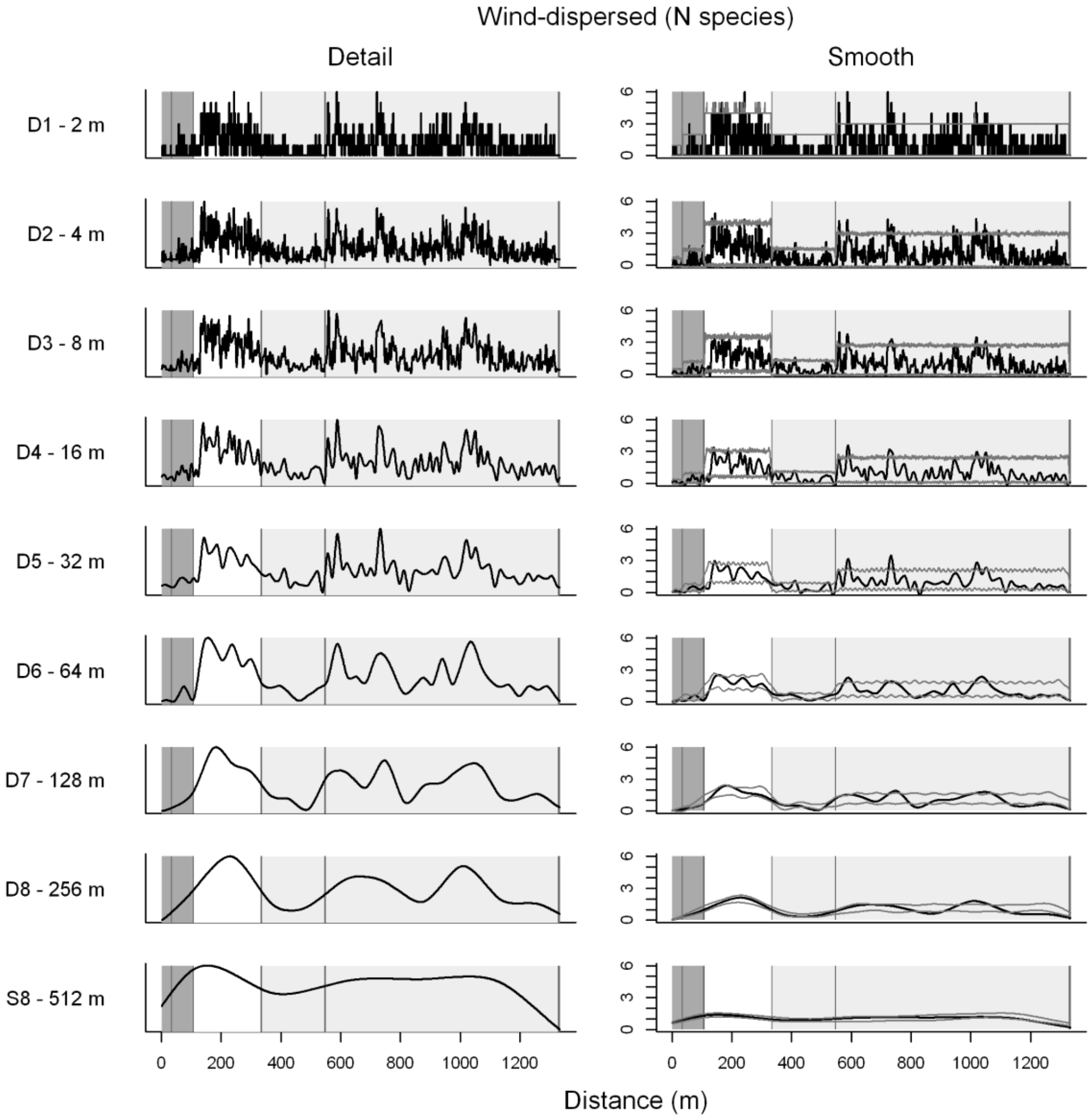
Wind-dispersed (N species)
Detail
Smooth
D1 - 2 m
D2 - 4 m
D3 - 8 m
D4 - 16 m
D5 - 32 m
D6 - 64 m
D7 - 128 m
D8 - 256 m
S8 - 512 m
0
3
6
0
200
400
600
800
1000
1200
Distance (m)

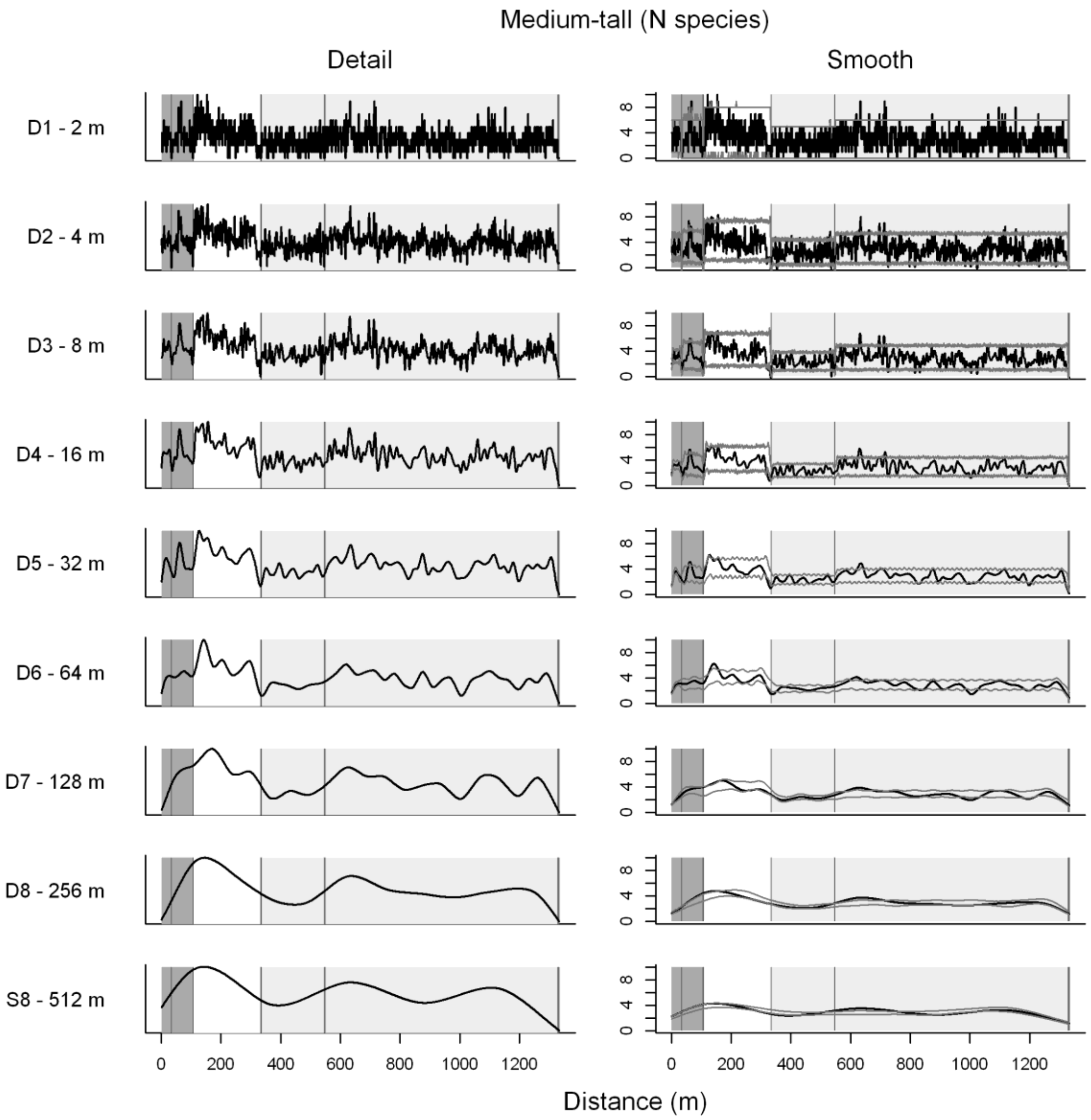
Medium-tall (N species)
Detail
Smooth
D1 - 2 m
D2 - 4 m
D3 - 8 m
D4 - 16 m
D5 - 32 m
D6 - 64 m
D7 - 128 m
D8 - 256 m
S8 - 512 m
0
4
8
0
200
400
600
800
1000
1200
Distance (m)

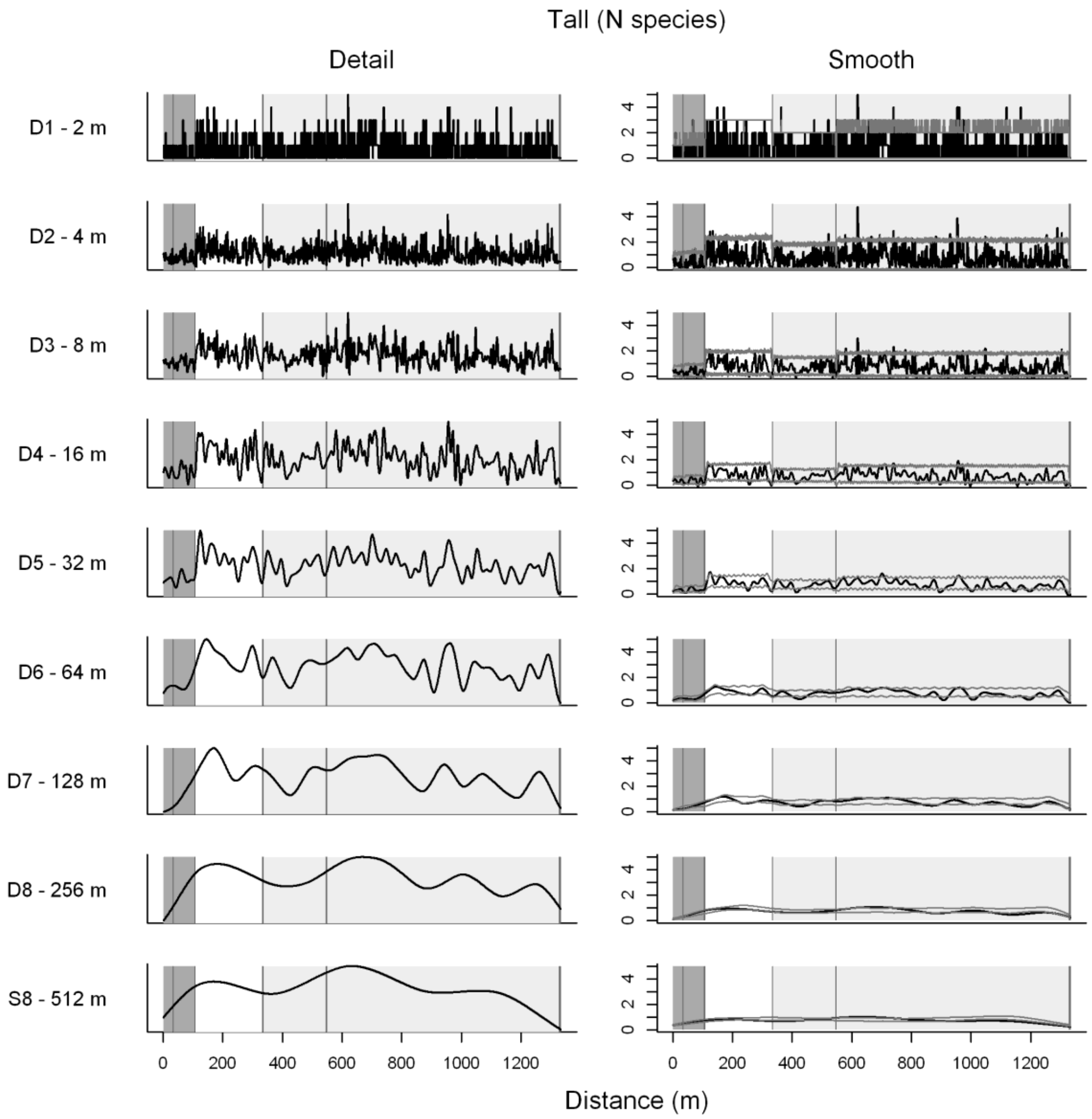
Tall (N species)
Detail
Smooth
D1 - 2 m
D2 - 4 m
D3 - 8 m
D4 - 16 m
D5 - 32 m
D6 - 64 m
D7 - 128 m
D8 - 256 m
S8 - 512 m
0
2
4
0
200
400
600
800
1000
1200
Distance (m)

SM 4.4 – Higher-resolution plot of the seriation analysis, with species names

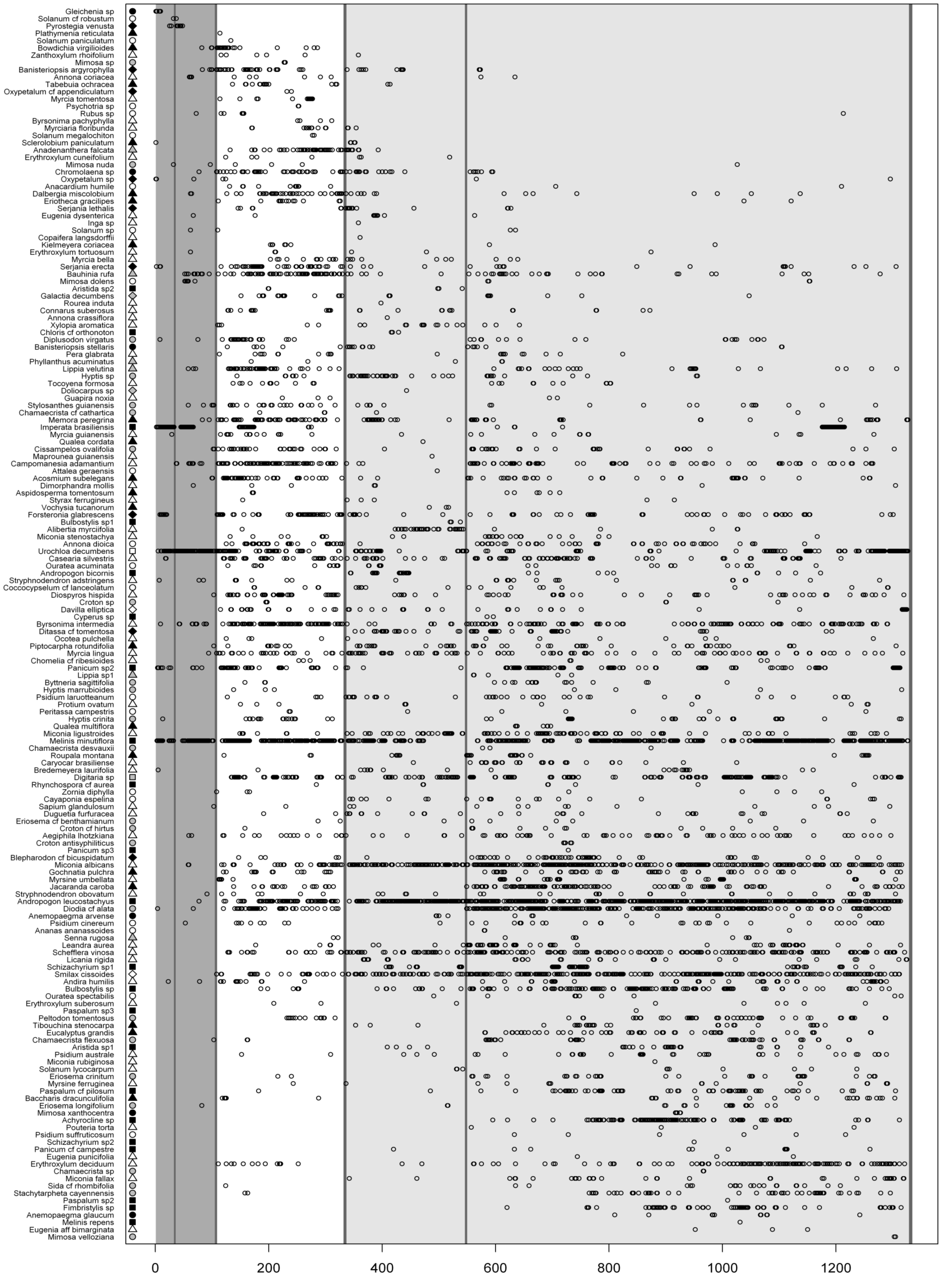

Seriation plot showing the variation in the plant community along the study transect. Each row corresponds to one species. Different symbol shapes represent different life forms and different colors represent the different dispersal syndromes: herbaceous and subshrubs: circle; graminoids: square; liana: diamond; shrubs and trees: triangle; animal-dispersed: white symbols; wind-dispersed: black symbols; self-dispersed: gray symbols. Background color represents the different plant communities: invaded grassland (dark gray), typical *cerrado* (white) and regenerating *cerrado* (light gray), and vertical lines represent the firebreaks.

SM 4.5 – Continuous wavelet transform plots for the 106 species used in the similarity analysis

Below are the results of the continuous wavelet transform for the 106 species used in the similarity analysis, in alphabetical order. Lighter colors represent low wavelet variance, usually corresponding to areas where the species is absent. The x axis is distance along the transect and the y axis is log(2) scale. The vertical lines are firebreaks.

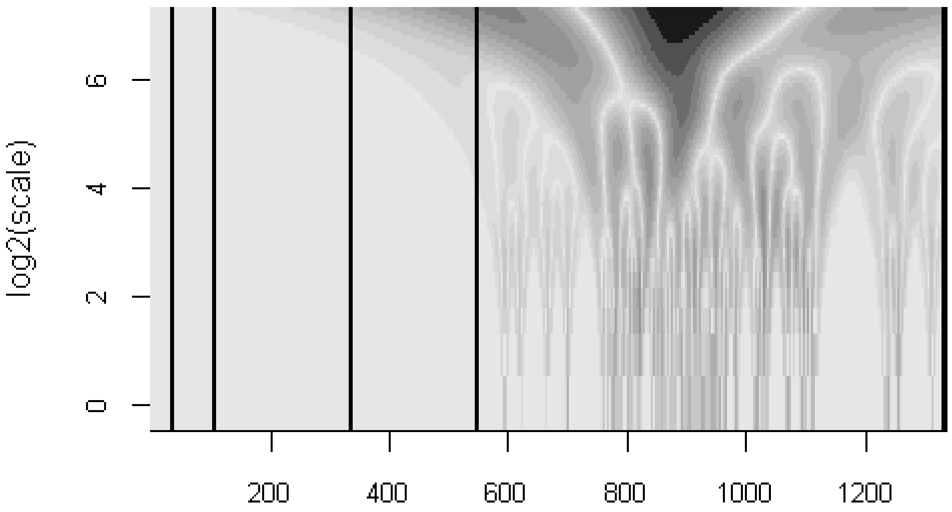
Achyrocline sp

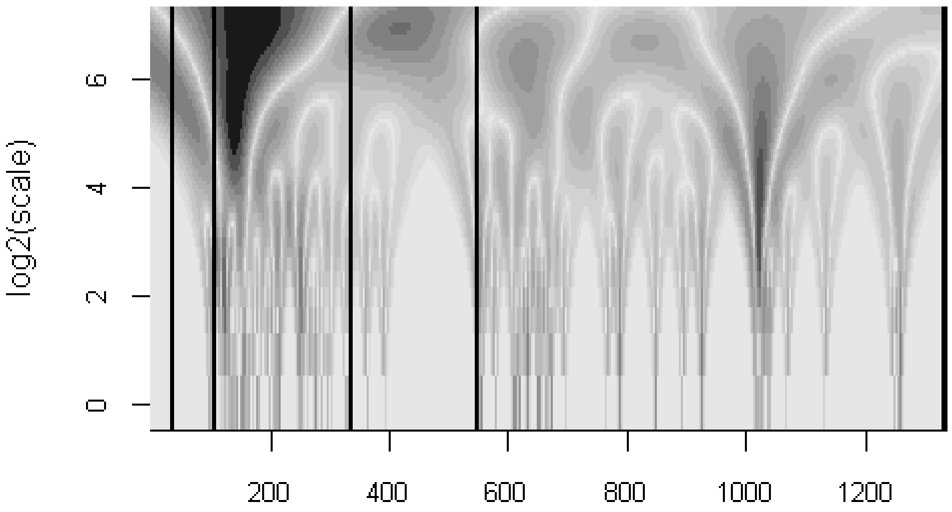
Acosmium subelegans

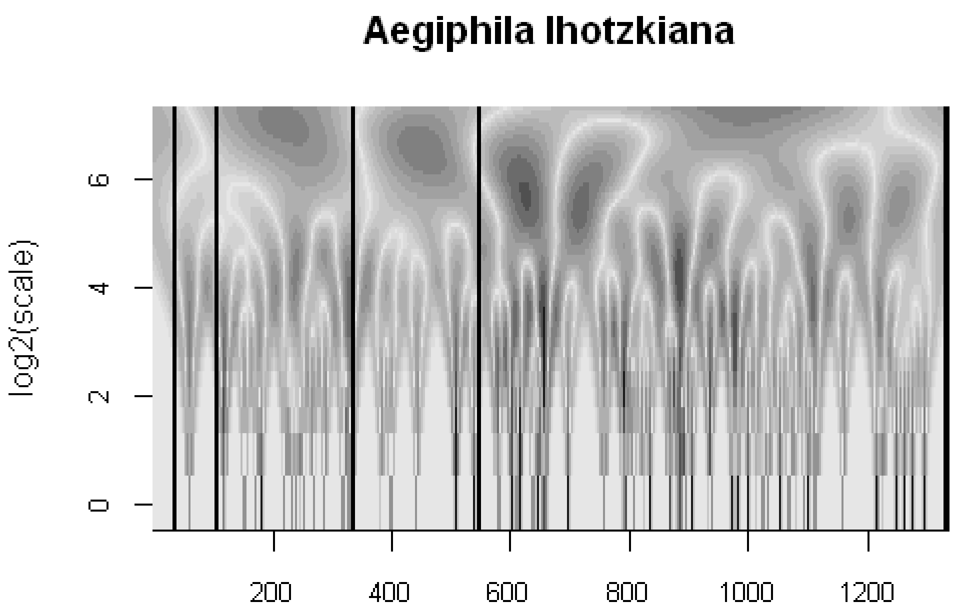

Aegiphila lhotzkiana

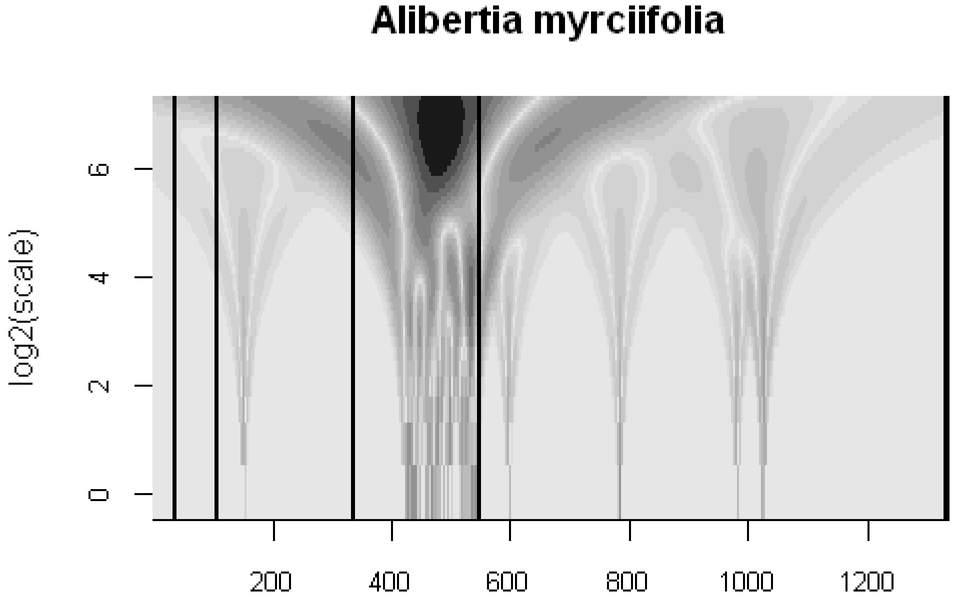

Alibertia myrciifolia

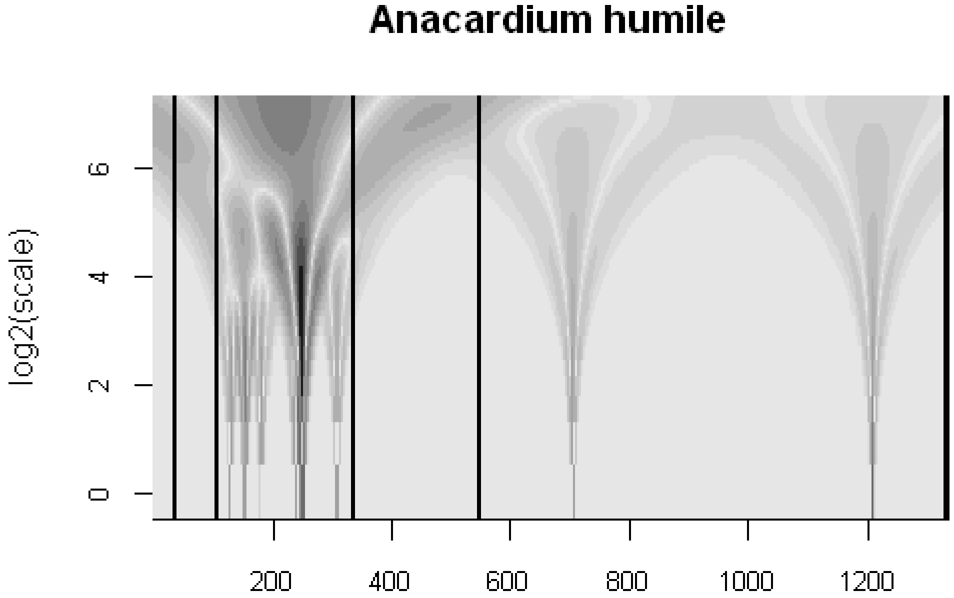

Anacardium humile

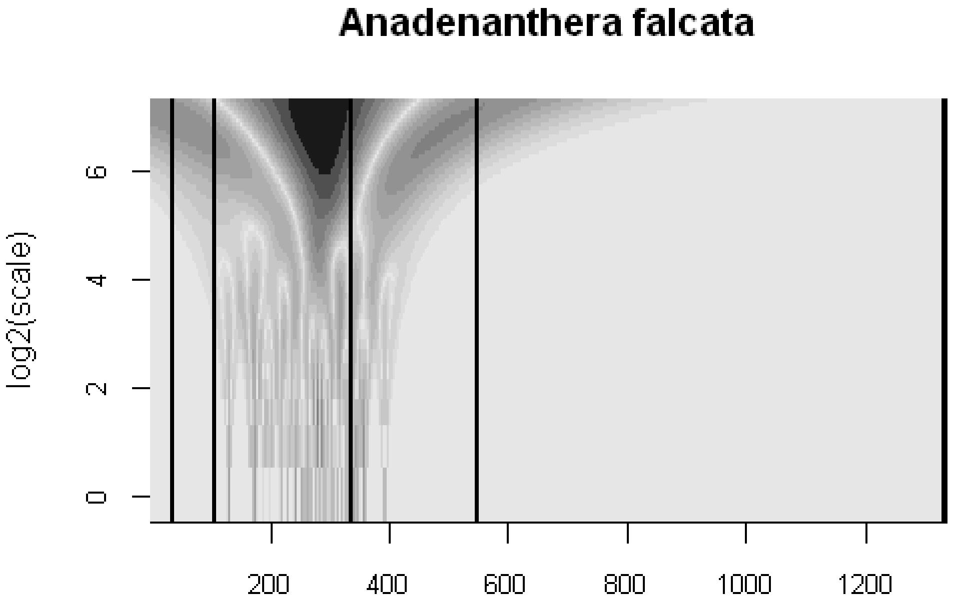

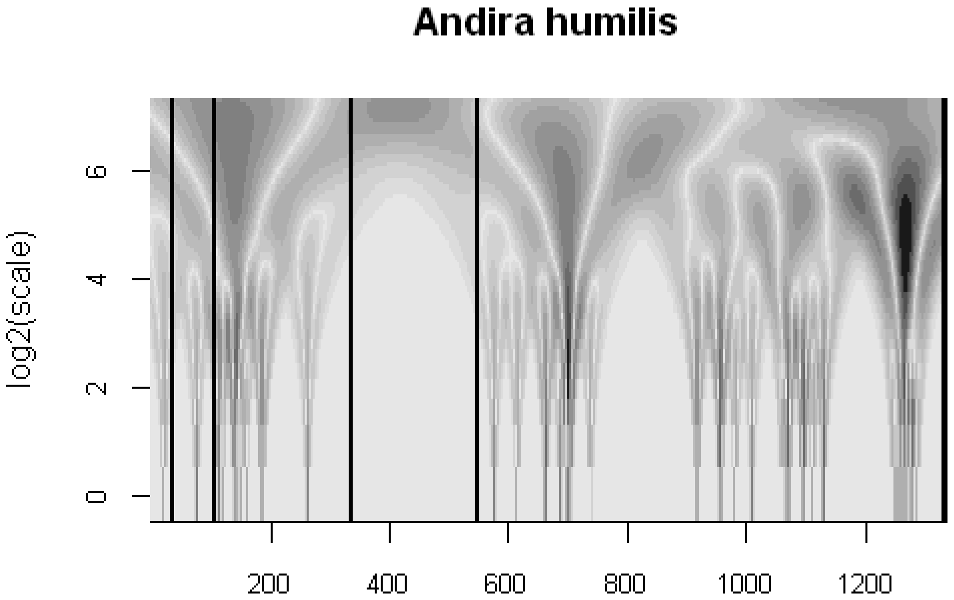

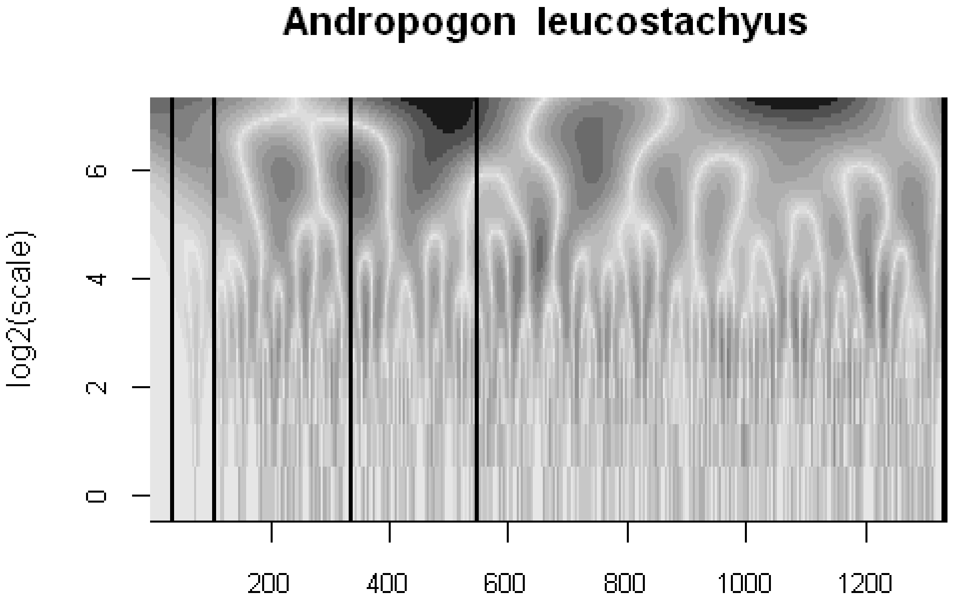

SM 4.5 – Continuous wavelet transform plots for the 106 species used in the similarity analysis

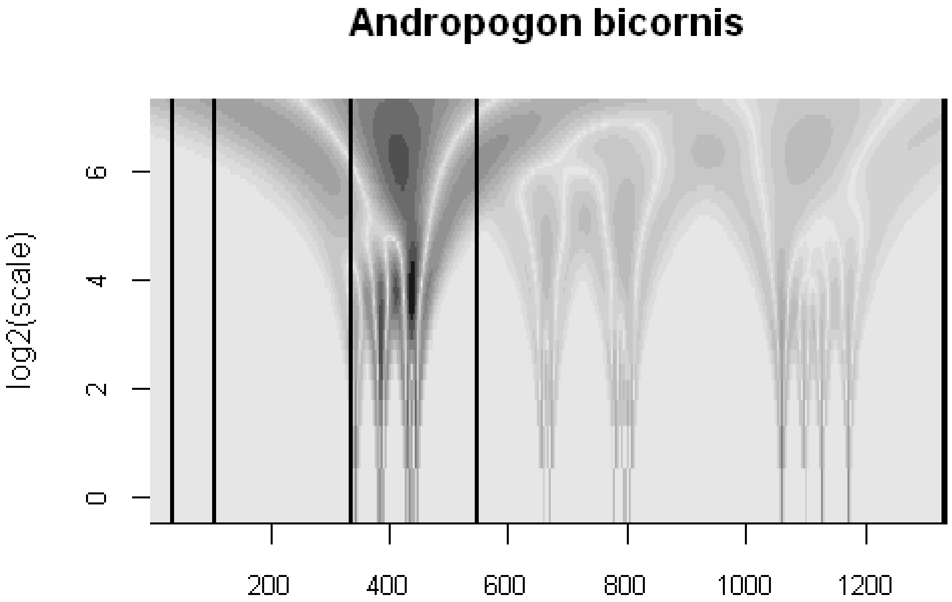

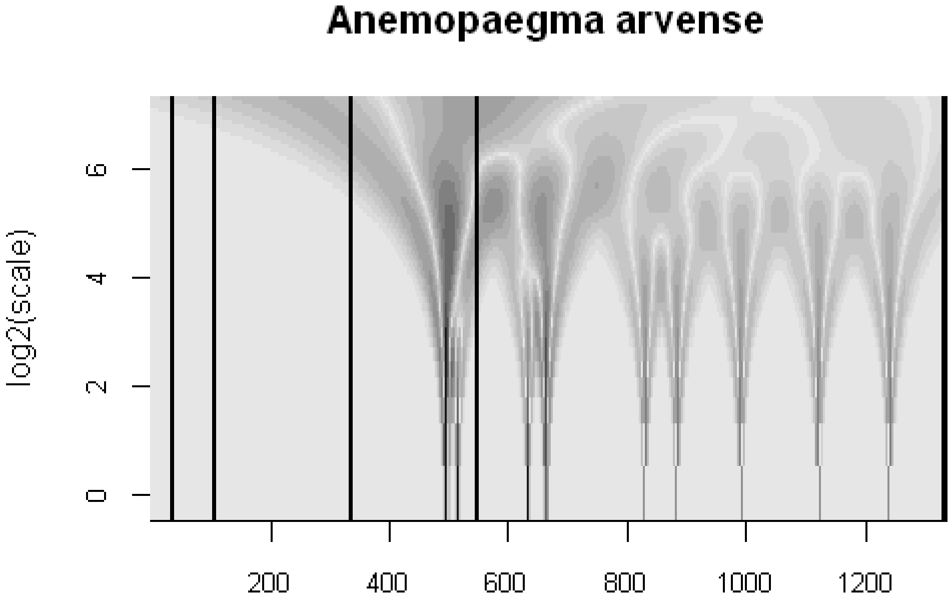

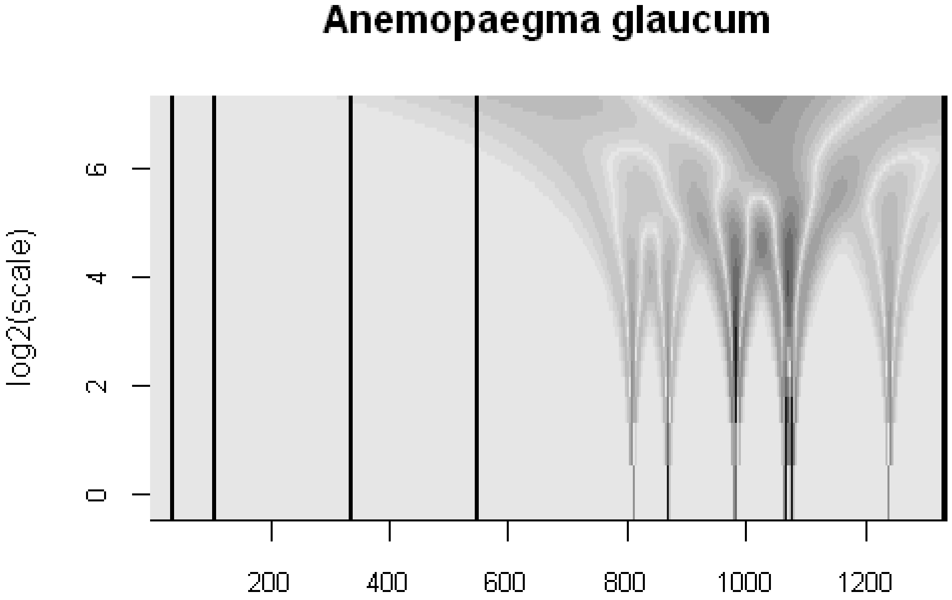

SM 4.5 – Continuous wavelet transform plots for the 106 species used in the similarity analysis

Annona coriacea

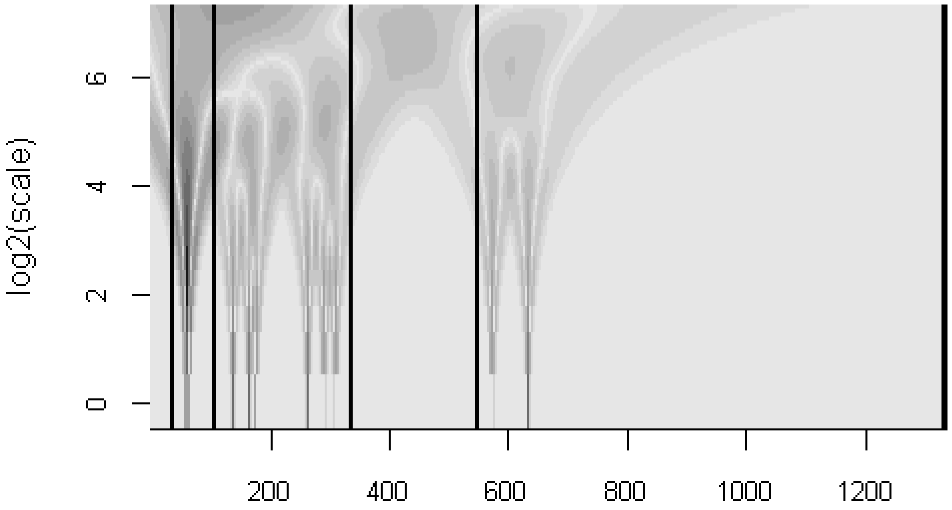

Annona dioica

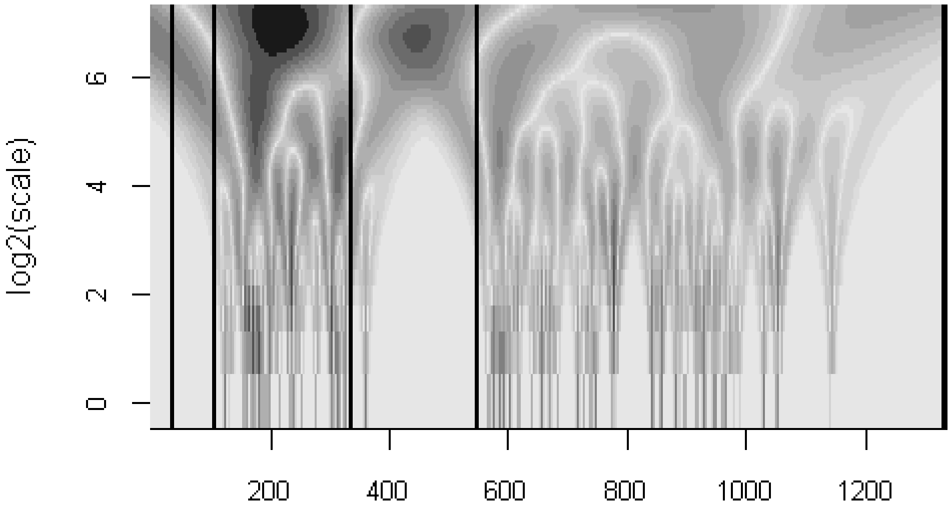

Aristida sp1

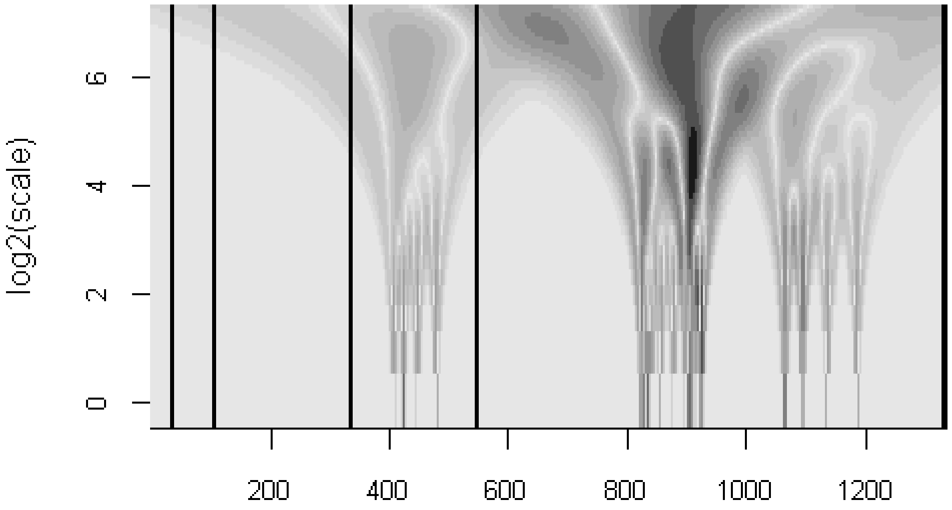

SM 4.5 – Continuous wavelet transform plots for the 106 species used in the similarity analysis

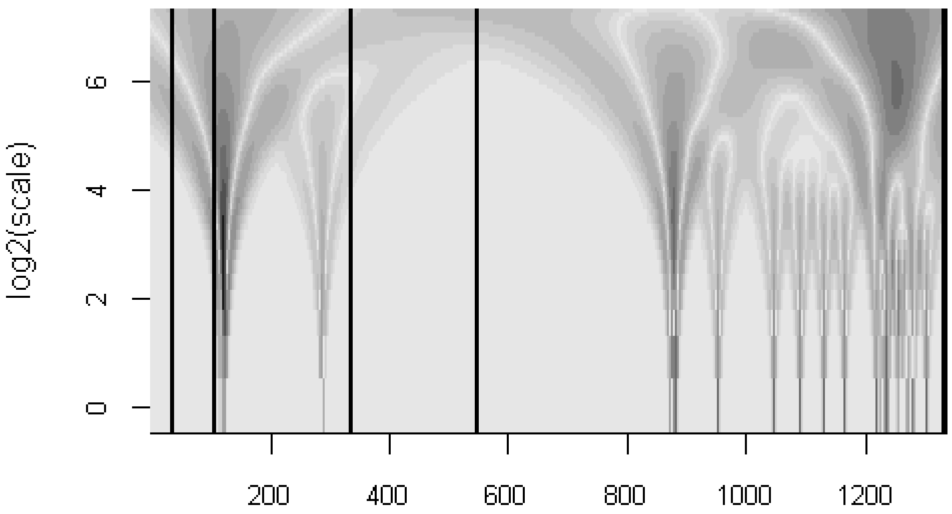

Baccharis dracunculifolia

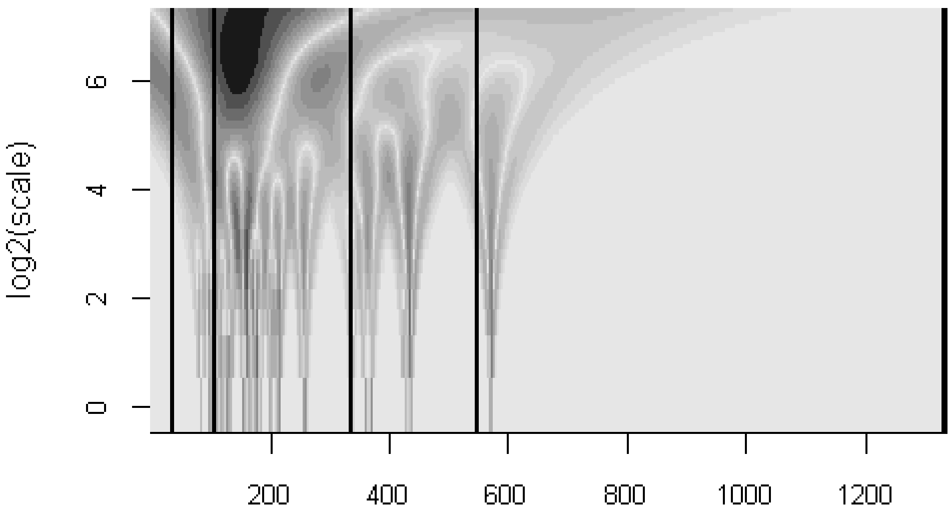

Banisteriopsis argyrophylla

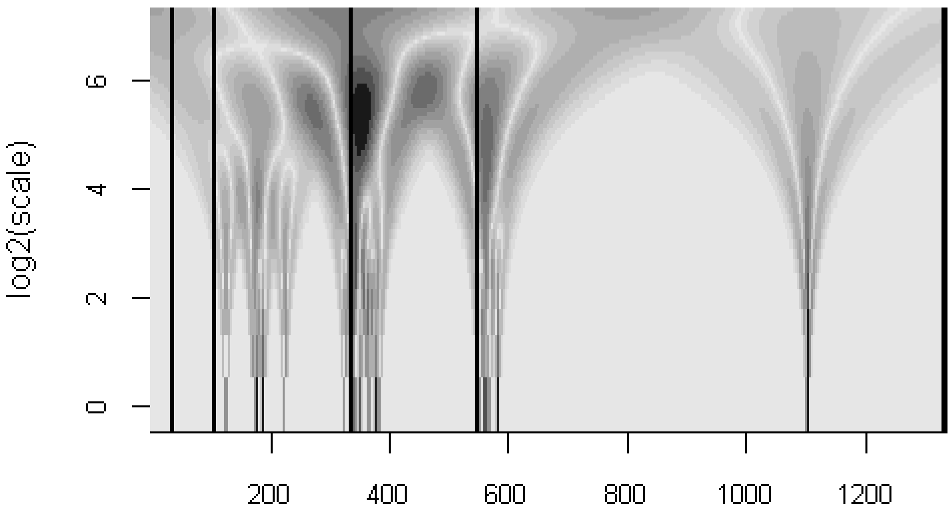

Banisteriopsis stellaris

SM 4.5 – Continuous wavelet transform plots for the 106 species used in the similarity analysis

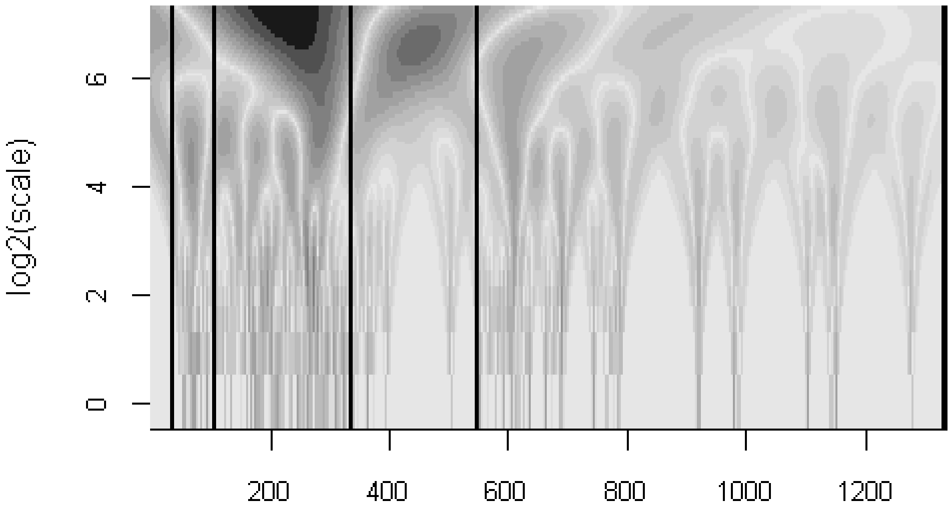

Bauhinia rufa

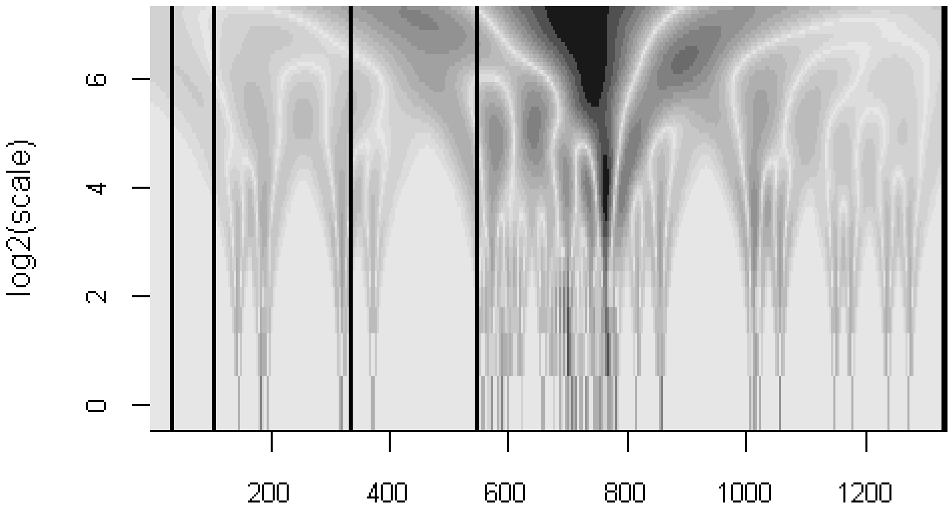

Blepharodon cf bicuspidatum

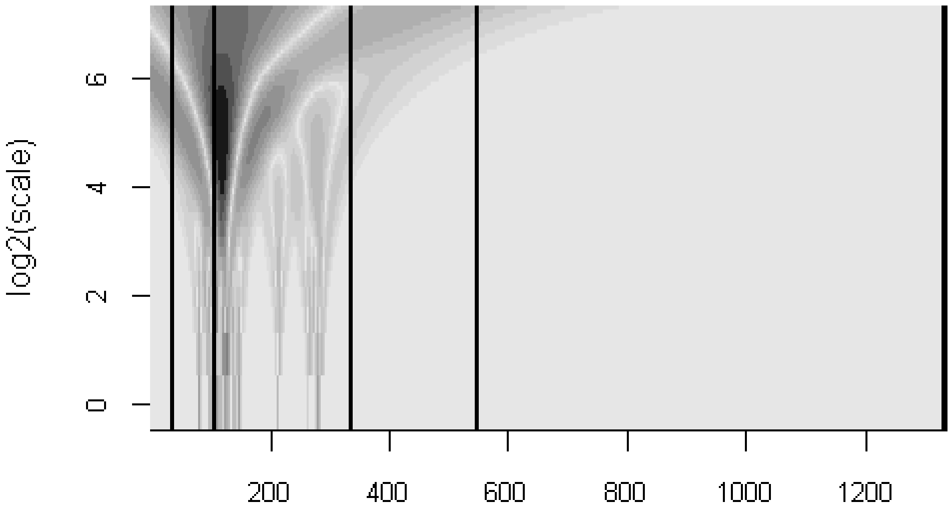

Bowdichia virgilioides

SM 4.5 – Continuous wavelet transform plots for the 106 species used in the similarity analysis

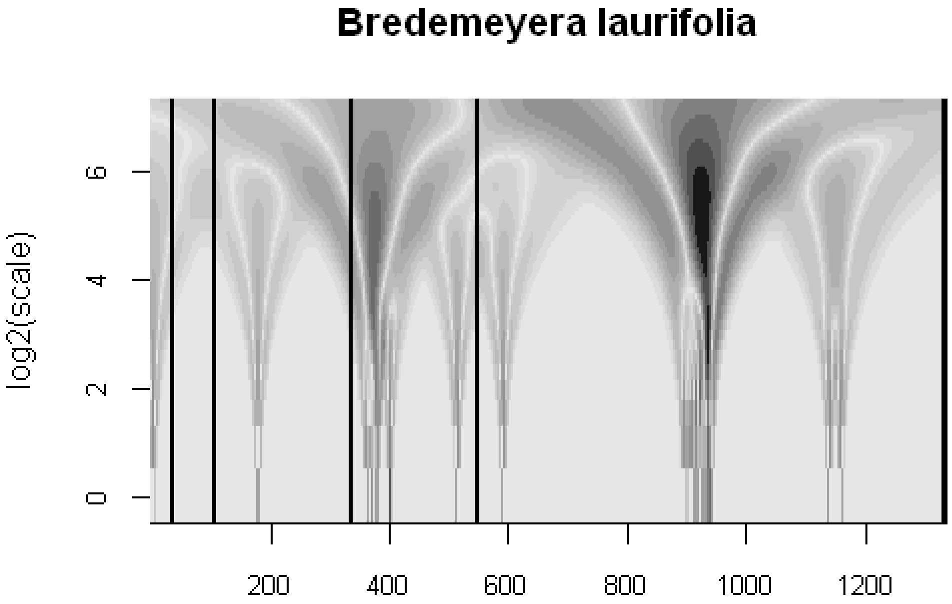
Bredemeyera laurifolia

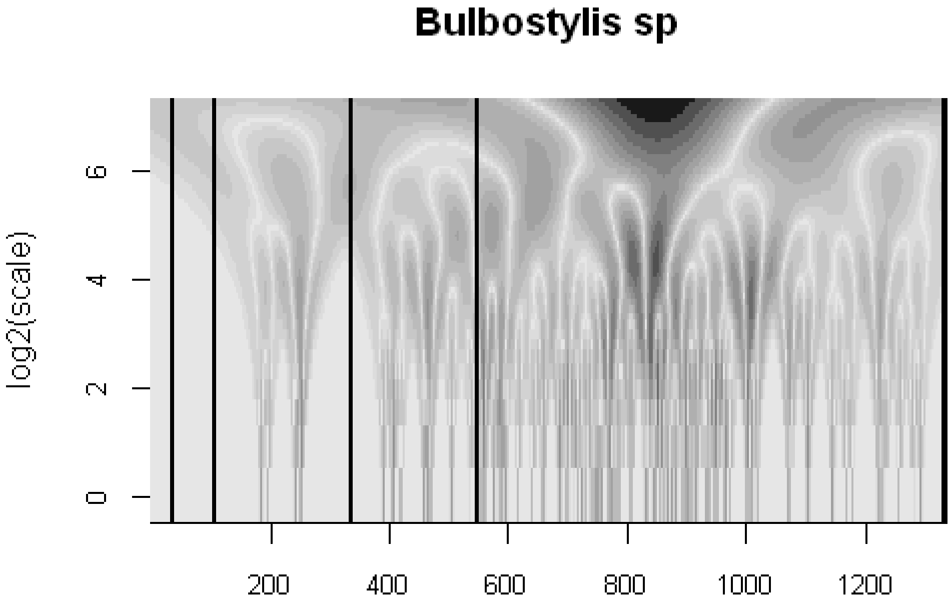
Bulbostylis sp

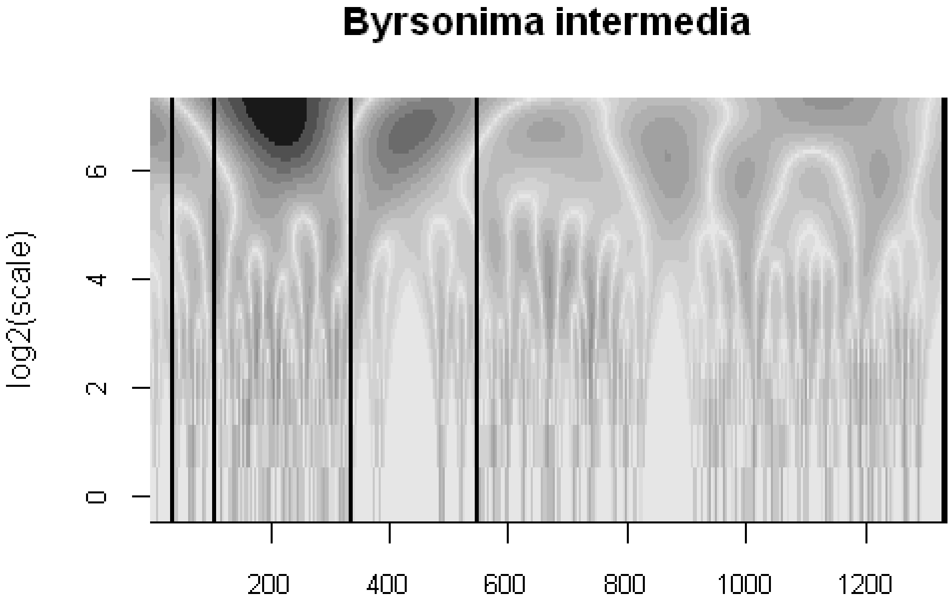
Byrsonima intermedia

SM 4.5 – Continuous wavelet transform plots for the 106 species used in the similarity analysis

Byttneria sagittifolia

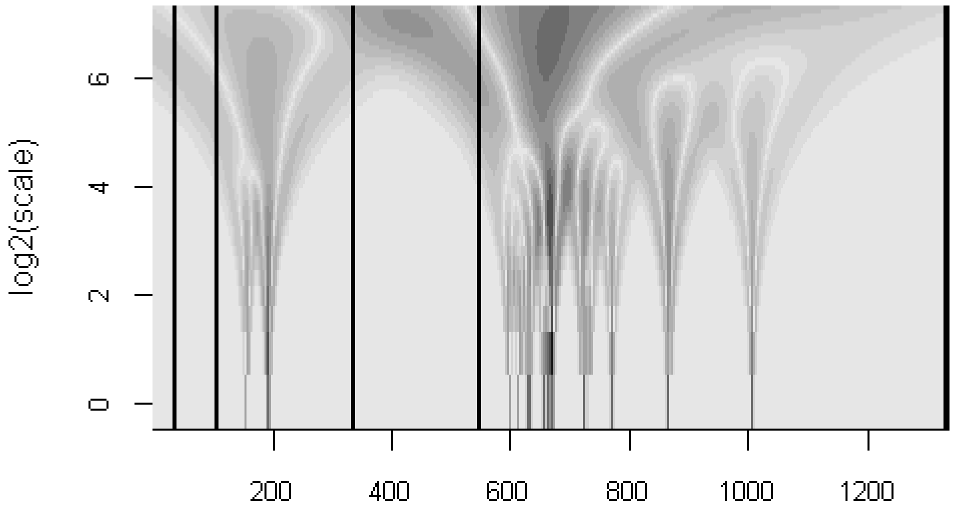

Campomanesia adamantium

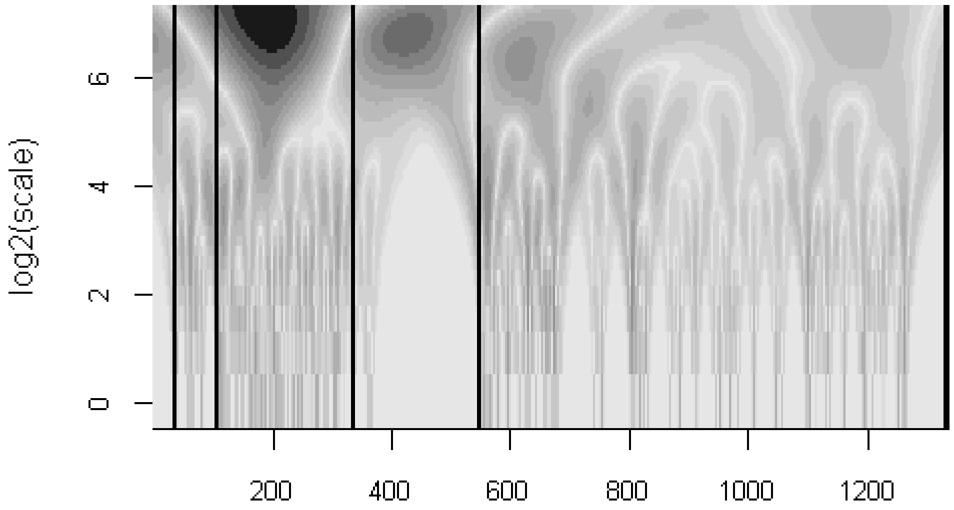

Caryocar brasiliense

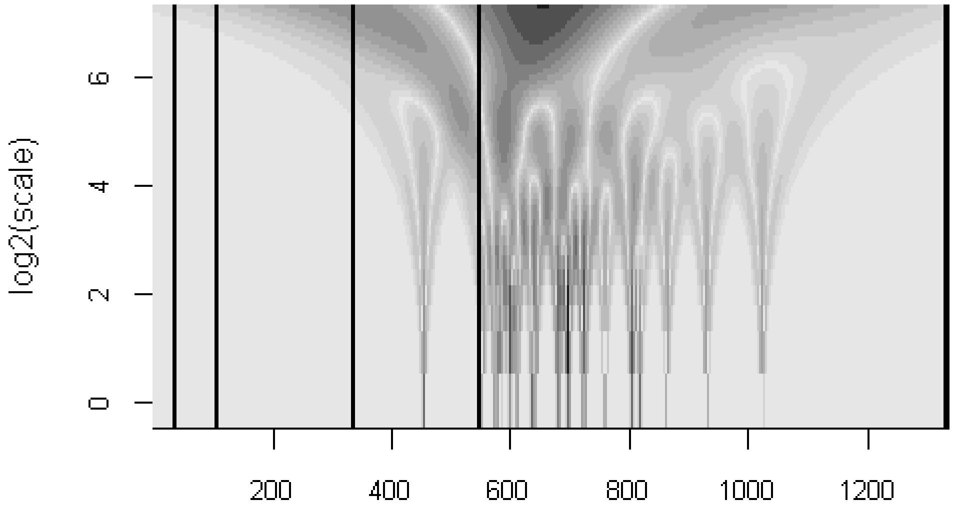

SM 4.5 – Continuous wavelet transform plots for the 106 species used in the similarity analysis

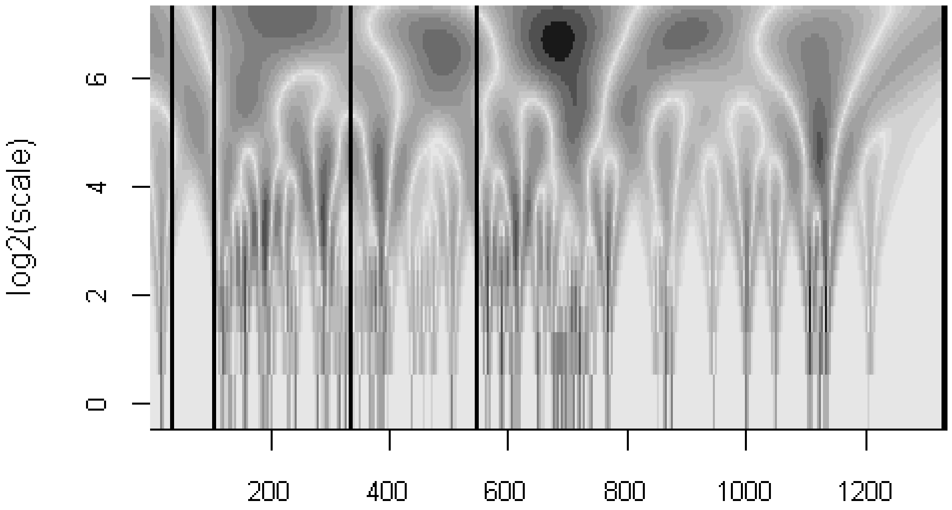

Casearia silvestris

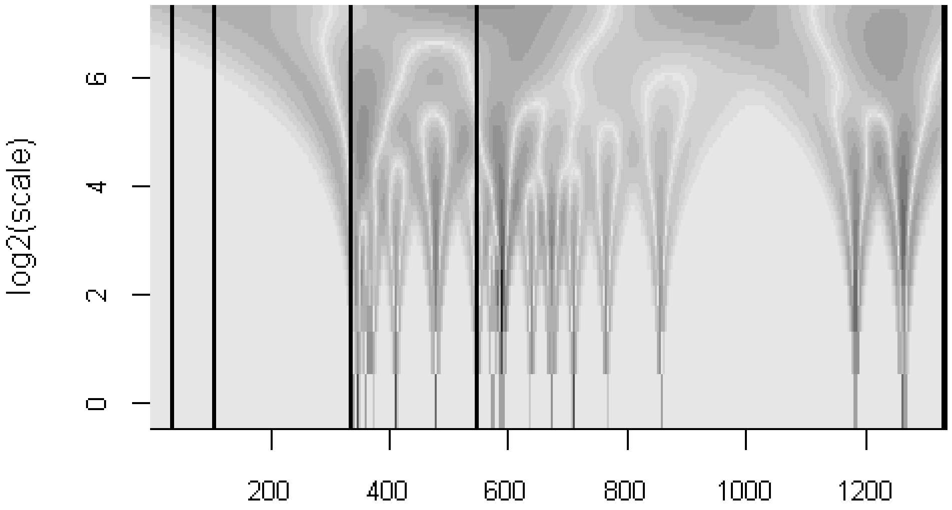

Cayaponia espelina

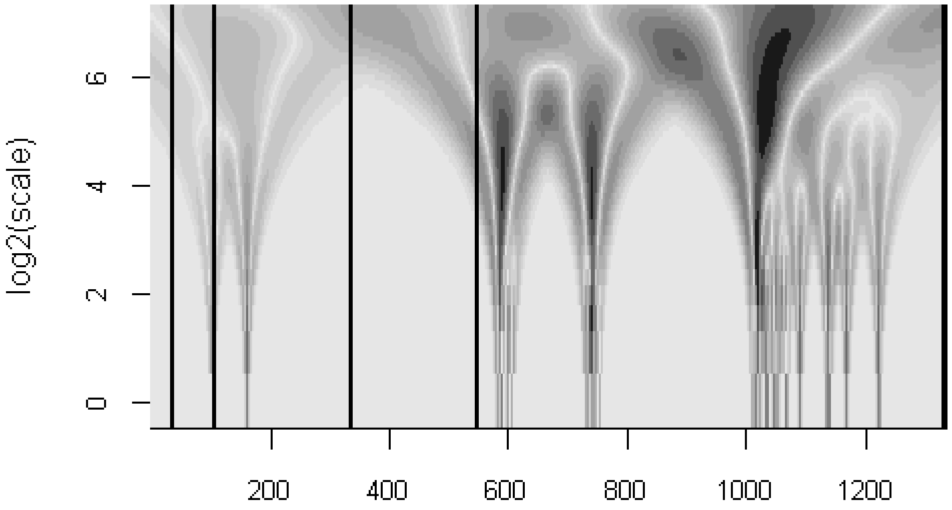

Chamaecrista flexuosa

SM 4.5 – Continuous wavelet transform plots for the 106 species used in the similarity analysis

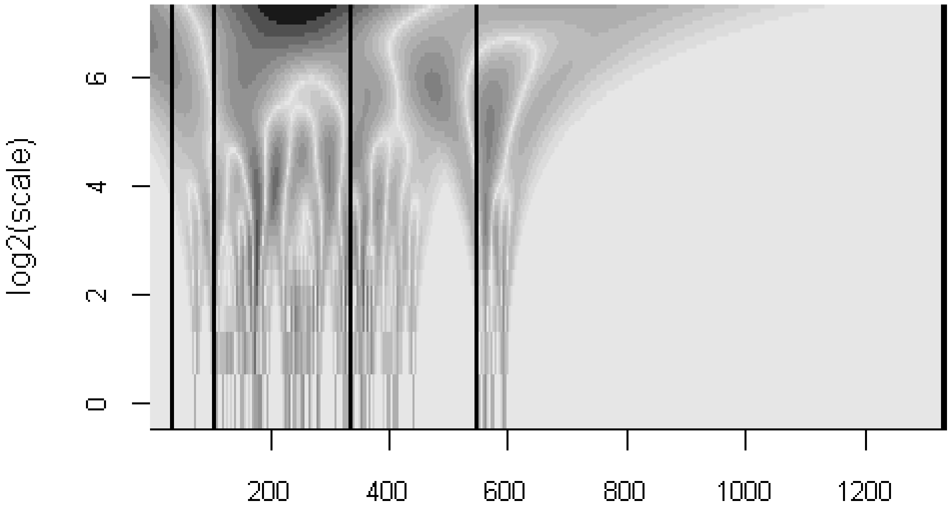

Chromolaena sp

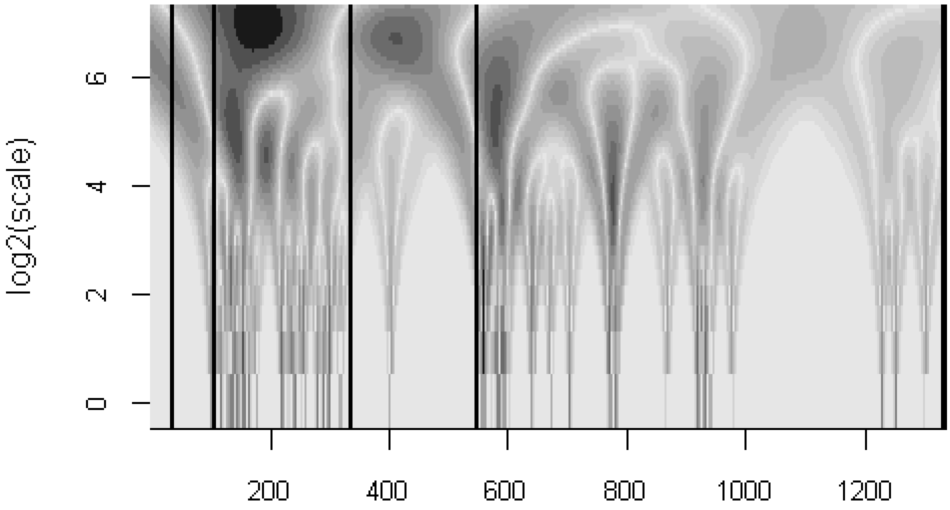

Cissampelos ovalifolia

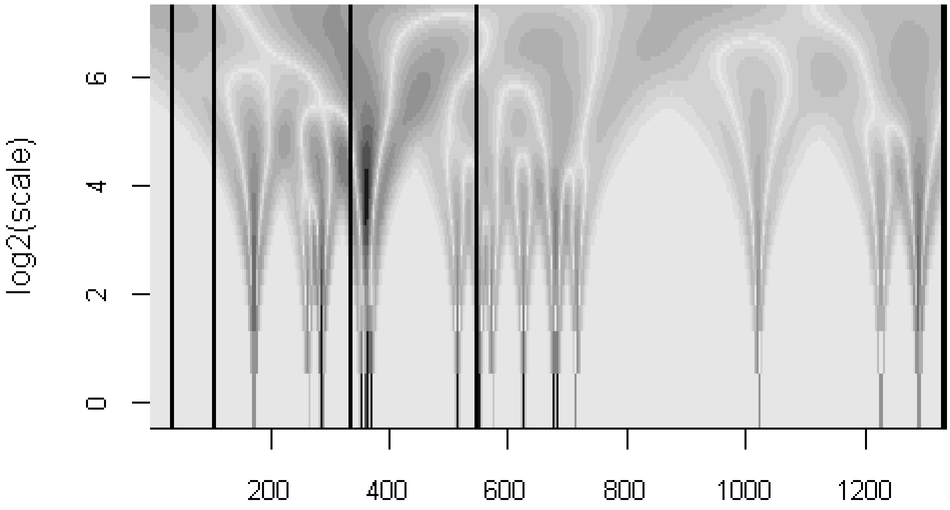

Coccocypselum cf lanceolatum

SM 4.5 – Continuous wavelet transform plots for the 106 species used in the similarity analysis

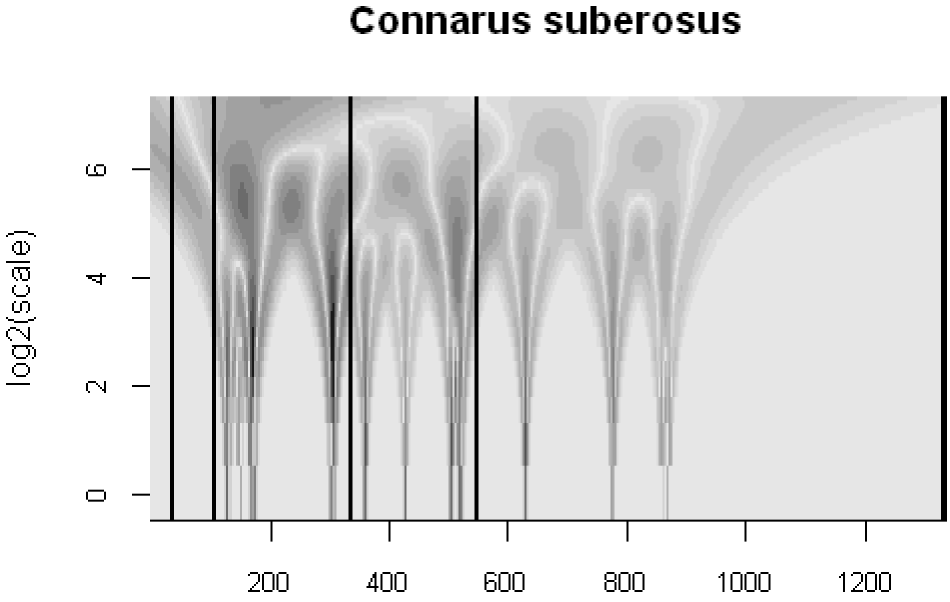

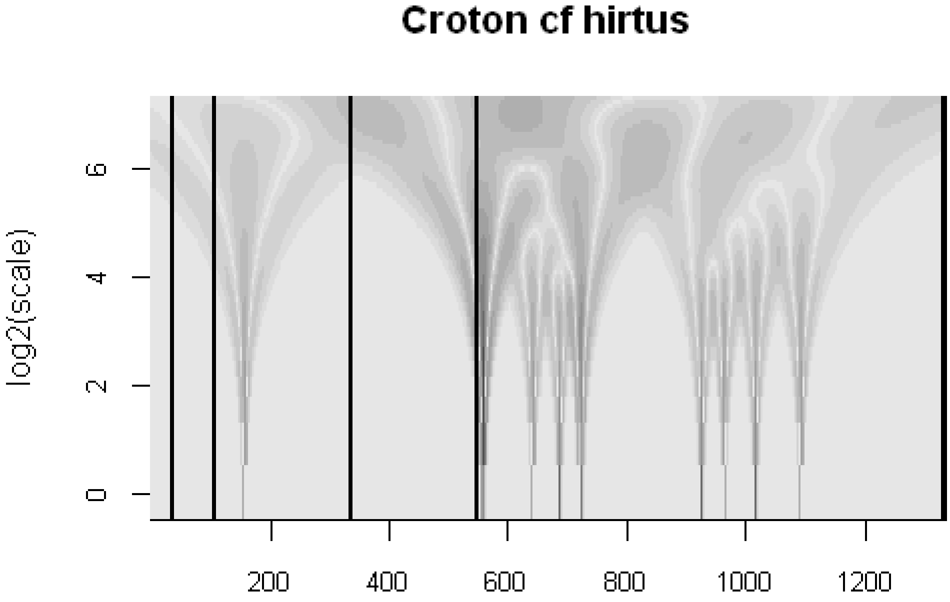

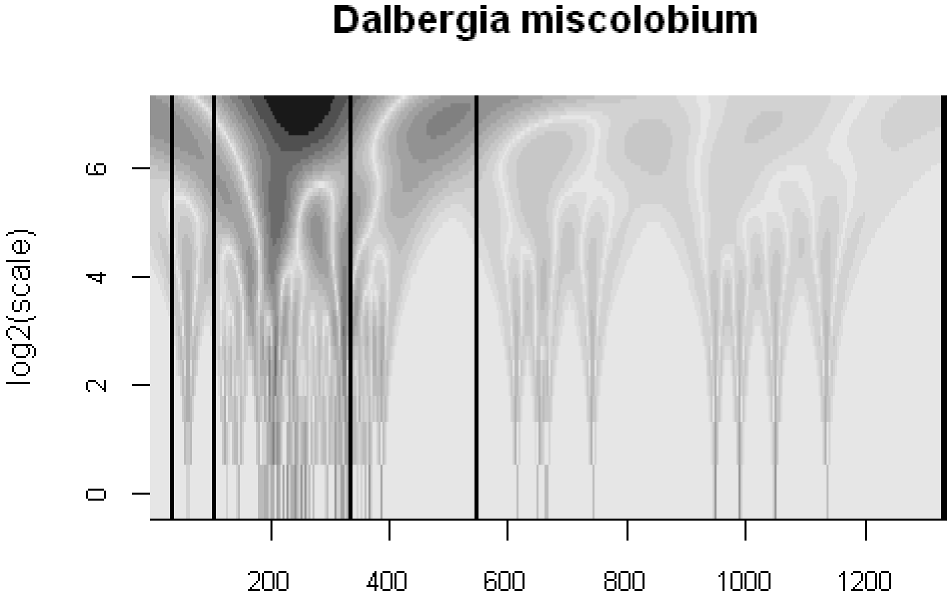

SM 4.5 – Continuous wavelet transform plots for the 106 species used in the similarity analysis

Davilla elliptica

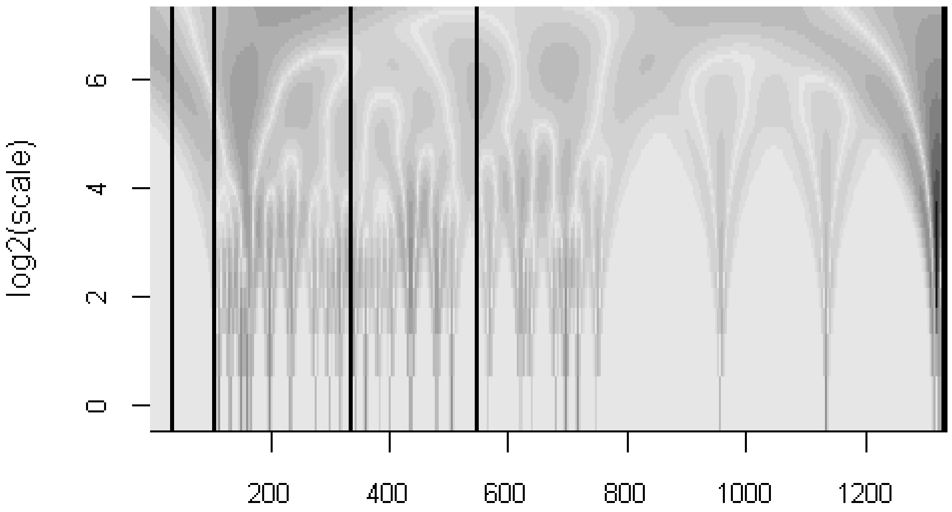

Digitaria sp

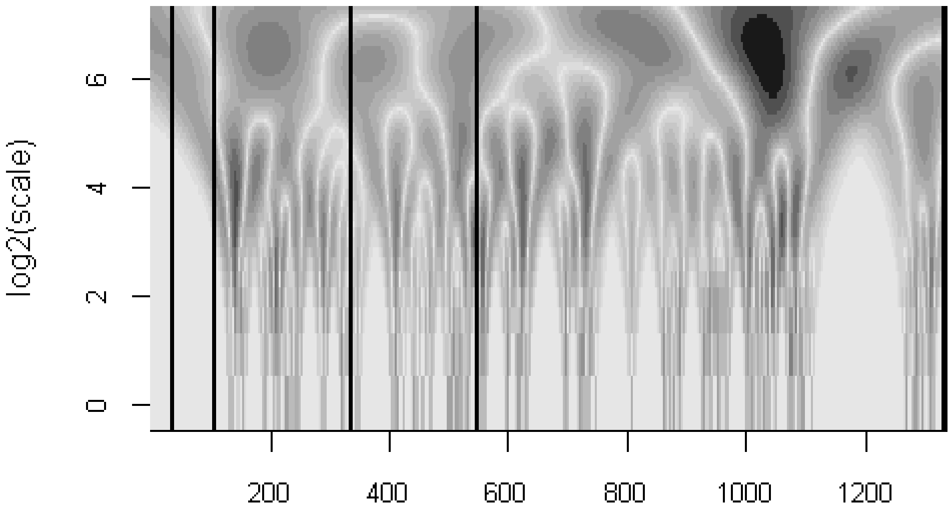

Diodia cf alata

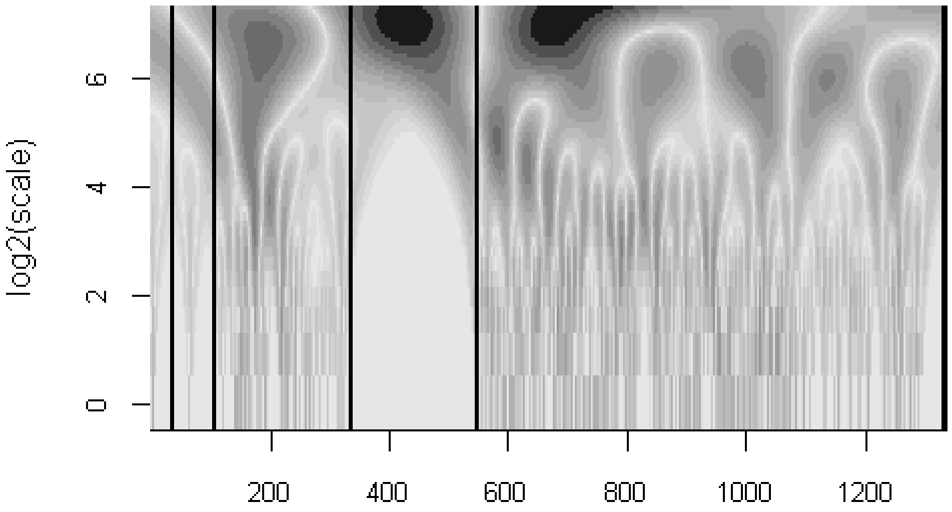

SM 4.5 – Continuous wavelet transform plots for the 106 species used in the similarity analysis

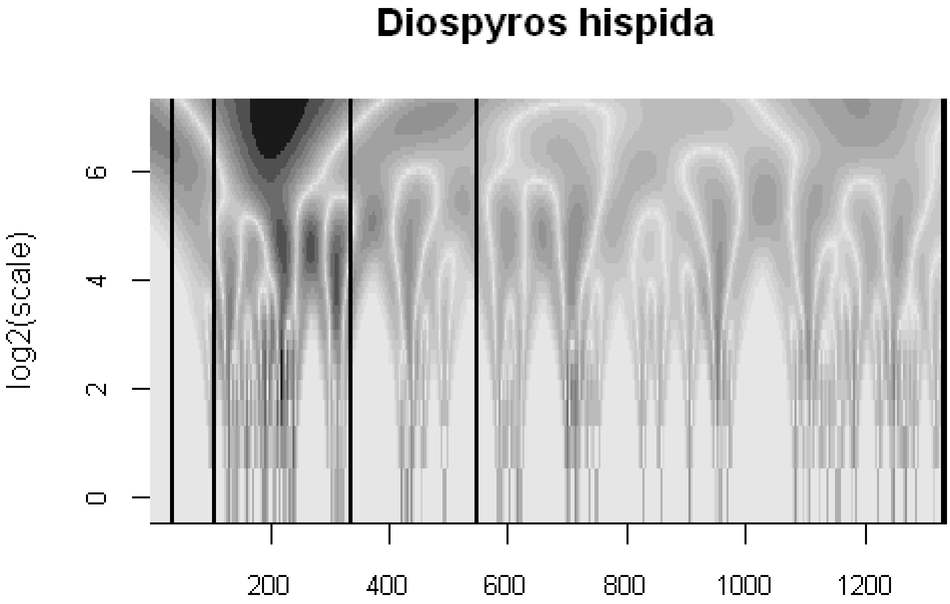
Diospyros hispida

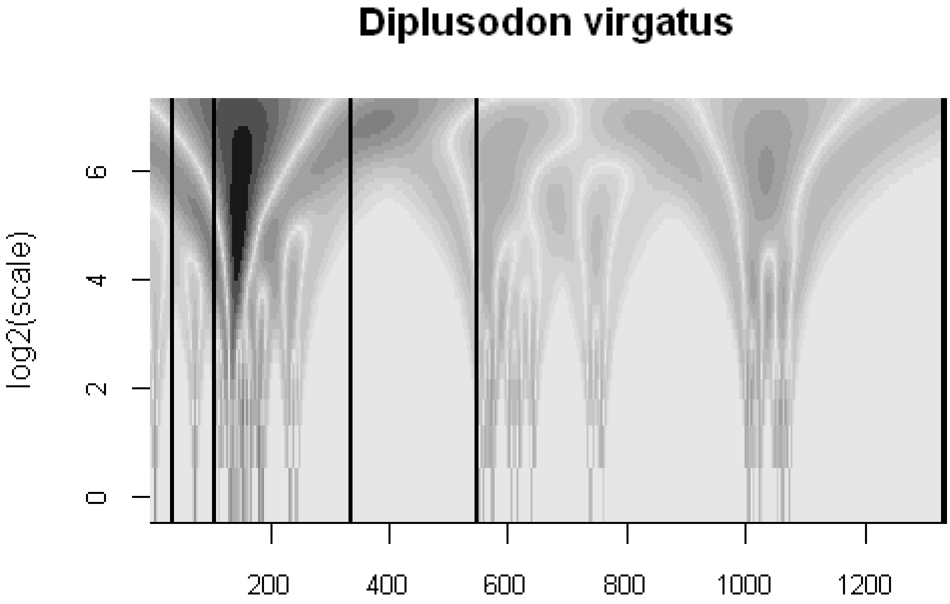
Diplusodon virgatus

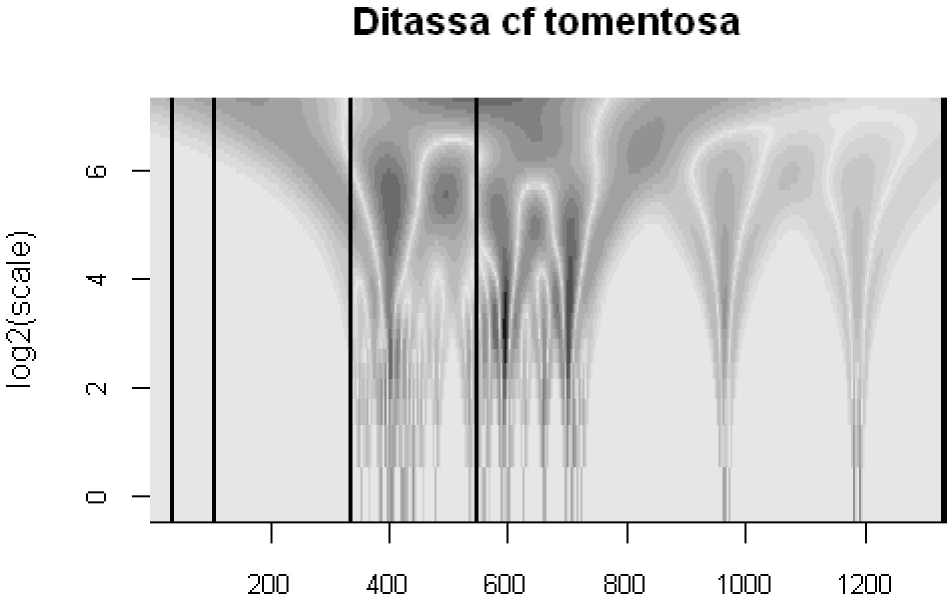
Ditassa cf tomentosa

SM 4.5 – Continuous wavelet transform plots for the 106 species used in the similarity analysis

Duguetia furfuracea

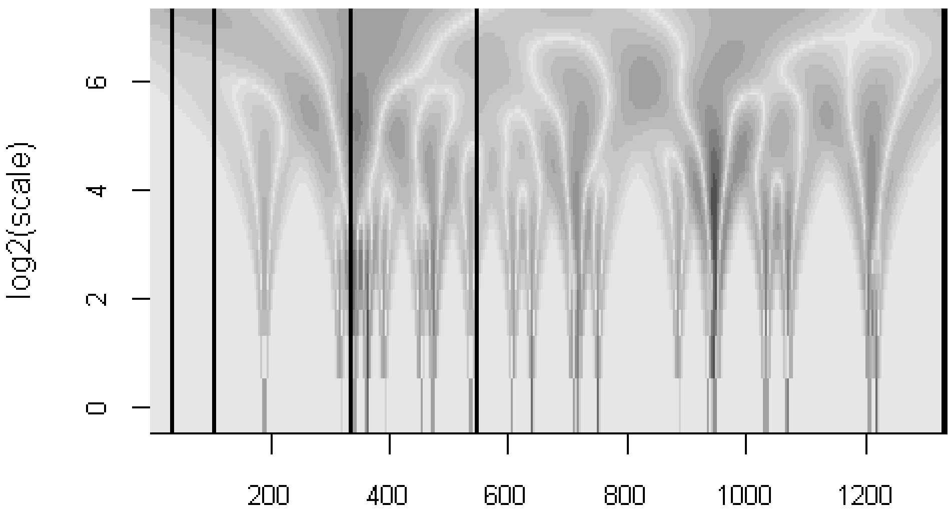

Eriosema cf benthamianum

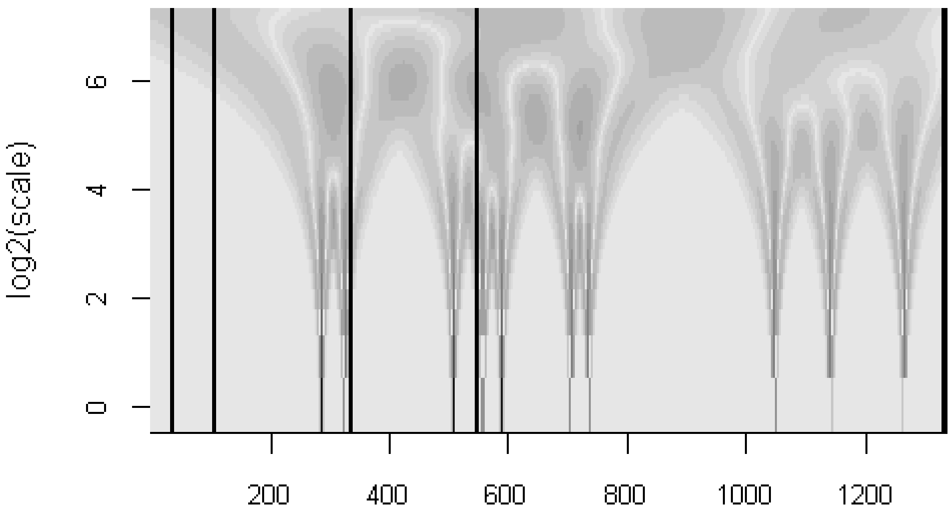

Eriosema crinitum

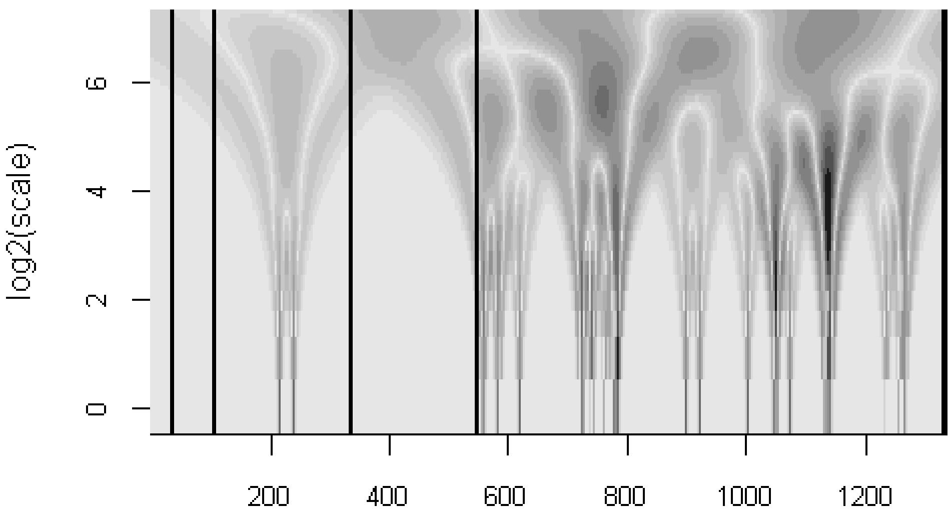

SM 4.5 – Continuous wavelet transform plots for the 106 species used in the similarity analysis

Eriosema longifolium

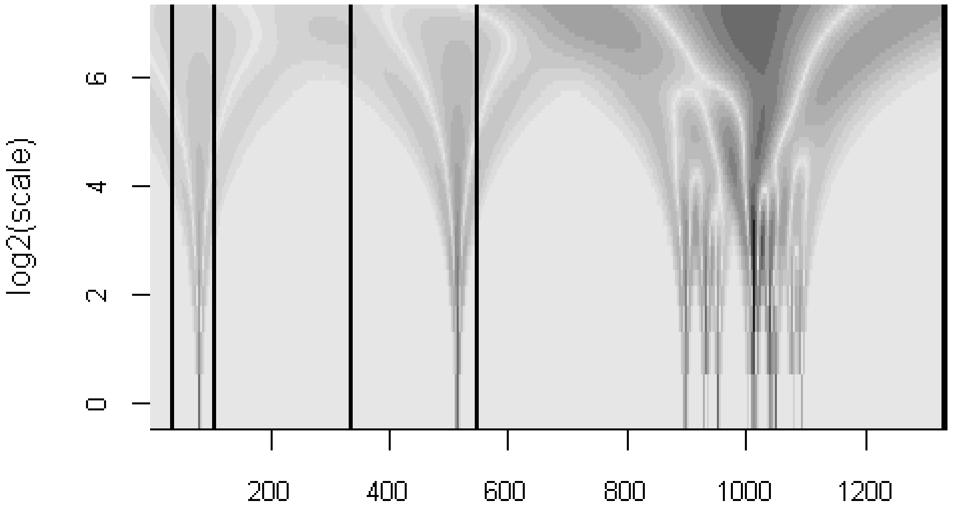

Eriotheca gracilipes

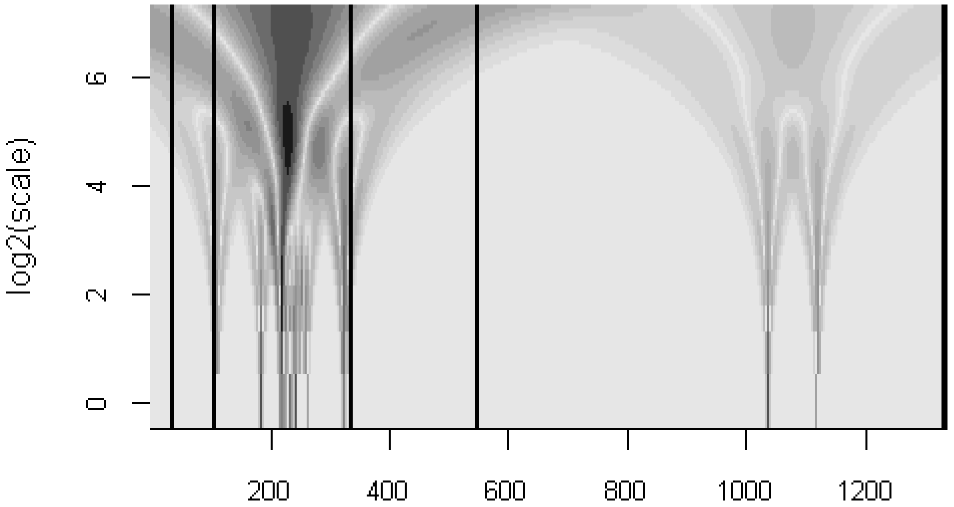

Erythroxylum deciduum

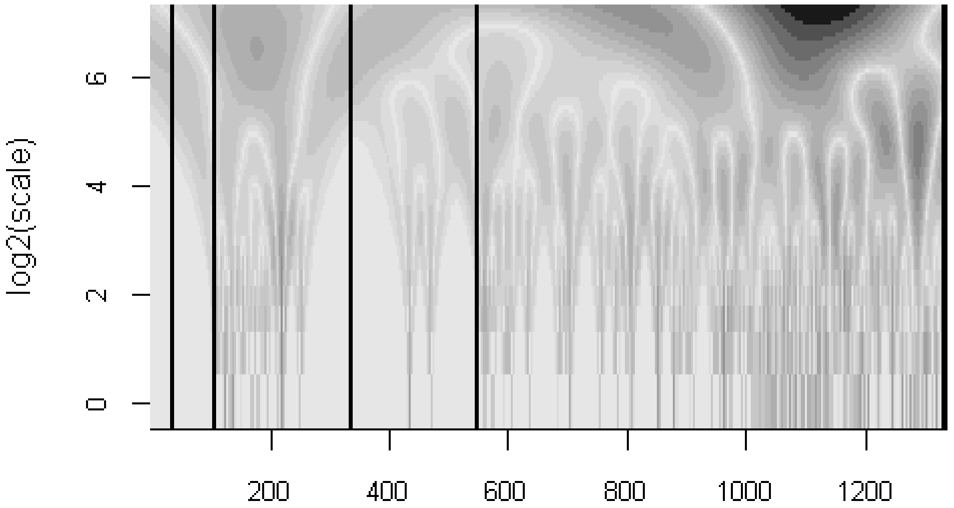

SM 4.5 – Continuous wavelet transform plots for the 106 species used in the similarity analysis

Eucalyptus grandis

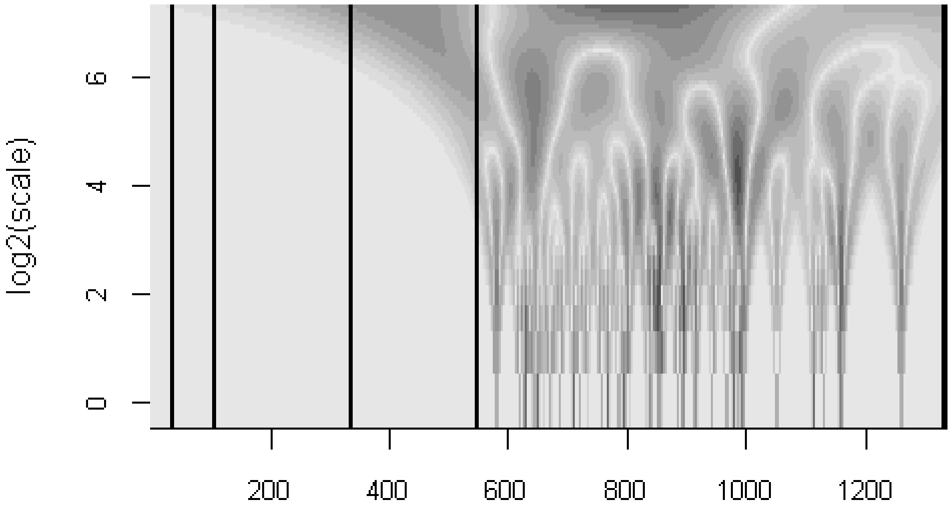

Eugenia dysenterica

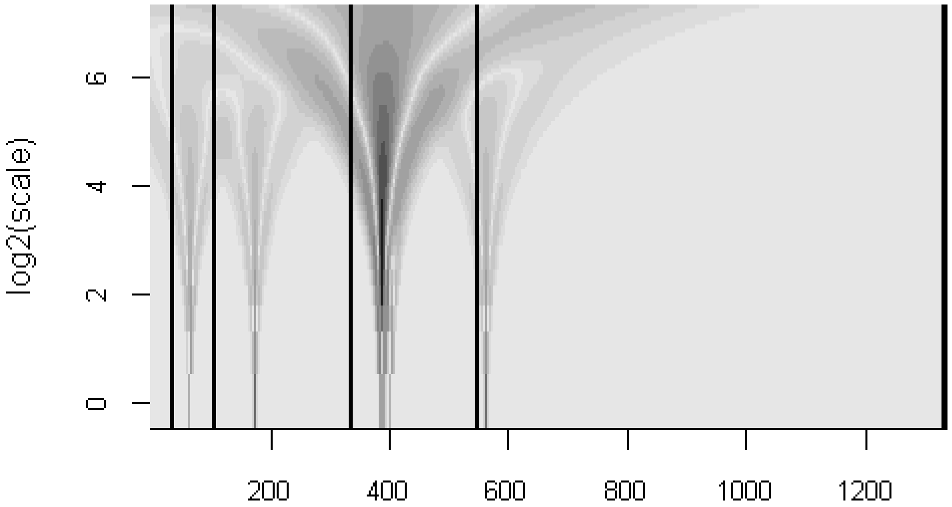

Fimbristylis sp

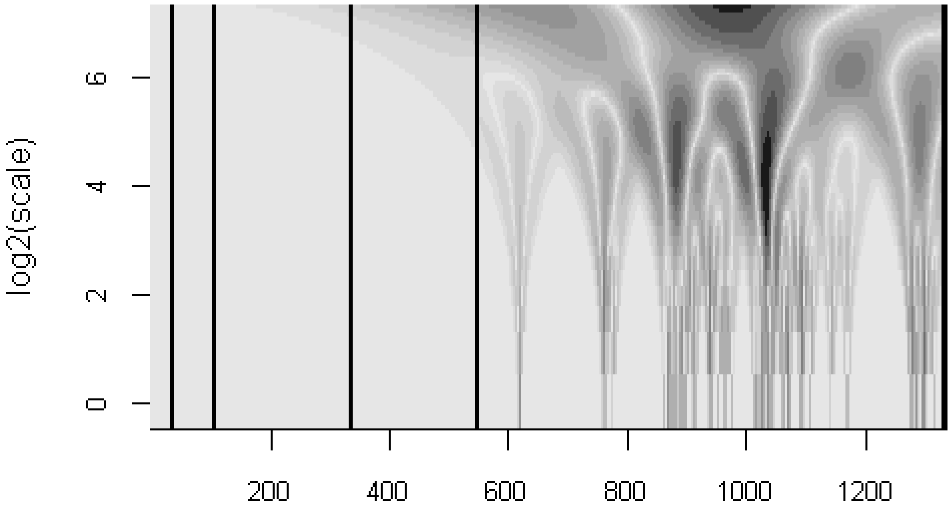

SM 4.5 – Continuous wavelet transform plots for the 106 species used in the similarity analysis

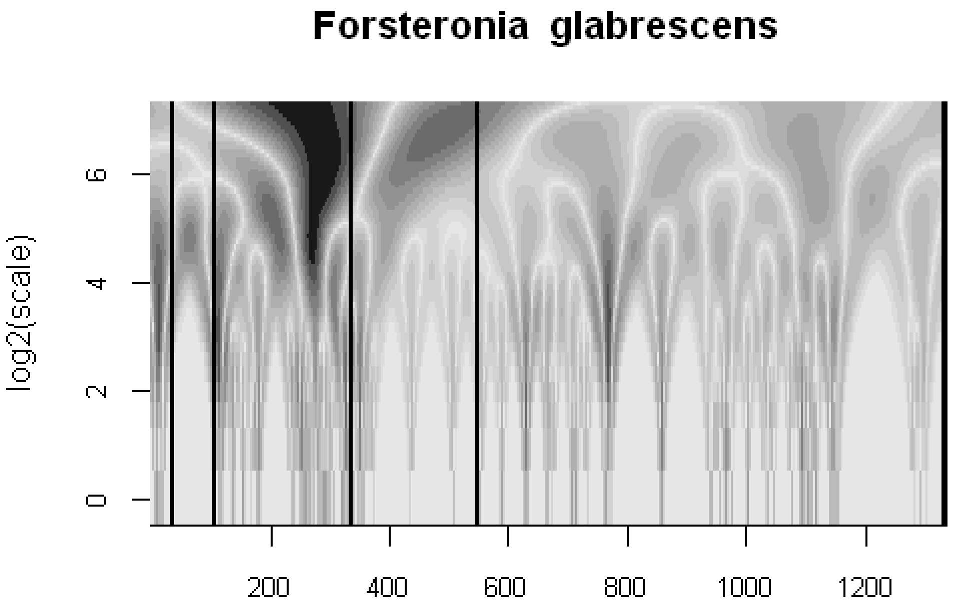

Forsteronia glabrescens

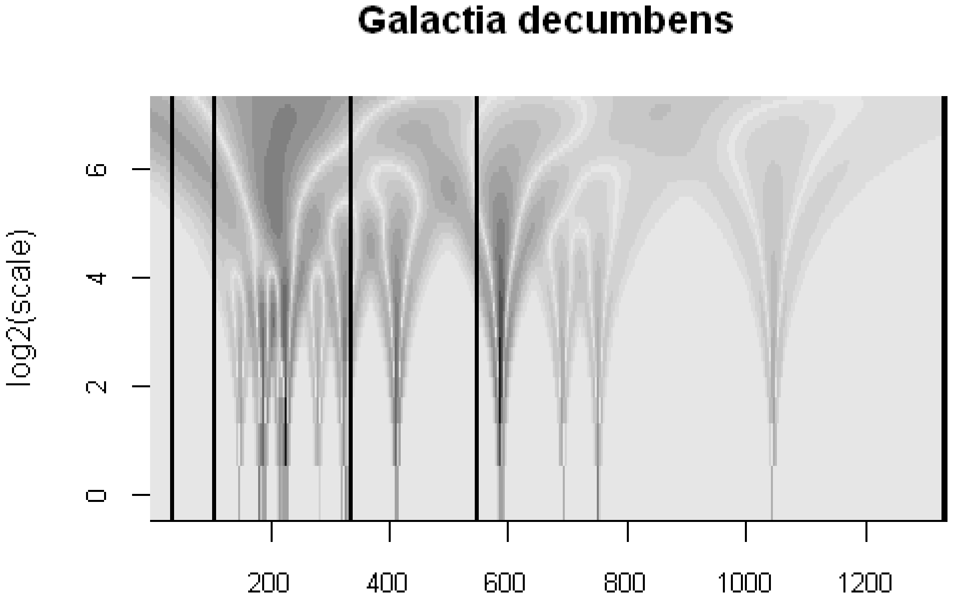

Galactia decumbens

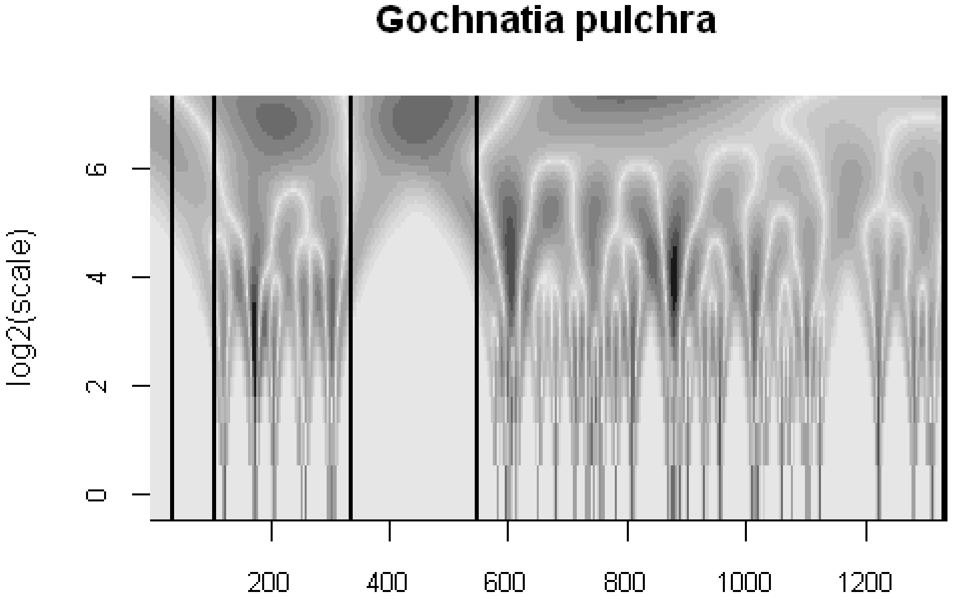

Gochnatia pulchra

SM 4.5 – Continuous wavelet transform plots for the 106 species used in the similarity analysis

Hyptis crinita

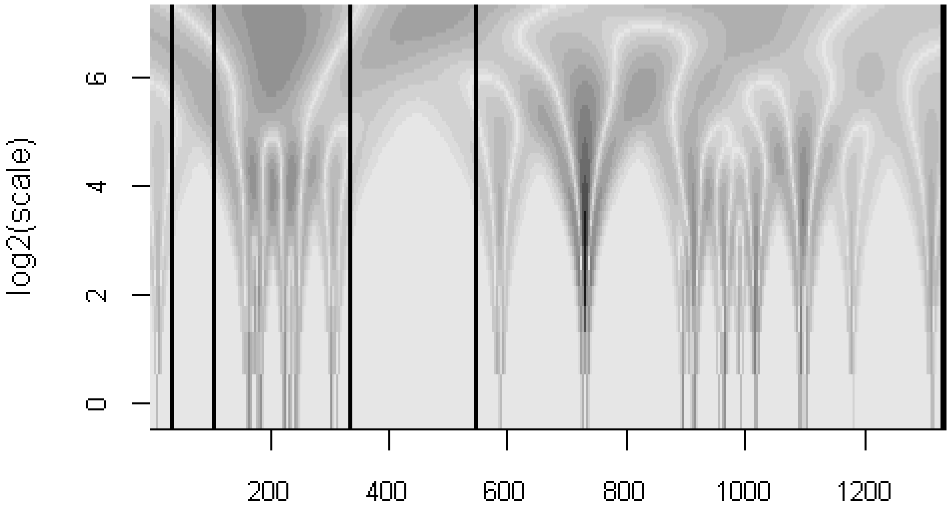

Hyptis sp

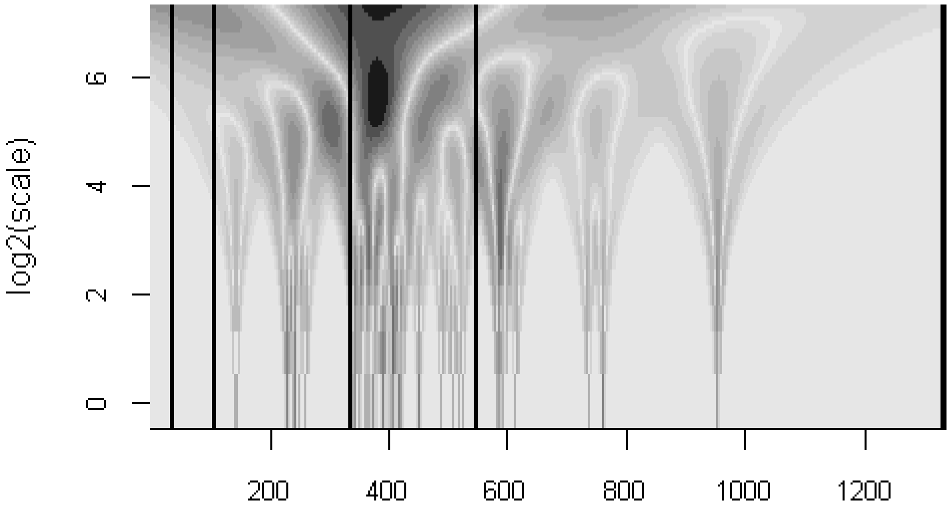

Imperata brasiliensis

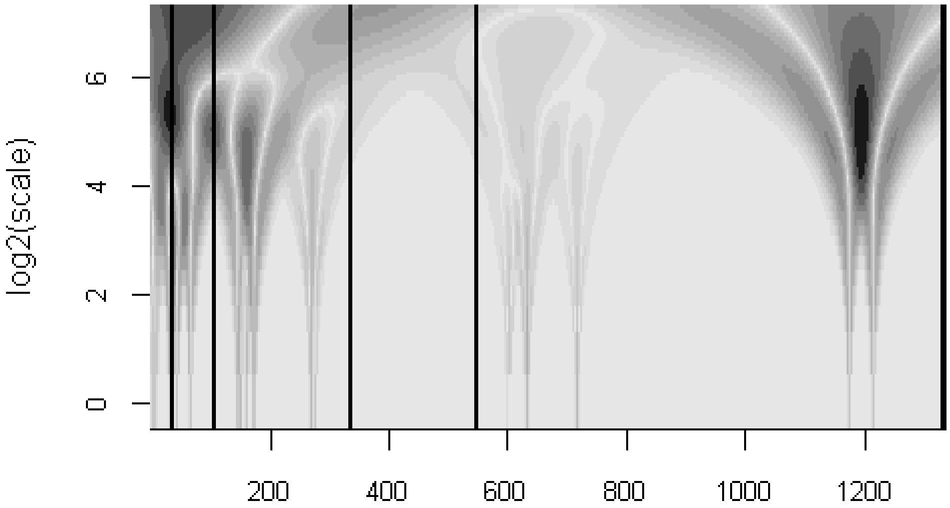

SM 4.5 – Continuous wavelet transform plots for the 106 species used in the similarity analysis

Jacaranda caroba

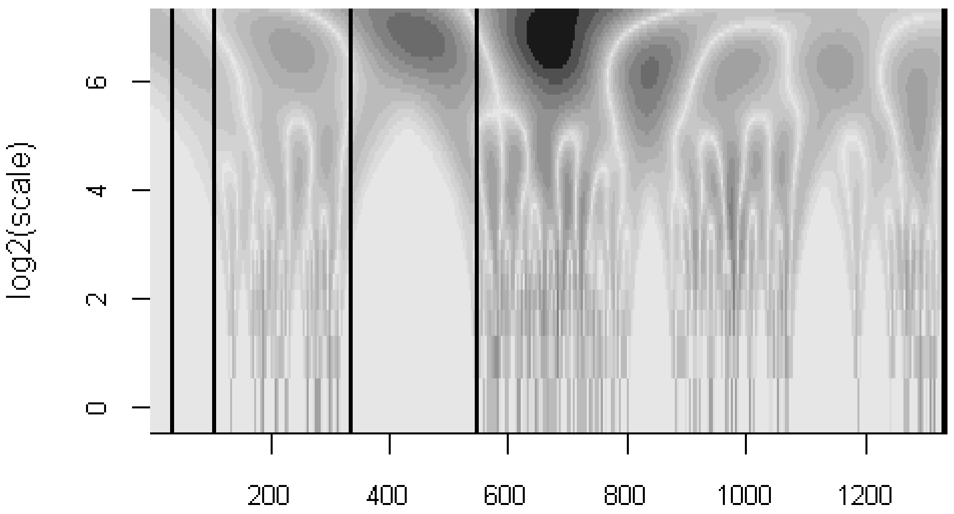

Leandra aurea

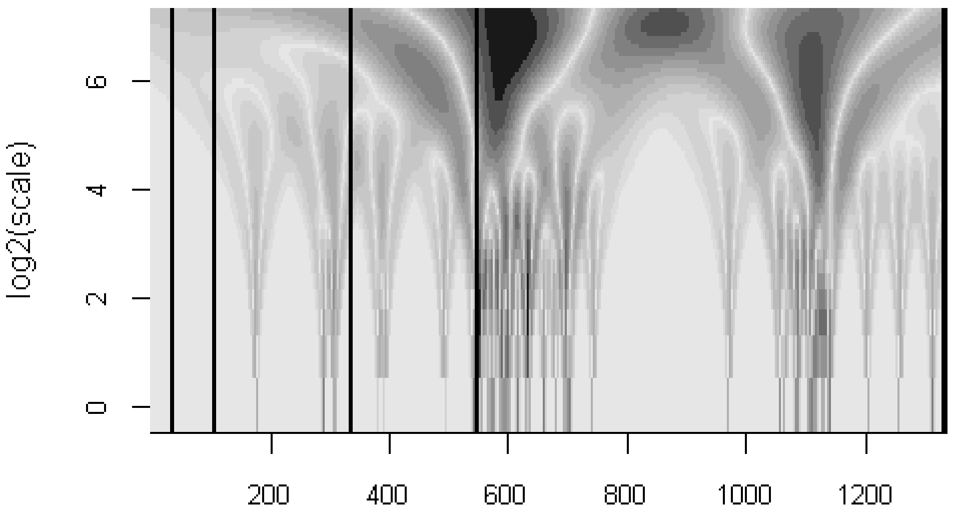

Licania rigida

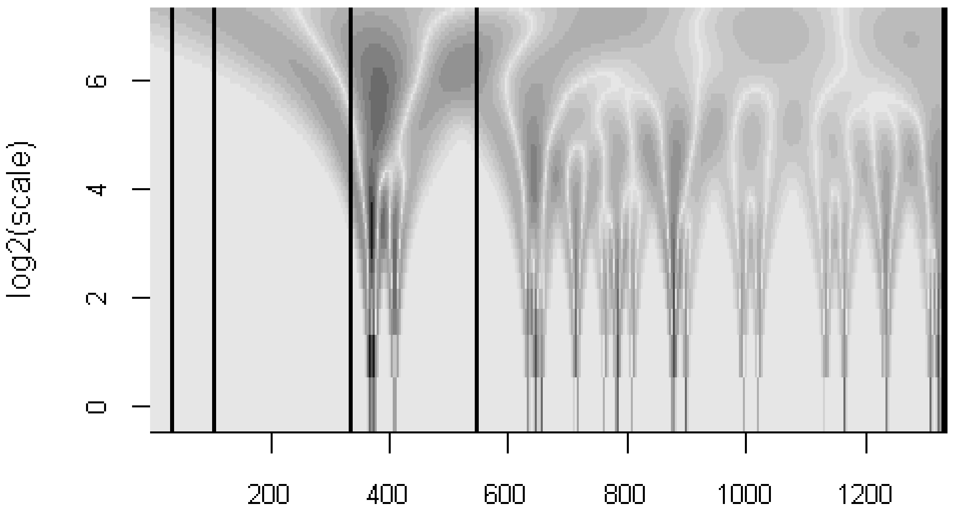

SM 4.5 – Continuous wavelet transform plots for the 106 species used in the similarity analysis

Lippia velutina

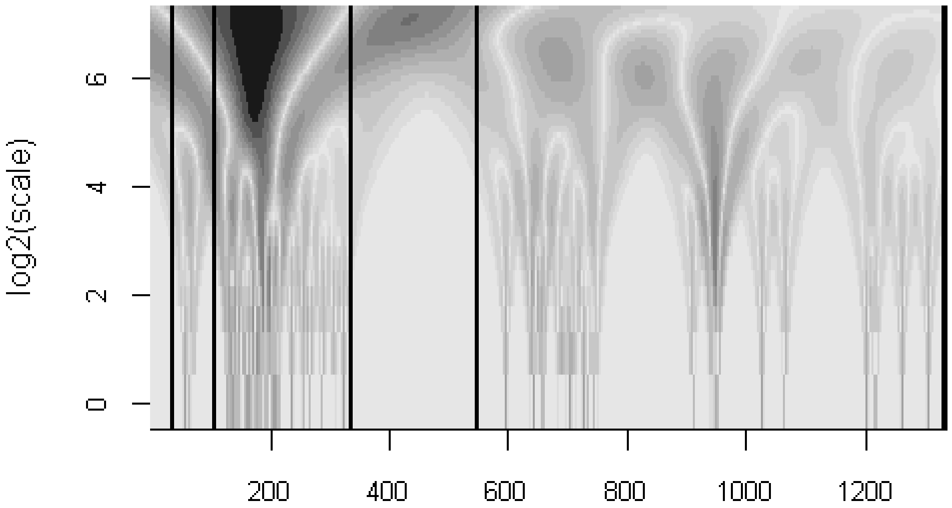

Melinis minutiflora

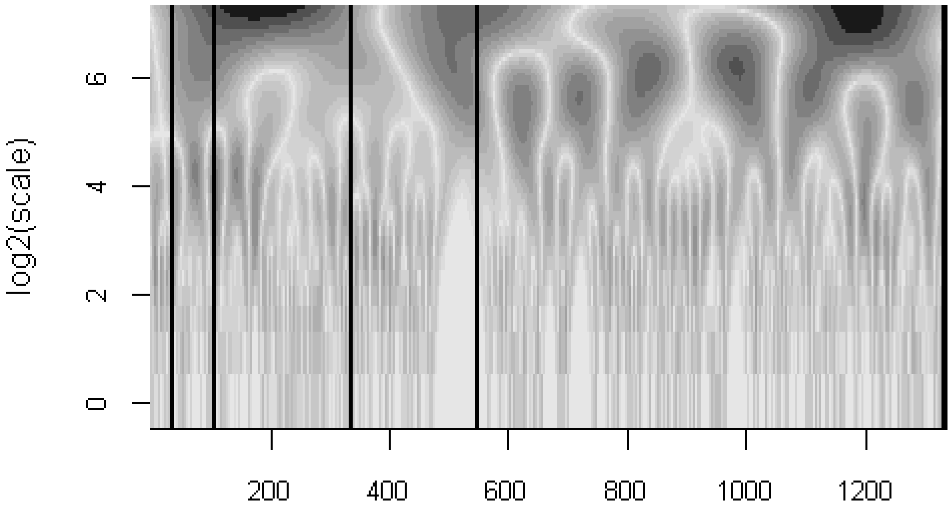

Memora peregrina

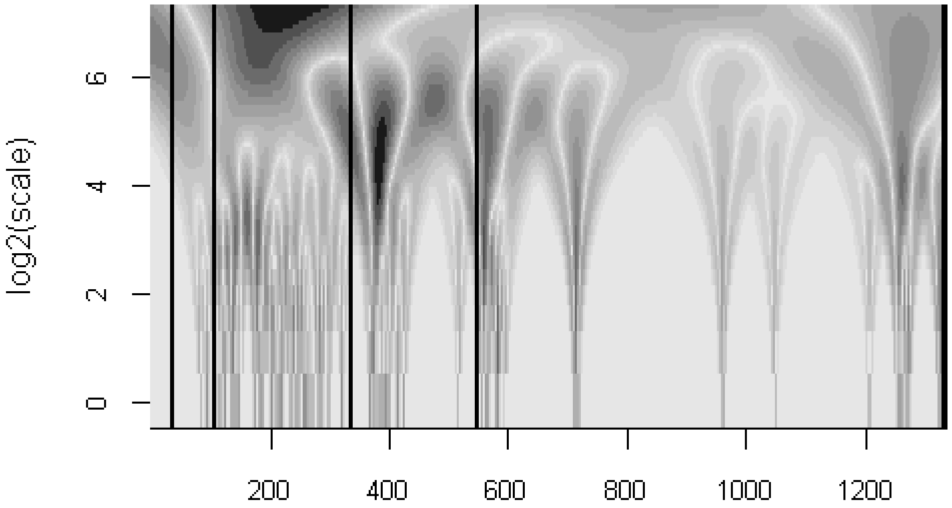

SM 4.5 – Continuous wavelet transform plots for the 106 species used in the similarity analysis

Miconia albicans

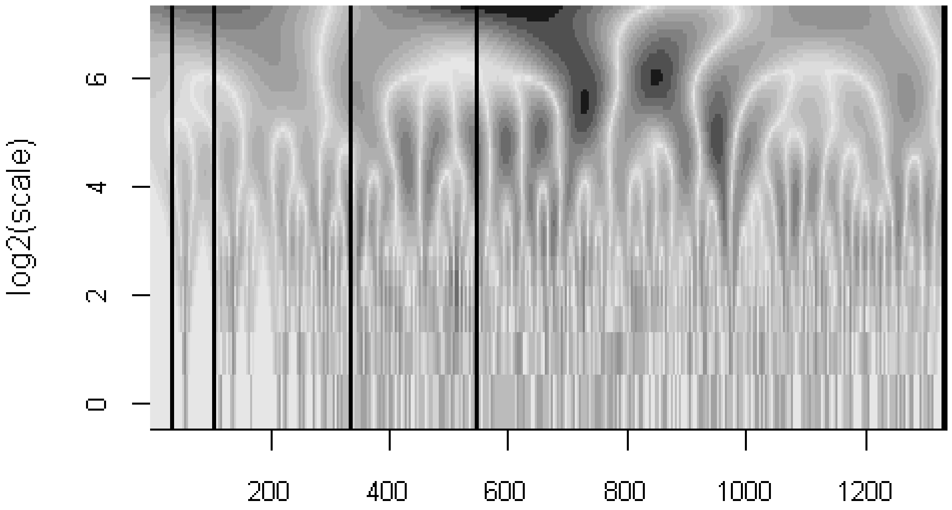

Miconia fallax

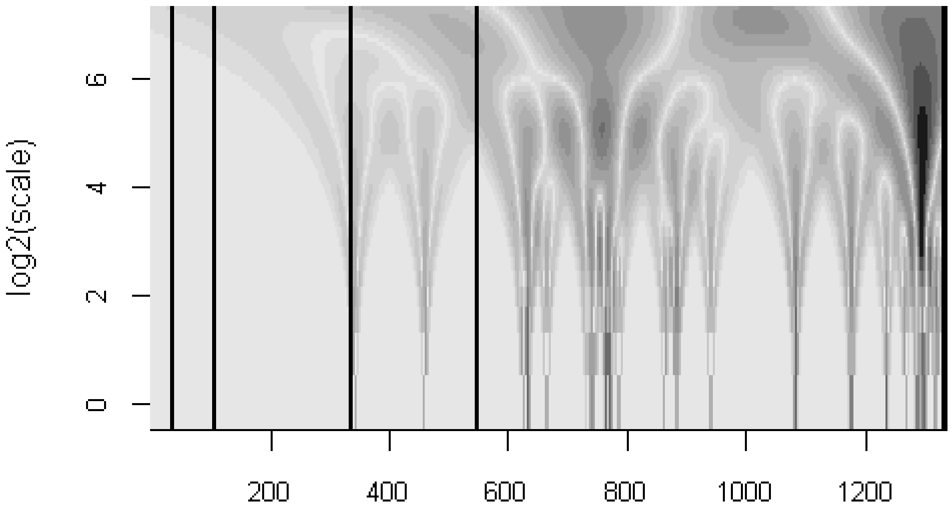

Miconia ligustroides

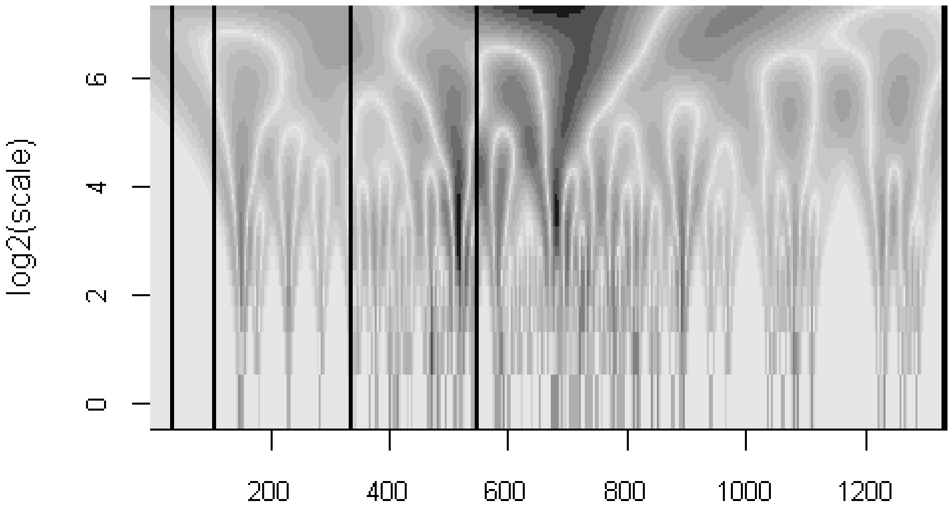

SM 4.5 – Continuous wavelet transform plots for the 106 species used in the similarity analysis

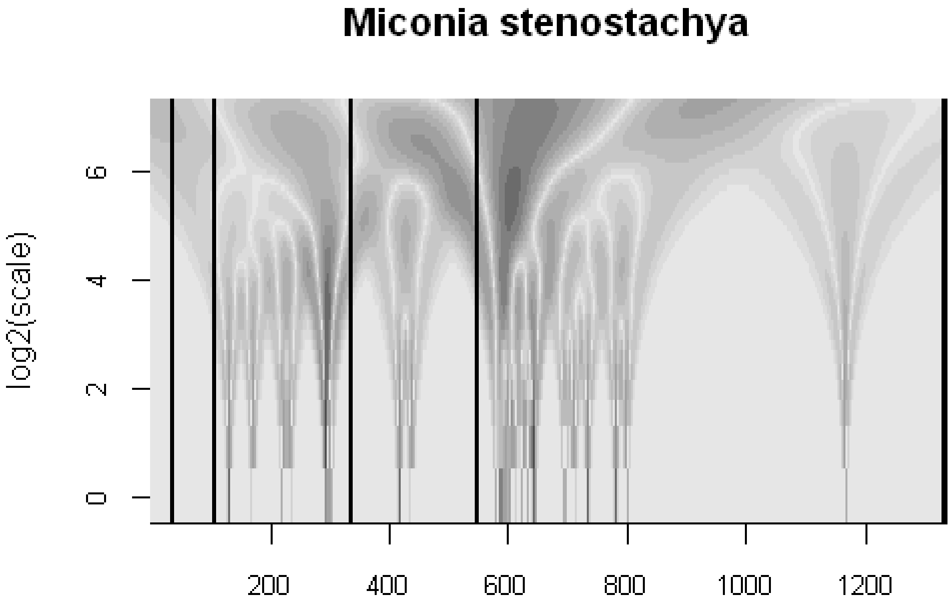

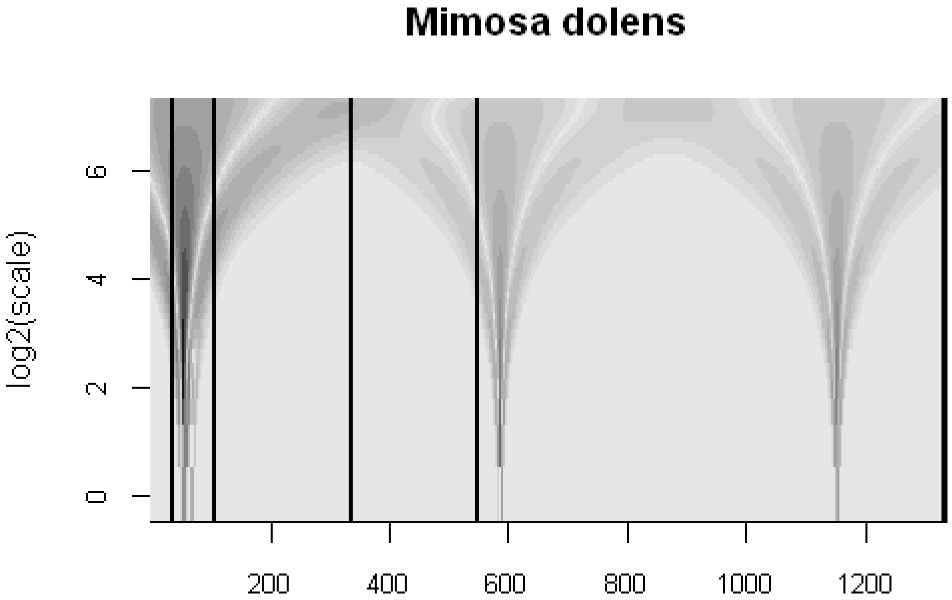

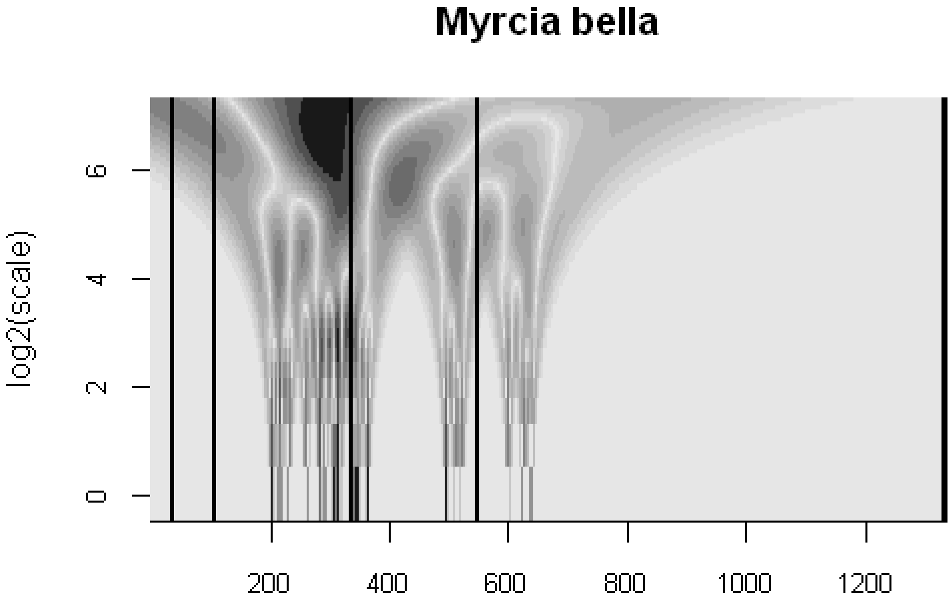

SM 4.5 – Continuous wavelet transform plots for the 106 species used in the similarity analysis

Myrcia guianensis

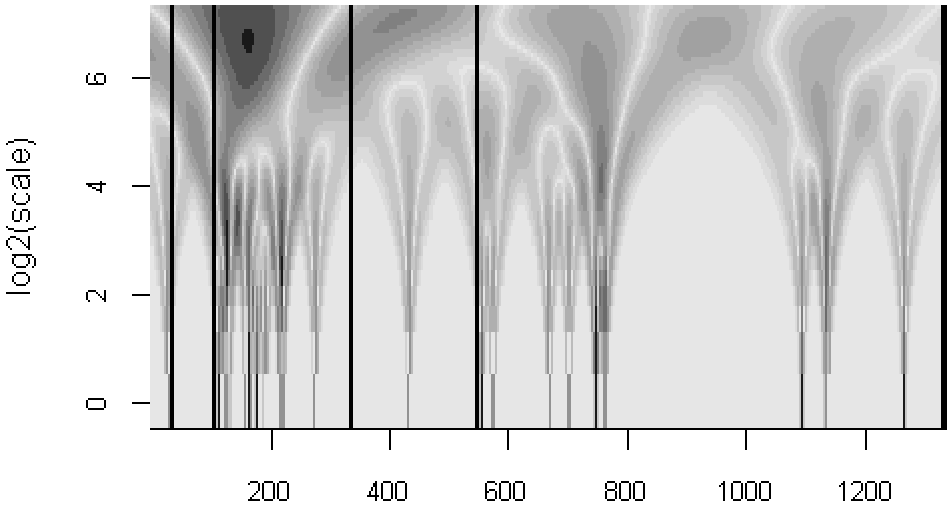

Myrcia lingua

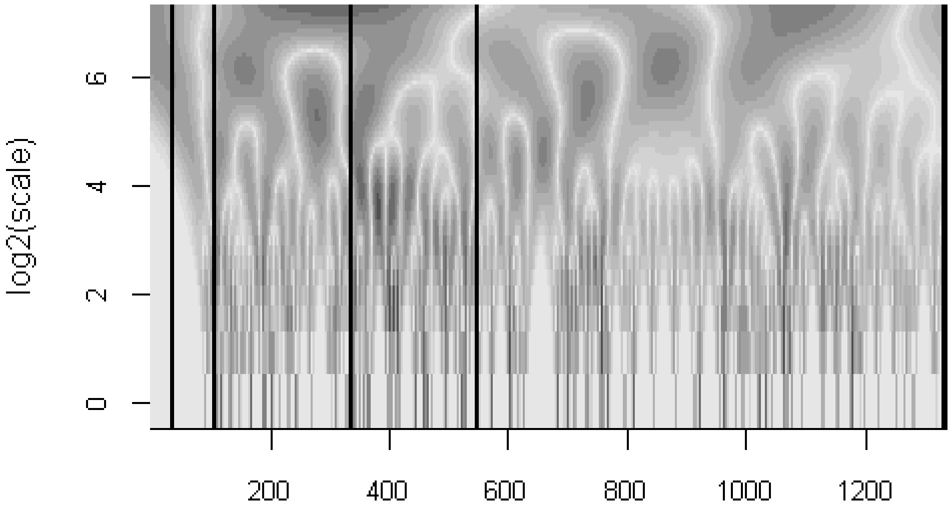

Myrcia tomentosa

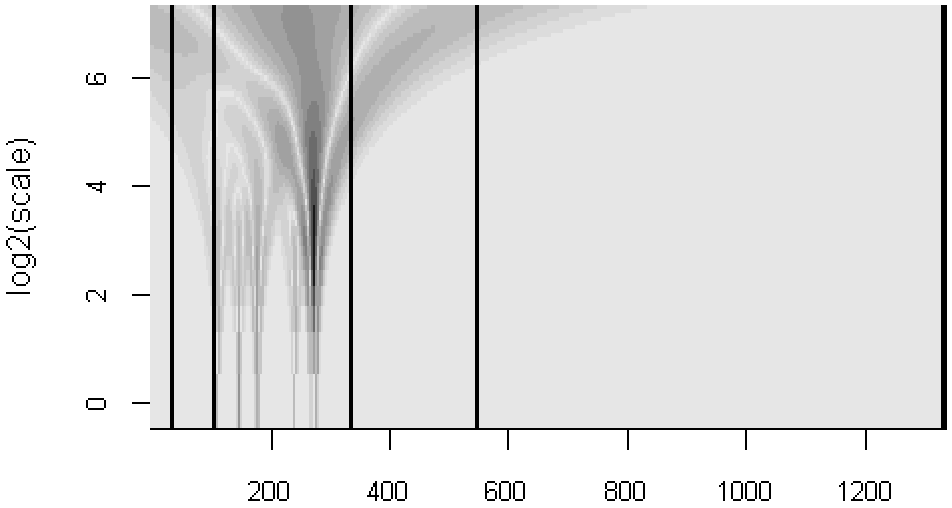

SM 4.5 – Continuous wavelet transform plots for the 106 species used in the similarity analysis

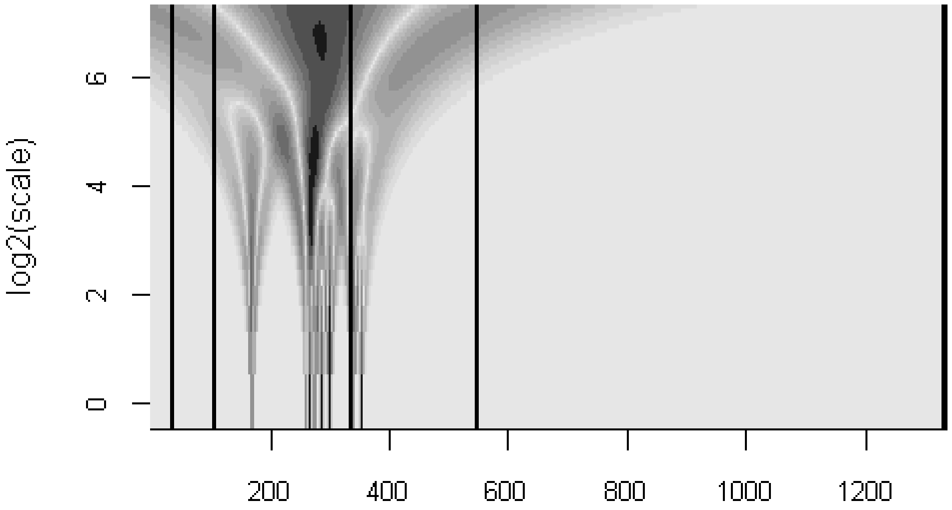

Myrciaria floribunda

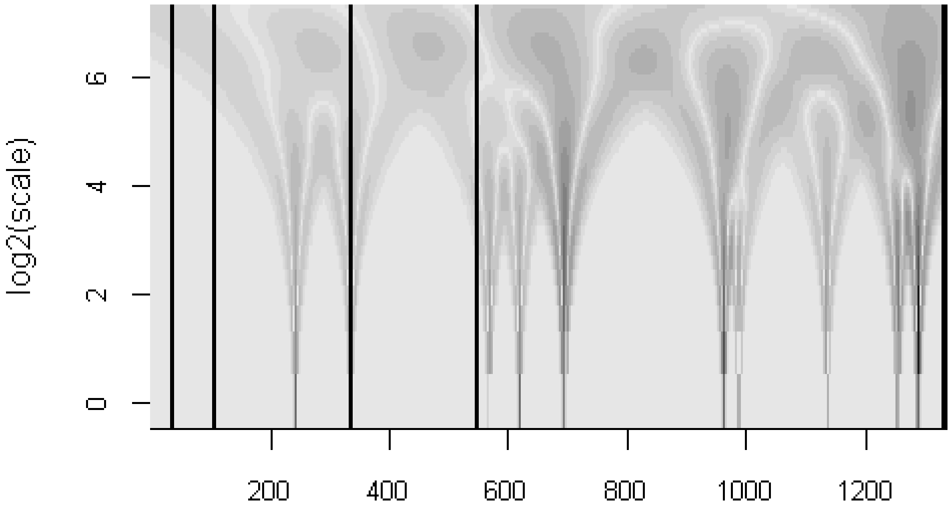

Myrsine ferruginea

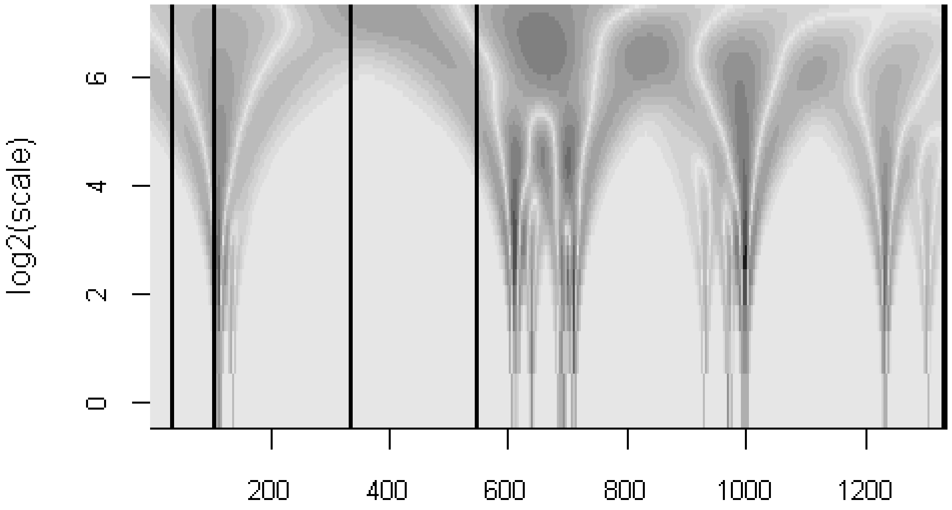

Myrsine umbellata

SM 4.5 – Continuous wavelet transform plots for the 106 species used in the similarity analysis

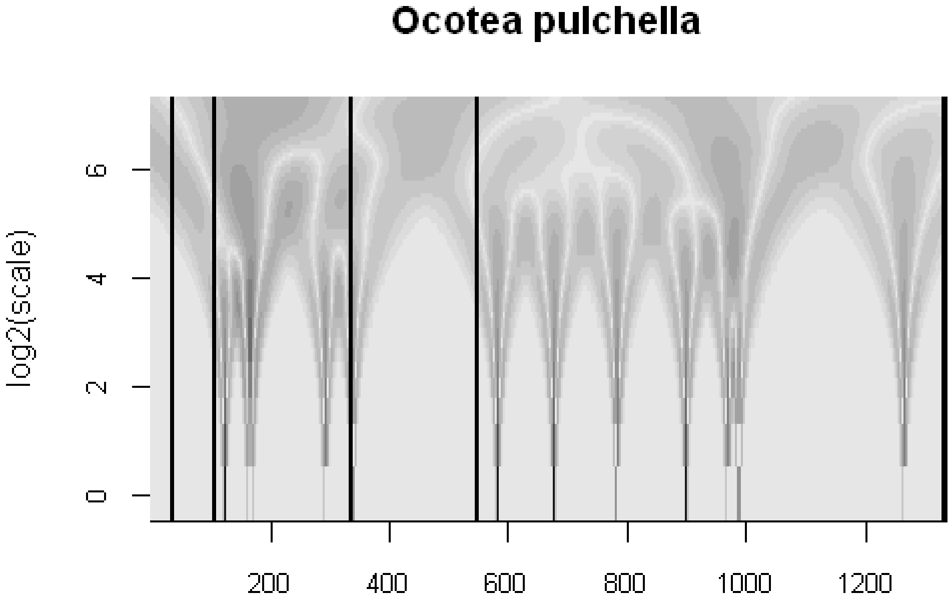

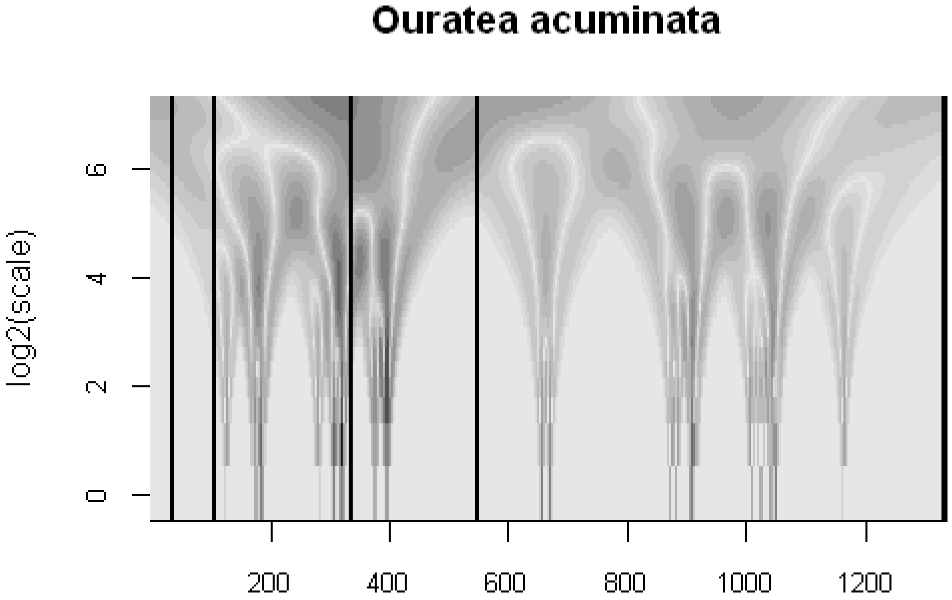

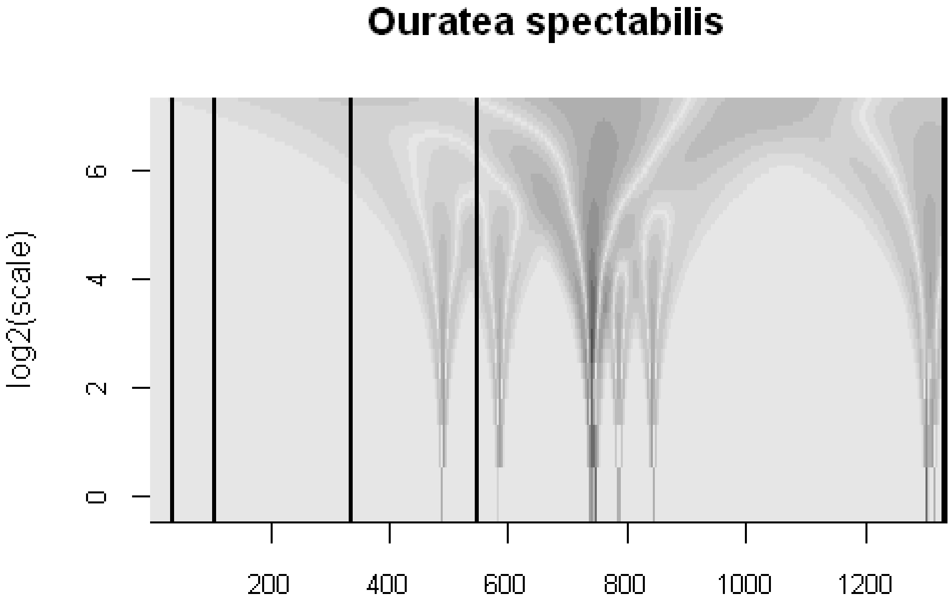

SM 4.5 – Continuous wavelet transform plots for the 106 species used in the similarity analysis

Panicum cf campestre

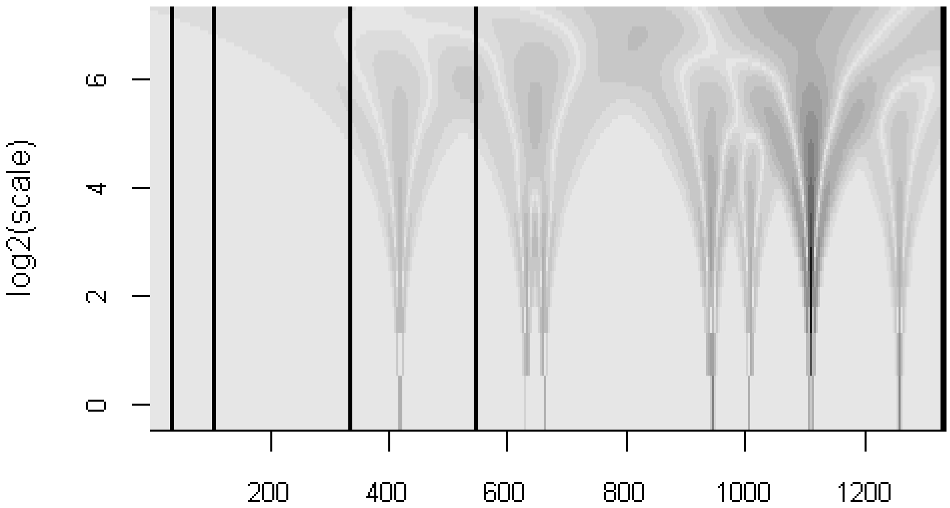

Panicum sp2

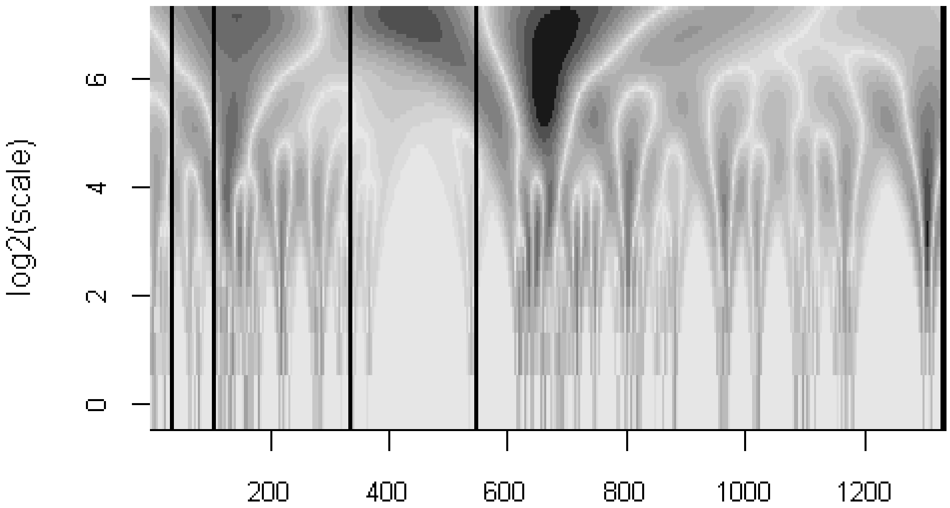

Paspalum cf pilosum

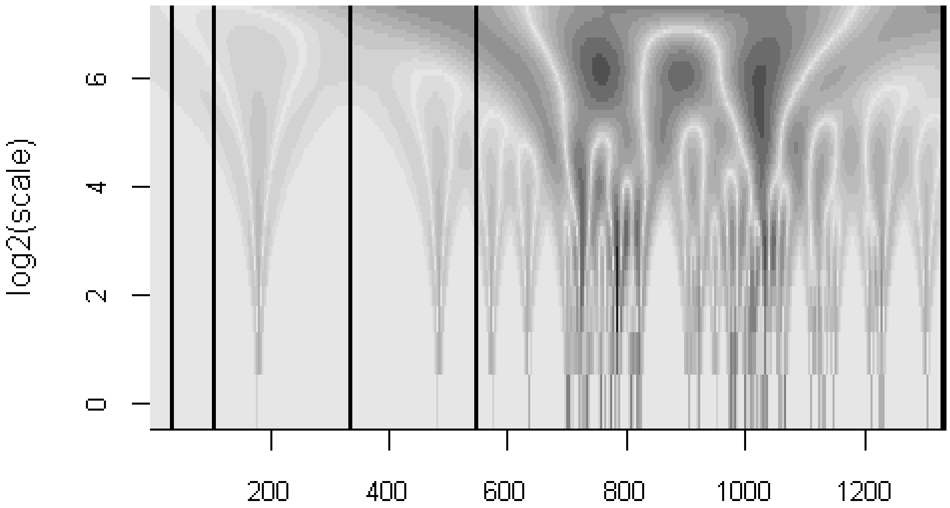

SM 4.5 – Continuous wavelet transform plots for the 106 species used in the similarity analysis

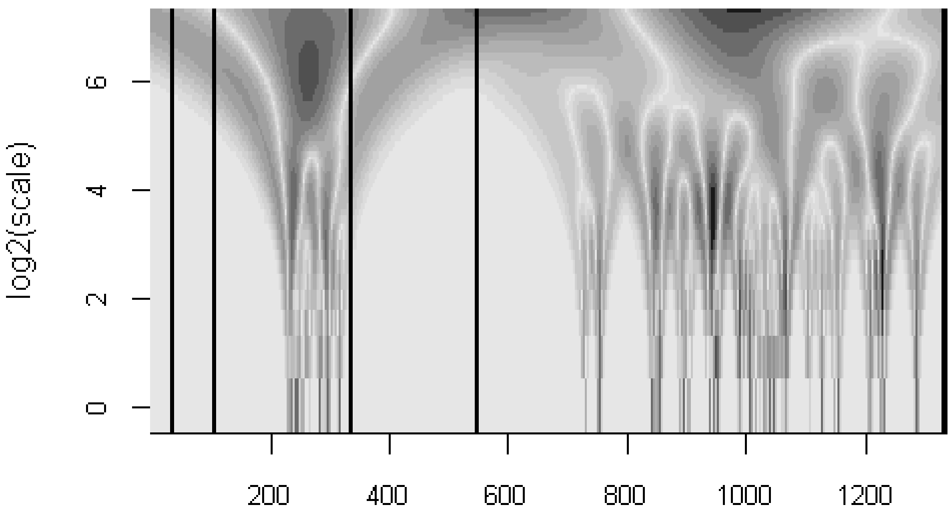

Peltodon tomentosus

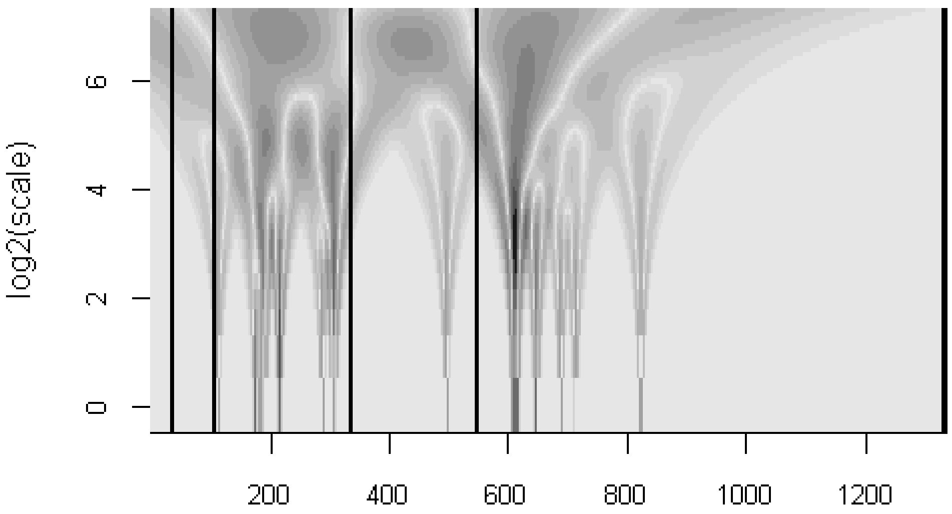

Pera glabrata

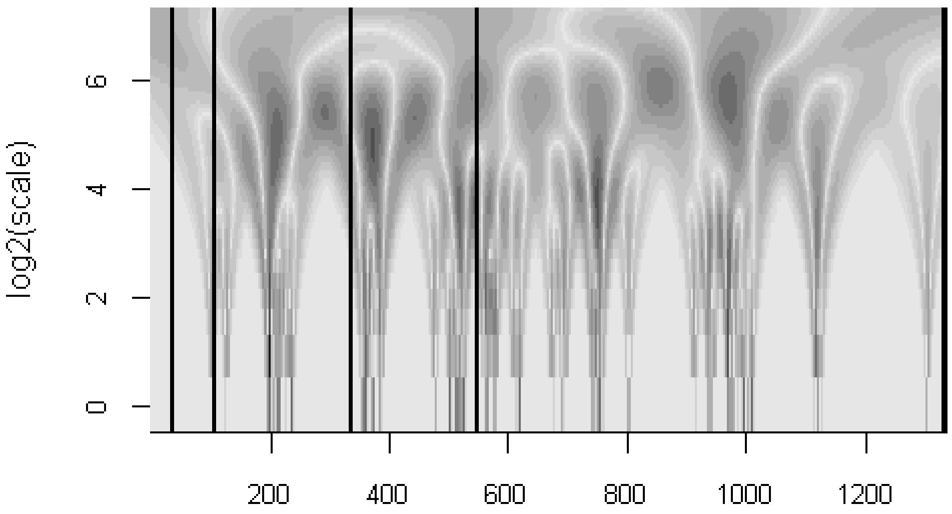

Piptocarpha rotundifolia

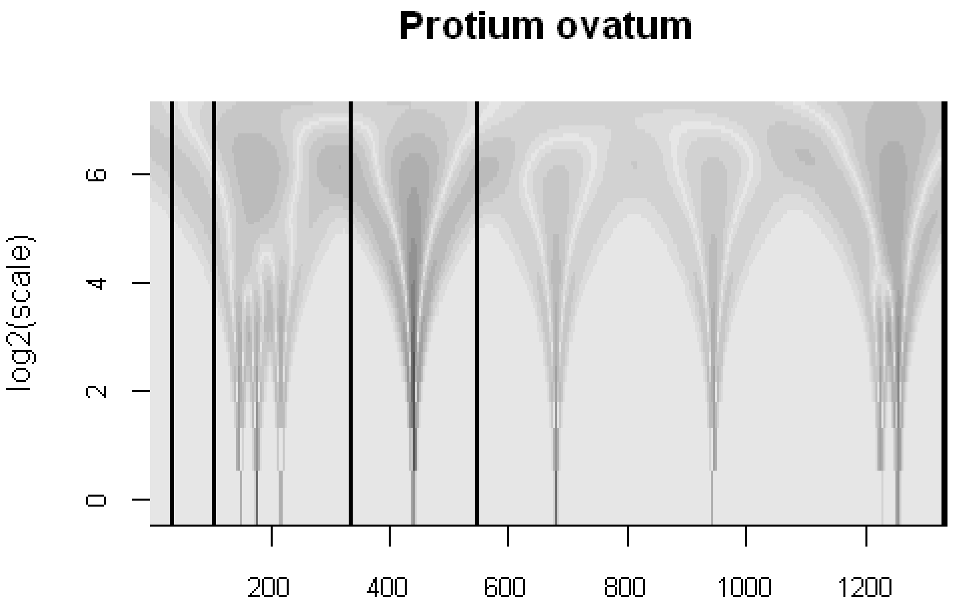

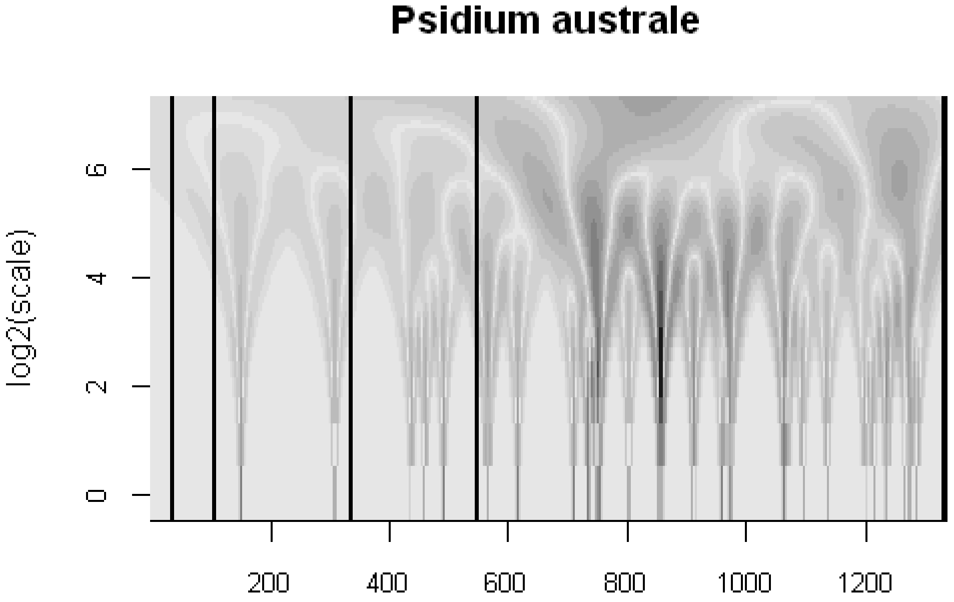

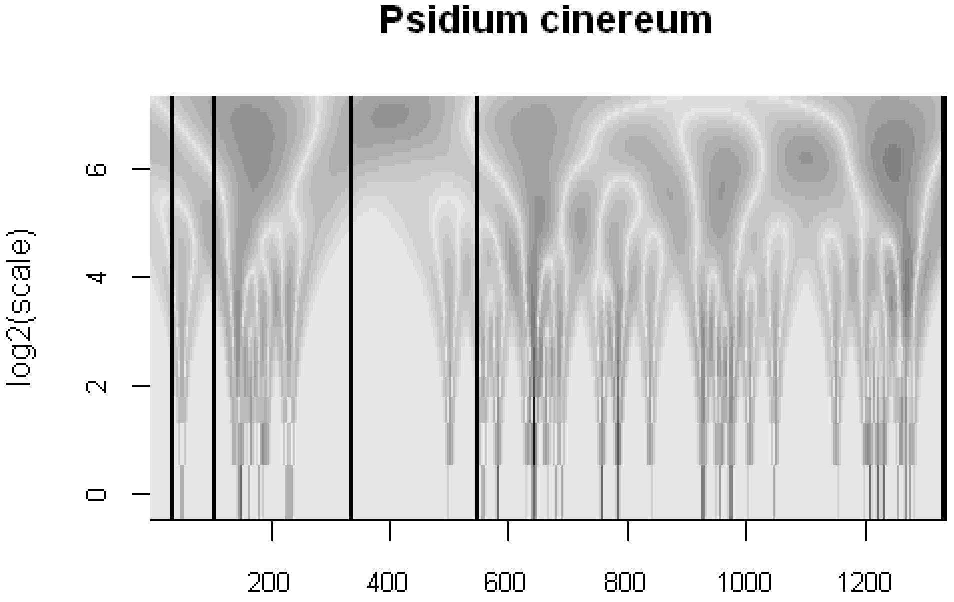

SM 4.5 – Continuous wavelet transform plots for the 106 species used in the similarity analysis

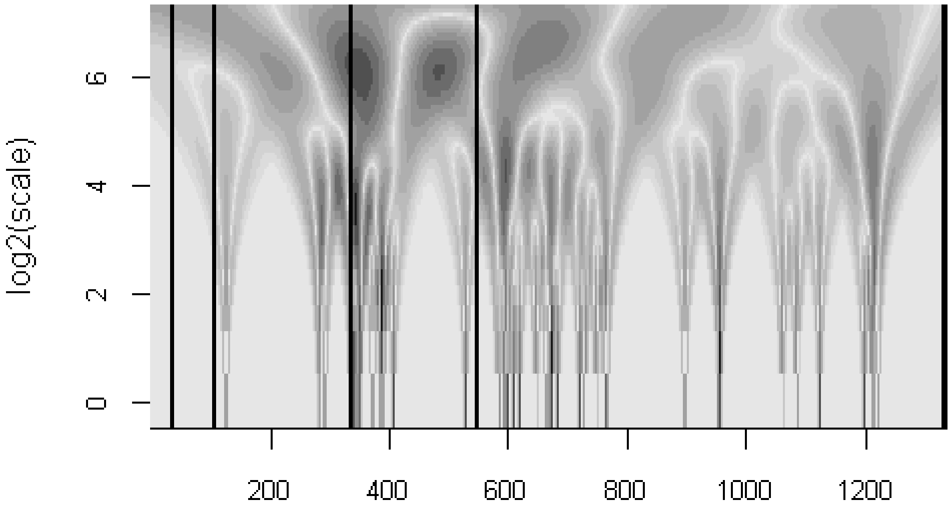
Psidium laruotteanum

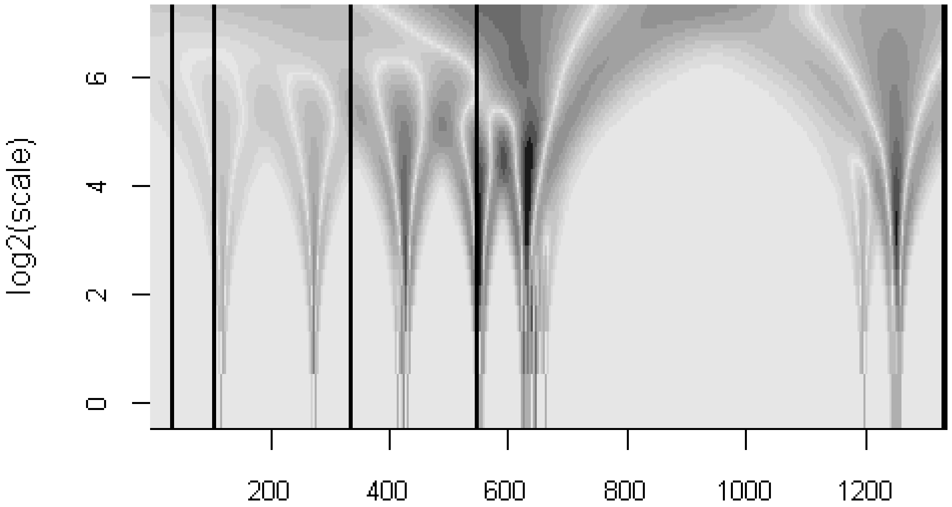
Roupala montana

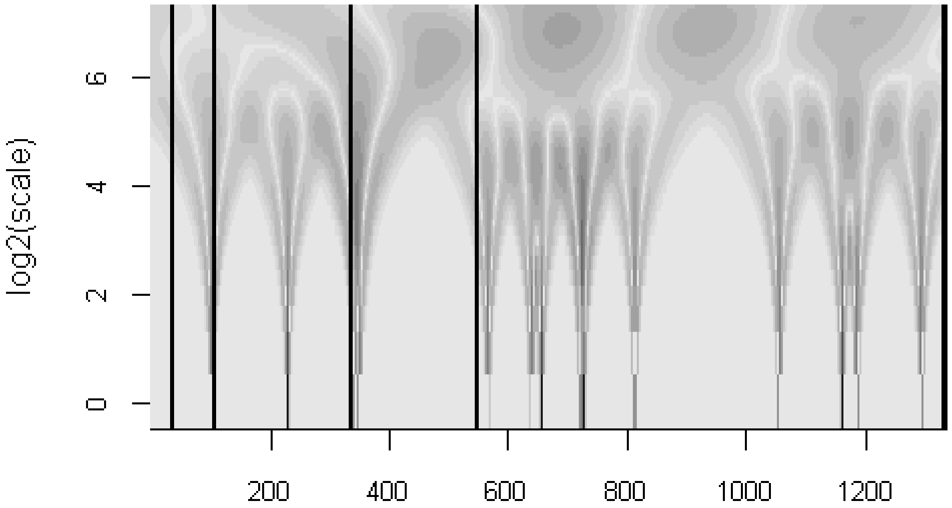
Sapium glandulosum

SM 4.5 – Continuous wavelet transform plots for the 106 species used in the similarity analysis

Schefflera vinosa

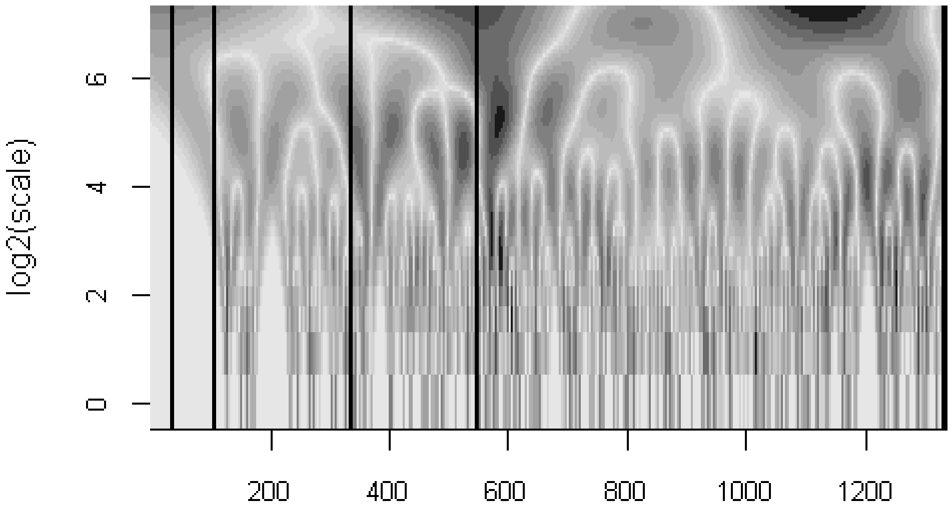

Schizachyrium sp1

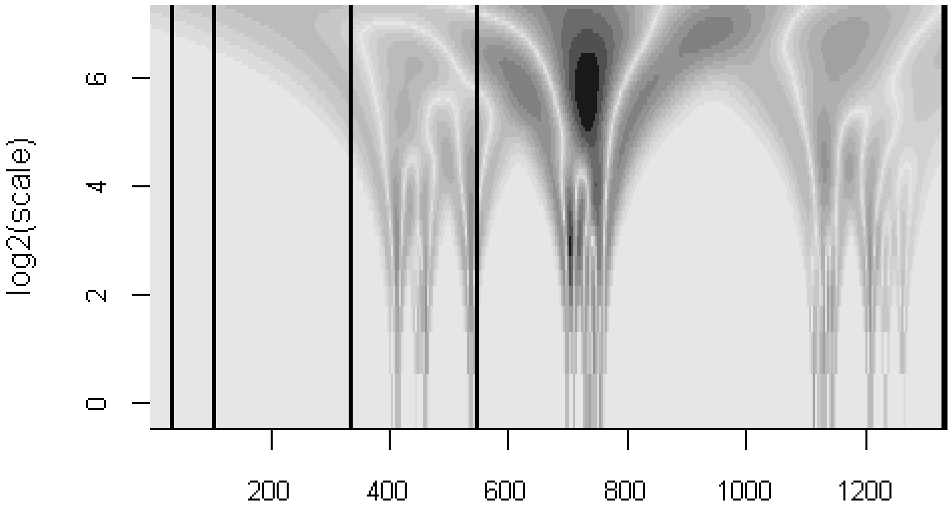

Senna rugosa

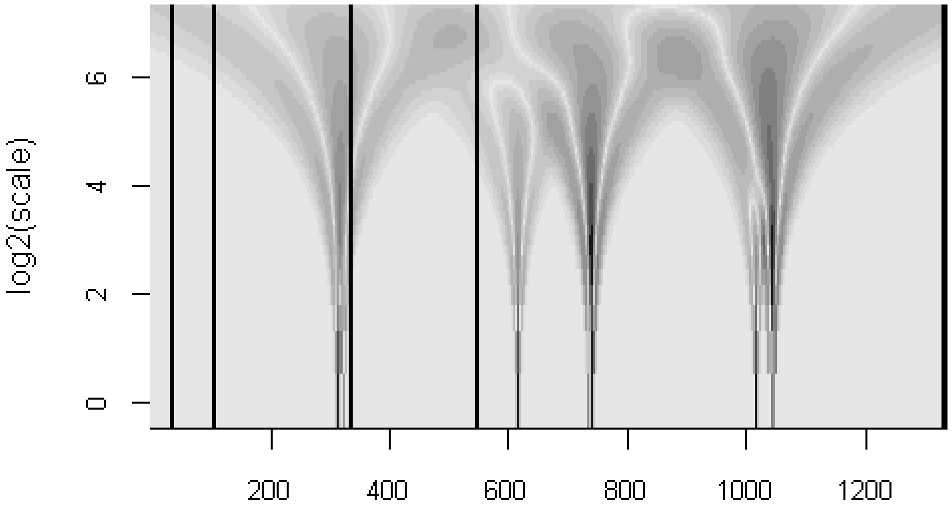

SM 4.5 – Continuous wavelet transform plots for the 106 species used in the similarity analysis

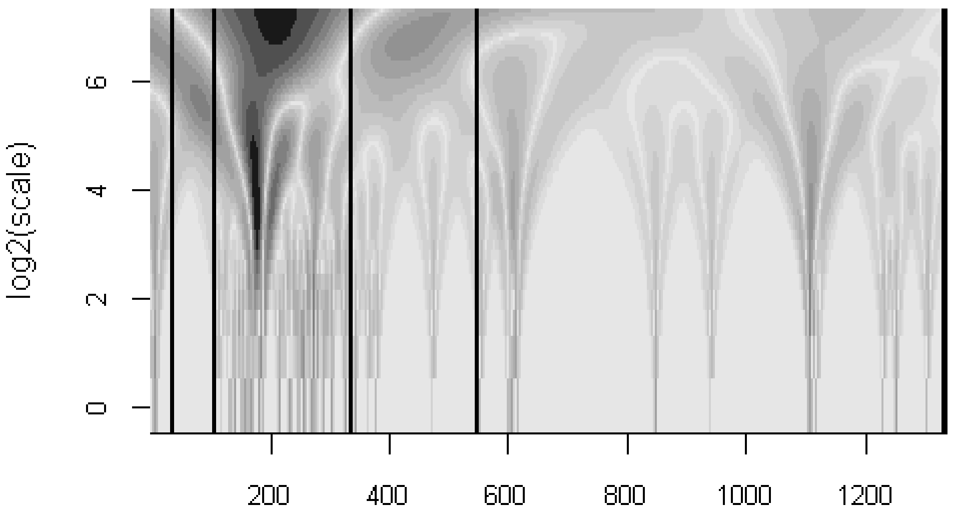

Serjania erecta

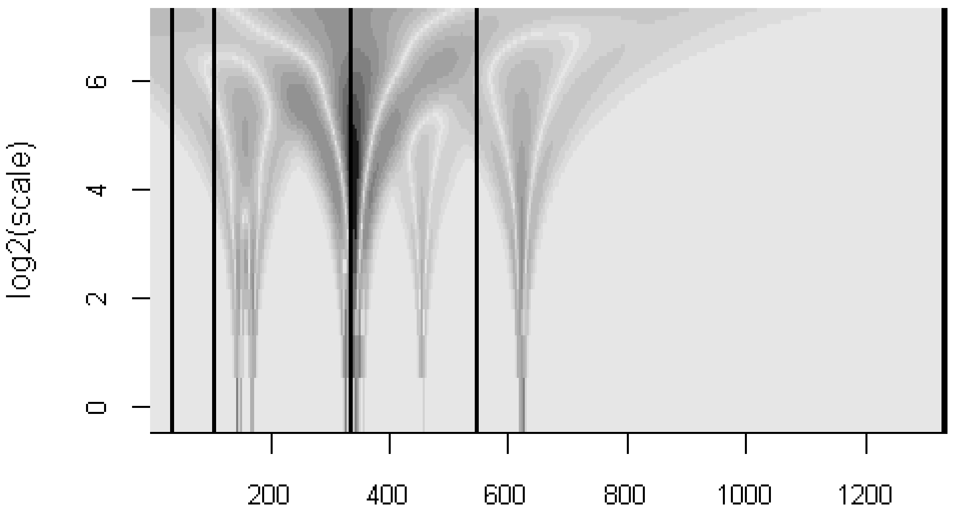

Serjania lethalis

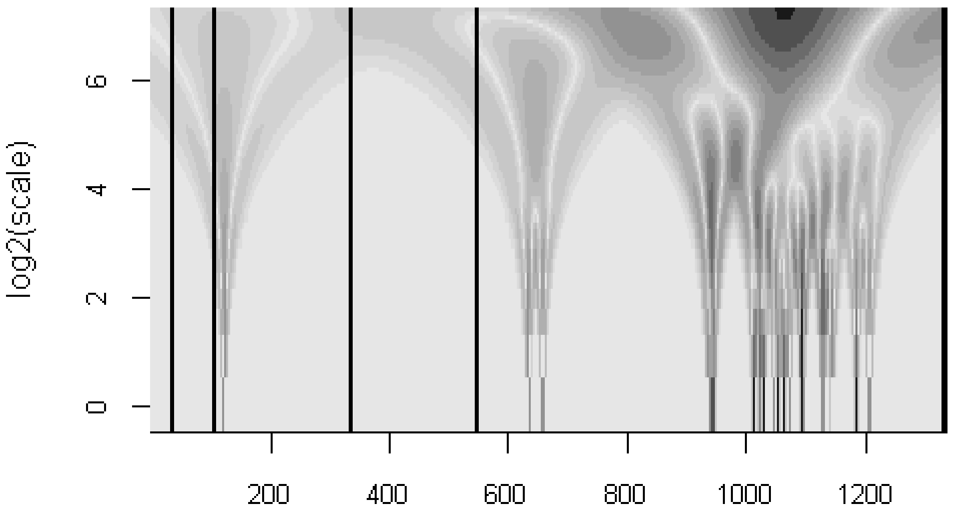

Sida cf rhombifolia

Smilax cissoides

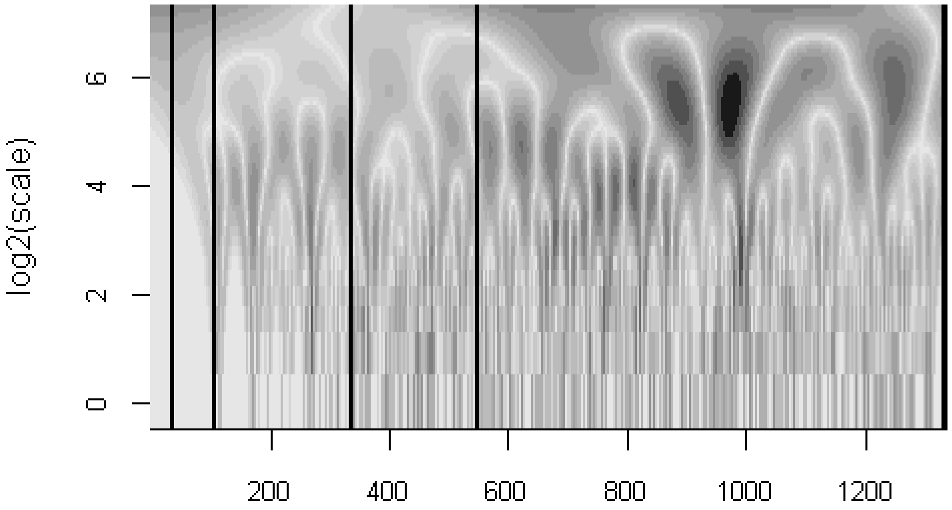

Solanum lycocarpum

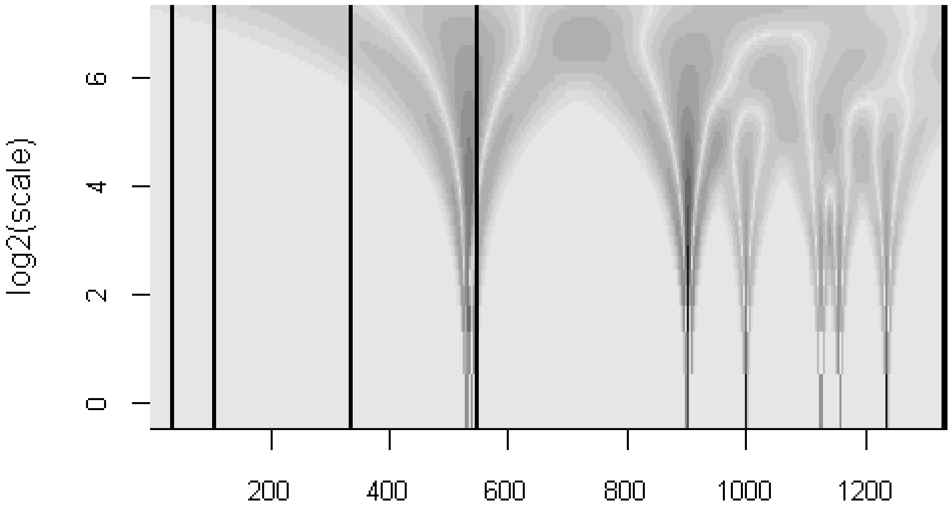

Stachytarpheta cayennensis

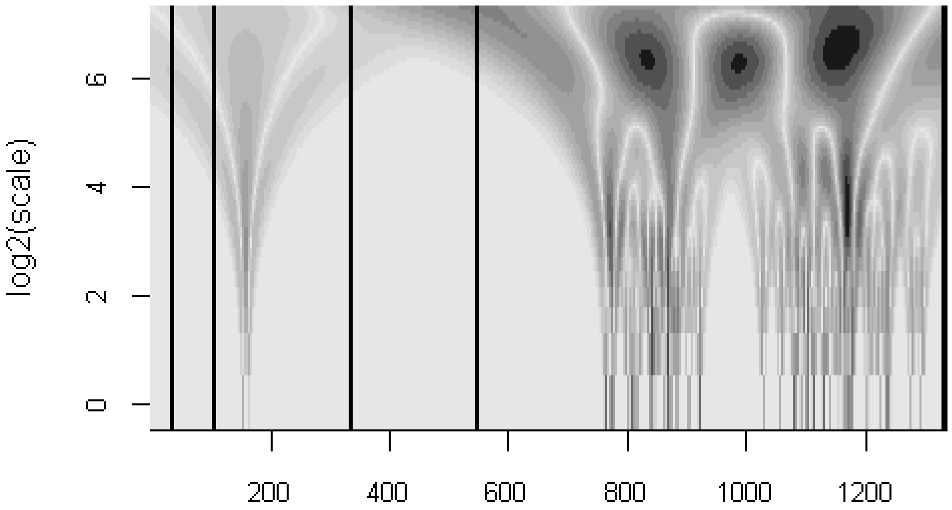

SM 4.5 – Continuous wavelet transform plots for the 106 species used in the similarity analysis

Stryphnodendron adstringens

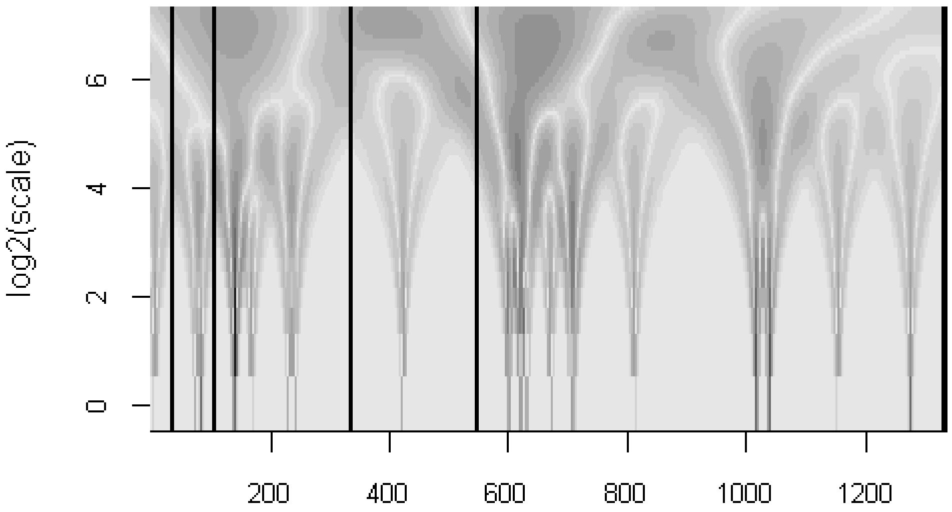

Stryphnodendron obovatum

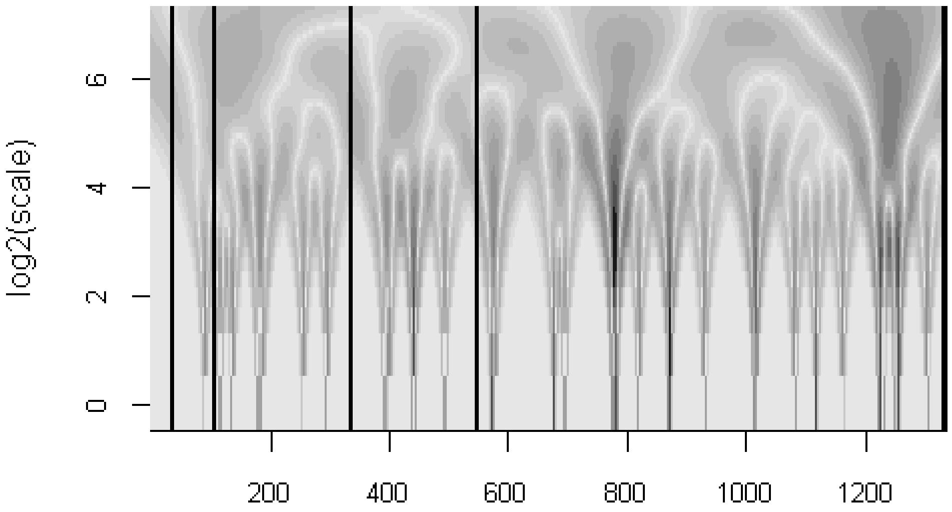

Stylosanthes guianensis

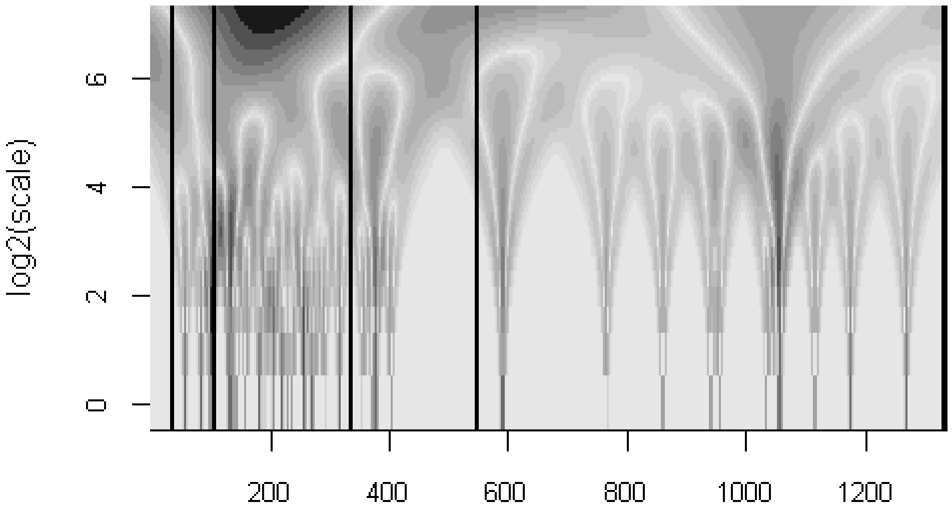

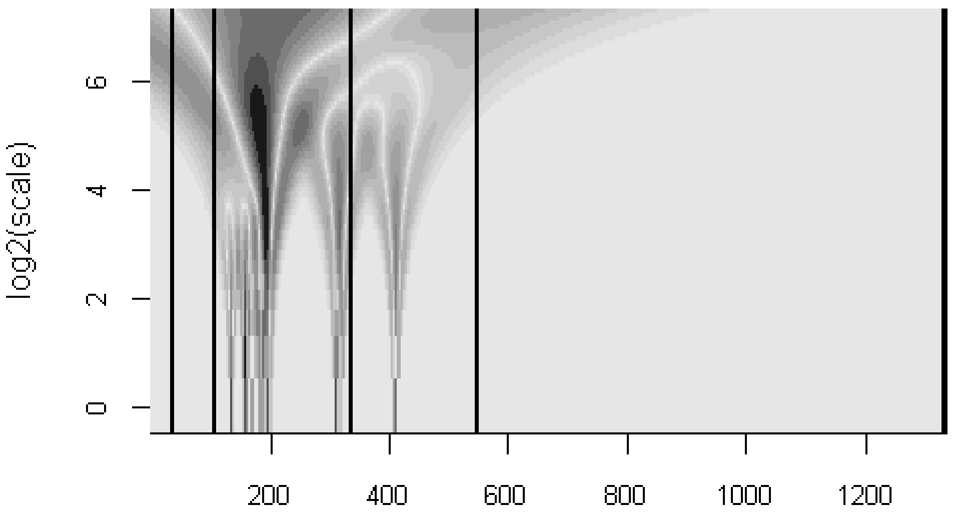
Tabebuia ochracea

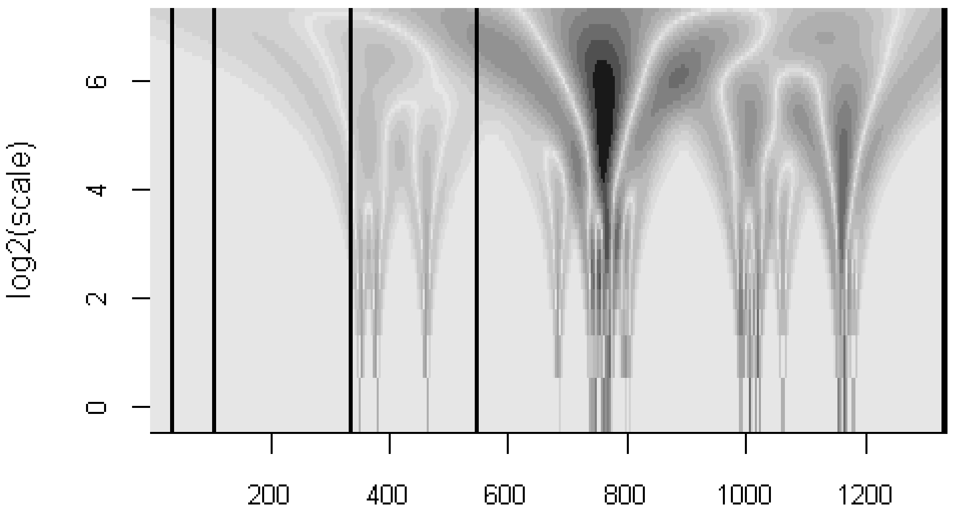
Tibouchina stenocarpa

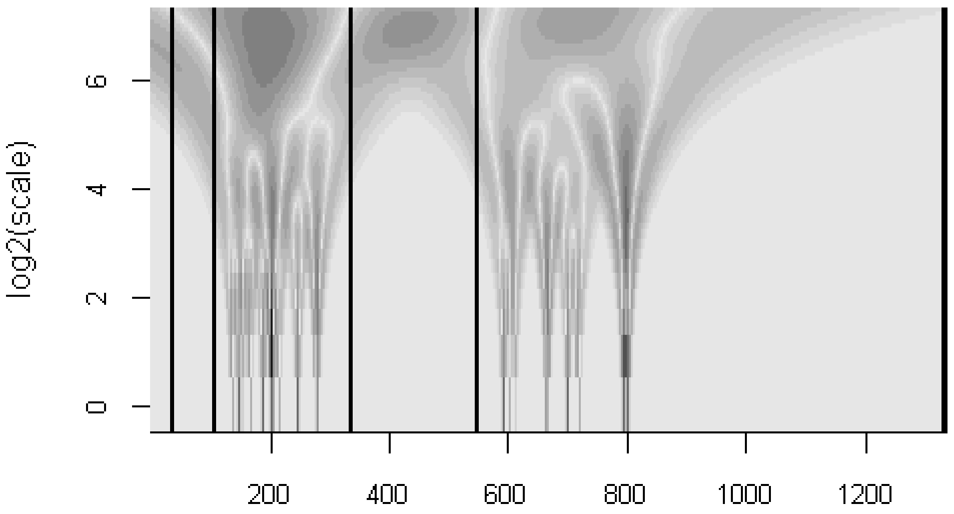
Tocoyena formosa

SM 4.5 – Continuous wavelet transform plots for the 106 species used in the similarity analysis

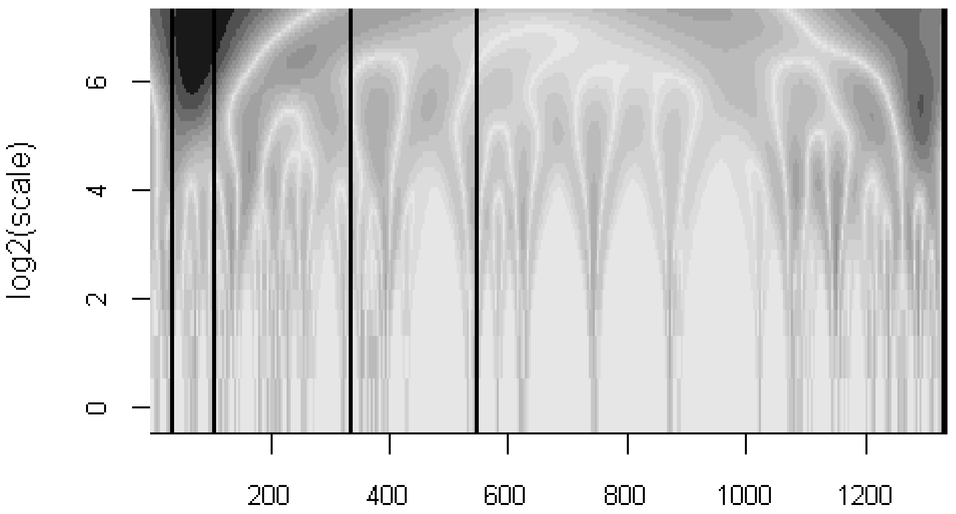
Urochloa decumbens

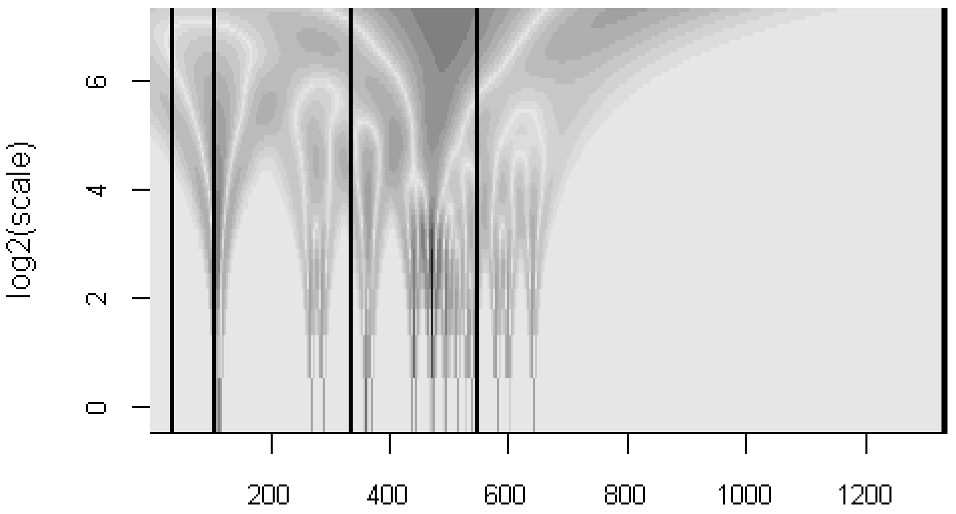
Xylopia aromatica